October 1962

Technical Report No. 16

A Linearized Theory for Rotational, Supercavitating Flow

by

Robert L. Street

This research was carried out under the
Bureau of Ships
Fundamental Hydromechanics Research Program
Project S-R009-01-01, ONR Contract Nonr 225(56)

Department of Civil Engineering
Stanford University
Stanford, California

A LINEARIZED THEORY FOR ROTATIONAL, SUPERCAVITATING FLOW

by

Robert L. Street

Technical Report No. 16

October 1962

This research was carried out under the Bureau of
Ships Fundamental Hydromechanics Research
Program Project S-R009-01-01,
ONR Contract Nonr 225(56)

ABSTRACT

This work is concerned with predicting the forces acting on slender bodies, namely hydrofoils and wedges, in rotational, supercavitating flow. Methods are given for establishing not only qualitative but quantitative measures of the effects of rotation in linearized, supercavitating flows.

A linearized theory is developed for steady, two-dimensional flow under the assumption that the flow has a constant vorticity throughout. The effects of gravity, viscosity, and surface tension are neglected. Tulin's original closed-cavity model is employed. A basic assumption of the theory is that the slender body-cavity combination causes only small perturbations in the velocity components of the basic shear flow. The stream function of the rotational flow satisfies Poisson's equation, which is a linear, inhomogeneous, partial differential equation. By using a particular solution of this equation, the linearized, rotational problem is reduced to a problem involving Laplace's equation and harmonic perturbation velocities. The boundary conditions for the perturbation velocities are established from facts known about the body-cavity combination in the supercavitating shear flow. The resulting boundary value problem is solved by the use of conformal mapping and singularities from thin airfoil theory.

The theory is applied to asymmetric shear flow past wedges and hydrofoils and to symmetric shear flow past wedges. Analytic expressions are given for pressure, drag, lift, and moment coefficients as well as cavity length, cavity area, and cavitation number relationships. The presence of vorticity is shown to create significant changes in those forces acting on the slender bodies and in the shape and size of the trailing cavities. The results are summarized in tables, graphs, and tabulated numerical calculations.

TABLE OF CONTENTS

	Page
1. INTRODUCTION	1
2. THE LINEARIZED THEORY	4
2.1 Notation and Boundary Conditions	4
2.2 Methods of Solution	13
2.3 Calculation of Results	18
3. APPLICATIONS OF THE LINEARIZED THEORY	22
3.1 Asymmetric Flow Past a Wedge	22
3.1.1 Solution of the boundary value problem	22
3.1.2 Results	24
3.1.3 Discussion	37
3.2 Symmetric Flow Past a Wedge	39
3.2.1 Solution of the boundary value problem	39
3.2.2 Results	40
3.2.3 Discussion	45
3.3 Asymmetric Flow Past a Hydrofoil	46
3.3.1 Solution of the boundary value problem	47
3.3.2 Results	51
3.3.3 Discussion	57
4. CONCLUDING REMARKS	59
APPENDIXES	
A. Solution of Singular Integral Equation	61
B. Expansions at $z = \ell$	63
C. Summary of Cavity Shape Integrals	66
D. Evaluation of Complex Integral	68
E. Solution of Quadratic Equation for $\bar{\epsilon}/U_\infty$	70
F. Computations	73
G. Supercavitating Flow about a Slender Wedge in a Transverse Gravity Field.	87
REFERENCES	97

TABLES

Table | Page

1. Boundary value problems for complex perturbation velocity . . 99
2. Transformations 99
3. Singularities 100
4. Pressure force coefficients 101
5. Flow circulations 102
6. Summary of results for asymmetric wedge flow 103
7. Symmary of results for symmetric wedge flow 104
8. Summary of results for hydrofoil flow 105
9. Summary of results for wedge flow in transverse gravity field 106

ILLUSTRATIONS

Figure | Page

1. Flow patterns and problems 107
2. Fully cavitated flows 108
3. Mapping of z-plane onto unit circle 109
4. Symmetric shear flow past a wedge 110
5. Mapping of z-plane onto unit circle 110
6. Contour paths for complex integration 111
7. Drag coefficient vs cavitation number for flow past a unit wedge 111
8. Cavity area vs cavitation number for flow past a unit wedge . 112
9. Vorticity parameter or gravity parameter vs cavitation number for flow past a unit wedge 113
10. Cavity shapes at constant cavitation number in uniform shear flow past a unit wedge 114

Figure		Page
11.	Lift coefficient for shear flow past a wedge	115
12.	Moment coefficient for shear flow past a wedge	115
13.	$\Sigma = 0.0865$, $\ell = 30$, $\alpha = 10^{\circ}$ pressure coefficient for shear flow past a wedge	116
14.	$\Sigma = 0.0483$, $\ell = 90$, $\alpha = 10^{\circ}$ pressure coefficient for shear flow past a wedge	116
15.	Center of lift for shear flow past a wedge	117
16.	Cavitation number vs cavity length for symmetric shear flow past a wedge: $\alpha = 5^{\circ}$	117
17.	Cavitation number vs cavity length for symmetric shear flow past a wedge: $\alpha = 10^{\circ}$	118
18.	Drag coefficient vs cavitation number for symmetric shear flow past a wedge	118
19.	Cavity shapes for wedge in symmetric shear flow at constant cavitation number	119
20.	Cavity length vs cavitation number for shear flow past a hydrofoil: $\alpha = 1^{\circ}$	120
21.	Cavity length vs cavitation number for shear flow past a hydrofoil: $\alpha = 4^{\circ}$	121
22.	Effect of vorticity and cavitation number on vorticity parameter for shear flow past a hydrofoil	122
23.	Cavity shapes at constant length in uniform shear flow . .	123
24.	Normal force coefficient vs cavitation number for shear flow past a hydrofoil	124
25.	Effect of vorticity on C_N : $\alpha = 3^{\circ}$	125
26.	Moment coefficient vs cavitation number for flow past a hydrofoil at $\epsilon/U_{\infty} = 0.04$	125
27.	Effect of vorticity on C_{MO}: $\alpha = 3^{\circ}$ flow past a hydrofoil	126
28.	Effect of vorticity on $\bar{x}$ at $\alpha = 3^{\circ}$ and varying Σ for flow past a hydrofoil	126

Figure | | Page
29. Effect of vorticity on pressure coefficient for shear flow past a hydrofoil: $\alpha = 1^{\circ}$ 127

30. Effect of cavitation number on C_p for shear flow past a hydrofoil: $\alpha = 4^{\circ}$, $\epsilon/U_{\infty} = 0.06$ 127

31. Supercavitating flow past a wedge in a transverse gravity field 128

32. Effect of cavitation number on lift coefficient in gravity field 129

33. Effect of cavitation number on moment coefficient in gravity field 129

34. $\sigma = 0.0865$, $\ell = 30$, $\alpha = 10^{\circ}$ effect of Froude number on C_p for flow past a wedge 130

35. $\sigma = 0.0483$, $\ell = 90$, $\alpha = 10^{\circ}$ effect of Froude Number on C_p for flow past a wedge 130

36. Effect of Froude number on cavity shape for wedge in transverse gravity field 131

37. Effect of cavitation number on $\bar{x}$ for arbitrary Froude number for flow past a wedge 131

LIST OF SYMBOLS

a	abscissa of trailing edge of body
a_o, a_1, etc.	coefficients of real part of Laurent's series
b_o, b_1, etc.	coefficients of imaginary part of Laurent's series
b_1	residue at pole of complex function
e	contour integral path at $z = \ell$
g	acceleration due to gravity
$\bar{g}/U_\infty$	non-dimensional gravity parameter
k	defined by $k = \sqrt{\ell - 1}$
ℓ	length of cavity measured from nose of body
p_c	pressure in cavity
p_o	pressure on body
p_∞	pressure at infinity
q	magnitude of total velocity; dummy variable in Q-plane
q_c	total velocity on cavity walls
q_o	total velocity on body
r	defined by $r = \sqrt{\sqrt{\ell}+1} + \sqrt{\sqrt{\ell}-1}$; radius; variable
s	defined by $s = \sqrt{\sqrt{\ell}+1} - \sqrt{\sqrt{\ell}-1}$
u	harmonic perturbation velocity in x-direction
v	harmonic perturbation velocity in y-direction
w	complex perturbation velocity $w = u - iv$
x, y	coordinate axes
$\bar{x}$	distance to center of lift from nose of body
$y_c(x)$, $y_o(x)$	ordinates of cavity surface and body
y_∞	ordinate of cavity streamline at $x = -\infty$
z	physical flow plane
A_c	cavity area
A_o	defined as $A_o = A/U_\infty$, A is a real constant
C_c	complex integral
C_D, C_L, C_{MO}, C_N, C_p	drag, lift, moment, normal, and pressure coefficients

D_o	defined as $D_o = D/U_\infty$, D is a real constant
F	Froude number, $F^2 = U_\infty^2/g(\text{CHORD})$
Im()	imaginary part of complex number
I_c, J_T	complex integrals
Q	solution plane in mapping sequence
R	defined by $R = 2\ell-1 - 2\sqrt{\ell(\ell-1)}$; radius
Real(), Re()	real part of complex number
S	area of body-cavity combination
T	defined by $T = 2\ell-1 + 2\sqrt{\ell(\ell-1)}$; contour integral path
U	flow velocity in x-direction
U_c	velocity in x-direction on cavity walls
U_o	velocity in x-direction on body
U_∞	flow velocity in x-direction at $(-\infty, 0)$; uniform flow velocity at infinity
V	flow velocity in y-direction
α	half-angle of wedge; angle of attack of hydrofoil
ϵ	small constant vorticity
ϵ/U_∞	relative vorticity (1/Length)
$\bar{\epsilon}/U_\infty$	non-dimensional vorticity parameter
ζ	vorticity component; solution plane in mapping sequence
θ	angular polar coordinate in ζ-plane
μ	source distribution strength
ρ	fluid density
σ	cavitation number, defined as $\sigma = p_\infty - p_c/\frac{1}{2}\rho U_\infty^2$
ϕ	velocity potential
ψ	stream function
ψ_H	harmonic stream function
ψ_P	particular solution of Poisson's equation (a stream function)
ω	rotation
Γ, $\bar{\Gamma}$	circulations
Σ	rotational cavitation number, defined as $\Sigma = q_c^2/U_\infty^2 - 1$

ACKNOWLEDGMENTS

The writer would like to express his sincere appreciation to Professor Byrne Perry for his interest, help, and encouragement during the course of this research.

1. INTRODUCTION

Cavitation occurs in a fluid flow as a consequence of local pressure reduction, generally brought about by high local velocities. The development of high-speed submarines, underwater missiles, and other vehicles, together with the surface-piercing hydrofoil ship, has renewed interest in the large scale effects of cavitation. The hydrofoil and wedge (or strut) are practical parts of the total hydrodynamic system of most of these vehicles. In many cases these parts have long and slender cross sections with their greatest dimension nearly parallel to the flow direction. At sufficiently high speeds, common for present vehicles, these slender bodies produce long, trailing, steady-state cavities as the result of air ventilation or cavitation. The characteristics of these so-called supercavitating flows about bodies are of particular interest to the design engineer. If the cavity pressure does not differ greatly from the free-stream static pressure, the velocities near the body and cavity do not differ greatly from the free-stream speed. It is possible, then, to study the flow by means of a linearized theory which is based on the well-known two-dimensional theory of thin airfoils.

Tulin [1][1] appears to be the first to have used the linearized theory. The work published since the appearance of Tulin's paper has been concerned with both higher order linearized theory [2] and extensions of the first order theory to include effects found in real flows, e.g., surface tension [3] and gravity [4,5]. The linearized theory has been applied to many practical problems which were insoluble by more classical means. The progress of this work up to 1960 is summarized in three papers, two by Tulin [6,7] and one by Parkin [8].

In the linearized, two-dimensional theory the effects of viscosity are usually neglected. The flow is assumed to be irrotational and the velocity is assumed to be uniform for points far from the slender body. However, since no fluid is completely inviscid all real flows are rotational. Even when viscosity is neglected, the flow picture may sometimes be best represented by a rotational flow.

---

[1]The numbers in brackets refer to the references listed at the end of the work.

Many rotational flows have already been studied empirically and analytically. For example, the only known exact solution for the problem of finite wave motion is Gerstner's trochoidal wave which, while producing a rotational flow, also satisfies exactly the constant pressure boundary condition at the free surface. Also, two common physical flows, the eye of a typhoon (a forced vortex) and uniform viscous open channel flow, are rotational. Lamb [9] and Groen [10] have studied another rotational flow - the propagation of small surface waves on a stratified fluid. The rotational flows studied by Yih [11] are of particular interest because his results show the importance of vorticity in reproducing physical effects. He considers the steady, rotational flow of an inviscid fluid in a two-dimensional channel or a circular tube toward a sink. His solutions show the unusual (for inviscid theory) features of separating streamlines and corner eddies. Note that for a viscous fluid flowing in a channel or pipe with an abrupt contraction, eddies occur in the corners formed by that contraction, but such eddies are not predicted by an irrotational analysis. In 1943, Tsien [12] recognized that there were many applications in two-dimensional airfoil theory where irrotational flow conditions are not satisfied. He states in his paper on airfoils in shear flow that, for example, the large vertical velocity gradient near the ground can be approximated to the first order by a flow with a linear velocity distribution (a shear flow). Thus, according to Kronauer, ". . . the discussion suggests that over a limited stream length the essential character of the motion may be closely approximated by specifically neglecting the viscous forces acting in that stream length, but by including (perhaps approximately) the effects of viscous forces up-stream [13]."

The present work may be regarded as an extension of both Tulin's linearized theory for supercavitating flow and Tsien's method for rotational, non-cavitating flow. Methods are given for establishing not only qualitative but quantitative measures of the effects of rotation in linearized, supercavitating flows. The effects of gravity and surface tension are specifically neglected. In the study a uniform, parallel, irrotational flow is perturbed by a uniform shear flow - the simplest perturbation of the parallel flow and a flow with constant vorticity. The vorticity is presumed to have come from some up-stream disturbance, e.g., a boundary layer developing on the body of a vessel or test tunnel walls. Hydrofoils and struts which lie in the slipstream or wake of other components would be in such a vortex field.

The perturbed flow and the physical problems to be studied are shown in Figure 1. The perturbed flow is also a uniform shear flow and, as such, is characterized by a linear velocity distribution and a constant vorticity ϵ throughout. The irrotational and rotational perturbed flows both satisfy the equation of continuity; therefore the stream function ψ exists in both. However, the velocity potential ϕ can, of course, exist only in the irrotational flow. Physically, the flow studied is two-dimensional, and the fluid is of infinite extent. The flow is supposed to detach at the leading and trailing edges of the hydrofoil and at both edges of the blunt base of the symmetric wedge. Finally, it is assumed that the cavity length, when measured from the leading edge of the body, is greater than that of the solid body, i.e., full cavitation occurs.

The main paper considers rotational, supercavitating flow past wedges and hydrofoils. The bodies chosen have been restricted to the slender wedge and the flat-plate hydrofoil. The Appendixes include a discussion of supercavitating flow past wedges in a transverse gravity field. The solution to this problem complements the gravity flow solutions already given by Parking [4] and Acosta [5] and arises directly from the solution of the rotational flow past a wedge.

2. THE LINEARIZED THEORY

In this section, a linearized theory is developed for two-dimensional, supercavitating flows under the assumption that the flow has a constant vorticity throughout. The effects of gravity and surface tension are neglected. The flows considered are those past slender wedges and flat-plate hydrofoils as shown in Figure 1. It is further assumed that the flow is steady and that the fluid is both incompressible and inviscid. Because of its simplicity and convenience, Tulin's original closed-cavity model is employed in this work. It should be noted that other linearized models are available [14,15].

2.1 Notation and Boundary Conditions

Figure 2 shows two typical fully cavitated flows; the notation used is introduced in the following discussion. The incompressible fluid has a constant density ρ. The base flow which is a parallel, uniform shear flow has been disturbed by the introduction of the slender body of unit length. The unit length body is used without loss of generality, since it is equivalent to normalizing the problem on the actual body length. Although it is certainly disturbed in the neighborhood of the slender body, the base flow is assumed to be undisturbed at infinity and is characterized there by a constant vorticity ϵ. The wedges are aligned symmetrically with their longitudinal center-lines parallel to the x-axis, and hydrofoils are placed at an angle of attack α with respect to the x-axis.

The origin of the rectangular coordinates is at the leading edge of the solid body. In terms of these coordinates, the velocity profile at $x = -\infty$ is $U_\infty - \epsilon y$, with U_∞ representing the velocity at $(-\infty, 0)$. The pressure at infinity is taken to be the undisturbed static pressure p_∞. The flow velocities U and V are in the x- and y-directions respectively. The total velocity at any point in the fluid is q, while the velocity on the cavity surfaces is q_c. The closed, trailing cavity which springs from the solid body is characterized by a length ℓ - greater than one, an ordinate $y_c(x)$, and a uniform, constant pressure p_c. It is presumed that the cavity is filled with air or water vapor. The pressure p_c is always less than or equal to p_∞.

In general, the only restriction imposed on the shape $y_o(x)$ of the slender bodies is that the flow over the body must satisfy a Brillouin-Villat separation condition [16]. Under this condition the maximum velocity on the surface of the body must occur at the separation point; this corresponds to requiring a fixed and known point of separation. In the flows considered, this condition is satisfied.

In a two-dimensional flow, the vorticity component is

$$\zeta = \frac{\partial V}{\partial x} - \frac{\partial U}{\partial y}$$

and the rotation $\omega = \zeta/2$. It is known that the flow has a constant vorticity $\zeta = \epsilon$ at $(-\infty, y)$. From the Helmholtz theorem on the permanence of rotation, it follows that the vorticity ϵ persists throughout the fluid; thus,

$$\frac{\partial V}{\partial x} - \frac{\partial U}{\partial y} = \epsilon \, . \tag{2.1}$$

Since the fluid is incompressible and the flow is steady, the continuity equation

$$\frac{\partial U}{\partial x} + \frac{\partial V}{\partial y} = 0 \tag{2.2}$$

must be satisfied throughout the fluid. In a rotational flow the stream function $\psi = \psi(x,y)$ exists and may be defined so that

$$U = -\frac{\partial \psi}{\partial y} \, , \; V = \frac{\partial \psi}{\partial x} \, . \tag{2.3}$$

The function ψ satisfies equation (2.2) identically, and Poisson's equation

$$\frac{\partial^2 \psi}{\partial x^2} + \frac{\partial^2 \psi}{\partial y^2} = \nabla^2 \psi(x,y) = \epsilon \tag{2.4}$$

is produced when ψ is introduced into equation (2.1).

The Bernoulli equation for rotational flow is found by integration of the Euler equations. They are, in this case,

$$U \frac{\partial U}{\partial x} + V \frac{\partial U}{\partial y} = - \frac{1}{\rho} \frac{\partial p}{\partial x}$$

$$U \frac{\partial V}{\partial x} + V \frac{\partial V}{\partial y} = - \frac{1}{\rho} \frac{\partial p}{\partial y} .$$

Following rearrangement, these equations become

$$V\left(\frac{\partial U}{\partial y} - \frac{\partial V}{\partial x}\right) = - \epsilon \frac{\partial \psi}{\partial x} = - \frac{\partial}{\partial x} \left(\frac{p}{\rho} + \frac{q^2}{2}\right)$$
$$U\left(\frac{\partial V}{\partial x} - \frac{\partial U}{\partial y}\right) = - \epsilon \frac{\partial \psi}{\partial y} = - \frac{\partial}{\partial y} \left(\frac{p}{\rho} + \frac{q^2}{2}\right).$$

Integration gives the Bernoulli equation for steady two-dimensional flow with constant vorticity (or rotation),

$$p + \tfrac{1}{2}\rho q^2 - \rho\epsilon\psi = \text{constant}. \tag{2.5}$$

Poisson's equation (2.4) is a linear, inhomogeneous, partial differential equation. Therefore, by the use of superposition, its solution can be written as $\psi = \psi_H + \psi_P$, with $\nabla^2\psi_H = 0$ and $\nabla^2\psi_P = \epsilon$. The stream function ψ_H represents a new harmonic flow; ψ_P is a particular solution of equation (2.4). From equation (2.3), then,

$$\left.\begin{aligned} U(x,y) &= U_H(x,y) + U_P(x,y) \\ V(x,y) &= V_H(x,y) + V_P(x,y) \end{aligned}\right\} . \tag{2.6}$$

If one lets $\psi_P = \frac{\epsilon y^2}{2}$, $\nabla^2\psi_P = \epsilon$ as desired, and

$$U_P = - \epsilon y,$$

$$V_P = 0.$$

Thus,

$$U = U_H - \epsilon y$$

$$V = V_H.$$

It is evident that any problem which requires a solution for U and V can be reduced to an equivalent problem for the harmonic velocity components U_H and V_H.

With the flow conditions at infinity known, it remains to establish the boundary conditions on the solid body and cavity walls. These conditions and a compatible boundary value problem are established in terms of a linearized theory. The basic assumption of such a theory is that a slender body-cavity system causes only small perturbations in the velocity components of the basic shear flow. This assumption does break down in the neighborhood of singular points. But, as Tulin [6] notes, the effect of this breakdown is usually restricted to the area of the singular points, and the overall characteristics of the flow are often well reproduced by linearized solutions. The flow pattern is a combination of parallel, uniform shear flow and, superposed on this, small velocity perturbations. Since it is desired to formulate eventually an harmonic boundary value problem, the flow velocities are written in terms of the harmonic perturbation velocities (u,v) in the x- and y- directions respectively. From equation (2.6)

$$\left.\begin{array}{l} U = U_\infty + u - \epsilon y \\ V = v \end{array}\right\} \qquad (2.6a)$$

in the linearized flow.

In a linearized theory for irrotational supercavitating flow, it is assumed that the perturbation velocities (u, v), the attack (or wedge semi-) angle α, the body shape (or camber) $y_o(x)$, and the cavity ordinate $y_c(x)$ are small. First order terms in these quantities are retained, but second and high order terms are neglected. The force coefficients obtained by such a linearized theory are generally correct only to the first order. In the present rotational development, terms of the form ϵy_c arise in the boundary conditions for the perturbation velocities; in order to preserve the first order smallness of these velocities, it is necessary to restrict the relative vorticity ϵ/U_∞ to a size of the order of one. In this case, then, the flow reversal, which occurs in a uniform shear flow at $y \approx U_\infty/\epsilon$, does not occur near the body-cavity combination, whose ordinates are usually very small compared to one. Finally, from the Cauchy-Riemann equations as applied to the harmonic perturbation velocities,[2] it is seen that these velocities change very slowly in space when the streamline slopes and curvatures are small [1]. For this reason, the linearized boundary conditions may be applied on the x-axis instead of the body-cavity surfaces. These boundary conditions for the harmonic perturbation velocities are established from facts known about the body-cavity system in the shear flow.

In order to formulate the boundary conditions on the cavity, it is first necessary to define a cavitation number. The cavitation number is the parameter which relates the pressure conditions in the fluid stream to those in the cavity. It indicates the degree of cavitation; as the cavitation number decreases, the cavity size increases. Recalling that $\psi = \psi_H + \epsilon y^2/2$, one has from equation (2.5), to the first order in ϵ,

$$\frac{p_\infty - p_c}{\frac{1}{2}\rho U_\infty^2} + \frac{2\epsilon\psi_H}{U_\infty^2} + \frac{\epsilon^2 y_\infty^2}{U_\infty^2} = \frac{q_c^2}{U_\infty^2} - 1 = \text{constant.}$$

The velocity U_∞ and pressure p_∞ are taken at $(-\infty, 0)$, while p_c and q_c are taken on the cavity streamline. In general, the extension of the cavity streamline does not coincide with the x-axis except at the leading edge of the slender body. The stream function ψ_H represents the difference between the harmonic stream function value on the x-axis and its value on the up-stream extension of the cavity streamline.

[2] See equations (2.13).

Thus, $\psi_H = -U_\infty y_\infty$ where y_∞ is the ordinate of the cavity streamline at $x = -\infty$. In the case of a uniform flow about a cylinder with circulation [17], $-y_\infty$ is infinite. However, in the present cases of a linearized uniform shear flow past slender wedges and hydrofoils, the value of y_∞ is not known a priori. It follows that in these rotational flows the cavitation number σ, defined in the usual sense as

$$\sigma = \frac{p_\infty - p_c}{\frac{1}{2}\rho U_\infty^2}, \tag{2.7}$$

cannot be used directly since

$$\sigma = \frac{q_c^2}{U_\infty^2} - 1 + \frac{2\epsilon y_\infty}{U_\infty} - \frac{\epsilon^2 y_\infty^2}{U_\infty^2}$$

and y_∞ is unknown. Therefore, it is convenient to define a rotational cavitation number Σ. Let Σ be defined so that

$$\Sigma = \frac{q_c^2}{U_\infty^2} - 1; \tag{2.7a}$$

then, in the following treatment most terms will retain the same form as their irrotational counterparts. When either $\epsilon \to 0$ or the flow is symmetric $\Sigma = \sigma$;[3] otherwise,

$$\sigma = \Sigma + \frac{2\epsilon y_\infty}{U_\infty}\left(1 - \frac{\epsilon y_\infty}{2U_\infty}\right).$$

This relationship provides a means for relating the pressure difference and flow velocities in experimental programs. The rotational cavitation number may be determined either by measuring the up-stream and cavity velocities directly or by first measuring the pressure difference, up-stream velocity, and vorticity and then measuring y_∞, the ordinate

[3] For a symmetric shear flow about a symmetric slender body, the x-axis and the bifurcated cavity streamline do coincide for $x \leq 0$ and equation (2.7) holds. In this case, $\sigma = \Sigma$. See Section 3.2 for discussion of such symmetric flow.

of the stagnation streamline.

On the cavity walls, from equation (2.5), the velocity q_c is constant because p_c is constant for a given vorticity ϵ. Writing q_c in terms of the perturbation velocities and introducing the result into equation (2.7a) yields

$$\Sigma = \frac{2u}{U_\infty} - \frac{2\epsilon y_c}{U_\infty} + \frac{1}{U_\infty^2} \{u^2 + v^2 + \epsilon^2 y_c^2 - 2u\epsilon y_c\}. \qquad (2.7b)$$

The cavity boundary condition is obtained by neglecting terms of order greater than one in equation (2.7b), thus producing

$$\frac{U_\infty \Sigma}{2} = u(x,0) - \epsilon y_c(x), \; a \leq x \leq \ell, \qquad (2.8)$$

which is applied on the x-axis. When equation (2.8) is applied to the upper cavity surface in the flow past a hydrofoil, the quantity a equals zero; otherwise, a is equal to one for flows past both wedges and hydrofoils. If one lets

$$U_c = U_\infty + u - \epsilon y_c$$

on the cavity, then $q_c^2 = U_c^2 + v^2$. Thus, from equation (2.7b), to the first order,

$$U_c = U_\infty (1 + \Sigma/2). \qquad (2.9)$$

From equation (2.7a) one obtains

$$U_c \approx q_c = U_\infty \sqrt{1 + \Sigma}\,.$$

In the present work equation (2.9), which is consistent with the linearization, is used; however, it should be noted that

$$1 + \Sigma/2 \approx \sqrt{1 + \Sigma}\,.$$

It was noted previously that the harmonic perturbation velocities change very slowly when the streamlines have small slope and curvature. For this reason, since the cavity is assumed to be long and slender, the variations in the quantity ϵy_c in equation (2.8) are certainly small over most of the cavity. It is reasonable, then, to replace ϵy_c with an average value $\pm \bar{\epsilon}$ on the upper and lower cavity surfaces respectively. This averaging technique was introduced by Parkin [4] in dealing with a linearized theory for flow past a hydrofoil in a transverse gravity field. The averaged quantity $\bar{\epsilon}/U_\infty$ is non-dimensional. It must be treated as part of the problem's solution and is used as a basic parameter when the results cannot be determined directly as a function of ϵ/U_∞. Note that the relative vorticity ϵ/U_∞, which has the dimensions (1/LENGTH), is independent of the length of the solid body and truly measures the relative size of the small constant vorticity and the up-stream velocity, i.e., the rate of change of velocity with y at infinity. Equation (2.8) now becomes

$$\left.\begin{aligned} u(x,0) &= U_\infty \Sigma/2 + \bar{\epsilon}, \quad a \le x \le \ell, \quad y \ge 0 \\ \text{and} \qquad u(x,0) &= U_\infty \Sigma/2 - \bar{\epsilon}, \quad 1 \le x \le \ell, \quad y \le 0. \end{aligned}\right\} \tag{2.8a}$$

These equations are applied on the upper and lower cavity surfaces respectively.

The total velocity on the solid body must be tangent to the surface of the body; hence, in terms of the perturbation velocities,

$$\frac{dy_o(x)}{dx} = \frac{v(x,y_o)}{U_\infty - \epsilon y_o + u(x,y_o)} .$$

The denominator may be written as

$$U_\infty - \epsilon y_o + u(x,y_o) = U_c + \eta,$$

with $\eta = (u(x,y_o) - u(x,y_c) - \epsilon y_o(x) + \epsilon y_c(x))$. From the basic assumptions of the theory, $\eta << U_c$. Since

$$\frac{dy_o(x)}{dx} = \frac{v}{U_c\left(1 + \frac{\eta}{U_c}\right)} ,$$

the denominator may be expanded in a binomial series. The result is

$$\frac{dy_o(x)}{dx} = \frac{v}{U_c}\left\{1 - \frac{\eta}{U_c} + 0\left[\left(\frac{\eta}{U_c}\right)^2\right]\right\} .$$

After linearization, the boundary condition is

$$\frac{dy_o(x)}{dx} = \frac{v(x,0)}{U_c} , \quad 0 \leq x \leq 1 , \tag{2.10}$$

and it is applied on the x-axis. Furthermore, this equation is also valid on the cavity surfaces and gives the surface slope at any point along the x-axis. In the cases of slender wedges or hydrofoils,

$$\frac{dy_o(x)}{dx} = \tan \alpha \approx \alpha .$$

Equation (2.10) becomes

$$v(x,0) = \pm \alpha U_c , \quad 0 \leq x \leq 1 , \tag{2.10a}$$

on the upper and lower wedge surfaces respectively, and

$$v(x,0) = - \alpha U_c , \quad 0 \leq x \leq 1 , \tag{2.10a}$$

on the solid surface of the hydrofoil.

Examination of equations (2.8a) and (2.10) shows that the result acquired in equation (2.10) provides automatically for smooth separation. This condition may be thought of as equivalent to the Kutta condition in airfoil theory in that both conditions serve to single out a unique solution to the flow boundary value problem.

The condition of cavity closure is characteristic of Tulin's model of the finite cavity. If the rotational and new irrotational flows are studied, it is seen that the subtracted portion ψ_P of the rotational flow makes no net contribution to the flow within the cavity-body shape. Hence, the cavity closure condition must hold in either flow, i.e., the net strength of sources within the body-cavity system must be zero.

Finally, since the base flow is undisturbed at infinity, the perturbation velocities (u,v) approach zero at great distances from the body-cavity system. In summary, the conditions to be imposed are:

$u = \frac{U_\infty \Sigma}{2} \pm \bar{\epsilon}$ on the cavity

$v = \pm \alpha U_c$ on the body

$(u,v) \rightarrow 0$ at infinity

The cavity is closed.

The flow must separate smoothly from the solid body.

These conditions are sufficient to determine the harmonic perturbation velocities (u,v).

2.2. Methods of Solution

Two methods of solution and their corresponding boundary value problems are given. The first is that method used originally by Tulin [1]. This method makes use of the velocity potential of a source distribution and singular integral equation theory. The second method is based on conformal mapping of the physical plane onto the exterior of the unit circle. This latter method, which has been used by others [4, 5, 8, 18], has proven most convenient for the present work; however, the former method is outlined here for completeness and comparison.

The first method is given here for a symmetric flow such as that found in Section 3.2 and Figure 4. The solution for the mathematical problem arising from the given conditions on (u,v) is found in terms of the velocity potential which exists for the harmonic flow represented by (u,v) and ψ_H. The potential of a distribution of sources along the x-axis between the leading edge of the body and the close of the cavity is

$$\phi(x,y) = -\frac{1}{2\pi}\int_0^{\ell} \mu(\xi)\,\ln r\,d\xi \ . \tag{2.11}$$

The distribution function $\mu(\xi)$ represents the source strength and

$$r^2 = (x - \xi)^2 + y^2.$$

This distribution produces a function with the required symmetry. The velocities are designated by

$$\begin{aligned} u(x,y) &= -\frac{\partial\phi}{\partial x} = \frac{1}{2\pi}\int_0^{\ell} \mu(\xi)\,\frac{(x-\xi)}{r^2}\,d\xi \\ v(x,y) &= -\frac{\partial\phi}{\partial y} = \frac{1}{2\pi}\int_0^{\ell} \mu(\xi)\,\frac{y}{r^2}\,d\xi \ . \end{aligned} \tag{2.12}$$

The given boundary conditions on (u,v) are applied on the x-axis, and one must pass to the limit $y \to 0$ in these equations. Taking the Cauchy principal value of the integrals when required and using the substitution $\tan\ t = (x - \xi)/y$, one obtains

$$\left.\begin{aligned} u(x,0) &= \frac{1}{2\pi}\int_0^{\ell}\frac{\mu(\xi)d\xi}{(x-\xi)} \\ v(x,0) &= \mu\ (x)\ /\ 2 \end{aligned}\right\} . \tag{2.12a}$$

Incorporating equations (2.12a) into the conditions given at the end of Section 2.1 produces the following complete boundary value problem:

To find $\mu(x)$ such that

a. $$\int_1^{\ell} \frac{\mu(\xi)d\xi}{x - \xi} = \Pi U_\infty \Sigma + 2\Pi\bar{\epsilon} - \int_0^1 \frac{2U_c \frac{dy_o(t)}{dt}}{x - t} dt = f(x),\ 1 < x < \ell.$$

b. $$\mu(x) = 2U_c \frac{dy_o(x)}{dx},\ 0 < x < 1.$$

c. The cavity is closed; hence
$$\int_1^{\ell} \mu(x)dx = - \int_0^1 2U_c \frac{dy_o(x)}{dx} dx = - 2U_c y_o(0).$$

d. The separation is smooth; hence $\mu(x)$ finite as $x \to 1^+$.

Since the flow is symmetric, it is sufficient to consider only $y \geq 0$. From equation (A-5) of Appendix A, one has

$$\mu(x) = - \frac{x}{\Pi^2 \sqrt{(\ell - x)\ (x - 1)}} \int_1^{\ell} \frac{\sqrt{(\ell - \xi)\ (\xi - 1)}}{\xi(x - \xi)} f(\xi)d\xi.$$

Once $\mu(x)$ is known, the cavity shape and pressure force coefficients can be calculated by using equations (2.12a) and the definitions given in Section 2.3.

The second method of solution also makes use of the new harmonic flow. In this case, it is convenient to work with complex variables. Following substitution of (u,v) and ψ_p into the vorticity equation (2.1) and continuity equation (2.2) they reduce to

$$\left.\begin{aligned} \frac{\partial v}{\partial x} &= \frac{\partial u}{\partial y} \\ \frac{\partial u}{\partial x} &= \frac{-\partial v}{\partial y} \end{aligned}\right\} \tag{2.13}$$

and

respectively. In terms of the complex variable $z = x + iy$, the total complex velocity may be defined as

$$W(z) = U_\infty + \tfrac{1}{2}\epsilon(z - \bar{z}) + w(z),$$

with $w(z)$, the complex perturbation velocity, given by $w(z) = u - iv$. Equations (2.13) are seen to be the Cauchy-Riemann equations for $w(z)$; from these equations and the continuity of the flow, it follows that $w(z)$ is analytic outside the cavity-body system. Also, since $(u,v) \rightarrow 0$ at infinity, $w(z)$ must vanish at infinity.

The boundary conditions are applied along a slit in the z-plane corresponding to the x-axis where $0 \leq z \leq 1$ and z is real. The complex velocity $w(z)$ is analytic in the region exterior to the slit in the z-plane. The complex z-plane and typical boundary conditions are shown in Figure 3. The mathematical problem is to ascertain an analytic function $w(z)$ subject to boundary conditions on both its real and imaginary parts, as given at the end of Section 2.1.

The specific problems for the wedge and hydrofoil are tabulated in Table 1. Note that in this table, conditions e. and f. are equivalent to requiring that

$$\mathrm{Im}(w) = O\left(\frac{1}{z}\right), \quad z \rightarrow \infty$$
$$\mathrm{Real}\,(w) = O\left(\frac{1}{z^2}\right), \quad z \rightarrow \infty.$$

The conditions listed in Table 1 are sufficient to determine $w(z)$. It is expected that the complex perturbation velocity $w(z)$ will exhibit singular behavior at those points on the slit where large changes occur in the magnitude and direction of the velocity. These large changes occur at the leading edge of the solid body and at the closure of the cavity. Condition g. in Table 1 is imposed to restrict the magnitude of the singular behavior so that the pressure distribution, which is proportional to $\mathrm{Re}(w)$, remains integrable.

The determination of $w(z)$ is accomplished by a method of conformal mapping which permits the use of results already known in airfoil theory. In accordance with Wu [18] and Parkin [4], the z-plane is mapped conformally by a succession of transformations onto the ζ-plane. The complex velocity w is held invariant at corresponding points of the mappings. The transformations are listed in Table 2, and the various mapped planes are shown in Figures 3 and 5, in which corresponding regions and boundary values are shown.

It is seen that the boundary value problem for w may be solved in any of the transformed planes. The ζ-plane is used directly for wedges, while the problem is solved in the Q-plane for hydrofoils. In either case, however, the singular functions which are the basis of the problem's solution are established in the ζ-plane. From Figures 3 and 5, it is clear that the real parts of the singular functions must satisfy particular conditions on the real axis, while the imaginary parts must satisfy other conditions on the unit circle. In addition, the limiting conditions on w as $z \to -\infty$ must be met at the corresponding points in the ζ-plane or Q-plane. A complete solution $w(\zeta)$ is formed from a series of singular complex functions. These functions, familiar in airfoil theory, and their properties are listed in Table 3. The strength of the singularities is limited by the pressure integrability condition previously noted. The singularities are not of higher order than simple poles at points on the slit. Figure 3 shows that the leading edge of the hydrofoil maps onto $\zeta = 1$, the leading edge of the wedge onto $\zeta = i$, and the cavity closure onto $\zeta = \infty$. These are the centers of the singular behavior in the linearized theory; hence, most of the $w_i(\zeta)$ in Table 3 are singular at these points. These functions in Table 3 have already been extensively used in linearized cavity theory and are discussed in some detail by Parkin [4, 8] and Wu [18, 19].

The solution $w(\zeta)$ to a particular problem is given in terms of the singular functions $w_i(\zeta)$ by

$$w(\zeta) = \sum_i K_i w_i + M + iN,$$

where the constants K_i, M, and N are assumed to be real. These constants are then determined by the conditions given in Table 1, since the $w(\zeta)$ formed is already analytic off the slit. In addition to establishing the constants, the given conditions also produce a relationship between the cavitation number Σ and the cavity length ℓ, with $\bar{\epsilon}$ and α as parameters. Following determination of w, the cavity shape and pressure force coefficients can be found by using equation (2.10) and the definitions given in the following part of this section.

2.3. Calculation of Results

The results of the linearized theory include the length-cavitation number ratio (already found in Section 2.2), the cavity shape, and the pressure force coefficients for lift (C_L), drag (C_D), and moment (C_{MO}). From equation (2.10), the cavity shape is given by

$$y_c(x) = \frac{1}{U_c}\int_a^x v\,dx + y_o(a),\quad a \leq x \leq \ell, \qquad (2.14)$$

For wedges, $a = 1$ on both surfaces, while $y_o(1) = \pm\alpha$ on the upper and lower surfaces respectively. For hydrofoils, $a = 0$ and $y_o(0) = 0$ on the upper cavity surface; $a = 1$ with $y_o(1) = -\alpha$ on the lower surface. Also, using equation (2.10), one may calculate the body-cavity area S, which is

$$S = \int_0^\ell (y_+ - y_-)dx.$$

This equation may be integrated by parts and, since the cavity must close, i.e., $\oint_{B+C} dy = 0$, one has

$$S = \oint_{B+C} \frac{dy}{dx}\,x\,dx = \frac{1}{U_c}\oint_{B+C} vx\,dx. \qquad (2.15)$$

The contour integral $B+C$ follows a closed, counter-clockwise path over the surfaces of the body-cavity combination. Recalling that $v = -\mathrm{Im}\,w(z)$, one may write the previous equations so that

$$y_c(x) = -\frac{1}{U_c}\,\mathrm{Im}\int_a^z w\,dz + y_o(a) \qquad (2.14a)$$

and

$$S = -\frac{1}{U_c}\,\mathrm{Im}\oint_{B+C} wz\,dz, \qquad (2.15a)$$

where $x = z$ on the slit in the complex z-plane. The latter result was first given by Geurst and Timman [20].

Calculation of the pressure force coefficients is based on the pressure coefficient C_p, which is given by

$$C_p = \frac{p - p_c}{\frac{1}{2}\rho U_\infty^2}. \qquad (2.16)$$

In each flow the solid body and cavity surfaces lie on the same streamline. Thus, the Bernoulli equation (2.5) yields

$$p - p_c = \tfrac{1}{2}\rho q_c^2 \,(1 - q_o^2/q_c^2).$$

The term on the right in this equation may be simplified by linearization. Writing $q_c^2 = U_c^2 + v^2$ and $q_o^2 = U_o^2 + v^2$, one has $q_c^2 = U_c^2$ to the first order and

$$\begin{aligned} 1 - q_o^2/q_c^2 &= -2(q_o - q_c)/q_c - (q_o - q_c)^2/q_c^2 \\ &= -2(U_o - U_c)/U_c - (U_o - U_c)^2/U_c^2 \\ &= -2(U_o - U_c)/U_c \end{aligned}$$

after linearization. The pressure coefficient may now be written as

$$C_p = -2U_c(U_o - U_c)/U_\infty^2,$$

with U_o and U_c being the x-components of velocity on the solid body and cavity surfaces respectively. From equation (2.6a), $U_o = u(x,y_o) - \epsilon y_o + U_\infty$, and from equation (2.9) $U_c = U_\infty + U_\infty\Sigma/2$. Thus,

$$C_p = - 2(1 + \tfrac{\Sigma}{2})\;(u(x,y_o) - \epsilon y_o - U_\infty\tfrac{\Sigma}{2})/U_\infty. \qquad (2.16a)$$

There has been considerable discussion [4, 8, 19] regarding the appropriate method of defining and linearizing the pressure coefficient so as not to lose any first order terms. The above result is consistent with that given by Wu [19], in that the flow is continuous and $C_p = 0$ at the trailing edges of the solid body for $\epsilon = 0$. As Parkin has pointed out [4], however, in order to be consistent with the averaging approximation when $\epsilon \neq 0$ and to have a continuous velocity at the trailing edge, one must take $|\epsilon y| = |\bar{\epsilon}|$ on the solid body for $x = 1$. On a wedge, $y = \pm \alpha x$; so, to the order of the approximation,

$$\epsilon y = \pm \bar{\epsilon} x$$

on the upper and lower wedge surfaces respectively. On a hydrofoil, $y = -\alpha x$, so

$$\epsilon y = -\bar{\epsilon} x$$

on the foil to the order of the averaging approximation. The final result for the pressure coefficient is given in Table 4. In addition, this table gives the remaining coefficients in terms of C_p. Note that the drag coefficient in the wedge flows is based on the base area of the wedge; the remaining coefficients use the unit chord of the body as a characteristic length. The method used to calculate these force coefficients follows that used by Wu [18] on wedges and Parkin [4] on the hydrofoil.

Finally, a rational means for evaluating the average parameter $\bar{\epsilon}/U_\infty$ must be determined. From the manner in which $\bar{\epsilon}/U_\infty$ arises, it is mathematically reasonable to let

$$\frac{\bar{\epsilon}}{U_\infty} = \left(\frac{\epsilon}{U_\infty}\right) \text{(cavity area)}/2(\ell - 1),$$

i.e., $\bar{\epsilon}/U_\infty$ equals the average value of $\epsilon|y_c|$ over the cavity. On the other hand, the vorticity ϵ creates an additional circulation in the flow, and it is this important flow property which characterizes the influence of the vorticity. (This result holds also in the case of a supercavitating flow past a hydrofoil in a transverse gravity field [4]). Thus, $\bar{\epsilon}/U_\infty$ is chosen so that the actual circulation Γ is equal to the circulation $\bar{\Gamma}$ based on the constant perturbation velocities associated with $\bar{\epsilon}/U_\infty$.

The circulation Γ is defined as

$$\Gamma = \oint \vec{q} \cdot \vec{ds}$$

where $\vec{q}$ is the total vector velocity and $\vec{ds}$ is the elemental vector path length on the closed contour where Γ is measured. Since the perturbation velocities are defined in the harmonic rather than the physical z-plane, it is convenient to balance Γ and $\bar{\Gamma}$ in the harmonic plane. From equations (2.6) and (2.6a), one finds that $U = U_\infty + u - \epsilon y$ implies that $U_H = U_\infty + u$ and $V = v$ implies that $V_H = v$. Therefore, on the cavity where $U \approx U_c$,

$$U_H = U_c + \epsilon y$$

and on the solid bodies,

$$U_H = U_\infty + u$$

$$V_H = v \ .$$

The actual circulation Γ and $\bar{\Gamma}$ are given to the first order in Table 5. Note that, to the first order on the solid bodies, the circulation integral

$$\int_{\text{body}} [(U_\infty + u)\ dx + v dy] = \int_{\text{body}} (U_\infty + u) dx.$$

Observe also that in the expression for $\bar{\epsilon}/U_\infty$ in Table 5, the terms in the large parenthesis are precisely equal to the cavity area for the wedge flow and equal to the cavity area less the triangular area between the hydrofoil and the x-axis for the hydrofoil flow. Thus, the matching of circulations at once provides a rigorous and intuitively satisfying result.

3. APPLICATIONS OF THE LINEARIZED THEORY

In this section the linearized theory developed in Section 2 is applied to three problems: the first two are the supercavitating, asymmetric and symmetric shear flows past slender wedges; the third concerns a supercavitating, uniform shear flow past a flat-plate hydrofoil. The solutions to all three problems are found by means of conformal mapping, using the singularities shown in Table 3.

3.1. Asymmetric Flow Past a Wedge

This first flow is a supercavitating, uniform shear flow past a wedge of unit length. The asymmetric, undisturbed velocity profile of the flow is shown in Figure 1 (solid line profile). The notation used is that given in Section 2 and Figure 2a.

3.1.1. Solution of the boundary value problem

The mapping of the physical z-plane and the appropriate boundary conditions are indicated in Figure 3a. From the conformal transformations in Table 2, it is easily shown [5] that

$$z = \ell \left[1 - \frac{4(\ell - 1)\,\zeta^2}{(\zeta^2 - \zeta_1^2)\,(\zeta^2 - \zeta_2^2)} \right] \tag{3.1}$$

where ζ_1 and ζ_2 are the roots of

$$\zeta^4 + 2\zeta^2(2\ell - 1) + 1 = (\zeta^2 - \zeta_1^2)\,(\zeta^2 - \zeta_2^2) = 0.$$

These roots are

$$\left.\begin{aligned} \zeta_1 &= i\,(\sqrt{\ell} + \sqrt{\ell - 1}) \\ \zeta_2 &= i\,(\sqrt{\ell} - \sqrt{\ell - 1}). \end{aligned}\right\} \tag{3.2}$$

It is seen from Figure 3a that ζ_1 is outside the unit circle and represents the point $z = \infty$, while ζ_2 is inside the unit circle and, hence, does not represent a point of the physical plane.

The complete boundary value problem for this wedge flow is given in Table 1, which was developed in Section 2. By using the singular functions listed in Table 3, it is possible to construct a solution function $w(\zeta)$. A comparison of the boundary conditions and available singularities shows that $w(\zeta)$ should have the form

$$w(\zeta) = -\frac{2\alpha U_c}{\Pi} \ln \frac{\zeta + i}{\zeta - i} + iA\left(\zeta - \frac{1}{\zeta}\right) + B$$
$$+ iC \ln\zeta + iD \frac{\zeta^2 - 1}{\zeta^2 + 1} . \tag{3.3}$$

The function $i(\zeta - 1/\zeta)$ is selected to provide the proper closure singularity, and the term $i(\zeta^2 - 1)/(\zeta^2 + 1)$ is used to satisfy the condition that $w(z) \rightarrow 0$ as $z \rightarrow \infty$. The remaining functions are needed to fulfill the boundary conditions (a) through (d) in Table 1. The real constants B and C are determined by considering $w(\zeta)$ on the real axis of the ζ-plane. Equating the values of $w(\zeta)$ and the boundary conditions there, one has

$$w(\zeta) = B = \frac{U_\infty \Sigma}{2} + \bar{\epsilon}, \ \zeta > 0$$

$$w(\zeta) = B - C\Pi = \frac{U_\infty \Sigma}{2} - \bar{\epsilon}, \ \zeta < 0.$$

Therefore, $B = U_\infty \Sigma/2 + \bar{\epsilon}$ and $C = 2\bar{\epsilon}/\Pi$. Equation (3.3) can now be rewritten as

$$w(\zeta) = \frac{U_\infty \Sigma}{2} + \bar{\epsilon} - \frac{2\alpha U_c}{\Pi} \ln \frac{\zeta + i}{\zeta - i} + i \frac{2}{\Pi} \bar{\epsilon} \ln\zeta$$
$$+ iA\left(\zeta - \frac{1}{\zeta}\right) + iD \frac{\zeta^2 - 1}{\zeta^2 + 1} . \tag{3.3a}$$

In this form $w(\zeta)$ satisfies the differential equation and conditions (a), (b), (c), (d), (g), and (h) of the boundary value problem. The remaining conditions will serve to establish A and D and to determine a unique relation between ℓ and Σ for given values of $\bar{\epsilon}$ and α.

3.1.2. Results

As Wu has pointed out [18], much can be learned by expanding $w(z)$ in negative powers of z as $z \to \infty$. The result is an infinite series of the form

$$w(z) = a_o + ib_o + \frac{a_1 + ib_1}{z} + \frac{a_2 + ib_2}{z^2} + O\left(\frac{1}{z^3}\right). \qquad (3.4)$$

From boundary conditions (e) and (f), one has

$$a_o = b_o = a_1 = 0.$$

As $z \to \infty$, $\zeta \to \zeta_1$; hence, using equations (3.1) and (3.2), ζ can be expanded in descending powers of z. Acosta [5] has shown that one obtains

$$\zeta = \zeta_1 \left\{1 + \frac{\sqrt{\ell(\ell - 1)}}{2z} + \frac{\sqrt{\ell(\ell - 1)}\,[2\ell + 1 + \sqrt{\ell(\ell - 1)}]}{8z^2} + O\left(\frac{1}{z^3}\right)\right\}. \qquad (3.5)$$

This result is now introduced into equation (3.3a) and the combination is simplified. This process is accomplished in several steps. First, from Acosta's work:

$$\frac{U_\infty \Sigma}{2} + \bar{\epsilon} - \frac{2\alpha U_c}{\Pi} \ln \frac{\zeta + 1}{\zeta - 1} + iA\left(\zeta - \frac{1}{\zeta}\right) = \left(\frac{U_\infty \Sigma}{2} + \bar{\epsilon} - \frac{\alpha U_c}{\Pi} \ln \frac{\sqrt{\ell} + 1}{\sqrt{\ell} - 1} - 2A\sqrt{\ell}\right) + \frac{1}{z}\left[\frac{\alpha U_c}{\Pi}\sqrt{\ell} - A(\ell - 1)\sqrt{\ell}\right] + \frac{1}{z^2}\left[\frac{\alpha U_c}{4\Pi}(\ell + 1)\sqrt{\ell} - \frac{A}{4}(\ell - 1)(3\ell + 1)\sqrt{\ell}\right] + O\left(\frac{1}{z^3}\right).$$

Second,

$$i\frac{2}{\Pi}\bar{\epsilon} \ln \zeta = i\frac{2}{\Pi}\bar{\epsilon}\,[\ln\zeta_1 + \ln(1 + Q)],$$

with $Q = M/z + N/z^2 + O(1/z^3)$, $M = \sqrt{\ell(\ell - 1)}/2$, and $N = \sqrt{\ell(\ell - 1)}$ $(2l + 1 + \sqrt{\ell(\ell - 1)})/8$. Following a series expansion on the small parameter Q, one has

$$i\frac{2\bar{\epsilon}}{\pi}\,\ell n\zeta = -\bar{\epsilon} + i\frac{2\bar{\epsilon}}{\pi}\,\ell n(\sqrt{\ell} + \sqrt{\ell-1}) + i\frac{2\bar{\epsilon}}{\pi}\left[\frac{\sqrt{\ell(\ell-1)}}{2z} + \frac{\sqrt{\ell(\ell-1)}\,(2\ell+1)}{8z^2}\right] + 0\left(\frac{1}{z^3}\right).$$

Finally,

$$iD\,\frac{\zeta^2 - 1}{\zeta^2 + 1} = iD\,\frac{\zeta_1^2\,(1 + Q)^2 - 1}{\zeta_1^2\,(1 + Q)^2 + 1},$$

with Q as before. Letting $\zeta_1^2 = -\,(2\ell - 1 + 2\sqrt{\ell(\ell - 1)}) = -\,T$, one obtains

$$iD\,\frac{\zeta^2 - 1}{\zeta^2 + 1} = iD\,\frac{(1 + T) + T(2Q + Q^2)}{(1 - T) - T(2Q + Q^2)},$$

and by setting

$$b = (1 + T)/T, \quad a = (1 - T)/T, \quad \text{and } \eta = 2Q + Q^2,$$

he has

$$iD\,\frac{\zeta^2 - 1}{\zeta^2 + 1} = -iD\,\frac{b}{a}\,\frac{(1 + \eta/b)}{(1 - \eta/a)}$$

for $\eta \ll (a,b)$. By expanding the denominator of this result, neglecting terms of order $(1/z^3)$, and simplifying the result, one obtains finally

$$iD\,\frac{\zeta^2 - 1}{\zeta^2 + 1} = -iD\left\{\frac{1 + T}{1 - T} + \frac{4T}{(1 - T)^2}\cdot\frac{M}{z} + \frac{4NT}{(1 - T)^2}\cdot\frac{1}{z^2} + \frac{2T(1 + 3T)}{(1 - T)^3}\cdot\frac{M^2}{z^2}\right\} + 0\left(\frac{1}{z^3}\right).$$

The series expansion of $w(z)$ in descending powers of z is a combination of these results, and

$$w(z) = \left[\frac{U_\infty \Sigma}{2} - 2A\sqrt{\ell} - \frac{\alpha U_c}{\Pi}\, \ell n\, \frac{\sqrt{\ell}+1}{\sqrt{\ell}-1} + i\frac{2}{\Pi}\bar{\epsilon}\, \ell n(\sqrt{\ell} + \sqrt{\ell - 1}) - iD\,\frac{1+T}{1-T}\right]$$

$$+ \frac{1}{z}\left[\frac{\alpha U_c \sqrt{\ell}}{\Pi} - A(\ell - 1)\sqrt{\ell} + i\,\frac{\bar{\epsilon}}{\Pi}\sqrt{\ell(\ell-1)} - iD\,\frac{2T\sqrt{\ell(\ell-1)}}{(1-T)^2}\right]$$

$$+ \frac{1}{z^2}\left\{\frac{\alpha U_c}{4\Pi}(\ell+1)\sqrt{\ell} - \frac{A}{4}(\ell-1)(3\ell+1)\sqrt{\ell} + \frac{i}{4\Pi}\bar{\epsilon}\sqrt{\ell(\ell-1)}\,(2\ell+1)\right.$$

$$\left. - iD\frac{T}{(1-T)^3}\left[\frac{\sqrt{\ell(\ell-1)}}{2}(2\ell+1+\sqrt{\ell(\ell-1)})(1-T) + \frac{1+3T}{2}\,\ell(\ell-1)\right]\right\}$$

$$+ O\left(\frac{1}{z^3}\right). \qquad (3.6)$$

Since it is required that $a_1 = b_o = 0$, it follows from equation (3.6) that

$$A = \alpha U_c/\Pi(\ell-1) \qquad (3.7a)$$

and

$$D = \frac{2}{\Pi}\bar{\epsilon}\,\frac{1-T}{1+T}\,\ell n(\sqrt{\ell} + \sqrt{\ell-1}). \qquad (3.7b)$$

Using these results and the further requirement that $a_o = 0$, one has

$$\frac{U_\infty \Sigma}{2} - \frac{\alpha U_c}{\Pi}\left(\ell n\frac{\sqrt{\ell}+1}{\sqrt{\ell}-1} + \frac{2\sqrt{\ell}}{\ell - 1}\right) = 0.$$

Because $U_c = U_\infty(1 + \Sigma/2)$, the above relation can be simplified to give

$$\frac{\Sigma}{2+\Sigma} = \frac{\alpha}{\Pi}\left(\ell n\,\frac{\sqrt{\ell}+1}{\sqrt{\ell}-1} + \frac{2\sqrt{\ell}}{\ell - 1}\right). \qquad (3.8)$$

This equation relates the cavitation number Σ, the cavity length ℓ, and the wedge semi-angle α. It is seen to be the same result as that obtained by Tulin [1] and Wu [18] for an irrotational wedge flow. In this case the rotationality of the flow has no first order effect on the cavity length. This same conclusion can be reached by purely physical reasoning as follows: if a first order length effect enters as $K\bar{\epsilon}$, then changing the sign of $\bar{\epsilon}$ reverses the first order effect but simply inverts the flow field. Hence, a contradiction would result from the presence of a first order length effect. This same reasoning applies to first-order changes in the drag and cavity area, but not to changes in the other pressure force coefficients or the cavity shape.

As a result of the above information, the complex perturbation velocity $w(z)$ may now be written as

$$w(z) = \frac{i}{z}\frac{\bar{\epsilon}}{\Pi}\sqrt{\ell(\ell-1)}\left[1 + \frac{4T}{T^2-1}\ln(\sqrt{\ell} + \sqrt{\ell-1})\right] + \frac{1}{z^2}\left\{-\frac{\alpha U_c \ell^{3/2}}{2\Pi}\right.$$

$$\left. + i\frac{\bar{\epsilon}}{4\Pi}\sqrt{\ell(\ell-1)}(2\ell+1)\left[1 + \frac{4T\ln(\sqrt{\ell} + \sqrt{\ell-1})}{(T^2-1)(1-T)}\left(1-T + \frac{2\sqrt{\ell(\ell-1)}(1+T)}{2\ell+1}\right)\right]\right\}$$

$$+ O\left(\frac{1}{z^3}\right). \tag{3.9}$$

The remaining calculations are based on equations (3.3a) and (3.9).

First, the cavity area and shape are calculated. From Section 2.3, the body-cavity area is

$$S = -\frac{1}{U_c}\,\mathrm{Im}\oint_{B+C} w(z)z\,dz. \tag{2.15a}$$

The cavity area A_c is

$$A_c = S - \alpha, \tag{3.10}$$

where it is seen that α is the area of the wedge. Because the complex velocity $w(z)$ is analytic off the slit,

$$\oint_{B+C} w(z)z\,dz = \oint_{T} w(z)z\,dz,$$

where T is a circle of large radius ($|z| \to \infty$) surrounding the slit. The slit and contour path lines are plotted in Figure 6. Applying the theory of residues, one has

$$\operatorname{Im}\oint_{T} w(z)z\,dz = 2\Pi a_2,$$

and from equation (3.9)

$$a_2 = -\alpha U_c \ell^{3/2}/2\Pi.$$

Thus,

$$S = \alpha\ell^{3/2} \tag{3.11a}$$

and

$$A_c = \alpha(\ell^{3/2} - 1). \tag{3.11b}$$

To find the cavity shape, one rewrites equation (2.14a) as

$$y_c = \alpha - \operatorname{Im}\int_1^t \frac{w(\zeta)}{U_c}\frac{dz}{d\zeta}\,d\zeta$$

on the upper cavity surface, and

$$y_c = -\alpha - \operatorname{Im}\int_{-1}^{-t} \frac{w(\zeta)}{U_c}\frac{dz}{d\zeta}\,d\zeta$$

on the lower surface. On the cavity surfaces (see Figure 3a), both ζ and z are real and $x = z$. The cavity ordinate y_c is related to the cavity abscissa x by determining x as a function of the parameter t. The derivative $dz/d\zeta$ is found by differentiating equation (3.1), and

$$\frac{dz}{d\zeta} = \frac{8\ell(\ell - 1)\zeta(\zeta^4 - 1)}{(\zeta^2 + T)^2\ (\zeta^2 + R)^2}. \tag{3.12}$$

The relations $\zeta_1^2\ \zeta_2^2 = 1$, $\zeta_1^2 = -T$, and $\zeta_2^2 = -R = -[2\ell - 1 - 2\sqrt{\ell(\ell-1)}]$ have been used to achieve this result. When ζ is real, the imaginary part of $w(\zeta)$ in equation (3.3a) becomes

$$\mathrm{Im}[w(\zeta)] = -\frac{4\alpha U_c}{\pi}\tan^{-1}\frac{1}{\zeta} + \frac{2}{\pi}\bar{\epsilon}\ \ln|\zeta| + A(\zeta - \frac{1}{\zeta}) + D\,\frac{\zeta^2 - 1}{\zeta^2 + 1}.$$

Combining the above results and using equations (3.7), one has on the cavity surfaces the following:

a. on the upper surface, $t \geq 1$,

$$y_c = \alpha - 8\ell(\ell-1)\int_1^t \left[\frac{\alpha}{\pi(\ell-1)}\,(\zeta - \frac{1}{\zeta}) + \frac{4}{\pi}\left(\frac{\bar{\epsilon}}{U_\infty}\right)\cdot\frac{(1-T)\ln(\sqrt{\ell} + \sqrt{\ell-1})}{(1+T)\ (2+\Sigma)}\cdot\frac{\zeta^2-1}{\zeta^2+1}\right.$$
$$\left. + \frac{4\bar{\epsilon}}{\pi U_\infty}\,\frac{\ln\zeta}{2+\Sigma} - \frac{4\alpha}{\pi}\tan^{-1}\frac{1}{\zeta}\right]\cdot\frac{\zeta(\zeta^4-1)d\zeta}{(\zeta^2+T)^2(\zeta^2+R)^2}\ . \tag{3.13a}$$

b. on the lower surface, $t \leq -1$,

$$y_c = -\alpha + 8\ell(\ell-1)\int_1^{|t|}\left[\frac{\alpha}{\pi(\ell-1)}(\zeta - \frac{1}{\zeta}) - \frac{4\bar{\epsilon}}{\pi U_\infty}\,\frac{1-T}{1+T}\cdot\frac{\ln(\sqrt{\ell} + \sqrt{\ell-1})}{(2+\Sigma)}\cdot\frac{\zeta^2-1}{\zeta^2+1}\right.$$
$$\left. - \frac{4\bar{\epsilon}}{\pi U_\infty}\,\frac{\ln\zeta}{2+\Sigma} - \frac{4\alpha}{\pi}\tan^{-1}\frac{1}{\zeta}\right]\cdot\frac{\zeta(\zeta^4-1)d\zeta}{(\zeta^2+T)^2(\zeta^2+R)^2}\ . \tag{3.13b}$$

c. from equation (3.1), for $|t| \geq 1$,

$$x = \ell\left[1 - \frac{4(\ell - 1)\ t^2}{(t^2+T)(t^2+R)}\right]. \tag{3.13c}$$

Next, the pressure force coefficients are determined. The pressure coefficient C_p was developed in Section 2.3 and is given explicitly in Table 4; the other coefficients are given in terms of C_p. From Table 4,

$$C_p = (2+\Sigma)\left[\pm \frac{\bar{\epsilon}}{U_\infty}x + \frac{\Sigma}{2} - \frac{u}{U_\infty}\right]. \tag{3.14}$$

On the wedge surfaces, $\zeta = e^{i\theta}$. The upper surface corresponds to the plus sign in the C_p expression and $0 \leq \theta \leq \Pi/2$, while the lower surface corresponds to the minus sign and $\Pi/2 \leq \theta \leq \Pi$. On the wedge, $0 \leq x \leq 1$. The combination of equations (3.3a) and (3.7) and the introduction of $\zeta = e^{i\theta}$ gives the complex velocity on the wedge

$$\frac{w(\theta)}{U_\infty} = \frac{\Sigma}{2} - (2+\Sigma)\frac{\alpha}{\Pi}\left[\ln\frac{e^{i\theta}+i}{e^{i\theta}-i} - \frac{i}{2(\ell-1)}(e^{i\theta} - e^{-i\theta})\right],$$

$$+ i\frac{2\bar{\epsilon}}{\Pi U_\infty}\frac{1-T}{1+T}\ln(\sqrt{\ell}+\sqrt{\ell-1})\frac{e^{i2\theta}-1}{e^{i2\theta}+1} + \frac{\bar{\epsilon}}{U_\infty}(1 - \frac{2}{\Pi}\theta).$$

Simplifying this result and taking the real part produces

$$\frac{u(\theta)}{U_\infty} = \frac{\Sigma}{2} - \frac{(2+\Sigma)}{(\ell-1)}\frac{\alpha}{\Pi}\sin\theta - \frac{2\bar{\epsilon}}{\Pi U_\infty}\frac{1-T}{1+T}\ln(\sqrt{\ell}+\sqrt{\ell-1})\tan\theta$$

$$+ \frac{\bar{\epsilon}}{U_\infty}(1 - \frac{2}{\Pi}\theta) - (2+\Sigma)\frac{\alpha}{\Pi}\ln\left|\frac{1+\sin\theta}{1-\sin\theta}\right|.$$

From the wedge flow transformations listed in Table 2,

$$\frac{1}{4}(\zeta + \frac{1}{\zeta})^2 = (\ell - 1)\frac{z}{\ell - z}.$$

Since $x = \mathrm{Re}(z)$ and $\zeta = e^{i\theta}$ on the wedge, one obtains, after some simplification,

$$x = \frac{\ell\cos^2\theta}{\ell - \sin^2\theta}. \tag{3.15}$$

The above results are now introduced into equation (3.14) and

$$C_p = (2+\Sigma)\left\{\frac{\alpha}{\Pi}(2+\Sigma)\left(\frac{\sin\theta}{\ell - 1} + \ln\left|\frac{1+\sin\theta}{1-\sin\theta}\right|\right)\right.$$
$$\left. + \frac{\bar{\epsilon}}{U_\infty}\left[\frac{2\theta}{\Pi} - 1 + \frac{2(1-T)}{\Pi(1+T)}\tan\theta \,.\, \ln\left(\sqrt{\ell} + \sqrt{\ell - 1}\right) \pm \frac{\ell\cos^2\theta}{\ell - \sin^2\theta}\right]\right\}. \tag{3.16}$$

The positive sign and $0 \leq \theta \leq \Pi/2$ are used on the upper wedge surface and the negative sign and $\Pi/2 \leq \theta \leq \Pi$ on the lower surface. Equations (3.15) and (3.16) then give the pressure coefficient C_p as a function of x on the wedge surfaces.

The drag coefficient based on the base width of the wedge is, from Table 4,

$$C_D = -\frac{1}{2\alpha}\oint_W C_p dy. \tag{3.17}$$

The contour integral W follows a closed, counter-clockwise path on the wedge surfaces. If equation (3.14) is introduced into (3.17), and the relationships $dy = \frac{v}{U_c}dx$ and $2uv = -\mathrm{Im}(w^2)$ are used, then

$$C_D = -\frac{1}{2\alpha}\left[\mathrm{Im}\oint_W \frac{w^2}{U_\infty^2}\, dz + (2+\Sigma)\oint_W\left(\mp\frac{\bar{\epsilon}}{U_\infty}x + \frac{\Sigma}{2}\right)dy\right], \tag{3.17a}$$

since $dx = dz$ on the slit. The first quantity in the brackets above can be written in terms of the contour integration paths shown in Figure 6 because w is analytic off the slit. Hence,

$$\oint_W w^2 dz = \oint_T w^2 dz - \oint_C w^2 dz.$$

The path T is a large radius circle, as before; the path C around the cavity on the slit consists of the cavity walls plus a small circle e (radius $r \to 0$) which surrounds the point $z = \ell$. On T, $w(z)$ is of the form

$$w(z) = \frac{ib_1}{z} + \frac{a_2 + ib_2}{z^2} + O(\frac{1}{z^3}),$$

so that

$$w^2(z) = -\frac{b_1^2}{z^2} + O(\frac{1}{z^3}).$$

Thus, by the theory of residues,

$$\oint_T w^2 dz = 0.$$

The integral over the cavity is given by

$$\mathrm{Im}\oint_C w^2 dz = -2\left[\int_S (\epsilon y_c + \Sigma U_\infty/2)_L\, U_c dy\right.$$

$$\left. + \int_S (\epsilon y_c + \Sigma U_\infty/2)_U\, U_c dy\right] + \mathrm{Im}\, J_T,$$

where $\mathrm{Im}\, w^2 = -2uv$ on the slit, and J_T is the integral over e. The integrals S over the slit are taken on the lower and upper cavity surfaces respectively as indicated by the subscript on the integrand. On the cavity $\epsilon y_c = \pm\bar{\epsilon}$, on the wedge $\pm\bar{\epsilon}x = \epsilon y_o = \bar{\epsilon}y/\alpha$. It follows from the definition of a closed contour integral that

$$\frac{1}{\alpha}\oint_W \bar{\epsilon} y dy = 0 \quad \text{and} \quad \oint_S \pm\bar{\epsilon} dy = 0.$$

Thus, equation (3.17a) may be simplified to

$$C_D = +\frac{1}{2\alpha}\,\mathrm{Im}(J_T/U_\infty^2). \tag{3.17b}$$

In order to evaluate this result, $w(z)$ must be expanded as $z \to \ell$. Taking equation (3.1) and letting $z \to \ell$ gives

$$\zeta \to \frac{2i\sqrt{\ell(\ell-1)}}{\sqrt{z-\ell}} \quad \text{as } z \to \ell.$$

The expansion of $w(z)$ about $z = \ell$ and evaluation of the resulting integrals over the e path are accomplished in Appendix B. There it is found that

$$J_T = \oint_e w^2 dz = 8\Pi\, iA^2 \ell(\ell - 1).$$

Introducing this result and the value for A given in equation (3.7a) into equation (3.17b) above gives the drag coefficient

$$C_D = \frac{\alpha(2 + \Sigma)^2 \ell}{\Pi(\ell - 1)}. \tag{3.18}$$

As expected, this result is precisely that given by Tulin [1] and Wu [18] for the irrotational flow about a wedge, and the rotation has no first order effect on the drag.

By utilizing the previously determined results of Table 4, the lift coefficient C_L is found to be

$$C_L = -(2 + \Sigma)\oint_W \frac{u}{U_\infty} dx + (2 + \Sigma)\oint_W \left(\frac{\Sigma}{2} \mp \frac{\bar{\epsilon}}{U_\infty} x\right) dx.$$

The real part of $w(z)dz$ is equal to udx on the wedge and

$$\oint_W \left(\frac{\Sigma}{2} \mp \frac{\bar{\epsilon}}{U_\infty} x\right) dx = -\frac{\bar{\epsilon}}{U_\infty}\left(\int_0^1 xdx - \int_1^0 xdx\right) = -\bar{\epsilon}/U_\infty,$$

so

$$C_L = -(2 + \Sigma)\,\mathrm{Re}\oint_W \frac{w}{U_\infty} dz - (2 + \Sigma)\left(\frac{\bar{\epsilon}}{U_\infty}\right). \tag{3.19}$$

From equation (3.9) and the theory of residues

$$\int_T wdz = 2\Pi i(ib_1),$$

since $a_1 = 0$, and $b_1 = \frac{\overline{\epsilon}}{\pi}\sqrt{\ell(\ell-1)} \left[1 + \frac{4T}{T^2-1} \ln(\sqrt{\ell} + \sqrt{\ell-1})\right]$.

Recalling that w is analytic off the slit, one may write

$$\oint_W wdz = \oint_T wdz - \oint_C wdz.$$

Then,

$$\mathrm{Re}\oint_W wdz = -2\overline{\epsilon}\sqrt{\ell(\ell-1)} \left[1 + \frac{4T}{T^2-1} \ln(\sqrt{\ell} + \sqrt{\ell-1})\right] - \mathrm{Re}\oint_c wdz$$

and

$$\mathrm{Re}\oint_C wdz = \mathrm{Re}\oint_S wdz + \mathrm{Re}\oint_e wdz.$$

The contour integral S follows a closed path over that part of the slit on the x-axis which corresponds to the cavity but excludes the point $z = \ell$. Upon using the fact that $\mathrm{Re}\, w = u$ and $u = U_\infty \Sigma/2 \pm \overline{\epsilon}$ on the cavity, it is found that

$$\mathrm{Re}\oint_S wdz = \oint_S udx = -\int_1^\ell \overline{\epsilon}\, dx + \int_\ell^1 \overline{\epsilon}\, dx = -2\overline{\epsilon}(\ell - 1).$$

Furthermore, from Appendix B, one sees that

$$\mathrm{Re}\int_e w\,dz = 0.$$

Using these results, equation (3.19) can be put into the form

$$C_L = 2(2+\Sigma)\left(\frac{\bar{\epsilon}}{U_\infty}\right)\left\{\sqrt{\ell(\ell-1)}\left[1+\frac{4T}{T^2-1}\ \ln\left(\sqrt{\ell}+\sqrt{\ell-1}\right)\right]-\frac{(2\ell-1)}{2}\right\}. \tag{3.20}$$

The moment coefficient about the nose of the wedge is defined as

$$C_{MO} = \frac{L\cdot \text{dist to } L}{\frac{1}{2}\rho U_\infty^2\cdot(\text{CHORD})^2},$$

positive in the counter-clockwise direction. The contribution due directly to pressure forces perpendicular to the x-axis is

$$C_{MOx} = \oint_W C_p x\,dx,$$

while the y-axis contribution is

$$C_{MOy} = \oint_W C_p\ |y|\,dy = \alpha^2\oint_W C_p x\,dx.$$

Hence, the total moment C_{MO} is

$$C_{MO} = (1 + \alpha^2) \oint_W C_p \, xdx,$$

but since α^2 is of second order it is properly neglected in this analysis. Again, using the results in Table 4, one has

$$C_{MO} = -(2 + \Sigma) \oint_W \frac{u}{U_\infty} xdx + (2 + \Sigma) \oint_W \left(\mp \frac{\bar{\epsilon}x}{U_\infty} + \Sigma/2 \right) xdx. \quad (3.21)$$

The real part of wzdz is equal to uxdx on the wedge and

$$\oint_W \left(\mp \frac{\bar{\epsilon}x}{U_\infty} + \frac{\Sigma}{2} \right) xdx = - \frac{\bar{\epsilon}}{U_\infty} \left(\int_0^1 x^2 dx - \int_1^0 x^2 dx \right) = - \frac{2}{3} \frac{\bar{\epsilon}}{U_\infty}.$$

Then,

$$\mathrm{Re} \oint_T wzdz = -2\Pi b_2$$

where from equation (3.9)

$$b_2 = \frac{\bar{\epsilon}}{4\Pi} \sqrt{\ell(\ell-1)} \, (2\ell+1) \left\{ 1 + \frac{4T\ell n(\sqrt{\ell} + \sqrt{\ell-1})}{(T^2-1)\,(1-T)} \left[\frac{2\sqrt{\ell(\ell-1)}\,(1+T)}{2\ell+1} + 1 - T \right] \right\} .$$

As before, one may write

$$\mathrm{Re} \oint_W wzdz = -2\Pi b_2 - \mathrm{Re} \oint_C wzdz.$$

From Appendix B,

$$\oint_e wzdz = 0,$$

and by using the cavity boundary conditions,

$$\mathrm{Re} \oint_S wzdz = \oint_S uxdx = -\bar{\epsilon} \left(\int_1^\ell xdx - \int_\ell^1 xdx \right) = -\bar{\epsilon}(\ell^2 - 1).$$

Thus, $\mathrm{Re} \oint_C wzdz = - \bar{\epsilon}(\ell^2 - 1)$.

After introducing the above into equation (3.21), the moment coefficient can be simplified to

$$C_{MO} = (2+\Sigma)\left(\frac{\bar{\epsilon}}{U_\infty}\right)\left\{\frac{\sqrt{\ell(\ell-1)}}{2}(2\ell+1)\left[1 + \frac{4T\ln(\sqrt{\ell}+\sqrt{\ell-1})}{(T^2-1)(1-T)} \cdot \left(1-T + \frac{2\sqrt{\ell(\ell-1)}(1+T)}{2\ell+1}\right)\right] + \frac{(1-3\ell^2)}{3}\right\}. \tag{3.22}$$

Finally, one must calculate the value of the parameter $\bar{\epsilon}/U_\infty$ and introduce it into the basic results. From Table 5,

$$\frac{\bar{\epsilon}}{U_\infty} = \frac{\epsilon}{U_\infty 2(\ell-1)}\left\{\int_1^\ell |y_c|_L \, dx + \int_1^\ell |y_c|_U \, dx\right\}.$$

In Section 2.3, it was noted that the quantity in the curly brackets is the cavity area A_c. Substituting the value of A_c from equation (3.11b) into the above equation yields

$$\frac{\bar{\epsilon}}{U_\infty} = \frac{\epsilon\, \alpha(\ell^{3/2}-1)}{U_\infty 2(\ell-1)}. \tag{3.23}$$

Equation (3.23) is now introduced into the previously obtained results.

3.1.3. Discussion

The results of the linearized analysis, which are summarized in Table 6, depend on the independent variables Σ(or ℓ), α, and relative vorticity ϵ/U_∞. Equation (3.8) gives Σ explicitly as a function of ℓ for fixed α. Numerical results, together with computation programs, are tabulated in Appendix F. Certain portions of these results have been plotted to illustrate the theory.

As predicted earlier, the cavity length - cavitation number relation, the cavity area, and the drag coefficient are independent of the relative vorticity ϵ/U_∞. On the other hand, the lift and moment coefficients depend linearly on ϵ/U_∞; both coefficients are, of course, zero in the irrotational, parallel flow past a wedge. For reference, Figures 7 and 8 show the drag coefficient C_D and cavity area A_c as functions of Σ, even though they are the same as those found in an irrotational flow. The $\ell - \Sigma$ relationship is plotted on Figures 16 and 17; the curve for asymmetric shear flow is the curve labelled $\frac{\epsilon}{U_\infty} = 0$, i.e., the irrotational flow. For this case, Wu [18] has shown that in the linearized theory, ℓ is limited to

$$1 + \frac{2\alpha}{\Pi}\left(1 + \frac{\alpha}{\Pi}\,\ln\frac{2\Pi}{\alpha}\right) < \ell < \infty.$$

Those results which are directly affected by vorticity are plotted in Figures 9 through 15. The first figure shows $\bar{\epsilon}/\epsilon$ as a function of Σ. The next is a plot of a typical cavity shape which shows a definite dependence on the relative vorticity. The two vorticity terms in equations (3.13) account for the airfoil shape of the cavity. The second, or logarithmic, term becomes large only near the end of the cavity and tends to pull the cavity end downward.

The key results of the theory are the pressure, lift, and moment coefficients. Since the latter two are linear in ϵ/U_∞, Figures 11 and 12 are plotted with $C_L/(\epsilon/U_\infty)$ and $C_{MO}/(\epsilon/U_\infty)$ as functions of Σ for various α's. The increase of both coefficients with (a) decreasing cavitation number, (b) increasing wedge angle, and (c) increasing relative vorticity is clearly seen. As Σ approaches zero, the cavity becomes infinitely long and the magnitudes of the lift and moment coefficients approach infinity. Tsien [12] found that this behavior also occurs in shear flow about an infinitely long, solid body. The pressure coefficient C_p is presented in Figures 13 and 14. The positive lift found above is represented here by the area between corresponding curves. On the upper wedge surface near the nose, the pressure coefficient of the linearized flow exhibits a large negative value. This phenomenon is associated with the high velocities required for the fluid to turn about the sharp nose point in the equivalent nonlinearized flow; here, the stagnation point on the wedge is below the x-axis and behind the nose. In a real flow a small cavity may occur on the upper surface at the nose. Such a cavity has been observed in experiments with wedges at a small angle of incidence [7, Chap. 12, Pt. 2, Fig. 12 II.13, p.33] where the flow patterns are essentially equivalent to those of the present rotational flow. Figure 15, the final figure in the series, shows the distance $\bar{x}$ of the center of lift from the nose of the wedge.

3.2. Symmetric Flow Past a Wedge

The undisturbed velocity profile of the supercavitating flow is shown in Figure 1 (dotted line profile) and again in Figure 4. The notation, which was introduced in Section 2, is shown on Figures 4 and 5. Note that Poisson's equation $\nabla^2\psi = \epsilon$ holds for $y > 0$, but $\nabla^2\psi = -\epsilon$ holds for $y < 0$, contrary to the asymmetric case. This change is, of course, due to the discontinuity in the vorticity at $y = 0$.

3.2.1. Solution of the boundary value problem

It is necessary to reformulate the wedge boundary value problem outlined in Table 1 because of the symmetric shear velocity profile at infinity. However, the same conformal mappings as were used in Section 3.1 may be used here.

In Section 2.1, the rotational flow was reduced to a harmonic or irrotational flow by introducing the stream function $\psi_P = \epsilon y^2/2$. In the case of the symmetric flow, it is necessary to use the function

$$\psi_{PU} = \epsilon y^2/2, \; y > 0$$

and the function

$$\psi_{PL} = -\epsilon y^2/2, \; y < 0.$$

Then, one has as desired

a. for $y > 0$: $\nabla^2\psi_P = \epsilon$, $U_P = -\epsilon y$
b. for $y < 0$: $\nabla^2\psi_P = \epsilon$, $U_P = +\epsilon y$.

The remainder of the development in Section 2 is unchanged.

By comparing Figures 2 and 3a to Figure 4, one can see that the boundary conditions in the symmetric flow are (a) the same on the upper and lower surfaces and (b) the same as those for the upper surface of the wedge in the asymmetric flow. The new boundary conditions on the slit and mapped planes are shown in Figure 5. The mapping (3.1) gives z as a function of ζ as before. The boundary value problem for symmetric flow in terms of the complex perturbation velocity $w = u - iv$ is the same as that given for the wedge flow in Table 1, except that condition (b) becomes Real $(w) = U_\infty \Sigma/2 + \bar{\epsilon}$, $1 \leq x \leq \ell$, $y = 0^-$. Note that in the symmetric flow,

$$\Sigma = \sigma = \frac{p_\infty - p_c}{\frac{1}{2}\rho U_\infty^2}.$$

It is seen from equation (3.3) that the function

$$w(\zeta) = -\frac{2\alpha U_c}{\pi} \ln \frac{\zeta + i}{\zeta - i} + iA(\zeta - 1/\zeta) + U_\infty\sigma/2 + \bar{\epsilon} \qquad (3.24)$$

satisfies the differential equation and conditions (a), (b), (c), (d), (g), and (h) of the revised boundary value problem. As before, the remaining conditions will serve to determine A and a relation between ℓ and σ for fixed $\bar{\epsilon}$ and α.

3.2.2. Results

The function $w(\zeta)$ can be expanded in descending powers of z as $z \to \infty$. The series has the form shown in equation (3.4); the boundary conditions (e) and (f) require that $a_o = b_o = a_1 = 0$. By using equations (3.5) and (3.6) of Section 3.1.2, one has

$$w(z) = \left[(U_\infty\sigma/2) + \bar{\epsilon} - \frac{\alpha U_c}{\pi} \ln \frac{\sqrt{\ell}+1}{\sqrt{\ell}-1} - 2A\sqrt{\ell}\right] + \frac{1}{z}\left[\frac{\alpha U_c\sqrt{\ell}}{\pi} - A(\ell-1)\sqrt{\ell}\right]$$

$$+ \frac{1}{z^2}\left[\frac{\alpha U_c}{\pi}(\ell+1)\sqrt{\ell} - \frac{A}{4}(\ell-1)(3\ell+1)\sqrt{\ell}\right] + O\left(\frac{1}{z^3}\right). \qquad (3.25)$$

It follows that

$$A = \frac{\alpha U_c}{\pi(\ell-1)}$$

and

$$- \frac{\alpha U_c}{\pi} \left(\ln \frac{\sqrt{\ell}+1}{\sqrt{\ell}-1} + \frac{2\sqrt{\ell}}{\ell-1} \right) + \frac{U_\infty \sigma}{2} + \bar{\epsilon} = 0.$$

Immediately, the relation between α, σ, $\bar{\epsilon}$, and ℓ is found to be

$$\frac{\sigma}{2+\sigma} = \frac{\alpha}{\pi} \left[\ln \frac{\sqrt{\ell}+1}{\sqrt{\ell}-1} + \frac{2\sqrt{\ell}}{\ell-1} \right] - \frac{2\bar{\epsilon}}{(2+\sigma)U_\infty} \tag{3.26}$$

The effect of positive vorticity is to shorten the cavity for fixed σ.

The complex velocity $w(z)$ can now be written as

$$w(z) = - \frac{1}{z^2}\left(\frac{\alpha U_c \ell^{3/2}}{2\,\pi}\right) + 0\left(\frac{1}{z^3}\right). \tag{3.27}$$

The remaining calculations are based on equations (3.24) and (3.27). Note that in this case the cavity remains symmetric in shape and, since the flow is symmetric, no lift or moments can be expected. The quantities of interest, then, are the cavity shape, cavity area, and the pressure and drag coefficients. Because the flow is symmetric, only the upper wedge surface C_p and upper cavity shape $y_c(x)$ need be calculated.

The cavity area and shape are found first. From Section 2.3, the body-cavity area is

$$S = A_c + \alpha = - \frac{1}{U_c} \operatorname{Im} \oint_{B+C} w(z) z dz. \tag{2.15a}$$

The function A_c is the cavity area and α is the area of the wedge. Using the contour paths in Figure 6 and the analyticity of $w(z)$ off the slit leads to

$$\oint_{B+C} wzdz = \oint_{T} w(z)zdz.$$

From equation (3.27) and the theory of residues, one has

$$\operatorname{Im} \oint_{B+C} wzdz = - \alpha U_c \ell^{3/2}.$$

Thus, $$S = \alpha \ell^{3/2} \tag{3.28a}$$
and $$A_c = \alpha(\ell^{3/2} - 1). \tag{3.28b}$$

Since a positive vorticity shortens the cavity length ℓ for a fixed σ, the area A_c is reduced also. The cavity shape is easily found by use of equation (2.14a) and several results from Section 3.1. From equation (3.24), the imaginary part of $w(\zeta)$ is

$$\mathrm{Im}\left[w(\zeta)\right] = -\frac{4\alpha U_c}{\pi}\tan^{-1}\zeta + A(\zeta - 1/\zeta),$$

when ζ is real (on the upper cavity surface). From equation (2.14a),

$$y_c = \alpha - \mathrm{Im}\int_1^t \frac{w(\zeta)}{U_c}\frac{dz}{d\zeta}\,d\zeta.$$

Introducing the above into this result, together with equation (3.12), gives

$$y_c = \alpha - \frac{8\alpha\ell}{\pi}\int_1^t \left[\zeta - \frac{1}{\zeta} - 4(\ell-1)\tan^{-1}\frac{1}{\zeta}\right]\frac{\zeta(\zeta^4-1)d\zeta}{(\zeta^2+T)^2(\zeta^2+R)^2},\quad t \geq 1. \tag{3.29a}$$

As before, x is given as a function of the parameter t by

$$x = \ell\left[1 - \frac{4(\ell-1)t^2}{(t^2+T)(t^2+R)}\right]; \tag{3.13c}$$

$$T = 2\ell - 1 + 2\sqrt{\ell(\ell-1)}$$

and $$R = 2\ell - 1 - 2\sqrt{\ell(\ell-1)}.$$

Although the vorticity parameter $\bar{\epsilon}/U_\infty$ does not enter explicitly in the above equations, its effect is felt through the change of ℓ for a given σ due to vorticity [see equation (3.26)].

Next, the pressure and drag coefficients are determined. The pressure coefficient C_p is given by

$$C_p = \frac{p - p_c}{\frac{1}{2}\rho U_\infty^2},$$

as before. Following the same procedures as in Section 2.3, one is lead to the result that

$$C_p = (2 + \sigma) \left[\left(\frac{\bar{\epsilon}}{U_\infty}\right) x + \sigma/2 - u/U_\infty \right], \quad 0 \leq x \leq 1. \qquad (3.30)$$

Since in this case C_p is symmetric with respect to the x-axis, equation (3.30) is valid on both upper and lower wedge surfaces. From the similar calculations in Section 3.1.2, it follows immediately that on the upper wedge surface,

$$\frac{u(\theta)}{U_\infty} = \mathrm{Re}\left(\frac{w(\theta)}{U_\infty}\right) = \frac{\sigma}{2} + \frac{\bar{\epsilon}}{U_\infty} - \frac{\alpha(2+\sigma)}{\Pi}\left[\frac{\sin\theta}{\ell - 1} + \ln\left|\frac{1+\sin\theta}{1-\sin\theta}\right|\right]$$

and

$$x = \ell \cos^2\theta/(\ell - \sin^2\theta) \qquad (3.31)$$

for $0 \leq \theta \leq \Pi/2$. Thus, equation (3.30) can be written in the form

$$C_p = (2+\sigma)\left\{\left(\frac{\bar{\epsilon}}{U_\infty}\right)(x-1) + \frac{\alpha}{\Pi}(2+\sigma)\left[\frac{\sin\theta}{\ell - 1} + \ln\left|\frac{1+\sin\theta}{1-\sin\theta}\right|\right]\right\},$$

$$0 \leq \theta \leq \Pi/2. \qquad (3.32)$$

The drag coefficient C_D for a wedge is given in Table 4 as

$$C_D = -\frac{1}{2\alpha}\oint_W C_p dy.$$

Utilizing the relationships developed in Section 3.1.2, one has, after allowing for the present symmetry of the boundary conditions,

$$C_D = -\frac{1}{2\alpha}\left[\mathrm{Im}\oint_W \frac{w^2}{U_\infty^2} dz + (2+\sigma)\oint_W \left(-\frac{\bar{\epsilon}}{U_\infty} x + \frac{\sigma}{2}\right) dy\right].$$

It follows immediately from the analytic character of w and equation (3.27) that

$$\mathrm{Im}\oint_W w^2 dz = \mathrm{Im}\oint_C w^2 dz,$$

since by the theory of residues

$$\oint_T w^2 dz = 0.$$

The integral over the cavity is given by

$$\mathrm{Im}\oint_C w^2 dz = -2\left\{\int_S (\epsilon|y_c| + U_\infty\sigma/2)_L U_c dy + \int_S (\epsilon|y_c| + U_\infty\sigma/2)_U U_c dy\right\} + \mathrm{Im}\oint_e w^2 dz,$$

where $\mathrm{Im}\, w^2 = -2uv$ on the slit. On the cavity $\epsilon|y_c| = \bar{\epsilon}$, and on the wedge $\bar{\epsilon}x = \epsilon|y_o| = \bar{\epsilon}|y|/\alpha$. Thus,

$$\oint_W \epsilon|y_o|dy = \bar{\epsilon}\oint_W xdy = \frac{\bar{\epsilon}}{\alpha}\oint_W |y|dy = 0,$$

and

$$\oint_S \epsilon|y_c|dy = \bar{\epsilon}\oint_S dy = 0.$$

Furthermore, from the cavity closure requirement, $\oint_{W+C} dy = 0$, with the contour integral W+C being taken over the wedge-cavity combination. Hence, one obtains

$$C_D = \frac{1}{2\alpha U_\infty^2}\,\mathrm{Im}\oint_e w^2 dz.$$

It is again necessary to expand $w(z)$ about $z = \ell$. Comparing equations (3.3a) and (3.24a), one sees that equation (B.1) in Appendix B becomes

$$w(z) \to \frac{U_\infty\sigma}{2} + \bar{\epsilon} - \frac{2A\sqrt{\ell(\ell-1)}}{\sqrt{z-\ell}}\,.$$

From this result, it follows that

$$\oint_e w^2 dz = J_T.$$

Using the value of J_T found in Appendix B plus the value of A found previously, one has

$$C_D = \frac{(2+\sigma)^2 \alpha \ell}{\Pi \, (\ell - 1)} \, . \tag{3.33}$$

This is formally the same equation found in the irrotational case; however the cavity length ℓ in equation (3.33) is altered by a first order vorticity effect. This alteration of ℓ causes a displacement of the curves of C_D versus σ.

In order to define a value for $\bar{\epsilon}$ to complete the solution of the symmetric problem, one must resort to physical and mathematical intuition. Since the circulation Γ is identically zero about the cavity in the symmetric flow, one cannot use the method of matching circulations which was so successful in Section 3.1.2. However, since $\bar{\epsilon}$ is to be a representative value of $\epsilon|y_c|$ over the whole cavity, it is reasonable to choose

$$\frac{\bar{\epsilon}}{U_\infty} = \left(\frac{\epsilon}{U_\infty}\right) \frac{A_c}{2(\ell-1)} = \left(\frac{\epsilon}{U_\infty}\right) \frac{\alpha(\ell^{3/2} - 1)}{2(\ell - 1)} \, , \tag{3.34}$$

i.e., the mathematical average value.

3.2.3. Discussion

The results of the symmetric flow analysis are summarized in Table 7. Appendix F lists the numerical computations which have been carried out by using the equations in Table 7. Three important results are presented in graphical form in Figures 16 through 19.

First, the cavitation number σ is plotted as a function of cavity length ℓ in Figures 16 and 17. It is evident that a positive vorticity ϵ causes a reduction in the cavity length for fixed values of σ. Although the cavity length is infinite when $\sigma \to 0$ in an irrotational flow ($\epsilon = 0$), there is a maximum ℓ corresponding to each value of the relative vorticity $\epsilon/U_\infty > 0$ in a rotational flow. When $\epsilon/U_\infty < 0$, the solution to the problem is no longer unique. Then, as seen in Figures 16 and 17 or in the tabulated data, there exists a minimum σ for each value of $\epsilon/U_\infty < 0$. For each σ greater than the minimum value, there are two possible cavity lengths - the conjugate lengths. When σ is less than the minimum value, no solutions exist to the linearized problem. When two solutions exist, both satisfy all imposed boundary conditions and produce physically reasonable drag coefficients and cavity shapes (see Figures 18 and 19). In spite of the large vorticity effects, the lower limit on the cavity length still seems to be that value determined for irrotational flow (see Section 3.1.3) and denoted by $1 + \frac{2\alpha}{\Pi}\left(1 + \frac{\alpha}{\Pi} \log \frac{2\Pi}{\alpha}\right) < \ell$.

Second, the drag coefficient C_D is given as a function of σ and α for two values of ϵ/U_∞ in Figure 18. A comparison of this figure with Figure 7 shows that when the vorticity is positive, the values of C_D for fixed α and σ are slightly increased over the corresponding irrotational values. However, when $\epsilon < 0$, the drag coefficient is reduced and the C_D curves in Figure 18 lie below the comparable curves in Figure 7. One should note the reappearance of a minimum cavitation number for $\epsilon < 0$ and the two possible C_D values for each σ above the minimum.

Finally, Figure 19 shows the shapes of the cavities trailing behind a wedge when the cavitation number is fixed and ϵ/U_∞ is varied. The two longest cavities shown are the conjugate length cavities for $\epsilon/U_\infty = -0.080$.

3.3 Asymmetric Flow Past a Hydrofoil

The final problem considered is a parallel, uniform shear flow past a supercavitating flat-plate hydrofoil. The unit length hydrofoil is placed at an angle α with the x-axis (as shown in Figure 1). The development, based on the methods outlined in Section 2, closely follows Parkin's solution of linearized cavity flow past a hydrofoil in a liquid with gravity [4]. The similarity between the present case and the gravity flow problem will be evident. In fact, the basic boundary value problems for the two flows differ only by a change in sign of the perturbation parameter, i.e., $\overline{\epsilon}/U_\infty = -\overline{u}/U_\infty$, where $\overline{u}/U_\infty$ represents Parkin's gravity parameter.

3.3.1. Solution of the boundary value problem

As before, the conformal mapping technique is used to solve the boundary value problem given in Table 1. The transformations are listed in Table 2; in Figure 3b the slit z-plane and transformed planes, together with corresponding boundary conditions, are shown.

The solution $w(\zeta)$ is constructed from the singularities in Table 3. By comparing the form of the boundary conditions and the available singularities, one can see that $w(\zeta)$ should have the form

$$w(\zeta) = iA\left(\zeta-\frac{1}{\zeta}\right) + iB + iC\ln\zeta + i\frac{D}{\zeta-1} + E. \qquad (3.35)$$

The boundary conditions in Table 1 are applied to equation (3.35) to determine the real constants. In summary, this leads to the following:

a. $Re(w) = U_\infty\Sigma/2 + \bar{\epsilon}$ for ζ real and ≥ 1, so that

$E = U_\infty\Sigma/2 + \bar{\epsilon}$.

b. $Re\ (w) = U_\infty\Sigma/2 - \bar{\epsilon}$ for ζ real and ≤ -1, so that

$-\Pi C+E = U_\infty\Sigma/2 - \bar{\epsilon}$ and $C = 2\bar{\epsilon}/\Pi$.

c. $Im(w) = +\alpha U_c$ for ζ on the unit semi-circle, so that

$-\frac{D}{2} + B = \alpha U_c$ and $B = \alpha U_c + \frac{D}{2}$.

d. $w(z) \to 0$ as $z \to -\infty$. In the Q-plane, as $z \to \infty$, $Q \to ik$ with $k = \sqrt{L-1}$, as before.

Equation (3.35) becomes

$$w(\zeta) = iA(\zeta-1/\zeta) + i\alpha U_c + \frac{i2\bar{\epsilon}}{\Pi}\ln\zeta$$
$$+ iD\left(\frac{1}{2} + \frac{1}{\zeta-1}\right) + U_\infty\Sigma/2 + \bar{\epsilon}. \qquad (3.35a)$$

In this form, w satisfies the differential equation and all boundary conditions except (e) and (f) in Table 1. These remaining boundary conditions allow determination of A and D and development of a cavitation-number - cavity-length relationship.

Following Parkin [4], one completes the solution of the problem in the Q-plane (see Figure 3b). From condition (f) and item d above, $w(z) \to 0$ as $z \to -\infty$, while in the Q-plane, $Q \to ik$ as $z \to -\infty$. Equation (3.35a) may then be written in terms of Q, and Q must be allowed to approach ik, where $w(Q)$ approaches 0. In accordance with the transformations of Table 2,

$$4Q + 2 = \zeta + 1/\zeta;$$

hence,

$$\zeta = 1 + 2Q \pm 2\sqrt{Q(Q+1)}. \qquad (3.36)$$

The negative root is chosen for Q real and ≤ -1; otherwise, the positive root is appropriate. When $Q = ik$,

$$\zeta = 2ik + 1 + 2\sqrt{ik-k}.$$

Letting $r = \sqrt{\sqrt{\ell}+1} + \sqrt{\sqrt{\ell}-1}$ and $s = \sqrt{\sqrt{\ell}+1} - \sqrt{\sqrt{\ell}-1}$, one obtains from equation (3.35a) and the above

$$w(ik) = iA\left[1 + \sqrt{k}\,s + i(2k + \sqrt{k}\,r) - \frac{1}{1+\sqrt{k}\,s + i(2k+\sqrt{k}\,r)}\right] + i\alpha U_c$$
$$+ iD(\tfrac{1}{2} + [\sqrt{k}\,s+i\sqrt{k}\,r]^{-1})+i(2\bar{\epsilon}/\Pi)\ln[(1+\sqrt{k}\,s)^2 + (2k + \sqrt{k}\,r)^2]$$
$$- (2\bar{\epsilon}/\Pi)\tan^{-1}\frac{2k+\sqrt{k}\,r}{1 + \sqrt{k}\,s} + U_\infty\Sigma/2 + \bar{\epsilon} = 0. \qquad (3.37)$$

Letting $A = A_o U_\infty$ and $D = D_o U_\infty$ as Parkin does, one obtains two equations for A_o and D_o from the real and imaginary parts of equation (3.37). These are

$$2\sqrt{k}\, rA_o - \frac{s}{4\sqrt{k}} D_o = \left(\frac{\bar{\epsilon}}{U_\infty}\right)\left(1 - \frac{2}{\pi}\tan^{-1}\left[\frac{2k + \sqrt{k}\, r}{1 + \sqrt{k}\, s}\right]\right) - \frac{\Sigma}{2}$$

and

$$2\sqrt{k}\, sA_o + \frac{r}{4\sqrt{k}} D_o = -\frac{\bar{\epsilon}}{U_\infty}\left\{\frac{1}{\pi}\ln\left[(1 + \sqrt{k}\, s)^2 + (2k + \sqrt{k}\, r)^2\right]\right\} - \alpha(1+\Sigma/2).$$

The equations are solved simultaneously to yield

$$A_o = \frac{1}{8\sqrt{\ell k}}\left[s\left\{-\frac{\bar{\epsilon}}{U_\infty}\frac{1}{\pi}\ln\left[(1+\sqrt{k}\, s)^2 + (2k+\sqrt{k}\, r)^2\right] - \alpha\left(1 + \frac{\Sigma}{2}\right)\right\}\right.$$
$$\left. + r\left\{\frac{\bar{\epsilon}}{U_\infty}\left[1 - \frac{2}{\pi}\tan^{-1}\left(\frac{2k + \sqrt{k}\, r}{1 + \sqrt{k}\, s}\right)\right] + \frac{\Sigma}{2}\right\}\right] \qquad (3.38a)$$

and

$$D_o = -\sqrt{\frac{k}{\ell}}\left[s\left\{\frac{\bar{\epsilon}}{U_\infty}\left[1 - \frac{2}{\pi}\tan^{-1}\left(\frac{2k+\sqrt{k}\, r}{1+\sqrt{k}\, s}\right)\right] + \frac{\Sigma}{2}\right\} + r\left\{\frac{\bar{\epsilon}}{U_\infty}\frac{1}{\pi}\ln\left[(1+\sqrt{k}\, s)^2\right.\right.\right.$$
$$\left.\left.\left. + (2k + \sqrt{k}\, r)^2\right] + \alpha\left(1+\frac{\Sigma}{2}\right)\right\}\right]. \qquad (3.38b)$$

In the Q-plane, using equation (3.36), the complex perturbation velocity is

$$w(Q)/U_\infty = i4A_o\sqrt{Q(Q+1)} + iD_o\sqrt{(Q+1)/Q}/2 + i\alpha(1+\Sigma/2)+\Sigma/2$$
$$+ \bar{\epsilon}/U_\infty + i\frac{\bar{\epsilon}}{U_\infty}\frac{2}{\pi}\ln\left[1+2Q+2\sqrt{Q(Q+1)}\right]. \qquad (3.39)$$

The remaining condition (e) is the closure condition. As noted previously, if the cavity is to close, the net strength of sources within the cavity must equal zero. It is equivalent to require that $w(z)$ have no real residue within an infinitely large circle T (see Figure 6) surrounding the cavity, i.e.,

$$\operatorname{Im}\oint_T w(z)dz = 0.$$

Because $w(z)$ is harmonic off the slit in the z-plane, it follows that

$$\operatorname{Im} \oint_{B+C} w(z)dz = 0, \tag{3.40}$$

with B+C the boundary of the foil-cavity system. Thus, in the Q-plane, the closure integral I_c is

$$I_c = \oint_{B+C} w(Q) \frac{dz}{dQ} dQ. \tag{3.41}$$

The foil-cavity system extends from $-\infty$ to $+\infty$ in the Q-plane. This integral is evaluated in the classical manner by using a semi-circle of radius R in the upper half plane to form a closed contour C_R. One has, from the given transforms,

$$\frac{dz}{dQ} = 2\ell k^2(k^2 + Q^2)^{-2}Q. \tag{3.42}$$

Thus,

$$\int_{\frown R} w(Q)\frac{dz}{dQ}\, dQ \to 0 \quad \text{as } R \to \infty$$

and

$$I_c = -2\ell k^2 \int_{-\infty}^{\infty} \frac{w(Q)QdQ}{(k^2 + Q^2)^2} = -2\Pi i \text{ (Residues within } C_R). \tag{3.41a}$$

The minus signs account for the reversal of the line integral orientation in the Q-plane. The only residue within C_R occurs at the second order pole $Q = ik$. The residue b_1 at the pole is given by [21]

$$b_1 = \frac{\ell k i}{2} \frac{dw(Q)}{dQ}\bigg|_{Q = ik}, \tag{3.43}$$

since $w(ik) = 0$. The introduction of equation (3.39) into equation (3.43) and the use of the subsequent result give

$$I_c = \frac{\Pi U_\infty}{8}\sqrt{\frac{\ell}{k}} \left\{s(16k^2A_o+D_o) - 8kr\left(A_o+\frac{1}{\Pi}\frac{\bar{\epsilon}}{U_\infty}\right) - i\left[8ks\left(A_o+\frac{1}{\Pi}\frac{\bar{\epsilon}}{U_\infty}\right) + r(16k^2A_o+D_o)\right]\right\}. \tag{3.44}$$

From equations (3.40) and (3.41), it follows that

$$8ks\left(A_o + \frac{1}{\Pi}\frac{\overline{\epsilon}}{U_\infty}\right) + r(16k^2A_o + D_o) = 0$$

for closure. By introducing the values of the constants A_o and D_o, one derives

$$-\frac{ks + 2k^2r}{\sqrt{\ell k}}\left(s\left\{\frac{\overline{\epsilon}}{\Pi U_\infty}\ln[(1+\sqrt{k}\,s)^2 + (2k+\sqrt{k}\,r)^2] + \alpha\left(1+\frac{\Sigma}{2}\right)\right\}\right.$$

$$\left.- r\left\{\frac{\overline{\epsilon}}{U_\infty}\left(1-\frac{2}{\Pi}\tan^{-1}\frac{2k+\sqrt{k}\,r}{1+\sqrt{k}\,s}\right) + \frac{\Sigma}{2}\right\}\right) + \frac{8ks\overline{\epsilon}}{\Pi U_\infty} - r\sqrt{\frac{k}{\ell}}\left(s\left\{\frac{\overline{\epsilon}}{U_\infty}\left[1-\frac{2}{\Pi}\tan^{-1}\frac{2k+\sqrt{k}\,r}{1+\sqrt{k}\,s}\right]\right.\right.$$

$$\left.\left.+\frac{\Sigma}{2}\right\} + r\left\{\frac{\overline{\epsilon}}{\Pi U_\infty}\ln[(1+\sqrt{k}\,s)^2 + (2k+\sqrt{k}\,r)^2] + \alpha\left(1+\frac{\Sigma}{2}\right)\right\}\right) = 0. \qquad (3.45)$$

3.3.2. <u>Results</u>

In the previous Section 3.3.1, the basic solution $w(Q)$ and a relation (equation (3.45)) between the problem parameters $\overline{\epsilon}/U_\infty$, ℓ, Σ, and α were found. Based on this information, the cavity characteristics -- length (closure condition), area, and shape -- may be found. In turn, one can determine the pressure force coefficients and, finally, the vorticity parameter $\overline{\epsilon}/U_\infty$.

Upon simplification, equation (3.45) yields the closure condition

$$\alpha = \frac{k\Sigma}{2+\Sigma} - \frac{2\epsilon}{\Pi(2+\Sigma)U_\infty}\left\{\ln[(1+\sqrt{k}\,s)^2 + (2k+\sqrt{k}\,r)^2] - \left[k\Pi\left(1-\frac{2}{\Pi}\tan^{-1}\frac{2k+\sqrt{k}\,r}{1+\sqrt{k}\,s}\right) + \frac{2s\sqrt{k\ell}}{k+\sqrt{\ell}}\right]\right\} \qquad (3.46)$$

As $(\overline{\epsilon}/U_\infty) \to 0$, this equation reduces to Tulin's condition for closure in the irrotational case [6], i.e.,

$$\alpha = \frac{k\Sigma}{2+\Sigma},$$

with $\Sigma = \sigma$ when $\bar{\epsilon}/U_\infty = 0$. When $\bar{\epsilon}/U_\infty$ is not zero, a positive $\bar{\epsilon}/U_\infty$ produces a lengthening of the cavity over the irrotational case for fixed α and Σ.

The cavity shape is found by integrating equation (2.14a) from the appropriate point on the hydrofoil, i.e., the leading or trailing edge. By employing the previously determined relation for dz/dQ and the fact that z and Q are real on the cavity, one can integrate equation (2.14a) directly in the Q-plane. For real Q,

$$\operatorname{Im} \frac{w}{U_\infty} = 4A_o\sqrt{Q(Q+1)} + D_o\frac{\sqrt{(Q+1)/Q}}{2} + \alpha\left(\frac{1+\Sigma}{2}\right) + \frac{2\bar{\epsilon}}{\Pi U_\infty} \ln\left|1+2Q \pm 2\sqrt{Q(Q+1)}\right| ,$$

on the upper and lower cavity surfaces respectively. It follows that

a. on the upper cavity surface, for $q \geq 0$ and real,

$$\frac{y_c}{\ell} = \frac{4k^2}{2+\Sigma}\int_0^q\left[4A_oQ\sqrt{Q(Q+1)} + \frac{D_o}{2}\sqrt{Q(Q+1)} + \frac{\alpha Q}{2}(2+\Sigma) + \frac{2\bar{\epsilon}}{\Pi U_\infty} Q\ln\left|1+2Q + 2\sqrt{Q(Q+1)}\right|\right]\frac{dQ}{(k^2+Q^2)^2} . \quad (3.47a)$$

b. on the lower surface, for $q \geq 1$ and real,

$$\frac{y_c}{\ell} = -\frac{\alpha}{\ell} + \frac{4k^2}{2+\Sigma}\int_1^q\left[4A_oQ\sqrt{Q(Q-1)} - \frac{D_o}{2}\sqrt{Q(Q-1)} - \frac{\alpha Q}{2}(2+\Sigma) - \frac{2\bar{\epsilon}}{\Pi U_\infty} Q\ln\left|1-2Q-2\sqrt{Q(Q-1)}\right|\right]\frac{dQ}{(k^2+Q^2)^2} . \quad (3.47b)$$

By use of the tabulated integrals from Appendix C, these equations may be written as

$$\frac{y_c}{\ell} = \frac{-4k^2}{(2+\Sigma)}\left\{4A_oI_1 + \frac{D_oI_2}{2} + \frac{2\bar{\epsilon}}{\Pi U_\infty} I_3 + \frac{\alpha(2+\Sigma)q^2}{4k^2(k^2+q^2)}\right\} \quad (3.48a)$$

on the upper surface and

$$\frac{y_c}{\ell} = -\frac{\alpha}{\ell} + \frac{4k^2}{2+\Sigma}\left(4A_oI_4 - \frac{D_oI_5}{2} - \frac{2\,\bar{\epsilon}}{\Pi U_\infty} I_6 - \frac{\alpha(2+\Sigma)(q^2-1)}{4\ell(k^2+q^2)}\right) \tag{3.48b}$$

on the lower cavity surface. The value of x for a corresponding q is found by integrating equation (3.42) and is given by

$$\frac{x}{\ell} = \frac{q^2}{(k^2+q^2)} . \tag{3.49}$$

Since the cavity and body-cavity areas are the same, the cavity area A_c is [from equation (2.15a)]

$$A_c = -\frac{2}{2+\Sigma} \operatorname{Im} \oint_{CAV} \frac{w(z)}{U_\infty} z dz.$$

The contour integral is again evaluated in the Q-plane, where

$$\oint_{CAV} \frac{w(z)}{U_\infty} z dz = -2k^2\ell^2 \oint_{C_R} \frac{w(Q)}{U_\infty} \frac{Q^3 dQ}{(k^2+Q^2)^3} .$$

As before, the theory of residues is applied. The only pole in the region is the third-order pole at $Q = ik$; the residue there is given by [21]

$$b_1 = \frac{k^2\ell^2}{U_\infty} \frac{d^2}{dQ^2} \left[\frac{w(Q)Q^3}{(Q+ik)^3}\right]_{Q=ik} .$$

This equation is reduced in Appendix D. The imaginary part of the result is

$$A_c = \frac{\Pi\sqrt{k\ell}}{16(2+\Sigma)} \left[4A_o[k(4k^2+5)r + (2k^2+1)s] - \frac{D_o}{2}\left[\left(2k+\frac{1}{k}\right) r - s\right] - \frac{4\bar{\epsilon}}{\Pi U_\infty}(kr-s)\right] , \tag{3.50}$$

with A_o and D_o given by equations (3.38).

The calculation of pressure force coefficients depends on the evaluation of the pressure coefficient, which represents the difference between the pressure p on the lower surface of the hydrofoil and the cavity pressure p_c on the upper surface. These relationships were defined in Section 2.3 and tabulated in Table 4. From that table,

$$C_p = -(2+\Sigma)\left(\frac{\bar{\epsilon}}{U_\infty} x + \frac{u}{U_\infty} - \frac{\Sigma}{2}\right). \tag{3.51}$$

In the Q-plane the lower side of the foil is represented by $Q = \xi e^{i\Pi}$,

$0 \leq \xi \leq 1$. Also, $u/U_\infty = \text{Real}\ (w/U_\infty)$. Using the above relations and equation (3.39), one has

$$\frac{u}{U_\infty} = -4A_o\sqrt{\xi(1-\xi)} + \frac{D_o}{2}\sqrt{\frac{1-\xi}{\xi}} - \frac{2\bar{\epsilon}}{\Pi U_\infty}\tan^{-1}\frac{2\sqrt{\xi(1-\xi)}}{1-2\xi} + \frac{\Sigma}{2} + \frac{\bar{\epsilon}}{U_\infty}.$$

Since $z = \ell Q^2/(k^2+Q^2)$, then $x = \ell\xi^2/(k^2+\xi^2)$ on the hydrofoil, and C_p can be written as

$$C_p = -(2+\Sigma)\left\{-4A_o\sqrt{\xi(1-\xi)} + \frac{D_o}{2}\sqrt{\frac{1-\xi}{\xi}} + \frac{\bar{\epsilon}}{U_\infty}\left[1 + \frac{\ell\xi^2}{k^2+\xi^2} - \frac{2}{\Pi}\cdot\tan^{-1}\left(\frac{2\sqrt{\xi(1-\xi)}}{1-2\xi}\right)\right]\right\}, \quad 0 \leq \xi \leq 1, \tag{3.52}$$

with $\tan^{-1}(\ ) \leq \Pi$.

The normal force coefficient C_N is given directly by integration of C_p over the foil. Thus, from Table 4,

$$C_N = \int_0^1 C_p dx$$

and, from equation (3.51),

$$C_N = -\frac{(2+\Sigma)}{2}\left(\frac{\bar{\epsilon}}{U_\infty} - \Sigma + 2\int_0^1 \frac{u}{U_\infty} dx\right). \tag{3.53}$$

The integral in this equation can be written in terms of a contour integral around the hydrofoil-cavity system, i.e.,

$$\int_0^1 \frac{u}{U_\infty} dx = \text{Re}\oint_{B+C} \frac{w}{U_\infty} dz - \int_1^\ell \frac{u}{U_\infty} dx - \int_\ell^0 \frac{u}{U_\infty} dx.$$

A comparison of the velocity functions used in the hydrofoil and wedge flows, together with the results of Appendix B, show that there is no contribution to the normal force from the integral of w around the end of the cavity. This is also true for the integral wz about the end of the cavity. Since $u/U_\infty = \Sigma/2 \pm \bar{\epsilon}/U_\infty$ on the upper and lower cavity surfaces respectively, one obtains

$$\int_0^1 \frac{u}{U_\infty}\, dx = \text{Real} \oint_{B+C} \frac{w(Q)}{U_\infty} \frac{dz}{dQ}\, dQ + \frac{\Sigma}{2} + \frac{\bar{\epsilon}}{U_\infty}\, (2\ell-1).$$

The introduction of this result and equation (3.41) into equation (3.53) produces

$$C_N = -(2+\Sigma)\left[\frac{\bar{\epsilon}}{U_\infty}\, \frac{4\ell-1}{2} + \text{Re}(I_c/U_\infty)\right] .$$

The final form for C_N is obtained by substituting the value of I_c from equation (3.44) and the values of the constants A_o and D_o into this result. After some manipulation, one has

$$C_N = \frac{\Pi}{4}\,(2+\Sigma)(\sqrt{\ell}-k)\left[\alpha k(2+\Sigma) + \Sigma + \frac{2\bar{\epsilon}}{U_\infty}\left\{\frac{k}{\Pi}\, \ln[(1+\sqrt{k}s)^2+(2k+\sqrt{k}\,r)^2] + 1 - \frac{2}{\Pi}\tan^{-1}\frac{2k+\sqrt{k}\,r}{1+\sqrt{k}\,s} + \frac{2\sqrt{\ell k}\,r-(4\ell-1)}{\Pi(\sqrt{\ell}-k)}\right\}\right], \tag{3.54}$$

where from Table 4, $C_L = C_N$, $C_D = \alpha C_N$, and $D/L = \alpha$.

The moment coefficient C_{MO} about the leading edge of the hydrofoil is, from Table 4,

$$C_{MO} = \int_0^1 C_p x\, dx.$$

When C_p is introduced into this result, one derives

$$C_{MO} = -(2+\Sigma)\left[\frac{\bar{\epsilon}}{3U_\infty} - \frac{\Sigma}{4} + \int_0^1 \frac{u}{U_\infty}\, x\, dx\right] . \tag{3.55}$$

As before, the integral on the foil is transformed into a contour integral with the result that

$$\int_0^1 \frac{u}{U_\infty} xdx = \mathrm{Re}\oint_{B+C} \frac{w}{U_\infty} zdz - \int_1^{\ell}\left(\frac{\Sigma}{2} - \frac{\bar{\epsilon}}{U_\infty}\right)xdx - \int_0^{\ell}\left(\frac{\Sigma}{2} + \frac{\bar{\epsilon}}{U_\infty}\right)xdx.$$

Thus,

$$C_{MO} = -(2+\Sigma)\left[\frac{\bar{\epsilon}}{U_\infty}\left(\frac{1}{3} + \frac{2\ell^2-1}{2}\right) + \mathrm{Re}\oint_{B+C} \frac{w(Q)}{U_\infty}\frac{zdz}{dQ}\,dQ\right].$$

The integral in this equation has been evaluated in Appendix D in connection with determination of the cavity area A_c. Taking the real part of that result and introducing it into the above equation produces

$$C_{MO} = +\,(2+\Sigma)\left\{-\frac{\bar{\epsilon}}{U_\infty}\left[\frac{1}{3} + \frac{(2\ell^2-1)}{2}\right] + \frac{\Pi\sqrt{\ell k}}{32}\left[4A_o([6\ell-1]r-[12\ell+1]ks)\right.\right.$$
$$\left.\left. + \frac{D_o}{2}\left(r-\left[2k + \frac{3}{k}\right]s\right) + \frac{4\bar{\epsilon}}{\Pi U_\infty}([4k^2+5]r+ks)\right]\right\}.$$

After minor re-arrangement, the moment coefficient has the form

$$C_{MO} = (2+\Sigma)\left\{\frac{\bar{\epsilon}}{U_\infty}\left[\frac{\sqrt{\ell k}}{8}([4\ell+1]r+ks)-\ell^2 + \frac{1}{6}\right]\right.$$
$$\left. + \frac{\Pi\sqrt{\ell k}}{32}\left[4A_o\,.\,([6\ell-1]r-[12\ell+1]ks)+\frac{D_o}{2}\left(r-\left[2k + \frac{3}{k}\right]s\right)\right]\right\}. \tag{3.56}$$

Finally one determines the vorticity parameter $\bar{\epsilon}/U_\infty$. From Table 5,

$$\frac{\bar{\epsilon}}{U_\infty} = \frac{\epsilon}{U_\infty\, 2(\ell-1)}\left\{\int_1^{\ell}|y_c|_L dx + \int_0^{\ell}|y_c|_U dx\right\}.$$

It has been noted that this result can be written directly as

$$\frac{\bar{\epsilon}}{U_\infty} = \frac{\epsilon(A_c-\alpha/2)}{U_\infty\, 2(\ell-1)} = \frac{\epsilon(A_c-\alpha/2)}{U_\infty(2k^2+1)}, \tag{3.57}$$

where $k = \sqrt{\ell-1}$. Recalling equation (3.50) which gives A_c, one can see that $\bar{\epsilon}/U_\infty$ may be found directly. This calculation involves solving a quadratic relation obtained by combining equations (3.50) and (3.57) and using equation (3.46), the closure condition, to eliminate Σ. The result obtained is

$$\frac{\bar{\epsilon}}{U_\infty} = \frac{\epsilon}{4(2\ell-1)U_\infty}\left\{\frac{-kX_4+(k-\alpha)X_3}{H} + \alpha X_1 + X_2 \right.$$
$$\left. (\pm)\ \sqrt{\left[\frac{-kX_4+(k-\alpha)X_3}{H} + \alpha X_1+X_2\right]^2 + \frac{4\alpha X_4}{H}\,(kX_1+X_2)}\right\} \qquad (3.58)$$

in terms of the notation introduced in Appendix E. For $\epsilon < 0$, the minus sign is taken to preserve the form of $\bar{\epsilon}/U_\infty$. This is required because $X_4 < 0$ when $\epsilon < 0$. With $\bar{\epsilon}/U_\infty$ known explicitly as a function of ϵ/U_∞, $\ell(\text{or}\Sigma)$, and α, the solution is complete.

3.3.3. Discussion

The solution to the hydrofoil problem is summarized in Table 8. Appendix F lists a sample of the numerical computations carried out by using the equations in that table. The results are presented graphically in Figures 20 through 30.

The cavity length ℓ is plotted as a function of cavitation number Σ for two values of the attack angle α in Figures 20 and 21. The effect of vorticity in the flow is clearly seen; for a given Σ the cavity is lengthened by positive vorticity. In Figure 22, the effect of vorticity on the size of the vorticity parameter $\bar{\epsilon}/U_\infty$ is shown. A typical cavity shape is plotted in Figure 23. The effect of positive vorticity is an increase in the cavity width and the cavitation number for a fixed cavity length. In contrast, Parkin [4] found that cavities effected by a transverse gravity field lie inside the corresponding gravity-free cavity.

The normal force and moment coefficients are pictured in Figures 24 through 27. (Recall that $C_L = C_N$ and $C_D = \alpha C_N$.) The coefficients are plotted versus Σ in Figures 24 and 26 for a relative vorticity $\epsilon/U_\infty = 0.04$. As the cavitation number approaches zero, both sets of curves turn upward and increase rapidly. This rapid increase in lift and moment as the cavity becomes infinite in length is consistent with the results of Tsien's investigations of shear flows [12] and the results of Section 3.1 (see Figures 11 and 12 and discussion on Page 37). Figures 25 and 27 show C_N and C_{MO} as functions of ϵ/U_∞. Generally, both increase as ϵ/U_∞ increases; however, the increase becomes pronounced only as Σ becomes small. The variation of the location of the center of lift as a function of Σ and ϵ/U_∞ is given in Figure 28.

Two sets of typical pressure coefficients are presented in Figures 29 and 30. The first shows the effect of vorticity on C_p at constant cavity length. The second shows the effect of the cavitation number Σ on C_p, when the angle of attack and vorticity are held constant. In this shear flow theory no pathological cases (i.e., cases in which C_p turns sharply downward) are found which would compare to those experienced by Parkin's gravity theory. The reason for this difference is that the change in sign of the coefficient D_o (Parkin's A_o), which causes negative lift in the gravity case, doesn't occur in the present problem because the perturbation parameter $\bar{\epsilon}/U_\infty$ differs from Parkin's gravity parameter $\bar{u}/U_\infty$ by a minus sign. Thus, while a strong gravity influence causes negative lift, a strong vorticity increases the lift.

Finally, from Figures 20 and 21 and the tabulated data it is seen that when $\epsilon/U_\infty > 0$, the problem solution is not unique. There is a minimum Σ for each value of $\epsilon/U_\infty > 0$. When Σ is greater than the minimum value, there are two possible cavity lengths- conjugate lengths; when Σ is less than the minimum value, no solutions exist to the problem. As in the case of symmetric flow past a wedge, when the two solutions do exist, they both satisfy all conditions of the problem and produce physically reasonable pressure force coefficients.

4. CONCLUDING REMARKS

In Section 3 the linearized theory has been applied to three rotational, supercavitating flows. From these applications it may be concluded that the effects of rotation (vorticity) are significant whenever the magnitude of the relative vorticity ϵ/U_∞ is greater than 0.02. Experimentally, the vorticity effects are most likely to be detected in measurements of lift and moment. In the cases of symmetric shear flow with negative vorticity and uniform shear flow past hydrofoils with positive vorticity, further analysis and experimentation will be required to determine (a) if the non-unique solutions found in Sections 3.2 and 3.3 do occur and (b) if the cavity might tend to oscillate between the conjugate lengths and hence cause some dynamic effects.

In the uniform shear flow about wedges and flat-plate hydrofoils, the positive rotation has been shown to cause an increase in lift and moment forces. In hydrofoil flows an attendant increase in the drag can be expected. It is also important to recall the large increase in the size of vorticity effects which occur as the cavity lengthens. The work of Parkin and others on associated problems suggests that the present linearized theory may over-estimate the vorticity effects when the cavity is extremely long; however, the theory gives no indication of failure in these regions. But, as the cavity length approaches infinity, the lift and moment coefficients do become infinite. On the other hand, in the symmetric flow, the cavitation number and cavity length as well as the effects of vorticity were generally found to be bounded.

The present application is limited in several ways. The wedge half-angles and the hydrofoil attack angles are bounded by the upper limits associated with the basic linearized theory. Chen [2] notes that the linear theory predicts the force coefficients with an error of 8 percent for a flat-plate hydrofoil at 5 degrees incidence and an error of 5 percent for a symmetric wedge of 15 degrees included angle. Finally, there is the method of determining the vorticity effect. The method chosen is arbitrary to be sure, but its value lies in the fact that the method (a) permits a comparitively simple solution of an otherwise difficult problem and (b) accounts, in general, for the over-all vorticity effects rather than the effects at one particular point in the flow. A specific objection which may be raised is that the present theory cannot be extended directly to the second order because of the averaging technique which is used. It is anticipated that the present method can be refined in future analyses and also extended to more general rotational flows.

APPENDIX A
Solution of the Singular Integral Equation

The solution of the singular integral equation of the first kind

$$\int_1^{\ell} \frac{\mu(\xi)d\xi}{x-\xi} = f(x), \; 1 \leq x \leq \ell, \tag{A-1}$$

is accomplished by reducing the integral equation to one of known type by a change of variables. Let

$$t = \frac{2(\xi-1)}{\ell-1} - 1 \quad \text{and} \quad r = \frac{2(x-1)}{\ell-1} - 1,$$

so that

$$d\xi = \frac{(\ell-1)}{2}\,dt, \; dx = \frac{(\ell-1)}{2}\,dr$$

$$\xi = \tfrac{1}{2}[(\ell-1)(t+1) + 2], \; x = \tfrac{1}{2}[(\ell-1)(r+1) + 2].$$

Then,

$$\mu(\xi) \to \phi(t) \quad \text{and} \quad f(x) \to f(r),$$

while equation (A-1) becomes

$$\frac{1}{\pi}\int_{-1}^{1} \frac{\phi(t)dt}{r-t} = \frac{1}{\pi}\,\tilde{f}(r). \tag{A-2}$$

This equation occurs in theory of airfoil motion and is often called the "airfoil equation." Note that improper integrals must be taken with their Cauchy principal value. The solution to (A-2) is provided by Tricomi [22]; it is

$$\phi(r) = \frac{1}{\pi^2\sqrt{1-r^2}}\int_{-1}^{1} \frac{\sqrt{1-t^2}}{t-r}\,\tilde{f}(t)dt + \frac{\tilde{C}}{\sqrt{1-r^2}}, \tag{A-3}$$

where $\gamma/\sqrt{1-r^2}$ represents the non-trivial solutions of the homogeneous equation

$$\int_{-1}^{1} \frac{\phi(t)dt}{t-r} = 0.$$

The solution to (A-2) is, as expected, non-unique; the constant γ is determined by the condition of smooth separation at the trailing edge of the wedge. Returning to the original variables,

$$\mu(x) = -\frac{1}{\pi^2\sqrt{(\ell-x)(x-1)}}\left[\int_1^{\ell} \frac{\sqrt{(\ell-\xi)(\xi-1)}}{x-\xi} f(\xi)d\xi + C\right], \qquad \text{(A-4)}$$

where C has replaced $2\gamma/\pi^2(\ell-1)$ to achieve the desired form. For $\mu(x)$ to remain finite at $x = 1$,

$$C = \int_1^{\ell} \frac{\sqrt{(\ell-\xi)(\xi-1)}}{\xi} f(\xi)d\xi.$$

Thus, the distribution function μ can be written as

$$\mu(x) = -\frac{x}{\pi^2\sqrt{(\ell-x)(x-1)}}\left[\int_1^{\ell} \frac{\sqrt{(\ell-\xi)(\xi-1)}}{\xi(x-\xi)} f(\xi)d\xi\right]. \qquad \text{(A-5)}$$

APPENDIX B
Expansions at $z = \ell$

In order to calculate the pressure force coefficients in a wedge flow, it is necessary to expand the complex perturbation velocity about $z = \ell$ and to calculate contour integrals over the circle e (see Figure 6). The velocity $w(z)$ becomes

$$w(z) \to \frac{\sigma U_\infty}{2} - \frac{2A\sqrt{\ell(\ell-1)}}{\sqrt{z-\ell}} + iD + i\frac{2}{\pi}\bar{\epsilon}\left(\ln 2\sqrt{\ell(\ell-1)} - \ln\sqrt{z-\ell}\right) \quad \text{(B-1)}$$

as $z \to \ell$ because, in equation (3.3a),

a. $\zeta \to -\frac{2\sqrt{\ell(\ell-1)}}{\sqrt{\ell - z}}, \ |\zeta| \to \infty$

b. $iD\frac{\zeta^2-1}{\zeta^2+1} \to iD$

c. $iA(\zeta - \frac{1}{\zeta}) \to -\frac{2A\sqrt{\ell(\ell-1)}}{\sqrt{z-\ell}} + O(\sqrt{z-\ell})$

d. $\ln\frac{\zeta + i}{\zeta - i} \to 0$

Thus, $w(z)$ may be written as

$$w(z) \to K - \frac{2A\sqrt{\ell(\ell-1)}}{\sqrt{z-\ell}} - i\frac{2\bar{\epsilon}}{\pi}\ln\sqrt{z-\ell} \quad \text{(B-2)}$$

where from above $K = O(\sigma, \bar{\epsilon})$. From equation (B-2)

$$w^2(z) = K^2 + \frac{4A^2\ell(\ell-1)}{\sqrt{z-\ell}} - \frac{4\bar{\epsilon}^2}{\pi^2}(\ln\sqrt{z-\ell})^2 - \frac{4KA\sqrt{\ell(\ell-1)}}{\sqrt{z-\ell}} - \frac{4iK\bar{\epsilon}}{\pi}\ln\sqrt{z-\ell} + \frac{8iA\bar{\epsilon}\sqrt{\ell(\ell-1)}}{\pi\sqrt{z-\ell}}\ln\sqrt{z-\ell}. \quad \text{(B-3)}$$

The integrals which occur in the linearized theory are of the form $\oint_e w\,dz$, $\oint_e wz\,dz$, $\oint_e w^2\,dz$. Since only singular terms may contribute to such contour integrals, one needs to evaluate contour integrals

J_i for the following singular functions:

a. $f_1 = \sqrt{z - \ell}$

b. $f_2 = \ln \sqrt{z - \ell}$

c. $f_3 = z/\sqrt{z - \ell}$

d. $f_4 = z \ln \sqrt{z - \ell}$

e. $f_5 = (\ln \sqrt{z - \ell})/\sqrt{z - \ell}$

f. $f_6 = (\ln \sqrt{z - \ell})^2$

g. $f_7 = \dfrac{1}{z - \ell}$

Near $z = \ell$, $z - \ell = re^{i\theta}$ and $z = re^{i\theta} + \ell$, where $r \to 0$ as $z \to \ell$. Then, $dz = ire^{i\theta}d\theta$ on e and an integral J_i is given by

$$J_i = \oint_e f_i dz = \lim_{r \to 0} ir \int_{-\Pi}^{\Pi} f_i \,(re^{i\theta})\, e^{i\theta} d\theta .$$

All integrals of the form

$$E = \int_{-\Pi}^{\Pi} f_i(e^{i\theta}, \theta) d\theta$$

are finite and if

$$J_i = \lim_{r \to 0} r^t E, \ t > 0,$$

then such $J_i = 0$.

Introducing the above notation into the f_i and writing the corresponding J_i gives

a. $$J_1 = \lim_{r \to 0} ir^{1/2} \int_{-\Pi}^{\Pi} e^{i\theta/2}\, d\theta = 0.$$

b. $J_2 = \lim_{r\to 0} ir \ln r^{1/2} \int_{-\Pi}^{\Pi} e^{i\theta} d\theta - \lim_{r\to 0} \frac{r}{2} \int_{-\Pi}^{\Pi} \theta e^{i\theta}\, d\theta = 0$

since $\lim_{r\to 0} r \ln r^t = 0$ for any finite t.

c. $J_3 = \lim_{r\to 0} ir^{3/2} \int_{-\Pi}^{\Pi} e^{i3\theta/2}\, d\theta + \ell J_1 = 0.$

d. $J_4 = \lim_{r\to 0} ir^2 \ln r^{1/2} \int_{-\Pi}^{\Pi} e^{2i\theta}\, d\theta - \lim_{r\to 0} \frac{r^2}{2} \int_{-\Pi}^{\Pi} \theta e^{i\theta} d\theta + \ell J_2 = 0.$

e. $J_5 = \lim_{r\to 0} ir^{1/2} \ln r^{1/2} \int_{-\Pi}^{\Pi} e^{i\theta/2}\, d\theta = 0$

since $\lim_{r\to 0} r^{1/2} \ln r^{1/2} = 0.$

f. $J_6 = \lim_{r\to 0} ir \int_{-\Pi}^{\Pi} \left[(\ln r^{1/2})^2 + i\theta \ln r^{1/2} - \frac{\theta^2}{4} \right] e^{i\theta} d\theta.$

Since all other terms go immediately to zero, one has

$$J_6 = i \lim_{r\to 0} (\ln r^{1/2})^2\, r \int_{-\Pi}^{\Pi} e^{i\theta}\, d\theta.$$

By L'Hospital's Rule

$$\lim_{r\to 0} \frac{(\ln r^{1/2})^2}{1/r} = \lim_{r\to 0} \frac{\frac{\ln r^{1/2}}{r}}{-\frac{1}{r^2}} = 0, \quad \text{and} \quad J_6 = 0.$$

g. $J_7 = \lim_{r\to 0} i \int_{-\Pi}^{\Pi} d\theta = 2\Pi i.$

It follows that

$$\oint_e w\,dz = 0,$$

$$\oint_e wz\,dz = 0,$$

and

$$J_T = \oint_e w^2 dz = 2\Pi i(4A^2 \ell(\ell-1)). \qquad \text{(B-4)}$$

APPENDIX C
Summary of Cavity Shape Integrals

The results listed below and the accompanying definition of terms are summarized from reference [4]. Appropriate changes of notation have been made to make the results compatible with this development. The new terms defined are as follows:

$$\omega^2 = k\sqrt{k^2+1} = \sqrt{\ell(\ell-1)}, \quad \beta_1 = -\sqrt{\frac{\omega^2-k^2}{2}}, \quad \beta_2 = -\sqrt{\frac{\omega^2+k^2}{2}},$$

$$\gamma_1 = \frac{1}{\omega^2}\left(k\beta_2 + \frac{1}{2}\beta_1\right), \quad \gamma_2 = \frac{1}{\omega^2}\left(k\beta_1 - \frac{1}{2}\beta_2\right), \quad \delta_1 = \frac{k\beta_2}{2\omega^2} \text{ and } \delta_2 = \frac{k\beta_1}{2\omega^2}.$$

One then has

$$I_1 = \int_0^q \frac{\sqrt{Q(Q+1)}\, Q\,dQ}{(k^2+Q^2)^2} = -\frac{\sqrt{q(q+1)}}{2(k^2+q^2)} + \frac{1}{4}\left\{\frac{\gamma_2}{k}\cdot \ln\left[\frac{\left([\gamma_1 q+\delta_1-\sqrt{q(q+1)}]^2 + [\gamma_2 q+\delta_2]^2\right)k^2}{(q^2+k^2)(\delta_1^2+\delta_2^2)}\right] + \frac{2\gamma_1}{k}\left[\tan^{-1}\frac{k}{q} + \tan^{-1}\frac{\gamma_2 q+\delta_2}{\gamma_1 q+\delta_1-\sqrt{q(q+1)}} - \frac{\Pi}{2} - \tan^{-1}\frac{\delta_2}{\delta_1}\right]\right\},$$

$$I_2 = \int_0^q \frac{\sqrt{Q(Q+1)}\,dQ}{(k^2+Q^2)^2} = \frac{1}{2(\ell-1)}\left\{\frac{q\sqrt{q(q+1)}}{(k^2+q^2)} + \frac{\beta_1}{4\omega^2}\ln\left[\frac{\left([\gamma_1 q-\delta_1-\sqrt{q(q+1)}]^2+[\gamma_2 q+\delta_2]^2\right)k^2}{(q^2+k^2)(\delta_1^2+\delta_2^2)}\right] + \frac{\beta_2}{2\omega^2}\left[\tan^{-1}\frac{k}{q} + \tan^{-1}\frac{\gamma_2 q+\delta_2}{\gamma_1 q+\delta_1-\sqrt{q(q+1)}} - \frac{\Pi}{2} - \tan^{-1}\frac{\delta_2}{\delta_1}\right]\right\},$$

$$I_3 = \int_0^q \frac{\ell n\left|1+2Q+2\sqrt{Q(Q+1)}\right| Q\,dQ}{(k^2 + Q^2)^2}$$

$$= -\frac{\ell n[1+2q+2\sqrt{q(q+1)}]}{2(k^2 + q^2)} + \frac{1}{2\omega^2}\left\{-\frac{\beta_2}{2k}\ \ell n\left[\frac{([\gamma_1 q+\delta_1-\sqrt{q(q+1)}]^2+[\gamma_2 q+\delta_2]^2)k^2}{(q^2 + k^2)(\delta_1^2 + \delta_2^2)}\right]\right.$$

$$\left. + \frac{\beta_1}{k}\left(\tan^{-1}\frac{k}{q} + \tan^{-1}\frac{\gamma_2 q+\delta_2}{\gamma_1 q+\delta_1-\sqrt{q(q+1)}} - \frac{\pi}{2} - \tan^{-1}\frac{\delta_2}{\delta_1}\right)\right\},$$

$$I_4 = \int_1^q \frac{Q\sqrt{Q(Q-1)}\,dQ}{(k^2 + Q^2)^2}$$

$$= -\frac{\sqrt{q(q-1)}}{2(k^2+q^2)} + \frac{1}{4}\left[-\frac{\gamma_2}{k}\ \ell n\left[\frac{([\gamma_1 q-\delta_1-\sqrt{q(q-1)}]^2+[-\gamma_2 q+\delta_2]^2)\ell}{(q^2+k^2)([\gamma_1-\delta_1]^2+[-\gamma_2+\delta_2]^2)}\right]\right.$$

$$\left. + \frac{2\gamma_1}{k}\left(\tan^{-1}\frac{k}{q} - \tan^{-1}k + \tan^{-1}\frac{-\gamma_2 q+\delta_2}{\gamma_1 q-\delta_1-\sqrt{q(q-1)}} - \tan^{-1}\frac{-\gamma_2+\delta_2}{\gamma_1-\delta_1}\right)\right],$$

$$I_5 = \int_1^q \frac{\sqrt{Q(Q-1)}\,dQ}{(k^2+Q^2)^2}$$

$$= \frac{1}{2(\ell-1)}\left\{\frac{q\sqrt{q(q-1)}}{(k^2+q^2)} + \frac{\beta_1}{4\omega^2}\cdot \ell n\left[\frac{([\gamma_1 q-\delta_1-\sqrt{q(q-1)}]^2+[-\gamma_2 q+\delta_2]^2)\ell}{(q^2+k^2)([\gamma_1-\delta_1]^2+[-\gamma_2+\delta_2]^2)}\right]\right.$$

$$\left. - \frac{\beta_2}{2\omega^2}\left(\tan^{-1}\frac{k}{q} - \tan^{-1}k + \tan^{-1}\frac{-\gamma_2 q+\delta_2}{\gamma_1 q-\delta_1-\sqrt{q(q-1)}} - \tan^{-1}\frac{-\gamma_2+\delta_2}{\gamma_1-\delta_1}\right)\right\},$$

and

$$I_6 = \int_1^q \frac{Q\ell n\left|1-2Q-2\sqrt{Q(Q-1)}\right| dQ}{(k^2 + Q^2)^2}$$

$$= -\frac{\ell n\left|1-2q-2\sqrt{q(q-1)}\right|}{2(k^2 + q^2)} - \frac{1}{2\omega^2}\left[\frac{\beta_2}{2k}\ \ell n\left[\frac{([\gamma_1 q-\delta_1-\sqrt{q(q-1)}]^2+[-\gamma_2 q+\delta_2]^2)\ell}{(q^2+k^2)([\gamma_1-\delta_1]^2+[-\gamma_2+\delta_2]^2)}\right]\right.$$

$$\left. + \frac{\beta_1}{k}\left(\tan^{-1}\frac{k}{q} - \tan^{-1}k + \tan^{-1}\frac{-\gamma_2 q + \delta_2}{\gamma_1 q-\delta_1-\sqrt{q(q-1)}} - \tan^{-1}\frac{-\gamma_2+\delta_2}{\gamma_1-\delta_1}\right)\right].$$

APPENDIX D
Evaluation of Complex Integral

In the hydrofoil analysis of Section 3.3, it is necessary to find the real and imaginary parts of

$$C_c = \oint_{\text{cavity}} \frac{w(z)}{U_\infty} z dz = -2k^2\ell^2 \int_{-\infty\,(\bar{C}_R)}^{\infty} \frac{w(Q)}{U_\infty} \frac{Q^3}{(k^2+Q^2)^3} dQ. \tag{D-1}$$

From the theory of residues,

$$C_c = -2\Pi i b_1 \tag{D-2}$$

with b_1 = the residue at the triple pole $Q = ik$. Now,

$$b_1 = k^2\ell^2 \frac{d^2}{dQ^2} \left[\frac{Q^3}{(Q+ik)^3} \frac{w(Q)}{U_\infty} \right] \Bigg|_{Q=ik} .$$

On performing the indicated differentiation and noting that $w(ik) = 0$, one obtains

$$b_1 = \frac{k^2\ell^2}{8} \left[\frac{d^2}{dQ^2} \left(\frac{w}{U_\infty} \right)_{ik} - i \frac{3d}{kdQ} \left(\frac{w}{U_\infty} \right)_{ik} \right] . \tag{D-3}$$

From equation (3.39), the derivatives of the complex velocity are

$$\frac{w'(Q)}{U_\infty} = \frac{i}{\sqrt{Q(Q+1)}} \left[(4Q+2)A_o - \frac{D_o}{4Q} + \frac{2\bar{\epsilon}}{\Pi U_\infty} \right]$$

and

$$\frac{w''(Q)}{U_\infty} = \frac{i}{2\sqrt{Q(Q+1)}^{\,3}} \left[-2A_o + \frac{D_o}{4Q}(3+4Q) - \frac{2\bar{\epsilon}}{\Pi U_\infty}(2Q+1) \right] .$$

These derivatives are evaluated at $Q = ik$ and introduced into equation (D-3). The resulting value of b_1 is then substituted into equation (D-2). After some simplification, including the use of equation (3.44) and the closure condition, C_c may be written as

$$
\begin{aligned}
C_c = -\frac{\Pi\sqrt{2k}}{32}\Bigg\{ & 4A_o[(6\ell-1)r-(12\ell+1)ks] + \frac{D_o}{2}[r-(2k+\tfrac{3}{k})s] \\
& + \frac{4\bar{\epsilon}}{\Pi U_\infty}\,[(4k^2+5)r+ks] + i\,\Bigg[4A_o(k[4k^2+5]r+[2k^2+1]s) - \frac{D_o}{2}\left([2k+\tfrac{1}{k}]r-s\right) \\
& - \frac{4\bar{\epsilon}}{\Pi U_\infty}\,(kr-s)\Bigg]\Bigg\} \; . \qquad\qquad (D\text{-}4)
\end{aligned}
$$

APPENDIX E
Solution of Quadratic Equation for $\bar{\epsilon}/U_\infty$

The vorticity parameter $\bar{\epsilon}/U_\infty$ is found as the solution to a quadratic equation. The equation is obtained by combining equations (3.50) and (3.57) and using equation (3.46), the closure condition, to eliminate Σ. Parkin has solved the analogous gravity parameter problem [4]. The nomenclature used here is essentially Parkin's, but the results are somewhat different.

The following simplifying and systematizing terms are introduced:

$$H(k) = \frac{1}{\Pi}\ln[(1+\sqrt{K}\,s)^2+(2k+\sqrt{K}\,r)^2] - k\left(1 - \frac{2}{\Pi}\tan^{-1}\frac{2k+\sqrt{K}\,r}{1+\sqrt{K}\,s}\right) - \frac{2\sqrt{k\ell}\,s}{\Pi(k+\sqrt{\ell})},$$

$$C_1(k) = \frac{1}{2}\sqrt{\frac{K}{\ell}}\,r, \qquad C_2(k) = \frac{1}{2}\sqrt{\frac{K}{\ell}}\,s,$$

$$C_3(k) = \frac{1}{2}\sqrt{\frac{K}{\ell}}\left\{\frac{r}{\Pi}\ln[(1+\sqrt{K}\,s)^2+(2k+\sqrt{K}\,r)^2] + s\left(1 - \frac{2}{\Pi}\tan^{-1}\frac{2k+\sqrt{K}\,r}{1+\sqrt{K}\,s}\right)\right\},$$

$$C_4(k) = \frac{s}{2\sqrt{\ell k}}, \qquad C_5(k) = \frac{r}{2\sqrt{\ell k}},$$

$$C_6(k) = \frac{1}{2\sqrt{\ell k}}\left\{\frac{s}{\Pi}\ln[(1+\sqrt{K}\,s)^2+(2k+\sqrt{K}\,r)^2] - r\left(1 - \frac{2}{\Pi}\tan^{-1}\frac{2k+\sqrt{K}\,r}{1+\sqrt{K}\,s}\right)\right\},$$

$$Q_1(k) = \frac{\Pi\sqrt{\ell k}}{16}\left[\left(2k + \frac{1}{k}\right)r - s\right],$$

$$Q_2(k) = \frac{\Pi\sqrt{\ell k}}{16}[k(4k^2+5)r + (2k^2+1)s],$$

$$Q_3(k) = \frac{\sqrt{\ell k}}{4}(kr-s),$$

and finally

$$X_1 = C_1Q_1 - C_4Q_2 - 1,$$

$$X_2 = C_2Q_1 + C_5Q_2,$$

$$X_3 = C_3Q_1 - C_6Q_2 - Q_3, \quad \text{and}$$

$$X_4 = 2(2k^2+1)\left(\frac{1}{\bar{\epsilon}/U_\infty}\right).$$

By using these terms one may now write

a. Equation (3.46) as

$$\alpha\left(1+\frac{\Sigma}{2}\right)=\frac{k\Sigma}{2}-\frac{\bar{\epsilon}}{U_\infty}H. \tag{E-1}$$

b. Equations (3.38) as

$$4A_o=-\alpha\left(1+\frac{\Sigma}{2}\right)C_4+\frac{\Sigma}{2}C_5-\frac{\bar{\epsilon}}{U_\infty}C_6$$

and

$$\frac{D_o}{2}=-\alpha\left(1+\frac{\Sigma}{2}\right)C_1-\frac{\Sigma}{2}C_2-\frac{\bar{\epsilon}}{U_\infty}C_3.$$

c. the combination of equations (3.57) and (3.50) as

$$X_4\frac{\bar{\epsilon}}{U_\infty}=\alpha Q_1C_1+Q_1C_2\frac{\Sigma}{2}\left(1+\frac{\Sigma}{2}\right)^{-1}+Q_1C_3\frac{\bar{\epsilon}}{U_\infty}\left(1+\frac{\Sigma}{2}\right)^{-1}-\alpha Q_2C_4$$
$$+Q_2C_5\frac{\Sigma}{2}\left(1+\frac{\Sigma}{2}\right)^{-1}-Q_2C_6\frac{\bar{\epsilon}}{U_\infty}\left(1+\frac{\Sigma}{2}\right)^{-1}-Q_3\frac{\bar{\epsilon}}{U_\infty}\left(1+\frac{\Sigma}{2}\right)^{-1}-\alpha.$$

Thus,

$$X_4\frac{\bar{\epsilon}}{U_\infty}=\alpha X_1+\frac{\Sigma}{2}\left(1+\frac{\Sigma}{2}\right)^{-1}X_2+\frac{\bar{\epsilon}}{U_\infty}\left(1+\frac{\Sigma}{2}\right)^{-1}X_3$$

and

$$-\frac{\bar{\epsilon}}{U_\infty}\frac{-X_4+X_3}{1+(\Sigma/2)}+\frac{X_2}{1+(\Sigma/2)}=\alpha X_1+X_2. \tag{E-2}$$

Now, solving equation (E-1) for $(1+\Sigma/2)$ produces

$$1+\frac{\Sigma}{2}=\frac{k+(\bar{\epsilon}/U_\infty)H}{k-\alpha}\ . \tag{E-3}$$

The combination of (E-2) and (E-3) in order to eliminate $(1+\Sigma/2)$ yields

$$\left(\frac{\bar{\epsilon}}{U_\infty}\right)^2HX_4-\frac{\bar{\epsilon}}{U_\infty}\left[-X_4k+X_3(k-\alpha)+HX_2+\alpha X_1H\right]-\alpha(X_1k+X_2)=0. \tag{E-4}$$

The solution of the quadratic equation (E-4) is

$$\frac{\bar{\epsilon}}{U_\infty} = \frac{1}{2X_4}\left\{\left[\frac{-kX_4 + (k-\alpha)X_3}{H} + \alpha X_1 + X_2\right] \pm \sqrt{\left[\frac{-kX_4+(k-\alpha)X_3}{H} + \alpha X_1+X_2\right]^2 + \frac{4X_4\alpha}{H}(kX_1+X_2)}\right\}. \tag{E-5}$$

When $(\epsilon/U_\infty) > 0$ $(X_4 > 0)$, the positive square root must be chosen because otherwise $(\bar{\epsilon}/U_\infty)$ approaches a finite limit as $\epsilon \to 0^+$; this is of course impossible. For $(\epsilon/U_\infty) < 0$ $(X_4 < 0)$, the negative square root is chosen.

APPENDIX F
Computations

The computations for the present work were accomplished at the Stanford University Computation Center on a Burroughs 220 Electronic Data Processing System. The installation at Stanford consists of a Burroughs Algebraic Compiler, the 220 digital computer with 10,000 words of core storage, and peripheral equipment. The compiler accepts symbolic programs written in BALGOL, an algorithmic language based on ALGOL [23] and produces machine-language programs for the computer [24].

The programs listed in this appendix are written in the Stanford version of BALGOL. The BALGOL language statements are reasonably self-evident. In the programs shown, use has been made of the computer's ability to perform repetitive and complex arithmetic calculations with great speed. Note that each FOR statement indicates a group of calculations (delineated by the BEGIN - END pair) which are to be repetitively done. These statements are sometimes nested within each other. For example, if a FOR group is to be repeated 10 times and it contains another FOR group which is to be repeated 10 times, 100 repetitions will occur within the second or nested group. The PROCEDURE SIMPSON 1() is a closed, independent routine which performs numerical integration according to Simpson's Rule; the procedure may be called and used at any time in a program in which the procedure is defined.

When the results are truncated by the computer during calculations and print-out, no rounding occurs. Thus, truncation causes an uncertainty of one unit in the last figure of all the tabulated data.

```
6/29/62   0002MIN                    CEDEPT
    BURROUGHS ALGEBRAIC COMPILER - STANFORD VERSION    7/25/61$
COMMENT  THIS PROGRAM CALCULATES FLOW PARAMETERS AND FORCE COEFFICIENTS
FOR UNIFORM SHEAR FLOW ABOUT CAVITATING WEDGES $
INTEGER I,J,K,N$ ARRAY L(40)$
INPUT DATA(N,FOR I=(1,1,N)$L(I))$ READ($$DATA)$
WRITE($$TOPU)$ FORMAT TOPW(B48,*UNIT WEDGE IN SHEAR FLOW*,W2)$
FOR J=(2,2,6)$
   BEGIN
      ALPHA= 0.04363(J)$ WRITE($$ANG,ANGF)$ WRITE($$FMT1)$
      FOR K=(1,1,N)$
         BEGIN
            Q= 0.3183.ALPHA(LOG((SQRT(L(K))+1)/(SQRT(L(K))-1))+2.0.SQRT
(L(K))/(L(K)-1))$
            SIGMA= 2.0.Q/(1.0-Q)$
            AC= ALPHA((L(K)*1.5)-1.0)$
            BAR= 0.5.AC/(L(K)-1)$
            CD= 0.3183.ALPHA((2+SIGMA)*2).L(K)/(L(K)-1)$
            BO= SQRT(L(K)(L(K)-1))$ T= 2.0.L(K)-1.0+2.0.BO$
            MUF= T*2-1$ DOR= 1-T$ NOR= LOG(SQRT(L(K))+SQRT(L(K)-1))$
            CL= 2.0(2+SIGMA).BAR(BO(1+4T.NOR/MUF)-L(K)+0.5)$
            CM= 0.5(2+SIGMA).BAR(BO(2.L(K)+1)(1+4T.NOR(DOR+2(T+1)BO/(2.
L(K)+1)))/(MUF.DOR))-2(L(K)*2)+2.0/3.0)$
            WRITE($$RESULTS,FMT2)$
         END$
      WRITE($$SPACE)$
   END$
OUTPUT ANG(ALPHA)$ FORMAT ANGF(B52,*ALPHA =*,S7.5,W2)$
OUTPUT RESULTS(SIGMA,L(K),AC,BAR,CD,CL,CM)$
FORMAT FMT1(B35,*SIGMA*,B5,*L*,B6,*AREA*,B3,*EPSIBAR*,B4,*CD*,B6,*CL*,B
6,*CM*,W0,B61,*EPSI*,B10,* EPSI/U  EPSI/U *,W2)$
FORMAT FMT2(B34,S6.4,S8.4,S9.5,4S8.4,W0)$ FORMAT SPACE(W0)$
FINISH$

6/29/62   0005MIN                    CEDEPT
    BURROUGHS ALGEBRAIC COMPILER - STANFORD VERSION    7/25/61$
COMMENT THIS PROGRAM CALCULATES THE PRESSURE COEFFICIENT FOR UNIFORM
SHEAR FLOW ABOUT CAVITATING WEDGES $
INTEGER I,J,K,N$ ARRAY L(40)$
INTEGER W$
INPUT DATA(N,FOR I=(1,1,N)$L(I))$ READ($$DATA)$
EPSI= 0.02$
FOR I=(1,1,2)$
   BEGIN
      EPSI= 2.0.EPSI$ WRITE($$VORT,VORTF)$
      FOR J=(2,2,6)$
         BEGIN
            ALPHA= 0.04363(J)$ WRITE($$ANG,ANGF)$
            FOR K=(1,1,N)$
               BEGIN
                  Q= 0.3183.ALPHA(LOG((SQRT(L(K))+1)/(SQRT(L(K))-1))+2.
0.SQRT(L(K))/(L(K)-1))$
                  SIGMA= 2.0.Q/(1.0-Q)$
                  AC= ALPHA((L(K)*1.5)-1.0)$
                  EPSIBAR= EPSI(0.5.AC/(L(K)-1))$
                  NOR= LOG(SQRT(L(K))+SQRT(L(K)-1))$
                  BO= SQRT(L(K)(L(K)-1))$ T= 2.0.L(K)-1.0+2.0.BO$
                  MUF= T*2-1.0$ DOR= 1.0-T$
                  WRITE($$EL,FMT3)$ WRITE($$FMT1)$
                  THETA = 0.0$
                  FOR W=(1,1,10)$
                     BEGIN
                        TP= THETA+1.72788$
                        X= L(K)(COS(THETA)*2)/(L(K)-(SIN(THETA)*2))$
                        XP= L(K)(COS(TP)*2)/(L(K)-(SIN(TP)*2))$
                        CPU= (2+SIGMA)(0.3183.ALPHA(2+SIGMA)(SIN(THETA)
/(L(K)-1)+LOG(ABS((1+SIN(THETA))/(1-SIN(THETA)))))+EPSIBAR(0.6366.THETA
-1+0.6366.DOR.NOR.TAN(THETA)/(1+T)+X))$
                        CPL= (2+SIGMA)(0.3183.ALPHA(2+SIGMA)(SIN(TP)/(L
(K)-1)+LOG(ABS((1+SIN(TP))/(1-SIN(TP)))))+EPSIBAR(0.6366.TP-1+0.6366.DO
R.NOR.TAN(TP)/(1+T)-XP))$
                        WRITE($$RESULTS2,FMT22)$
                        THETA= THETA+0.15708$
                     END$
                  WRITE($$SPACE)$ FORMAT SPACE(W0)$
               END$
         END$
   END$
OUTPUT VORT(EPSI)$ FORMAT VORTF(B51,*EPSILON/U =*,S4.2,W2)$
OUTPUT ANG(ALPHA)$ FORMAT ANGF(B52,*ALPHA =*,S7.5,W2)$
OUTPUT EL(L(K),SIGMA)$
OUTPUT RESULTS2(X,CPU,XP,CPL)$
FORMAT FMT1(B46,*XU*,B6,*CPU*,B5,*XL*,B6,*CPL*,W2)$
FORMAT FMT22(B44,S5.4,B2,S7.4,B2,S5.4,B2,S7.4,W0)$
FORMAT FMT3(B46,*L =*,S7.5,B2,*SIGMA =*,S6.4,W2)$
FINISH$

6/29/62   0009MIN                    CEDEPT
    BURROUGHS ALGEBRAIC COMPILER - STANFORD VERSION    7/25/61$
COMMENT CALCULATION OF CAVITY SHAPE FOR ASYMMETRIC WEDGE FLOW$
INTEGER I,J,K,N,P$ ARRAY L(10),SIGMA(10),EPSIBAR(10)$
INPUT DATA(N,P,ALPHA,FOR K=(1,1,N)$(L(K),SIGMA(K),EPSIBAR(K)))$
READ($$DATA)$
WRITE($$TOPCP,FMT5)$
PROCEDURE SIMPSON1(X,Y,TERM,P$$F())$
   BEGIN
      INTEGER I,P$
      H=0.5(X-Y)/P$
      S=F(Y)+F(X)+4.0F(X-H)$
      FOR I=(1,2,2P-3)$
      S=S+4.0F(Y+I.H)+2.0F(Y+(I+1)H)$
      SIMPSON1()=0.3333333(S.H)$
      RETURN$
   END$
FUNCTION FU(X)=(A(X-1/X)+E(X*2-1)/(X*2+1)+0.6366.EPSIBAR(K).LOG(X)/(1+0
.5SIGMA(K))-1.2732.ALPHA.ARCTAN(1/X))(X(X*4-1)/(((X*2+T)*2)((X*2+R)*2))
) $
FUNCTION FL(X)=(A(X-1/X)-E(X*2-1)/(X*2+1)-0.6366.EPSIBAR(K).LOG(X)/(1+0
.5SIGMA(K))-1.2732.ALPHA.ARCTAN(1/X))(X(X*4-1)/(((X*2+T)*2)((X*2+R)*2))
) $
INTEGER W$ W=P$
FOR K=(1,1,N)$
   BEGIN
      NOR= LOG(SQRT(L(K))+SQRT(L(K)-1))$
      T= 2.0L(K)-1.0+2.0.SQRT(L(K)(L(K)-1))$ DOR= 1.0-T$
      R= 2.0L(K)-1.0-2.0.SQRT(L(K)(L(K)-1))$
      A= ALPHA/(3.14159(L(K)-1))$
      E= 0.6366.EPSIBAR(K).NOR.DOR/((1+T)(1+0.5.SIGMA(K)))$
      X= 1.0      $
      TERMU= 0.0$ TERML= 0.0$ YCU= ALPHA$ YCL= -ALPHA$
      WRITE($$EPS,FMT6)$
      WRITE($$FMT4)$
      FOR J=(1,1,15)$
         BEGIN
            Y=X$
            X= X+J$
            XC= L(K)(1-4(L(K)-1)(X*2)/((X*2+T)(X*2+R)))$
            YCU= YCU-8L(K)(L(K)-1)SIMPSON1(X,Y,TERMU,P$$FU())$
            YCL= YCL+8L(K)(L(K)-1)SIMPSON1(X,Y,TERML,P$$FL())$
            P= P+1$
            WRITE($$RESULT,FMT)$
         END$
      P=W$
      WRITE($$SPACE)$ FORMAT SPACE(W0)$
   END$
OUTPUT RESULT(XC,YCU,YCL)$
OUTPUT TOPCP(ALPHA)$
OUTPUT EPS(EPSIBAR(K),L(K),SIGMA(K))$
FORMAT FMT(B44,3S9.4,W0)$
FORMAT FMT4(B50,*X*,B8,*YU*,B7,*YL*,W2)$
FORMAT FMT5(B46,*CAVITY SHAPE-ASYM WEDGE FLOW*,W2,B52,*ALPHA =*,S7.5,W2
)$
```

```
FORMAT FMT6(B49,*EPSIBAR/U =*,S8.6,W2,B48,*L =*,S5.3,B2,*SIGMA =*,S6.4,
W2)$
FINISH$

6/29/62  0003MIN                    CEDEPT
    BURROUGHS ALGEBRAIC COMPILER - STANFORD VERSION   7/25/61$
COMMENT  THIS PROGRAM CALCULATES FLOW PARAMETERS AND FORCE COEFFICIENTS
FOR SYMMETRIC SHEAR FLOW ABOUT CAVITATING WEDGES$
INTEGER I,J,K,N$ ARRAY L(40)$
INPUT DATA(N,FOR I=(1,1,N)$L(I))$ READ($$DATA)$
WRITE($$SYM)$ FORMAT SYM(B43,*UNIT WEDGE IN SYMMETRIC SHEAR FLOW*,W2)$
EPSI= 0.02$
IN..FOR I=(1,1,2)$
   BEGIN
      EPSI= 2.0.EPSI$ WRITE($$VORT,VORTF)$
      FOR J=(2,2,6)$
         BEGIN
            ALPHA= 0.04363(J)$ WRITE($$ANG,ANGF)$ WRITE($$FMT1)$
            FOR K=(1,1,N)$
               BEGIN
                  Q= 2.ALPHA(LOG((SQRT(L(K))+1)/(SQRT(L(K))-1))+2.SQRT(
L(K))/(L(K)-1))(0.3183)$
                  AC= ALPHA(L(K)*1.5-1)$
                  EPSIBAR= EPSI.AC/(2(L(K)-1))$
                  E= 2.EPSIBAR$
                  SIGMA= (Q-E)/(1-0.5.Q)$
                  CD= 1.2732.ALPHA((1+0.5.SIGMA)*2).L(K)/(L(K)-1)$
                  WRITE($$RESULTS,FMT2)$
               END$
            WRITE($$SPACE)$ FORMAT SPACE(W0)$
         END$
   END$
IF EPSI GTR 0.0$
   BEGIN
      EPSI= -0.02$
      GO TO IN$
   END$
OUTPUT VORT(EPSI)$ FORMAT VORTF(B51,*EPSILON/U =*,S4.2,W2)$
OUTPUT ANG(ALPHA)$ FORMAT ANGF(B53,*ALPHA =*,S7.5,W2)$
OUTPUT RESULTS(SIGMA,L(K),AC,EPSIBAR,CD)$
FORMAT FMT1(B39,*SIGMA*,B5,*L*,B6,*AREA*,B4,*EPSILON/U*,B5,*CD*,W2)$
FORMAT FMT2(B38,S6.4,S8.4,S9.5,S12.8,S8.4,W0)$
FINISH$

6/29/62  0003MIN                    CEDEPT
    BURROUGHS ALGEBRAIC COMPILER - STANFORD VERSION   7/25/61$
COMMENT CALCULATION OF CAVITY SHAPE FOR SYMMETRIC WEDGE FLOW $
INTEGER I,J,K,N,P$ ARRAY L(10),SIGMA(10),EPSI(10)$
INPUT DATA(N,P,ALPHA,FOR K=(1,1,N)$(L(K),SIGMA(K),EPSI(K)))$
READ($$DATA)$
WRITE($$TOPCP,FMT5)$
PROCEDURE SIMPSON1(X,Y,TERM,P$$F())$
   BEGIN
      INTEGER I,P$
      H=0.5(X-Y)/P$
      S=F(Y)+F(X)+4.0F(X-H)$
      FOR I=(1,2,2P-3)$
      S=S+4.0F(Y+I.H)+2.0F(Y+(I+1)H)$
      SIMPSON1()=0.3333333(S.H)$
      RETURN$
   END$
FUNCTION FU(X)=(A(X-1/X)-1.2732.ALPHA.ARCTAN(1/X))(X(X*4-1)/(((X*2+T)*2
)((X*2+R)*2)))$
INTEGER W$ W=P$
FOR K=(1,1,N)$
   BEGIN
      T= 2.0L(K)-1.0+2.0.SQRT(L(K)(L(K)-1))$
      R= 2.0L(K)-1.0-2.0.SQRT(L(K)(L(K)-1))$
      A= ALPHA/(3.14159(L(K)-1))$
      X= 1.0      $
      TERMU= 0.0$ TERML= 0.0$ YCU= ALPHA$ YCL= -ALPHA$
      WRITE($$EPS,FMT6)$
      WRITE($$FMT4)$
      FOR J=(1,1,15)$
         BEGIN
            Y=X$
            X= X+J$
            XC= L(K)(1-4(L(K)-1)(X*2)/((X*2+T)(X*2+R)))$
            YCU= YCU-8L(K)(L(K)-1)SIMPSON1(X,Y,TERMU,P$$FU())$
            YCL=-YCU$
            P= P+1$
            WRITE($$RESULT,FMT)$
         END$
      P=W$
      WRITE($$SPACE)$ FORMAT SPACE(W0)$
   END$
OUTPUT RESULT(XC,YCU,YCL)$
OUTPUT TOPCP(ALPHA)$
OUTPUT EPS(EPSI(K),L(K),SIGMA(K))$
FORMAT FMT(B44,3S9.4,W0)$
FORMAT FMT4(B50,*X*,B8,*YU*,B7,*YL*,W2)$
FORMAT FMT5(B46,*CAVITY SHAPE- SYM WEDGE FLOW*,W2,B52,*ALPHA =*,S7.5,W2
)$
FORMAT FMT6(B52,*EPSILON/U =*,S5.3,W2,B48,*L =*,S5.3,B2,*SIGMA =*,S6.4,
W2)$
FINISH$

6/29/62  0008MIN                    CEDEPT
    BURROUGHS ALGEBRAIC COMPILER - STANFORD VERSION   7/25/61$
COMMENT THIS PROGRAM CALCULATES FLOW PARAMETERS AND FORCE COEFFICIENTS
FOR UNIFORM SHEAR FLOW ABOUT CAVITATING HYDROFOILS $
INTEGER I,J,N,P$ ARRAY L(40)$
INPUT DATA(N,FOR P=(1,1,N)$L(P))$ READ($$DATA)$
EPSI= 0.06
WRITE($$TOP)$ FORMAT TOP(B46,*UNIT HYDROFOIL IN SHEAR FLOW*,W2)$
FOR I=(1,1,3)$
   BEGIN
      WRITE($$VORT,VORTF)$
      FOR J=(1,1,5)$
         BEGIN
            ALPHA= 0.0174533(J)$ WRITE($$ANG,ANGF)$ WRITE($$FMT1H)$
            FOR P=(1,1,N)$
               BEGIN
                  K=SQRT(L(P)-1)$ F=SQRT(K.L(P))$ G=SQRT(K/L(P))$
                  R=SQRT(SQRT(L(P))+1)+SQRT(SQRT(L(P))-1)$
                  S=SQRT(SQRT(L(P))+1)-SQRT(SQRT(L(P))-1)$
                  T=1+S.SQRT(K)$ U=2.K+R.SQRT(K)$
                  H=0.31831.LOG(T*2+U*2)-K(1-0.63662.ARCTAN(U/T))-0.636
62.S.F/(K+SQRT(L(P)))$
                  C1=0.5.R.G$ C2=0.5.S.G$
                  C3=0.5.G(0.31831.R.LOG(T*2+U*2)+S(1-0.63662.ARCTAN(U/
T)))$
                  C4=0.5.S/F$ C5=0.5.R/F$
                  C6=0.5(0.31831.S.LOG(T*2+U*2)-R(1-0.63662.ARCTAN(U/T)
))/F$
                  Q1=0.3927.F((2K+1/K)R-S)/2$
                  Q2=0.3927.F(K(4(K*2)+S)R+(2(K*2)+1)S)/2$
                  Q3=0.2500.F(K.R-S)$
                  X1= C1.Q1-C4.Q2-1$ X2= C2.Q1+C5.Q2$
                  IF EPSI EQL 0.06
                     BEGIN
                        EPSIBAR= 0.0$ GO TO SKIP$
                     END$
                  X3= C3.Q1-C6.Q2-Q3$ X4= 2(2(K*2)+1)/EPSI$
                  PART= (-K.X4+(K-ALPHA)X3)/H+ALPHA.X1+X2$
                  EPSIBAR= EPSI(PART+SQRT((PART)*2+4.ALPHA.X4(K.X1+X2)/
H))/(4(2.L(P)-1))$
               SKIP..M= 0.63662.EPSIBAR(LOG(T*2+U*2)-3.1416.K(1-0.63662.AR
CTAN(U/T))-2.S.F/(K+SQRT(L(P))))$
                  SIGMA= (2.ALPHA+M)/(K-ALPHA)$
                  A=(S(-0.31831.EPSIBAR.LOG(T*2+U*2)-ALPHA(1+0.5.SIGMA)
)+R(EPSIBAR(1-0.63662.ARCTAN(U/T))+0.5.SIGMA))/(8.F)$
                  D=-G(S(EPSIBAR(1-0.63662.ARCTAN(U/T))+( 5.SIGMA)+R(0.
```

```
31831.EPSIBAR.LOG(T*2+U*2)+ALPHA(1+0.5.SIGMA)))$
                    AC=0.3927.F(4A(K(4(K*2)+5)R+(2(K*2)+1)S)-0.5D((2K+1/K
)R-S)-1.2732.EPSIBAR(K.R-S))/(2(2+SIGMA))$
                    CN=0.7854(2+SIGMA)(SQRT(L(P))-K)(ALPHA.K(2+SIGMA)+SIG
MA+0.63662.EPSIBAR(K.LOG(T*2+U*2)+3.1416-2.ARCTAN(U/T)+(2F.R-4L(P)+1)/(
SQRT(L(P))-K)))$
                    CM=3.1416.F(2+SIGMA)(1.2732.EPSIBAR(8(1/6-L(P)*2)/F+(
4L(P)+1)R+K.S)+4A((6L(P)-1)R-(12L(P)+1)K.S)+0.5D(R-(2K+3/K)S))/32$
                    WRITE($$RESULTSH.FMT2H)$
                 ENDS
              WRITE($$SPACE)$
           ENDS
        EPSI= EPSI+0.04$
     ENDS
OUTPUT VORT(EPSI)$FORMAT VORTF(B52.*EPSILON/U =*.S4.2.W2)$
OUTPUT ANG(ALPHA)$FORMAT ANGF(B53.*ALPHA =*.S7.5.W2)$
OUTPUT RESULTSH(SIGMA.L(P).AC.EPSIBAR.CN.CM)$
FORMAT FMT1H(B35.*SIGMA*.B5.*L*.B6.*AREA*.B4.*EPSIBAR/U*.B5.*CN*.B6.*CM
*.W2)$
FORMAT FMT2H(B34.S6.4.S8.4.S9.5.S12.8.2S8.4.W0)$
FORMAT SPACE(W0)$
FINISH$

6/29/62  0002MIN                 CEDEPT
    BURROUGHS ALGEBRAIC COMPILER - STANFORD VERSION   7/25/61$
COMMENT THIS PROGRAM CALCULATES THE PRESSURE COEFFICIENT FOR UNIFORM
SHEAR FLOW ABOUT CAVITATING HYDROFOILS $
INTEGER I.J.N.P.W$ ARRAY L(10).SIGMA(10).ALPHA(10).EPBAR(10)$
INPUT DATA(N.FOR I=(1.1.N)$(L(I).SIGMA(I).ALPHA(I).EPBAR(I)))$
READ($$DATA)$ WRITE($$TOP)$
FOR I=(1.1.N)$
    BEGIN
        WRITE($$INFO.INFOF)$
        K=SQRT(L(I)-1)$ F=SQRT(K.L(I))$ G=SQRT(K/L(I))$
        R=SQRT(SQRT(L(I))+1)+SQRT(SQRT(L(I))-1)$
        S=SQRT(SQRT(L(I))+1)-SQRT(SQRT(L(I))-1)$
        T=1+S.SQRT(K)$ U=2.K+R.SQRT(K)$
        A=(S(-0.31831.EPBAR(I).LOG(T*2+U*2)-ALPHA(I)(1+0.5.SIGMA(I)))+R(E
PBAR(I)(1-0.63662.ARCTAN(U/T))+0.5.SIGMA(I)))/(8.F)$
        D=-G(S(EPBAR(I)(1-0.63662.ARCTAN(U/T))+0.5.SIGMA(I))+R(0.31831.EP
BAR(I).LOG(T*2+U*2)+ALPHA(I)(1+0.5.SIGMA(I))))$
        WRITE($$FMT1)$
      - PSI= 0.05$
        FOR W=(1.1.15)$
            BEGIN
                X=L(I)(PSI*2/(K*2+PSI*2))$
                IF PSI GTR 0.5$
                    BEGIN
                        CP=-(2+SIGMA(I))(-4A.SQRT(PSI(1-PSI))+0.5D.SQRT((1-PS
I)/PSI)+EPBAR(I)(1+X-0.63662(3.14159+ARCTAN(2.SQRT(PSI(1-PSI))/(1-2PSI)
)))))$
                        PSI=PSI+0.05$ GO TO STEP$
                    ENDS
                CP=-(2+SIGMA(I))(-4A.SQRT(PSI(1-PSI))+0.5D.SQRT((1-PSI)/PSI
)+EPBAR(I)(1+X-0.63662.ARCTAN(2.SQRT(PSI(1-PSI))/(1-2PSI))))$
                PSI=PSI+0.1$
                STEP..WRITE($$RESULTS2.FMT22)$
            ENDS
        WRITE($$SPACE)$ FORMAT SPACE(W0)$
    ENDS
OUTPUT INFO(EPBAR(I).ALPHA(I).L(I).SIGMA(I))$
OUTPUT RESULTS2(X.CP)$
FORMAT INFOF(B49.*EPSIBAR/U =*.S8.6.W2.B52.*ALPHA =*.S7.5.W2.B48.*L =*.
S5.3.B2.*SIGMA =*.S6.4.W2)$
FORMAT TOP(B46.*UNIT HYDROFOIL IN SHEAR FLOW*.W2)$
FORMAT FMT1(B54.*X*.B8.*CP*.W2)$
FORMAT FMT22(B52.S5.4.B2.S7.4.W0)$
FINISH$
```

```
6/29/62  0004MIN                 CEDEPT
    BURROUGHS ALGEBRAIC COMPILER - STANFORD VERSION   7/25/61$
COMMENT THIS PROGRAM CALCULATES THE CAVITY SHAPE FOR UNIFORM SHEAR FLOW
PAST SUPERCAVITATING HYDROFOILS$
INTEGER I.J.N.P.W.Z$ ARRAY L(10).SIGMA(10).EPBAR(10)$
INPUT DATA(N.ALPHA.FOR I=(1.1.N)$(L(I).SIGMA(I).EPBAR(I)))$
IN..READ($$DATA)$ WRITE($$TOP.FMT5)$
FOR I=(1.1.N)$
    BEGIN
        WRITE($$EPS.FMT6)$ WRITE($$FMT4)$
        K=SQRT(L(I)-1)$ F=SQRT(K.L(I))$ G=SQRT(K/L(I))$
        R=SQRT(SQRT(L(I))+1)+SQRT(SQRT(L(I))-1)$
        S=SQRT(SQRT(L(I))+1)-SQRT(SQRT(L(I))-1)$
        T=1+S.SQRT(K)$ U=2.K+R.SQRT(K)$
        W2=SQRT(L(I)(L(I)-1))$
        B1=-SQRT(0.5(W2-(K*2)))$ B2=-SQRT(0.5(W2+(K*2)))$
        G1=(K.B2+0.5.B1)/W2$ G2=(K.B1-0.5.B2)/W2$ D1=K.B2/(2.W2)$ D2=K.B1
/(2.W2)$ Q=0.05$
        A=(S(-0.31831.EPBAR(I).LOG(T*2+U*2)-   ALPHA(1+0.5.SIGMA(I)))+R(E
PBAR(I)(1-0.63662.ARCTAN(U/T))+0.5.SIGMA(I)))/(8.F)$
        D=-G(S(EPBAR(I)(1-0.63662.ARCTAN(U/T))+0.5.SIGMA(I))+R(0.31831.EP
BAR(I).LOG(T*2+U*2)+   ALPHA(1+0.5.SIGMA(I))))$
        FOR J=(1.1.20)$
            BEGIN
                X=L(I)(Q*2/(Q*2+K*2))$
                IF X GEQ 1.0$
                    BEGIN
                        I4=-SQRT(Q(Q-1))/(2(K*2+Q*2))-0.25((G2/K)LOG(L(I)((G1
.Q-D1-SQRT(Q(Q-1)))*2+(-G2.Q+D2)*2)/((Q*2+K*2)((G1-D1)*2+(-G2+D2)*2)))-
2G1(ARCTAN(K/Q)-ARCTAN(K)+ARCTAN((-G2.Q+D2)/(G1.Q-D1-SQRT(Q(Q-1))))-ARC
TAN((-G2+D2)/(G1-D1)))/K)$
                        I5=(Q.SQRT(Q(Q-1))/(K*2+Q*2)+D2.LOG(L(I)((G1.Q-D1-SQR
T(Q(Q-1)))*2+(-G1.Q+D2)*2)/((Q*2+K*2)((G1-D1)*2+(-G2+D2)*2)))/(2K)-D1(A
RCTAN(K/Q)-ARCTAN(K)+ARCTAN((-G2.Q+D2)/(G1.Q-D1-SQRT(Q(Q-1))))-ARCTAN((
-G2+D2)/(G1-D1)))/K)/(2(L(I)-1))$
                        I6=-0.5.LOG(ABS(1-2Q-2SQRT(Q(Q-1))))/(Q*2+K*2)-0.5(0.
5.B2.LOG(L(I)((G1.Q-D1-SQRT(Q(Q-1)))*2+(-G2.Q+D2)*2)/((Q*2+K*2)((G1-D1)
*2+(-G2+D2)*2)))/K+B1(ARCTAN(K/Q)-ARCTAN(K)+ARCTAN((-G2.Q+D2)/(G1.Q-D1-
SQRT(Q(Q-1))))-ARCTAN((-G2+D2)/(G1-D1)))/K)/W2$
                        YCL=-ALPHA+4L(I)(K*2)(4A.I4-0.5D.I5-0.63662.EPBAR(I).
I6-ALPHA(2+SIGMA(I))(Q*2-1)/(4L(I)(K*2+Q*2)))/(2+SIGMA(I))$
                        GO TO UPPER$
                    ENDS
                YCL=-ALPHA.X$
                UPPER..T1= LOG((K*2)((G1.Q+D1-SQRT(Q(Q+1)))*2+(G2.Q+D2)*2)/
((D1*2+D2*2)(Q*2+K*2)))$
                T2= ARCTAN(K/Q)+ARCTAN((G2.Q+D2)/(G1.Q+D1-SQRT(Q(Q+1))))-1.
5708-ARCTAN(D2/D1)$
                I1=-0.5.SQRT(Q(Q+1))/(K*2+Q*2)+0.25(G2.T1/K+2G1.T2/K)$
                I2= (Q.SQRT(Q(Q+1))/(K*2+Q*2)+0.25.B1.T1/W2+0.5.B2.T2/W2)/(
2(L(I)-1))$
                I3=-0.5.LOG(1+2Q+2SQRT(Q(Q+1)))/(K*2+Q*2)+(-B2.T1/(2K)+B1.T
2/K)/(2.W2)$
                YCU=-4L(I)(K*2)(4A.I1+0.5D.I2+0.63662.EPBAR(I).I3+ALPHA(2+S
IGMA(I))(Q*2)/(4(K*2)(K*2+Q*2)))/(2+SIGMA(I))$
                WRITE($$RESULT.FMT)$
                Q=Q+0.125.J$
            ENDS
        WRITE($$SPACE)$ FORMAT SPACE(W0)$
    ENDS
OUTPUT RESULT(X.YCU.YCL)$
OUTPUT TOP(ALPHA)$
OUTPUT EPS(EPBAR(I).L(I).SIGMA(I))$
FORMAT FMT4(B50.*X*.B8.*YU*.B7.*YL*.W2)$
FORMAT FMT5(B46.*UNIT HYDROFOIL IN SHEAR FLOW*.W2.B52.*ALPHA =*.S7.5.W2
)$
FORMAT FMT6(B49.*EPSIBAR/U =*.S8.6.W2.B48.*L =*.S5.3.B2.*SIGMA =*.S6.4.
W2)$
FORMAT FMT(B44.3S9.4.W0)$
FINISH$
```

```
6/29/62  0001MIN                 CEDEPT
    BURROUGHS ALGEBRAIC COMPILER - STANFORD VERSION   7/25/61$
COMMENT  THIS PROGRAM CALCULATES FLOW PARAMETERS AND FORCE COEFFICIENTS
FOR SUPERCAVITATING FLOW ABOUT WEDGES IN A TRANSVERSE GRAVITY FIELD $
INTEGER I,J,K,N$ ARRAY L(40)$
INPUT DATA(N,FOR I=(1,1,N)$L(I))$ READ($$DATA)$
WRITE($$TOPW)$ FORMAT TOPW(B47,*UNIT WEDGE IN GRAVITY FLOW*,W2)$
FOR J=(2,2,6)$
   BEGIN
      ALPHA= 0.04363(J)$ WRITE($$ANG,ANGF)$ WRITE($$FMT1)$
      FOR K=(1,1,N)$
         BEGIN
            Q= 0.3183.ALPHA(LOG((SQRT(L(K))+1)/(SQRT(L(K))-1))+2.0.SQRT
(L(K))/(L(K)-1))$
            SIGMA= 2.0.Q/(1.0-Q)$
            AC= ALPHA((L(K)*1.5)-1.0)$
            BAR= 0.5.AC/(L(K)-1)$
            CD= 0.3183.ALPHA((2+SIGMA)*2).L(K)/(L(K)-1)$
            BO= SQRT(L(K)(L(K)-1))$ T= 2.0.L(K)-1.0+2.0.BO$
            MUF= T*2-1$ DOR= 1-T$ NOR= LOG(SQRT(L(K))+SQRT(L(K)-1))$
            CL= 2.BAR(1-(2+SIGMA)(BO(1+4T.NOR/MUF)-L(K)+1))$
            CM= BAR(4.0/3.0-0.5(2+SIGMA)(BO(2.L(K)+1)(1+4T.NOR(DOR+2(T+
1)BO/(2.L(K)+1))/(MUF.DOR))-2(L(K)*2)+2.0))$
            WRITE($$RESULTS,FMT2)$
         END$
      WRITE($$SPACE)$
   END$
OUTPUT ANG(ALPHA)$ FORMAT ANGF(B52,*ALPHA =*,S7.5,W2)$
OUTPUT RESULTS(SIGMA,L(K),AC,BAR,CD,CL,CM)$
FORMAT FMT1(B25,*SIGMA*,B5,*L*,B6,*AREA*,B2,*GBAR(F2)/U*,B2,*CD*,B3,*CL
(F2)*,B2,*CM(F2)*,W2)$
FORMAT FMT2(B24,S6.4,S8.4,S9.5,4S8.4,W0)$  FORMAT SPACE(W0)$
FINISH$

6/29/62  0008MIN                 CEDEPT
    BURROUGHS ALGEBRAIC COMPILER - STANFORD VERSION   7/25/61$
COMMENT THIS PROGRAM CALCULATES THE PRESSURE COEFFICIENT FOR UNIFORM
GRAV. FLOW ABOUT CAVITATING WEDGES $
INTEGER I,J,K,N$ ARRAY L(40)$
INTEGER W$
INPUT DATA(N,FOR I=(1,1,N)$L(I))$ READ($$DATA)$
FOR I= 1,2,4,6$
   BEGIN
      F2=(I*2)$ WRITE($$FROUDE,FROUDEF)$
      FOR J=(2,2,6)$
         BEGIN
            ALPHA= 0.04363(J)$ WRITE($$ANG,ANGF)$
            FOR K=(1,1,N)$
               BEGIN
                  Q= 0.3183.ALPHA(LOG((SQRT(L(K))+1)/(SQRT(L(K))-1))+2.
0.SQRT(L(K))/(L(K)-1))$
                  SIGMA= 2.0.Q/(1.0-Q)$
                  AC= ALPHA((L(K)*1.5)-1.0)$
                  GBAR=(1/F2)(0.5.AC/(L(K)-1))$
                  NOR= LOG(SQRT(L(K))+SQRT(L(K)-1))$
                  BO= SQRT(L(K)(L(K)-1))$ T= 2.0.L(K)-1.0+2.0.BO$
                  MUF= T*2-1.0$ DOR= 1.0-T$
                  WRITE($$EL,FMT3)$ WRITE($$FMT1)$
                  THETA = 0.0$
                  FOR W=(1,1,10)$
                     BEGIN
                        TP= THETA+1.72788$
                        X= L(K)(COS(THETA)*2)/(L(K)-(SIN(THETA)*2))$
                        XP= L(K)(COS(TP)*2)/(L(K)-(SIN(TP)*2))$
                        CPU= (2+SIGMA)(0.3183.ALPHA(2+SIGMA)(SIN(THETA)
/(L(K)-1)+LOG(ABS((1+SIN(THETA))/(1-SIN(THETA)))))-   GBAR(0.6366.THETA
-1+0.6366.DOR.NOR.TAN(THETA)/(1+T)))-2.GBAR.X$
                        CPL= (2+SIGMA)(0.3183.ALPHA(2+SIGMA)(SIN(TP)/(L
(K)-1)+LOG(ABS((1+SIN(TP))/(1-SIN(TP)))))-   GBAR(0.6366.TP-1+0.6366.DO
R.NOR.TAN(TP)/(1+T)))+2.GBAR.XP$
                        WRITE($$RESULTS2,FMT22)$
                        THETA= THETA+0.15708$
                     END$
                  WRITE($$SPACE)$ FORMAT SPACE(W0)$
               END$
         END$
   END$
OUTPUT FROUDE(SQRT(F2)+0.01)$FORMAT FROUDEF(B51,*FROUDE NO =*,S4.2,W2)$
OUTPUT ANG(ALPHA)$ FORMAT ANGF(B52,*ALPHA =*,S7.5,W2)$
OUTPUT EL(L(K),SIGMA)$
OUTPUT RESULTS2(X,CPU,XP,CPL)$
FORMAT FMT1(B46,*XU*,B6,*CPU*,B5,*XL*,B6,*CPL*,W2)$
FORMAT FMT22(B44,S5.4,B2,S7.4,B2,S5.4,B2,S7.4,W0)$
FORMAT FMT3(B46,*L =*,S7.5,B2,*SIGMA =*,S6.4,W2)$
FINISH$

6/29/62  0010MIN                 CEDEPT
    BURROUGHS ALGEBRAIC COMPILER - STANFORD VERSION   7/25/61$
COMMENT CALCULATION OF CAVITY SHAPE FOR WEDGE-GRAVITY FLOW $
INTEGER I,J,K,N,P$ ARRAY L(10),SIGMA(10),GBAR(10)$
INPUT DATA(N,P,ALPHA,FOR K=(1,1,N)$(L(K),SIGMA(K),GBAR(K)))$
READ($$DATA)$
WRITE($$TOPCP,FMT5)$
PROCEDURE SIMPSON1(X,Y,TERM,P$$F())$
   BEGIN
      INTEGER I,P$
      H=0.5(X-Y)/P$
      S=F(Y)+F(X)+4.0F(X-H)$
      FOR I=(1,2,2P-3)$
      S=S+4.0F(Y+I.H)+2.0F(Y+(I+1)H)$
      SIMPSON1()=0.3333333(S.H)$
      RETURN$
   END$
FUNCTION FU(X)=(A(X-1/X)+E(X*2-1)/(X*2+1)    -0.6366.GBAR(K).LOG(X)/(1+0
.5SIGMA(K))-1.2732.ALPHA.ARCTAN(1/X))(X(X*4-1)/(((X*2+T)*2)((X*2+R)*2))
) $
FUNCTION FL(X)=(A(X-1/X)-E(X*2-1)/(X*2+1)    +0.6366.GBAR(K).LOG(X)/(1+0
.5SIGMA(K))-1.2732.ALPHA.ARCTAN(1/X))(X(X*4-1)/(((X*2+T)*2)((X*2+R)*2))
) $
INTEGER W$ W=P$
FOR K=(1,1,N)$
   BEGIN
      NOR= LOG(SQRT(L(K))+SQRT(L(K)-1))$
      T= 2.0L(K)-1.0+2.0.SQRT(L(K)(L(K)-1))$ DOR= 1.0-T$
      R= 2.0L(K)-1.0-2.0.SQRT(L(K)(L(K)-1))$
      A= ALPHA/(3.14159(L(K)-1))$
      E=   -0.6366.GBAR(K).NOR.DOR/((1+T)(1+0.5.SIGMA(K)))$
      X= 1.0      $
      TERMU= 0.0$ TERML= 0.0$ YCU= ALPHA$ YCL= -ALPHA$
      WRITE($$EPS,FMT6)$
      WRITE($$FMT4)$
      FOR J=(1,1,15)$
         BEGIN
            Y=X$
            X= X+J$
            XC= L(K)(1-4(L(K)-1)(X*2)/((X*2+T)(X*2+R)))$
            YCU= YCU-8L(K)(L(K)-1)SIMPSON1(X,Y,TERMU,P$$FU())/(1-GBAR(K
)/(1+0.5.SIGMA(K)))$
            YCL= YCL+8L(K)(L(K)-1)SIMPSON1(X,Y,TERML,P$$FL())/(1+GBAR(K
)/(1+0.5.SIGMA(K)))$
            P= P+1$
            WRITE($$RESULT,FMT)$
         END$
      P=W$
      WRITE($$SPACE)$ FORMAT SPACE(W0)$
   END$
OUTPUT RESULT(XC,YCU,YCL)$
OUTPUT TOPCP(ALPHA)$
OUTPUT EPS(SIGMA(K),GBAR(K))$
FORMAT FMT(B44,3S9.4,W0)$
FORMAT FMT4(B50,*X*,B8,*YU*,B7,*YL*,W2)$
FORMAT FMT5(B46,*CAVITY SHAPE-GRAV-WEDGE FLOW*,W2,B52,*ALPHA =*,S7.5,W2
)$
FORMAT FMT6(B45,*SIGMA =*,S5.4,B2,*GBAR/U =*,S6.5,W2)$
FINISH$
```

UNIT WEDGE IN SHEAR FLOW

ALPHA = .08726

SIGMA	L	AREA	EPSIBAR / EPSI	CD	CL / (EPSI/U)	CM / (EPSI/U)
.4991	1.500	.07304	.0730	.5204	.1915	.0264
.2923	2.000	.15994	.0797	.2918	.2909	.0566
.2221	2.500	.25766	.0858	.2205	.3695	.0779
.1850	3.000	.34615	.0915	.1989	.4383	.0959
.1448	4.000	.61081	.1018	.1703	.5594	.1267
.1081	6.000	1.1951	.1195	.1401	.7668	.1782
.0783	10.00	2.6721	.1404	.1333	1.113	.2635
.0619	15.00	4.9820	.1779	.1265	1.403	.3539
.0527	20.00	7.7175	.2030	.1232	1.810	.4339
.0423	30.00	14.251	.2457	.1198	2.309	.5754
.0323	50.00	30.763	.3139	.1170	3.370	.8152
.0238	90.00	74.416	.4180	.1150	4.973	1.206
.0141	250.0	344.83	.6924	.1131	9.630	2.333
.0100	500.0	979.50	.9774	.1124	14.93	3.621
.0070	1000.	2759.3	1.381	.1119	22.98	5.220

ALPHA = .17452

SIGMA	L	AREA	EPSIBAR / EPSI	CD	CL / (EPSI/U)	CM / (EPSI/U)
1.330	1.500	.14609	.1460	1.048	.5104	.0703
.6847	2.000	.31909	.1595	.8007	.6815	.1325
.4997	2.500	.51533	.1717	.5789	.8315	.1754
.4078	3.000	.73231	.1830	.4830	.9660	.2114
.3123	4.000	1.2216	.2036	.3960	1.206	.2732
.2286	6.000	2.3903	.2390	.3310	1.621	.3769
.1631	10.00	5.3442	.2969	.2888	2.318	.5486
.1278	15.00	9.9641	.3558	.2694	3.001	.7304
.1084	20.00	15.435	.4061	.2599	3.719	.8915
.0865	30.00	28.502	.4914	.2501	4.882	1.175
.0657	50.00	61.527	.6278	.2418	6.852	1.657
.0483	90.00	148.83	.8361	.2356	10.06	2.442
.0289	250.0	689.67	1.384	.2295	19.39	4.701
.0201	500.0	1951.0	1.954	.2271	30.01	7.279
.0141	1000.	5518.6	2.762	.2255	46.13	10.47

ALPHA = .26178

SIGMA	L	AREA	EPSIBAR / EPSI	CD	CL / (EPSI/U)	CM / (EPSI/U)
2.990	1.500	.21914	.2191	6.225	1.147	.1981
1.239	2.000	.47864	.2393	1.748	1.233	.2399
.8567	2.500	.77299	.2576	1.133	1.425	.3008
.6811	3.000	1.0984	.2746	.8984	1.613	.3531
.5002	4.000	1.8326	.3054	.6989	1.962	.4445
.3637	6.000	3.5855	.3585	.5506	2.579	.5996
.2551	10.00	8.0164	.4453	.4708	3.626	.8579
.1981	15.00	14.946	.5337	.4313	4.743	1.131
.1671	20.00	23.152	.6092	.4119	5.795	1.374
.1327	30.00	42.755	.7371	.3920	7.406	1.802
.1003	50.00	92.291	.9417	.3750	10.45	2.527
.0733	90.00	223.26	1.254	.3622	15.28	3.709
.0431	250.0	1094.5	2.077	.3492	29.30	7.102
.0303	500.0	2926.5	2.932	.3441	45.24	10.97
.0213	1000.	8277.9	4.143	.3407	69.45	15.77

EPSILON/U = .04

ALPHA = .08726

L = 2.0000 SIGMA = .2923

XU	CPU	XL	CPL
1.000	.0000	.0477	.9048
.9876	.0690	.1743	.6858
.9498	.1385	.3417	.5519
.8851	.2090	.5135	.4493
.7911	.2818	.6666	.3621
.6666	.3587	.7911	.2833
.5135	.4430	.8851	.2093
.3417	.5411	.9498	.1381
.1743	.6675	.9876	.0686
.0477	.8674	1.000	-.0000

L = 10.000 SIGMA = .0783

XU	CPU	XL	CPL
1.000	.0000	.0271	.7096
.9779	.0387	.1049	.4977
.9132	.0777	.2238	.3817
.8105	.1180	.3696	.2995
.6779	.1607	.5263	.2341
.5263	.2076	.6779	.1785
.3696	.2615	.8106	.1290
.2238	.3267	.9132	.0837
.1049	.4119	.9779	.0411
.0271	.5366	1.000	-.0000

L = 30.000 SIGMA = .0423

XU	CPU	XL	CPL
1.000	.0000	.0252	.7836
.9763	.0339	.0984	.5250
.9073	.0676	.2117	.3947
.7993	.1020	.3532	.3059
.6621	.1380	.5084	.2368
.5084	.1772	.6621	.1791
.3531	.2215	.7993	.1285
.2117	.2735	.9074	.0828
.0984	.3365	.9763	.0403
.0252	.4022	1.000	-.0000

L = 90.000 SIGMA = .0238

XU	CPU	XL	CPL
1.000	.0000	.0247	.9799
.9757	.0286	.0964	.6178
.9054	.0561	.2079	.4525
.7957	.0831	.3480	.3452
.6570	.1103	.5027	.2643
.5027	.1385	.6570	.1980
.3480	.1683	.7957	.1408
.2079	.1990	.9054	.0899
.0964	.2231	.9757	.0434
.0247	.1793	1.000	-.0000

ALPHA = .17452

L = 2.0000 SIGMA = .6847

XU	CPU	XL	CPL
1.000	.0000	.0477	2.474
.9876	.1893	.1743	1.877
.9498	.3798	.3417	1.511
.8851	.5736	.5135	1.231
.7911	.7736	.6666	.9928
.6666	.9849	.7911	.7769
.5135	1.216	.8851	.5741
.3417	1.486	.9498	.3791
.1743	1.835	.9876	.1885
.0477	2.387	1.000	-.0000

L = 10.000 SIGMA = .1631

XU	CPU	XL	CPL
1.000	.0000	.0271	1.530
.9779	.0840	.1049	1.074
.9132	.1687	.2238	.8247
.8105	.2561	.3696	.6473
.6779	.3490	.5263	.5061
.5263	.4510	.6779	.3859
.3696	.5681	.8106	.2792
.2238	.7101	.9132	.1812
.1049	.8961	.9779	.0889
.0271	1.170	1.000	-.0000

L = 30.000 SIGMA = .0865

XU	CPU	XL	CPL
1.000	.0000	.0252	1.627
.9763	.0710	.0984	1.091
.9073	.1416	.2117	.8213
.7993	.2135	.3532	.6367
.6621	.2891	.5084	.4931
.5084	.3713	.6621	.3729
.3531	.4643	.7993	.2677
.2117	.5737	.9074	.1725
.0984	.7066	.9763	.0841
.0252	.8481	1.000	-.0000

L = 90.000 SIGMA = .0483

XU	CPU	XL	CPL
1.000	.0000	.0247	1.997
.9757	.0589	.0964	1.260
.9054	.1155	.2079	.9239
.7957	.1710	.3480	.7052
.6570	.2271	.5027	.5400
.5027	.2853	.6570	.4045
.3480	.3470	.7957	.2878
.2079	.4108	.9054	.1839
.0964	.4619	.9757	.0889
.0247	.3772	1.000	-.0000

ALPHA = .26178

L = 2.0000 SIGMA = 1.239

XU	CPU	XL	CPL
1.000	.0000	.0477	5.387
.9876	.4133	.1743	4.092
.9498	.8293	.3417	3.296
.8851	1.252	.5135	2.686
.7911	1.689	.6666	2.166
.6666	2.152	.7911	1.695
.5135	2.659	.8851	1.253
.3417	3.250	.9498	.8280
.1743	4.014	.9876	.4117
.0477	5.229	1.000	-.0000

L = 10.000 SIGMA = .2551

XU	CPU	XL	CPL
1.000	.0000	.0271	2.482
.9779	.1371	.1049	1.746
.9132	.2755	.2238	1.340
.8105	.4183	.3696	1.052
.6779	.5701	.5263	.8233
.5263	.7371	.6779	.6280
.3696	.9288	.8106	.4544
.2238	1.161	.9132	.2950
.1049	1.466	.9779	.1448
.0271	1.919	1.000	-.0000

L = 30.000 SIGMA = .1327

XU	CPU	XL	CPL
1.000	.0000	.0252	2.537
.9763	.1115	.0984	1.704
.9073	.2224	.2117	1.282
.7993	.3355	.3532	.9948
.6621	.4544	.5084	.7706
.5084	.5839	.6621	.5830
.3531	.7305	.7993	.4187
.2117	.9033	.9074	.2699
.0984	1.113	.9763	.1316
.0252	1.342	1.000	-.0000

L = 90.000 SIGMA = .0733

XU	CPU	XL	CPL
1.000	.0000	.0247	3.055
.9757	.0908	.0964	1.930
.9054	.1781	.2079	1.415
.7957	.2639	.3480	1.080
.6570	.3506	.5027	.8275
.5027	.4409	.6570	.6201
.3480	.5367	.7957	.4413
.2079	.6361	.9054	.2820
.0964	.7173	.9757	.1363
.0247	.5948	1.000	-.0000

EPSILON/U = .08

ALPHA = .08726

L = 2.0000 SIGMA = .2923

XU	CPU	XL	CPL
1.000	.0000	.0477	.9235
.9876	.0692	.1743	.6949
.9498	.1386	.3417	.5972
.8851	.2089	.5135	.4525
.7911	.2811	.6666	.3638
.6666	.3971	.7911	.2840
.5135	.4398	.8851	.2094
.3417	.5357	.9498	.1380
.1743	.6584	.9876	.0685
.0477	.8487	1.000	-.0000

L = 10.000 SIGMA = .0783

XU	CPU	XL	CPL
1.000	.0000	.0271	.7960
.9779	.0375	.1049	.5406
.9132	.0747	.2238	.4093
.8105	.1124	.3696	.3185
.6779	.1518	.5263	.2473
.5263	.1944	.6779	.1873
.3696	.2424	.8106	.1346
.2238	.2991	.9132	.0867
.1049	.3690	.9779	.0422
.0271	.4502	1.000	-.0000

L = 30.000 SIGMA = .0423

XU	CPU	XL	CPL
1.000	.0000	.0252	.9743
.9763	.0307	.0984	.6193
.9073	.0600	.2117	.4593
.7993	.0887	.3532	.3480
.6621	.1175	.5084	.2666
.5084	.1474	.6621	.1996
.3531	.1793	.7993	.1418
.2117	.2129	.9074	.0904
.0984	.2422	.9763	.0435
.0252	.2115	1.000	-.0000

L = 90.000 SIGMA = .0238

XU	CPU	XL	CPL
1.000	.0000	.0247	1.300
.9757	.0212	.0964	.8152
.9054	.0392	.2079	.5792
.7957	.0542	.3480	.4337
.6570	.0664	.5027	.3272
.5027	.0756	.6570	.2418
.3480	.0798	.7957	.1697
.2079	.0722	.9054	.1068
.0964	.0257	.9757	.0509
.0247	-.2209	1.000	-.0000

ALPHA = .17452

L = 2.0000 SIGMA = .6847

XU	CPU	XL	CPL
1.000	.0000	.0477	2.518
.9876	.1897	.1743	1.899
.9498	.3802	.3417	1.524
.8851	.5733	.5135	1.238
.7911	.7719	.6666	.9967
.6666	.9810	.7911	.7785
.5135	1.209	.8851	.5744
.3417	1.474	.9498	.3780
.1743	1.813	.9876	.1880
.0477	2.343	1.000	-.0000

L = 10.000 SIGMA = .1631

XU	CPU	XL	CPL
1.000	.0000	.0271	1.710
.9779	.0815	.1049	1.163
.9132	.1624	.2238	.8820
.8105	.2446	.3696	.6869
.6779	.3305	.5263	.5336
.5263	.4235	.6779	.4044
.3696	.5285	.8106	.2907
.2238	.6527	.9132	.1875
.1049	.8068	.9779	.0914
.0271	.9900	1.000	-.0000

L = 30.000 SIGMA = .0865

XU	CPU	XL	CPL
1.000	.0000	.0252	2.017
.9763	.0644	.0984	1.284
.9073	.1261	.2117	.9451
.7993	.1864	.3532	.7229
.6621	.2471	.5084	.5539
.5084	.3104	.6621	.4149
.3531	.3781	.7993	.2949
.2117	.4499	.9074	.1880
.0984	.5140	.9763	.0907
.0252	.4585	1.000	-.0000

L = 90.000 SIGMA = .0483

XU	CPU	XL	CPL
1.000	.0000	.0247	2.808
.9757	.0439	.0964	1.660
.9054	.0813	.2079	1.180
.7957	.1126	.3480	.8842
.6570	.1383	.5027	.6673
.5027	.1580	.6570	.4933
.3480	.1679	.7957	.3462
.2079	.1542	.9054	.2181
.0964	.0623	.9757	.1039
.0247	-.4330	1.000	-.0000

ALPHA = .26178

L = 2.0000 SIGMA = 1.239

XU	CPU	XL	CPL
1.000	.0000	.0477	5.466
.9876	.4140	.1743	4.130
.9498	.8300	.3417	3.319
.8851	1.252	.5135	2.699
.7911	1.686	.6666	2.173
.6666	2.145	.7911	1.698
.5135	2.646	.8851	1.254
.3417	3.228	.9498	.8274
.1743	3.976	.9876	.4109
.0477	5.149	1.000	-.0000

L = 10.000 SIGMA = .2551

XU	CPU	XL	CPL
1.000	.0000	.0271	2.763
.9779	.1333	.1049	1.885
.9132	.2657	.2238	1.430
.8105	.4003	.3696	1.114
.6779	.5412	.5263	.8663
.5263	.6941	.6779	.6569
.3696	.8669	.8106	.4724
.2238	1.071	.9132	.3048
.1049	1.327	.9779	.1487
.0271	1.637	1.000	-.0000

L = 30.000 SIGMA = .1327

XU	CPU	XL	CPL
1.000	.0000	.0252	3.134
.9763	.1014	.0984	1.999
.9073	.1986	.2117	1.472
.7993	.2939	.3532	1.127
.6621	.3901	.5084	.8640
.5084	.4986	.6621	.6473
.3531	.5984	.7993	.4603
.2117	.7135	.9074	.2936
.0984	.8186	.9763	.1417
.0252	.7449	1.000	-.0000

L = 90.000 SIGMA = .0733

XU	CPU	XL	CPL
1.000	.0000	.0247	4.285
.9757	.0680	.0964	2.537
.9054	.1262	.2079	1.804
.7957	.1752	.3480	1.352
.6570	.2159	.5027	1.020
.5027	.2476	.6570	.7548
.3480	.2648	.7957	.5300
.2079	.2466	.9054	.3339
.0964	.1106	.9757	.1591
.0247	-.6354	1.000	-.0000

CAVITY SHAPE-ASYM WEDGE FLOW

ALPHA = .17452

EPSIBAR/U = .000000

L = 30.0 SIGMA = .0865

X	YU	YL
1.533	.2398	-.2398
4.041	.4064	-.4064
9.164	.5626	-.5626
15.43	.6152	-.6152
20.69	.5710	-.5710
24.21	.4875	-.4875
26.37	.4032	-.4032
27.65	.3317	-.3317
28.44	.2745	-.2745
28.93	.2294	-.2294
29.24	.1938	-.1938
29.45	.1656	-.1656
29.59	.1429	-.1429
29.69	.1244	-.1244
29.76	.1092	-.1092

EPSIBAR/U = .019656

L = 30.0 SIGMA = .0865

X	YU	YL
1.533	.2432	-.2363
4.041	.4325	-.3804
9.164	.6186	-.5065
15.43	.6792	-.5513
20.69	.6184	-.5236
24.21	.5099	-.4651
26.37	.4028	-.4037
27.65	.3137	-.3498
28.44	.2436	-.3054
28.93	.1892	-.2695
29.24	.1470	-.2406
29.45	.1139	-.2172
29.59	.0876	-.1981
29.69	.0665	-.1823
29.76	.0493	-.1691

EPSIBAR/U = .039313

L = 30.0 SIGMA = .0865

X	YU	YL
1.533	.2467	-.2328
4.041	.4585	-.3543
9.164	.6747	-.4505
15.43	.7431	-.4873
20.69	.6658	-.4763
24.21	.5322	-.4428
26.37	.4026	-.4041
27.65	.2957	-.3678
28.44	.2127	-.3363
28.93	.1491	-.3097
29.24	.1002	-.2874
29.45	.0623	-.2688
29.59	.0324	-.2533
29.69	.0087	-.2401
29.76	-.0105	-.2290

EPSIBAR/U = .000000

L = 90.0 SIGMA = .0483

X	YU	YL
1.552	.2427	-.2427
4.345	.4370	-.4370
11.28	.6926	-.6926
23.11	.9210	-.9210
37.81	1.043	-1.043
51.94	1.045	-1.045
63.27	.9677	-.9677
71.44	.8570	-.8570
77.04	.7437	-.7437
80.82	.6410	-.6410
83.38	.5528	-.5528
85.14	.4787	-.4787
86.36	.4170	-.4170
87.23	.3656	-.3656
87.86	.3226	-.3226

EPSIBAR/U = .033445

L = 90.0 SIGMA = .0483

X	YU	YL
1.552	.2518	-.2336
4.345	.5164	-.3576
11.28	.9190	-.4661
23.11	1.308	-.5331
37.81	1.522	-.5647
51.94	1.517	-.5742
63.27	1.365	-.5695
71.44	1.159	-.5549
77.04	.9533	-.5341
80.82	.7720	-.5100
83.38	.6206	-.4851
85.14	.4969	-.4606
86.36	.3965	-.4375
87.23	.3150	-.4162
87.86	.2485	-.3967

EPSIBAR/U = .066891

L = 90.0 SIGMA = .0483

X	YU	YL
1.552	.2610	-.2245
4.345	.5958	-.2782
11.28	1.145	-.2396
23.11	1.696	-.1452
37.81	2.001	-.0859
51.94	1.988	-.1027
63.27	1.764	-.1712
71.44	1.461	-.2528
77.04	1.163	-.3244
80.82	.9030	-.3790
83.38	.6883	-.4173
85.14	.5150	-.4425
86.36	.3768	-.4581
87.23	.2644	-.4668
87.86	.1743	-.4708

UNIT WEDGE IN SYMMETRIC SHEAR FLOW

EPSILON/U = .04

ALPHA = .08726

SIGMA	L	AREA	EPSILON/U	CD
.4918	1.500	.07304	.00292187	.5174
.2849	2.000	.15954	.00319097	.2900
.2145	2.500	.25766	.00343553	.2270
.1770	3.000	.36615	.00366156	.1974
.1361	4.000	.61081	.00407213	.1689
.0980	6.000	1.1951	.00478077	.1467
.0660	10.00	2.6721	.00593809	.1317
.0472	15.00	4.9820	.00711726	.1247
.0361	20.00	7.7175	.00812369	.1212
.0223	30.00	14.251	.00982828	.1175
.0068	50.00	30.763	.01255665	.1141
-.0099	90.00	74.416	.01672283	.1112
-.0415	250.0	344.83	.02769784	.1069
-.0685	500.0	975.50	.03909856	.1038
-.1038	1000.	2759.3	.05524151	.0999

ALPHA = .17452

SIGMA	L	AREA	EPSILON/U	CD
1.310	1.500	.14609	.00584374	1.826
.6675	2.000	.31909	.00638194	.7905
.4826	2.500	.51533	.00687107	.5706
.3901	3.000	.73231	.00732312	.4760
.2935	4.000	1.2216	.00814426	.3896
.2073	6.000	2.3903	.00956155	.3247
.1374	10.00	5.3442	.01187619	.2819
.0975	15.00	9.9641	.01423453	.2618
.0741	20.00	15.435	.01624739	.2515
.0455	30.00	28.502	.01965657	.2404
.0139	50.00	61.527	.02511331	.2298
-.0201	90.00	148.83	.03344567	.2201
-.0837	250.0	689.67	.05539568	.2047
-.1378	500.0	1951.0	.07819712	.1930
-.2083	1000.	5518.6	.11048302	.1784

ALPHA = .26178

SIGMA	L	AREA	EPSILON/U	CD
2.946	1.500	.21914	.00876562	6.116
1.208	2.000	.47864	.00957291	1.715
.8272	2.500	.77299	.01030661	1.110
.6517	3.000	1.0984	.01098468	.8788
.4776	4.000	1.8324	.01221639	.6820
.3298	6.000	3.5855	.01434233	.5427
.2149	10.00	8.0164	.01781428	.4562
.1511	15.00	14.946	.02135180	.4131
.1143	20.00	23.152	.02437108	.3921
.0698	30.00	42.753	.02948486	.3693
.0212	50.00	92.291	.03766996	.3473
-.0306	90.00	223.24	.05016851	.3267
-.1265	250.0	1034.5	.08309352	.2936
-.2078	500.0	2926.5	.11729568	.2681
-.3136	1000.	8277.9	.16572453	.2371

EPSILON/U = .08

ALPHA = .08726

SIGMA	L	AREA	EPSILON/U	CD
.4845	1.500	.07304	.00584374	.5143
.2776	2.000	.15954	.00638194	.2881
.2068	2.500	.25766	.00687107	.2254
.1690	3.000	.36615	.00732312	.1960
.1274	4.000	.61081	.00814426	.1676
.0879	6.000	1.1951	.00956155	.1453
.0536	10.00	2.6721	.01187619	.1301
.0325	15.00	4.9820	.01423453	.1229
.0194	20.00	7.7175	.01624739	.1192
.0022	30.00	14.251	.01965657	.1151
-.0186	50.00	30.763	.02511331	.1112
-.0438	90.00	74.416	.03344567	.1074
-.0973	250.0	344.83	.05539568	.1009
-.1471	500.0	975.50	.07819712	.0955
-.2146	1000.	2759.3	.11048302	.0886

ALPHA = .17452

SIGMA	L	AREA	EPSILON/U	CD
1.291	1.500	.14609	.01168749	1.805
.6504	2.000	.31909	.01276388	.7804
.4654	2.500	.51533	.01374215	.5627
.3725	3.000	.73231	.01464624	.4690
.2747	4.000	1.2216	.01628852	.3832
.1860	6.000	2.3903	.01912311	.3185
.1117	10.00	5.3442	.02375238	.2792
.0672	15.00	9.9641	.02846907	.2543
.0399	20.00	15.435	.03249477	.2433
.0045	30.00	28.502	.03931315	.2309
-.0379	50.00	61.527	.05022662	.2182
-.0806	90.00	148.83	.06689134	.2092
-.1961	250.0	689.67	.11079136	.1814
-.2958	500.0	1951.0	.15639423	.1616
-.4308	1000.	5518.6	.22096605	.1369

ALPHA = .26178

SIGMA	L	AREA	EPSILON/U	CD
2.902	1.500	.21914	.01753124	6.008
1.177	2.000	.47864	.01914582	1.682
.7978	2.500	.77299	.02061323	1.087
.6222	3.000	1.0984	.02196937	.8594
.4469	4.000	1.8324	.02443279	.6652
.2959	6.000	3.5855	.02868467	.5270
.1747	10.00	8.0164	.03562857	.4378
.1042	15.00	14.946	.04270360	.3953
.0615	20.00	23.152	.04874217	.3727
.0069	30.00	42.753	.05896972	.3472
-.0578	50.00	92.291	.07533993	.3206
-.1346	90.00	223.24	.10033701	.2931
-.2963	250.0	1034.5	.16618705	.2428
-.4459	500.0	2926.5	.23459136	.2016
-.6486	1000.	8277.9	.33144908	.1523

EPSILON/U =-.04

ALPHA = .08726

SIGMA	L	AREA	EPSILON/U	CD
.5064	1.500	.07304	-.00292187	.5234
.2996	2.000	.15954	-.00319097	.2937
.2297	2.500	.25766	-.00343553	.2301
.1930	3.000	.36615	-.00366156	.2003
.1536	4.000	.61081	-.00407213	.1717
.1182	6.000	1.1951	-.00478077	.1495
.0907	10.00	2.6721	-.00593809	.1348
.0766	15.00	4.9820	-.00711726	.1283
.0694	20.00	7.7175	-.00812369	.1252
.0624	30.00	14.251	-.00982828	.1222
.0578	50.00	30.763	-.01255665	.1200
.0577	90.00	74.416	-.01672283	.1189
.0699	250.0	344.83	-.02769784	.1194
.0885	500.0	975.50	-.03909856	.1214
.1179	1000.	2759.3	-.05524151	.1247

ALPHA = .17452

SIGMA	L	AREA	EPSILON/U	CD
1.349	1.500	.14609	-.00584374	1.870
.7018	2.000	.31909	-.00638194	.8110
.5169	2.500	.51533	-.00687107	.5865
.4254	3.000	.73231	-.00732312	.4901
.3312	4.000	1.2216	-.00814426	.4025
.2499	6.000	2.3903	-.00956155	.3374
.1888	10.00	5.3442	-.01187619	.2957
.1581	15.00	9.9641	-.01423453	.2772
.1426	20.00	15.435	-.01624739	.2684
.1276	30.00	28.502	-.01965657	.2601
.1176	50.00	61.527	-.02511331	.2541
.1168	90.00	148.83	-.03344567	.2517
.1409	250.0	689.67	-.05539568	.2556
.1780	500.0	1951.0	-.07819712	.2640
.2364	1000.	5518.6	-.11048302	.2781

ALPHA = .26178

SIGMA	L	AREA	EPSILON/U	CD
3.034	1.500	.21914	-.00876562	6.334
1.270	2.000	.47864	-.00957291	1.782
.8861	2.500	.77299	-.01030661	1.156
.7106	3.000	1.0984	-.01098468	.9183
.5309	4.000	1.8324	-.01221639	.7161
.3976	6.000	3.5855	-.01434233	.5748
.2952	10.00	8.0164	-.01781428	.4877
.2450	15.00	14.946	-.02135180	.4499
.2199	20.00	23.152	-.02437108	.4322
.1956	30.00	42.753	-.02948486	.4155
.1794	50.00	92.291	-.03766996	.4036
.1774	90.00	223.24	-.05016851	.3994
.2129	250.0	1034.5	-.08309352	.4096
.2684	500.0	2926.5	-.11729568	.4296
.3563	1000.	8277.9	-.16572453	.4630

EPSILON/U =-.08

ALPHA = .08726

SIGMA	L	AREA	EPSILON/U	CD
.5137	1.500	.07304	-.00584374	.5265
.3069	2.000	.15954	-.00638194	.2956
.2374	2.500	.25766	-.00687107	.2317
.2010	3.000	.36615	-.00732312	.2018
.1623	4.000	.61081	-.00814426	.1731
.1282	6.000	1.1951	-.00956155	.1509
.1030	10.00	2.6721	-.01187619	.1364
.0912	15.00	4.9820	-.01423453	.1301

.0861	20.00	7.7175	-.01624739	.1272
.0825	30.00	14.291	-.01966657	.1246
.0834	50.00	30.763	-.02511331	.1250
.0915	90.00	74.416	-.03244567	.1228
.1257	250.0	344.83	-.05539568	.1260
.1671	500.0	975.50	-.07519712	.1307
.2288	1000.	2759.3	-.11040302	.1381

ALPHA = .17452

SIGMA	L	AREA	EPSILON/U	CD
1.369	1.500	.14609	-.01148749	1.891
.7189	2.000	.31909	-.01276380	.8213
.5341	2.500	.51535	-.01374215	.5945
.4430	3.000	.73251	-.01464624	.4973
.3900	4.000	1.2216	-.01628852	.4090
.2712	6.000	2.3903	-.01912311	.3438
.2145	10.00	5.3442	-.02375238	.3026
.1884	15.00	9.9641	-.02846907	.2850
.1769	20.00	15.435	-.03249477	.2771
.1686	30.00	28.502	-.03951315	.2702
.1695	50.00	61.527	-.05022662	.2668
.1853	90.00	140.83	-.06689134	.2682
.2533	250.0	689.67	-.11079136	.2831
.3360	500.0	1951.0	-.15639423	.3037
.4592	1000.	5518.6	-.22096605	.3362

ALPHA = .26178

SIGMA	L	AREA	EPSILON/U	CD
3.077	1.500	.21914	-.01753124	6.445
1.301	2.000	.47866	-.01914582	1.816
.9156	2.500	.77299	-.02061323	1.180
.7400	3.000	1.0984	-.02196937	.9384
.5695	4.000	1.8324	-.02443279	.7335
.4315	6.000	3.5855	-.02868467	.5911
.3394	10.00	8.0164	-.03562857	.5049
.2919	15.00	14.946	-.04270360	.4689
.2727	20.00	23.152	-.04874217	.4530
.2585	30.00	42.753	-.05896972	.4396
.2585	50.00	92.291	-.07533993	.4337
.2814	90.00	223.24	-.10035701	.4385
.3827	250.0	1034.5	-.16618708	.4749
.5065	500.0	2926.5	-.23460136	.5265
.6912	1000.	8277.9	-.33144908	.6041

CAVITY SHAPE- SYM WEDGE FLOW

ALPHA = .08726

EPSILON/U = .000

L = 5.20 SIGMA = .1000

X	YU	YL
1.409	.1102	-.1102
2.694	.1394	-.1394
3.911	.1200	-.1200
4.575	.0911	-.0911
4.882	.0673	-.0673
5.026	.0505	-.0505
5.098	.0389	-.0389
5.137	.0308	-.0308
5.159	.0248	-.0248
5.172	.0205	-.0205
5.180	.0171	-.0171
5.186	.0145	-.0145
5.189	.0125	-.0125
5.192	.0108	-.0108
5.194	.0095	-.0095

EPSILON/U =-.000

L = 10.8 SIGMA = .1000

X	YU	YL
1.485	.1161	-.1161
3.406	.1712	-.1712
6.107	.1874	-.1874
8.190	.1631	-.1631
9.375	.1293	-.1293
9.993	.1005	-.1005
10.32	.0789	-.0789
10.49	.0629	-.0629
10.60	.0511	-.0511
10.66	.0422	-.0422
10.70	.0354	-.0354
10.73	.0301	-.0301
10.75	.0259	-.0259
10.76	.0225	-.0225
10.77	.0197	-.0197

EPSILON/U = .000

L = 6.70 SIGMA = .1000

X	YU	YL
1.441	.1126	-.1126
2.961	.1489	-.1489
4.630	.1421	-.1421
5.652	.1126	-.1126
6.155	.0849	-.0849
6.399	.0644	-.0644
6.523	.0498	-.0498
6.590	.0395	-.0395
6.628	.0319	-.0319
6.651	.0263	-.0263
6.666	.0220	-.0220
6.675	.0187	-.0187
6.682	.0161	-.0161
6.686	.0140	-.0140
6.689	.0122	-.0122

EPSILON/U =-.000

L = 120. SIGMA = .1000

X	YU	YL
1.555	.1216	-.1216
4.394	.2209	-.2209
11.60	.3506	-.3506
24.95	.4971	-.4971
43.11	.5948	-.5948
62.58	.6299	-.6299
79.06	.6107	-.6107
93.39	.5601	-.5601
103.2	.4982	-.4982
110.1	.4368	-.4368
114.9	.3812	-.3812
118.3	.3328	-.3328
120.7	.2915	-.2915
122.4	.2566	-.2566
123.7	.2271	-.2271

UNIT HYDROFOIL IN SHEAR FLOW

EPSILON/U = .00

ALPHA = .01745

SIGMA	L	AREA	EPSIBAR/U	CN	CM
.0723	1.250	.02242	.00000000	.0909	.0349
.0626	1.330	.02368	.00000000	.0781	.0293
.0567	1.400	.02500	.00000000	.0706	.0261
.0506	1.500	.02713	.00000000	.0632	.0229
.0411	1.750	.03317	.00000000	.0527	.0185
.0355	2.000	.03994	.00000000	.0470	.0162
.0289	2.500	.05507	.00000000	.0410	.0138
.0249	3.000	.07196	.00000000	.0378	.0125
.0203	4.000	.11023	.00000000	.0344	.0112
.0176	5.000	.15373	.00000000	.0329	.0106
.0137	7.500	.28191	.00000000	.0309	.0098
.0117	10.00	.43378	.00000000	.0300	.0095
.0080	20.00	1.2262	.00000000	.0287	.0090
.0056	40.00	3.4679	.00000000	.0280	.0088
.0045	60.00	6.3709	.00000000	.0278	.0087
.0035	100.0	13.707	.00000000	.0277	.0086

ALPHA = .03490

SIGMA	L	AREA	EPSIBAR/U	CN	CM
.1501	1.250	.04485	.00000000	.1958	.0752
.1293	1.330	.04736	.00000000	.1665	.0625
.1160	1.400	.05001	.00000000	.1497	.0553
.1038	1.500	.05426	.00000000	.1332	.0483
.0839	1.750	.06635	.00000000	.1099	.0386
.0725	2.000	.07989	.00000000	.0975	.0336
.0586	2.500	.11014	.00000000	.0845	.0284
.0506	3.000	.14392	.00000000	.0777	.0257
.0411	4.000	.22046	.00000000	.0706	.0230
.0355	5.000	.30747	.00000000	.0670	.0216
.0277	7.500	.56382	.00000000	.0627	.0200
.0235	10.00	.86756	.00000000	.0607	.0192
.0161	20.00	2.4525	.00000000	.0579	.0182
.0112	40.00	6.9359	.00000000	.0565	.0177
.0091	60.00	12.741	.00000000	.0560	.0175
.0070	100.0	27.415	.00000000	.0556	.0174

ALPHA = .05235

SIGMA	L	AREA	EPSIBAR/U	CN	CM
.2339	1.250	.06728	.00000000	.3170	.1218
.2005	1.330	.07105	.00000000	.2660	.1001
.1805	1.400	.07502	.00000000	.2383	.0880
.1599	1.500	.08139	.00000000	.2106	.0764
.1287	1.750	.09953	.00000000	.1720	.0604
.1105	2.000	.11984	.00000000	.1517	.0523
.0893	2.500	.16522	.00000000	.1305	.0439
.0768	3.000	.21588	.00000000	.1195	.0396
.0623	4.000	.33069	.00000000	.1082	.0352
.0537	5.000	.46120	.00000000	.1023	.0330
.0419	7.500	.84574	.00000000	.0953	.0304
.0355	10.00	1.3013	.00000000	.0921	.0292
.0243	20.00	3.6787	.00000000	.0875	.0275
.0169	40.00	10.403	.00000000	.0852	.0267
.0137	60.00	19.112	.00000000	.0844	.0264
.0105	100.0	41.123	.00000000	.0837	.0262

ALPHA = .06981

SIGMA	L	AREA	EPSIBAR/U	CN	CM
.3245	1.250	.08971	.00000000	.4577	.1758
.2766	1.330	.09473	.00000000	.3868	.1429
.2481	1.400	.10003	.00000000	.3378	.1267
.2190	1.500	.10852	.00000000	.2964	.1075
.1753	1.750	.13271	.00000000	.2395	.0842
.1501	2.000	.15979	.00000000	.2099	.0723
.1208	2.500	.22029	.00000000	.1794	.0603
.1038	3.000	.28784	.00000000	.1636	.0542
.0839	4.000	.44092	.00000000	.1473	.0480
.0723	5.000	.61494	.00000000	.1389	.0448
.0563	7.500	1.1276	.00000000	.1289	.0411
.0476	10.00	1.7351	.00000000	.1243	.0394
.0325	20.00	4.9050	.00000000	.1176	.0370
.0226	40.00	13.871	.00000000	.1143	.0358
.0183	60.00	25.483	.00000000	.1130	.0354
.0141	100.0	54.831	.00000000	.1120	.0350

ALPHA = .08726

SIGMA	L	AREA	EPSIBAR/U	CN	CM
.4228	1.250	.11214	.00000000	.6216	.2387
.3582	1.330	.11841	.00000000	.5107	.1917
.3201	1.400	.12504	.00000000	.4498	.1661
.2815	1.500	.13565	.00000000	.3917	.1421
.2241	1.750	.16589	.00000000	.3129	.1100
.1912	2.000	.19973	.00000000	.2726	.0939
.1534	2.500	.27536	.00000000	.2312	.0777
.1315	3.000	.35981	.00000000	.2099	.0695
.1061	4.000	.55115	.00000000	.1881	.0613
.0912	5.000	.76067	.00000000	.1768	.0571

.0708	7.500	1.4095	.00000000	.1635	.0521
.0599	10.00	2.1689	.00000000	.1573	.0499
.0408	20.00	6.1313	.00000000	.1483	.0467
.0283	40.00	17.339	.00000000	.1436	.0450
.0229	60.00	31.854	.00000000	.1420	.0444
.0176	100.0	68.539	.00000000	.1405	.0440

EPSILON/U = .04

ALPHA = .01745

SIGMA	L	AREA	EPSIBAR/U	CN	CM
.0725	1.250	.02254	.00036900	.0912	.0348
.0628	1.330	.02382	.00036409	.0785	.0292
.0569	1.400	.02516	.00036572	.0710	.0260
.0508	1.500	.02732	.00037230	.0637	.0228
.0414	1.750	.03347	.00039620	.0532	.0185
.0358	2.000	.04037	.00042226	.0476	.0162
.0292	2.500	.05583	.00047145	.0417	.0138
.0253	3.000	.07318	.00051600	.0387	.0125
.0208	4.000	.11275	.00059474	.0356	.0113
.0180	5.000	.15808	.00066411	.0341	.0107
.0143	7.500	.29342	.00081378	.0325	.0100
.0123	10.00	.45649	.00094300	.0320	.0097
.0087	20.00	1.3407	.00136646	.0320	.0095
.0065	40.00	4.0420	.00204253	.0337	.0097
.0056	60.00	7.8584	.00263809	.0357	.0101
.0048	100.0	18.763	.00377025	.0398	.0109

ALPHA = .03490

SIGMA	L	AREA	EPSIBAR/U	CN	CM
.1504	1.250	.04508	.00073773	.1965	.0749
.1298	1.330	.04763	.00072801	.1673	.0623
.1172	1.400	.05032	.00073122	.1505	.0551
.1043	1.500	.05463	.00074440	.1341	.0482
.0845	1.750	.06693	.00079282	.1109	.0385
.0729	2.000	.08072	.00084430	.0987	.0335
.0593	2.500	.11165	.00094272	.0859	.0284
.0514	3.000	.14634	.00103180	.0794	.0258
.0420	4.000	.22544	.00118924	.0727	.0231
.0365	5.000	.31609	.00132800	.0695	.0218
.0288	7.500	.58668	.00162707	.0660	.0204
.0247	10.00	.91269	.00188542	.0648	.0198
.0176	20.00	2.6803	.00273189	.0646	.0192
.0131	40.00	8.0797	.00408291	.0679	.0196
.0112	60.00	15.706	.00527453	.0718	.0204
.0096	100.0	37.493	.00753381	.0800	.0220

ALPHA = .05235

SIGMA	L	AREA	EPSIBAR/U	CN	CM
.2348	1.250	.06761	.00110620	.3182	.1214
.2012	1.330	.07143	.00109168	.2680	.0999
.1812	1.400	.07547	.00109650	.2396	.0878
.1606	1.500	.08193	.00111630	.2120	.0762
.1295	1.750	.10038	.00118824	.1736	.0604
.1114	2.000	.12106	.00126620	.1536	.0522
.0904	2.500	.16744	.00141372	.1328	.0439
.0781	3.000	.21946	.00154736	.1222	.0397
.0637	4.000	.33809	.00178338	.1114	.0355
.0552	5.000	.47402	.00199144	.1061	.0334
.0436	7.500	.87976	.00243985	.1004	.0310
.0373	10.00	1.3685	.00282721	.0984	.0300
.0265	20.00	4.0189	.00409617	.0978	.0291
.0197	40.00	12.113	.00612113	.1025	.0297
.0169	60.00	23.544	.00790635	.1082	.0307
.0144	100.0	56.191	.01129070	.1205	.0332

ALPHA = .06981

SIGMA	L	AREA	EPSIBAR/U	CN	CM
.3253	1.250	.09013	.00147440	.4594	.1754
.2775	1.330	.09523	.00145512	.3826	.1426
.2491	1.400	.10060	.00146155	.3397	.1245
.2201	1.500	.10922	.00148795	.2985	.1075
.1765	1.750	.13381	.00158396	.2418	.0841
.1514	2.000	.16139	.00168783	.2126	.0723
.1223	2.500	.22322	.00188450	.1825	.0604
.1054	3.000	.29256	.00206258	.1672	.0544
.0858	4.000	.45068	.00237727	.1518	.0484
.0743	5.000	.63186	.00265455	.1441	.0453
.0585	7.500	1.1726	.00325221	.1358	.0419
.0501	10.00	1.8242	.00376836	.1328	.0405
.0355	20.00	5.3563	.00545993	.1315	.0392
.0263	40.00	16.142	.00815708	.1375	.0398
.0226	60.00	31.372	.01053521	.1450	.0412
.0195	100.0	74.855	.01504110	.1615	.0445

ALPHA = .08726

SIGMA	L	AREA	EPSIBAR/U	CN	CM
.4239	1.250	.11264	.00184240	.6239	.2382
.3594	1.330	.11901	.00181831	.5132	.1913
.3213	1.400	.12573	.00182638	.4523	.1658
.2829	1.500	.13651	.00185940	.3944	.1419
.2256	1.750	.16724	.00197944	.3160	.1100

.1928	2.000	.20170	.00210926	.2760	.0940
.1553	2.500	.27896	.00235507	.2352	.0779
.1335	3.000	.36562	.00257762	.2146	.0698
.1084	4.000	.56321	.00297078	.1938	.0618
.0937	5.000	.78963	.00331722	.1835	.0578
.0737	7.500	1.4654	.00408480	.1723	.0532
.0630	10.00	2.2795	.00470894	.1680	.0513
.0446	20.00	6.6927	.00682138	.1658	.0494
.0330	40.00	20.166	.01019088	.1729	.0501
.0283	60.00	39.189	.01316842	.1822	.0518
.0242	100.0	93.487	.01878487	.2024	.0558

EPSILON/U = .08

ALPHA = .01745

SIGMA	L	AREA	EPSIBAR/U	CN	CM
.0727	1.250	.02266	.00074520	.0915	.0346
.0630	1.330	.02396	.00073590	.0788	.0291
.0572	1.400	.02532	.00073944	.0714	.0259
.0511	1.500	.02751	.00075320	.0641	.0228
.0417	1.750	.03377	.00080304	.0537	.0184
.0361	2.000	.04080	.00085693	.0482	.0161
.0296	2.500	.05663	.00095965	.0424	.0138
.0257	3.000	.07446	.00105320	.0395	.0126
.0212	4.000	.11540	.00122065	.0367	.0114
.0186	5.000	.16271	.00137024	.0354	.0108
.0149	7.500	.30595	.00169997	.0343	.0102
.0129	10.00	.48177	.00199326	.0342	.0100
.0096	20.00	1.4789	.00301745	.0361	.0101
.0078	40.00	4.8437	.00489810	.0417	.0111
.0075	60.00	10.249	.00688672	.0484	.0124
.0076	100.0	29.688	.01193467	.0662	.0160

ALPHA = .03490

SIGMA	L	AREA	EPSIBAR/U	CN	CM
.1508	1.250	.04531	.00148946	.1972	.0747
.1302	1.330	.04790	.00147084	.1681	.0621
.1177	1.400	.05063	.00147880	.1514	.0550
.1048	1.500	.05501	.00150560	.1350	.0481
.0851	1.750	.06752	.00160528	.1120	.0385
.0736	2.000	.08158	.00171306	.0999	.0335
.0601	2.500	.11321	.00191825	.0875	.0285
.0522	3.000	.14885	.00210540	.0811	.0259
.0429	4.000	.23068	.00243991	.0750	.0233
.0375	5.000	.32525	.00273895	.0721	.0221
.0300	7.500	.61152	.00339775	.0696	.0208
.0261	10.00	.96285	.00398368	.0694	.0203
.0194	20.00	2.9549	.00602887	.0729	.0208
.0157	40.00	9.6726	.00978113	.0839	.0224
.0146	60.00	20.453	.01374289	.0972	.0250
.0152	100.0	59.117	.02376462	.1328	.0321

ALPHA = .05235

SIGMA	L	AREA	EPSIBAR/U	CN	CM
.2351	1.250	.06794	.00223253	.3193	.1211
.2018	1.330	.07182	.00220481	.2693	.0996
.1819	1.400	.07592	.00221966	.2410	.0876
.1614	1.500	.08249	.00225710	.2135	.0761
.1304	1.750	.10124	.00240664	.1794	.0603
.1124	2.000	.12232	.00256826	.1555	.0522
.0915	2.500	.16975	.00287590	.1352	.0440
.0793	3.000	.22318	.00319652	.1249	.0399
.0651	4.000	.34586	.00369791	.1149	.0358
.0568	5.000	.48761	.00410604	.1102	.0336
.0454	7.500	.91670	.00509325	.1060	.0316
.0394	10.00	1.4432	.00597115	.1053	.0309
.0293	20.00	4.4279	.00903425	.1102	.0310
.0236	40.00	14.486	.01464906	.1267	.0339
.0220	60.00	30.612	.02056885	.1466	.0377
.0228	100.0	88.292	.03549246	.1998	.0484

ALPHA = .06981

SIGMA	L	AREA	EPSIBAR/U	CN	CM
.3261	1.250	.09055	.00297466	.4611	.1749
.2784	1.330	.09573	.00293783	.3844	.1422
.2501	1.400	.10119	.00295244	.3416	.1242
.2211	1.500	.10995	.00300770	.3008	.1071
.1777	1.750	.13494	.00320712	.2442	.0840
.1527	2.000	.16303	.00342293	.2153	.0723
.1239	2.500	.22624	.00383255	.1858	.0605
.1071	3.000	.29744	.00420644	.1709	.0546
.0877	4.000	.46091	.00487457	.1564	.0487
.0764	5.000	.64979	.00547135	.1497	.0459
.0610	7.500	1.2215	.00678634	.1434	.0428
.0528	10.00	1.9229	.00795578	.1422	.0418
.0392	20.00	5.8980	.01203364	.1463	.0418
.0319	40.00	19.285	.01950210	.1700	.0455
.0294	60.00	40.727	.02736499	.1964	.0506
.0304	100.0	117.21	.04712080	.2671	.0648

ALPHA = .08726

SIGMA	L	AREA	EPSIBAR/U	CN	CM
.4249	1.250	.11315	.00371573	.6262	.2377
.3605	1.330	.11962	.00366987	.5156	.1909
.3226	1.400	.12645	.00368822	.4569	.1655
.2842	1.500	.13738	.00375750	.3972	.1417
.2272	1.750	.16862	.00400672	.3192	.1099
.1946	2.000	.20371	.00427593	.2795	.0940
.1572	2.500	.28268	.00478820	.2395	.0781
.1357	3.000	.37164	.00525528	.2194	.0701
.1108	4.000	.57585	.00608982	.1998	.0623
.0964	5.000	.81180	.00683546	.1906	.0585
.0768	7.500	1.5259	.00847760	.1818	.0544
.0664	10.00	2.4019	.00993747	.1800	.0529
.0492	20.00	7.3653	.01502702	.1870	.0527
.0395	40.00	24.070	.02434032	.2138	.0572
.0368	60.00	50.798	.03413173	.2467	.0636
.0380	100.0	145.90	.05865206	.3349	.0813

UNIT HYDROFOIL IN SHEAR FLOW

EPSIBAR/U = .000000

ALPHA = .01745

L = 4.00 SIGMA = .0203

X	CP
.0033	.1623
.0297	.0899
.0816	.0664
.1569	.0530
.2529	.0436
.3663	.0362
.4285	.0329
.4937	.0298
.5616	.0267
.6315	.0237
.7032	.0207
.7763	.0175
.8503	.0140
.9250	.0097
1.000	.0000

EPSIBAR/U = .000594

ALPHA = .01745

L = 4.00 SIGMA = .0208

X	CP
.0033	.1682
.0297	.0931
.0816	.0687
.1569	.0548
.2529	.0451
.3663	.0373
.4285	.0339
.4937	.0306
.5616	.0275
.6315	.0244
.7032	.0212
.7763	.0179
.8503	.0142
.9250	.0098
1.000	-.0000

EPSIBAR/U = .001220

ALPHA = .01745

L = 4.00 SIGMA = .0212

X	CP
.0033	.1743
.0297	.0963
.0816	.0710
.1569	.0566
.2529	.0465
.3663	.0384
.4285	.0349
.4937	.0315
.5616	.0282
.6315	.0250
.7032	.0217
.7763	.0182
.8503	.0145
.9250	.0099
1.000	-.0000

EPSIBAR/U = .002221

ALPHA = .06981

L = 1.25 SIGMA = .3257

X	CP
.0123	1.121
.1032	.6825
.2500	.5475
.4110	.4706
.5593	.4141
.6843	.3652
.7377	.3415
.7853	.3177
.8277	.2930
.8653	.2668
.8988	.2384
.9286	.2064
.9551	.1686
.9788	.1194
1.000	-.0000

EPSIBAR/U = .003124

ALPHA = .06981

L = 3.00 SIGMA = .1063

X	CP
.0037	.7484
.0333	.4167
.0909	.3094
.1731	.2484
.2758	.2053
.3961	.1711
.4576	.1557
.5232	.1411
.5903	.1269
.6585	.1127
.7272	.0983
.7961	.0832
.8647	.0664
.9328	.0459
.9999	-.0000

EPSIBAR/U = .004041

ALPHA = .06981

L = 5.00 SIGMA = .0793

X	CP
.0031	.7219
.0279	.3977
.0769	.2923
.1485	.2324
.2409	.1904
.3515	.1572
.4128	.1424
.4776	.1285
.5456	.1150
.6164	.1017
.6896	.0882
.7649	.0742
.8419	.0589
.9204	.0404
1.000	-.0000

EPSIBAR/U = .005805

ALPHA = .06981

L = 10.0 SIGMA = .0514

X	CP
.0027	.7252
.0249	.3966
.0689	.2897
.1342	.2290
.2200	.1865
.3251	.1530
.3846	.1382
.4483	.1243
.5163	.1108
.5882	.0976
.6639	.0843
.7431	.0706
.8256	.0557
.9113	.0380
1.000	-.0000

EPSIBAR/U = .027560

ALPHA = .06981

L = 100. SIGMA = .0236

X	CP
.0025	1.155
.0227	.6240
.0630	.4531
.1235	.3563
.2041	.2886
.3044	.2350
.3623	.2113
.4249	.1888
.4925	.1671
.5649	.1458
.6423	.1245
.7245	.1026
.8115	.0793
.9033	.0525
1.000	-.0000

UNIT HYDROFOIL IN SHEAR FLOW

ALPHA = .06981

EPSIBAR/U = .000000

L = 7.50 SIGMA = .0563

X	YU	YL
.0028	.0010	-.0002
.0351	.0058	-.0024
.2027	.0183	-.0141
.6722	.0372	-.0469
1.547	.0564	-.0985
2.723	.0683	-.1223
3.930	.0696	-.1311
4.947	.0628	-.1289
5.707	.0522	-.1211
6.240	.0409	-.1115
6.604	.0305	-.1022
6.853	.0214	-.0938
7.024	.0137	-.0866
7.144	.0073	-.0805
7.229	.0019	-.0754
7.290	-.0025	-.0710
7.335	-.0062	-.0674
7.369	-.0094	-.0643
7.395	-.0121	-.0616
7.414	-.0145	-.0593

EPSIBAR/U = .003252

L = 7.50 SIGMA = .0585

X	YU	YL
.0028	.0011	-.0002
.0351	.0063	-.0024
.2027	.0200	-.0141
.6722	.0411	-.0469
1.547	.0627	-.0987
2.723	.0762	-.1221
3.930	.0779	-.1309
4.947	.0706	-.1290
5.707	.0589	-.1216
6.240	.0468	-.1124
6.604	.0350	-.1033
6.853	.0250	-.0952
7.024	.0166	-.0881
7.144	.0096	-.0822
7.229	.0038	-.0771
7.290	-.0010	-.0728
7.335	-.0050	-.0692
7.369	-.0085	-.0661
7.395	-.0114	-.0634
7.414	-.0139	-.0612

EPSIBAR/U = .006706

L = 7.50 SIGMA = .0610

X	YU	YL
.0028	.0012	-.0002
.0351	.0069	-.0024
.2027	.0220	-.0141
.6722	.0454	-.0469
1.547	.0695	-.0989
2.723	.0848	-.1219
3.930	.0869	-.1306
4.947	.0788	-.1290
5.707	.0659	-.1219
6.240	.0522	-.1131
6.604	.0395	-.1043
6.853	.0286	-.0964
7.024	.0194	-.0895
7.144	.0117	-.0836
7.229	.0054	-.0786
7.290	.0001	-.0743
7.335	-.0042	-.0707
7.369	-.0079	-.0676
7.395	-.0111	-.0650
7.414	-.0138	-.0627

UNIT WEDGE IN GRAVITY FLOW

ALPHA = .08726

SIGMA	L	AREA	GBAR(F2)/U	CD	CL(F2)	CM(F2)
.4991	1.500	.07304	.0730	.5204	-.2279	-.0507
.2923	2.000	.15954	.0797	.2918	-.3142	-.0721
.2221	2.500	.25764	.0858	.2285	-.3886	-.0907
.1850	3.000	.36615	.0915	.1989	-.4552	-.1072
.1448	4.000	.61081	.1018	.1703	-.5742	-.1365
.1081	6.000	1.1951	.1195	.1481	-.7797	-.1868
.0783	10.00	2.6721	.1484	.1333	-1.125	-.2713
.0619	15.00	4.9820	.1779	.1265	-1.494	-.3612
.0527	20.00	7.7175	.2030	.1232	-1.821	-.4411
.0423	30.00	14.251	.2457	.1198	-2.400	-.5823
.0323	50.00	30.763	.3139	.1170	-3.380	-.8219
.0238	90.00	74.416	.4180	.1150	-4.983	-1.213
.0141	250.0	344.83	.6924	.1131	-9.639	-2.340
.0100	500.0	975.50	.9774	.1124	-14.94	-3.628
.0070	1000.	2759.3	1.381	.1119	-22.99	-5.226

ALPHA = .17452

SIGMA	L	AREA	GBAR(F2)/U	CD	CL(F2)	CM(F2)
1.330	1.500	.14609	.1460	1.848	-.7047	-.1999
.6847	2.000	.31909	.1595	.8007	-.7908	-.2054
.4997	2.500	.51533	.1717	.5785	-.9173	-.2327
.4078	3.000	.73231	.1830	.4830	-1.040	-.2612
.3125	4.000	1.2216	.2036	.3960	-1.269	-.3156
.2206	6.000	2.3903	.2390	.3310	-1.675	-.4133
.1631	10.00	5.3442	.2969	.2888	-2.367	-.5809
.1278	15.00	9.9641	.3558	.2694	-3.106	-.7608
.1084	20.00	15.435	.4061	.2599	-3.764	-.9208
.0865	30.00	28.502	.4914	.2501	-4.925	-1.204
.0657	50.00	61.527	.6278	.2418	-6.893	-1.684
.0483	90.00	148.83	.8361	.2356	-10.10	-2.469
.0285	250.0	689.67	1.384	.2295	-19.43	-4.727
.0201	500.0	1951.0	1.954	.2271	-30.05	-7.305
.0141	1000.	5518.6	2.762	.2255	-46.17	-10.50

ALPHA = .26178

SIGMA	L	AREA	GBAR(F2)/U	CD	CL(F2)	CM(F2)
2.990	1.500	.21914	.2191	6.225	-1.802	-.5950
1.239	2.000	.47864	.2393	1.748	-1.530	-.4376
.8567	2.500	.77299	.2576	1.133	-1.646	-.4479
.6811	3.000	1.0984	.2746	.8984	-1.800	-.4778
.5082	4.000	1.8324	.3054	.6989	-2.117	-.5480
.3637	6.000	3.5855	.3585	.5586	-2.709	-.6866
.2551	10.00	8.0164	.4453	.4708	-3.739	-.9337
.1981	15.00	14.946	.5337	.4313	-4.849	-1.202
.1671	20.00	23.152	.6092	.4119	-5.837	-1.442
.1327	30.00	42.753	.7371	.3920	-7.584	-1.867
.1003	50.00	92.291	.9417	.3790	-10.54	-2.590
.0733	90.00	223.24	1.254	.3622	-15.37	-3.770
.0431	250.0	1034.5	2.077	.3492	-29.39	-7.162
.0303	500.0	2926.5	2.932	.3441	-45.33	-11.03
.0213	1000.	8277.9	4.143	.3407	-69.53	-15.83

FROUDE NO = 1.0

ALPHA = .08726

L = 2.0000 SIGMA = .2923

XU	CPU	XL	CPL
1.000	.0233	.0477	.4174
.9876	.0873	.1743	.4446
.9498	.1566	.3417	.4038
.8851	.2329	.5135	.3551
.7911	.3188	.6666	.3028
.6666	.4180	.7911	.2464
.5135	.5372	.8851	.1854
.3417	.6892	.9498	.1200
.1743	.9087	.9876	.0503
.0477	1.354	1.000	-.0233

L = 10.000 SIGMA = .0783

XU	CPU	XL	CPL
1.000	.0116	.0271	-1.538
.9779	.0809	.1049	-.6185
.9132	.1665	.2238	-.3368
.8105	.2715	.3696	-.1994
.6779	.3996	.5263	-.1159
.5263	.5577	.6779	-.0603
.3696	.7605	.8106	-.0243
.2238	1.045	.9132	-.0049
.1049	1.528	.9779	-.0010
.0271	2.785	1.000	-.0116

L = 30.000 SIGMA = .0423

XU	CPU	XL	CPL
1.000	.0104	.0252	-4.174
.9763	.1277	.0984	-1.926
.9073	.2742	.2117	-1.182
.7993	.4554	.3532	-.7946
.6621	.6786	.5084	-.5431
.5084	.9573	.6621	-.3614
.3531	1.322	.7993	-.2248
.2117	1.851	.9074	-.1236
.0984	2.788	.9763	-.0533
.0252	5.361	1.000	-.0103

L = 90.000 SIGMA = .0238

XU	CPU	XL	CPL
1.000	.0099	.0247	-9.427
.9757	.2311	.0964	-4.515
.9054	.5046	.2079	-2.845
.7957	.8414	.3480	-1.958
.6570	1.256	.5027	-1.376
.5027	1.779	.6570	-.9483
.3480	2.472	.7957	-.6173
.2079	3.496	.9054	-.3583
.0964	5.356	.9757	-.1589
.0247	10.58	1.000	-.0099

ALPHA = .17452

L = 2.0000 SIGMA = .6847

XU	CPU	XL	CPL
1.000	.1092	.0477	1.330
.9876	.2862	.1743	1.303
.9498	.4743	.3417	1.146
.8851	.6779	.5135	.9827
.7911	.9032	.6666	.8175
.6666	1.160	.7911	.6472
.5135	1.465	.8851	.4699
.3417	1.852	.9498	.2847
.1743	2.409	.9876	.0916
.0477	3.531	1.000	-.1092

L = 10.000 SIGMA = .1631

XU	CPU	XL	CPL
1.000	.0484	.0271	-3.151
.9779	.1955	.1049	-1.251
.9132	.3756	.2238	-.6765
.8105	.5953	.3696	-.4003
.6779	.8627	.5263	-.2352
.5263	1.192	.6779	-.1277
.3696	1.615	.8106	-.0598
.2238	2.211	.9132	-.0256
.1049	3.222	.9779	-.0224
.0271	5.851	1.000	-.0483

L = 30.000 SIGMA = .0865

XU	CPU	XL	CPL
1.000	.0425	.0252	-8.504
.9763	.2833	.0984	-3.920
.9073	.5830	.2117	-2.406
.7993	.9527	.3532	-1.619
.6621	1.407	.5084	-1.111
.5084	1.976	.6621	-.7455
.3531	2.720	.7993	-.4713
.2117	3.801	.9074	-.2687
.0984	5.719	.9763	-.1280
.0252	10.98	1.000	-.0424

L = 90.000 SIGMA = .0483

XU	CPU	XL	CPL
1.000	.0404	.0247	-19.06
.9757	.4884	.0964	-9.130
.9054	1.041	.2079	-5.755
.7957	1.722	.3480	-3.964
.6570	2.560	.5027	-2.790
.5027	3.616	.6570	-1.929
.3480	5.017	.7957	-1.262
.2079	7.090	.9054	-.7419
.0964	10.85	.9757	-.3404
.0247	21.44	1.000	-.0402

ALPHA = .26178

L = 2.0000 SIGMA = 1.239

XU	CPU	XL	CPL
1.000	.2965	.0477	3.311
.9876	.6862	.1743	3.035
.9498	1.094	.3417	2.601
.8851	1.528	.5135	2.185
.7911	2.002	.6666	1.783
.6666	2.535	.7911	1.382
.5135	3.160	.8851	.9775
.3417	3.946	.9498	.5633
.1743	5.071	.9876	.1389
.0477	7.304	1.000	-.2965

L = 10.000 SIGMA = .2551

XU	CPU	XL	CPL
1.000	.1136	.0271	-4.839
.9779	.3485	.1049	-1.895
.9132	.6337	.2238	-1.015
.8105	.9794	.3696	-.5996
.6779	1.399	.5263	-.3560
.5263	1.916	.6779	-.2009
.3696	2.581	.8106	-.1065
.2238	3.517	.9132	-.0630
.1049	5.108	.9779	-.0664
.0271	9.241	1.000	-.1135

L = 30.000 SIGMA = .1327

XU	CPU	XL	CPL
1.000	.0978	.0252	-12.99
.9763	.4689	.0984	-5.983
.9073	.9287	.2117	-3.672
.7993	1.495	.3532	-2.475
.6621	2.191	.5084	-1.706
.5084	3.060	.6621	-1.153
.3531	4.201	.7993	-.7406
.2117	5.859	.9074	-.4362
.0984	8.802	.9763	-.2255
.0252	16.87	1.000	-.0977

L = 90.000 SIGMA = .0733

XU	CPU	XL	CPL
1.000	.0920	.0247	-28.93
.9757	.7729	.0964	-13.85
.9054	1.611	.2079	-8.732
.7957	2.643	.3480	-6.020
.6570	3.914	.5027	-4.244
.5027	5.513	.6570	-2.943
.3480	7.638	.7957	-1.937
.2079	10.78	.9054	-1.151
.0964	16.49	.9757	-.5455
.0247	32.58	1.000	-.0918

FROUDE NO = 2.0

ALPHA = .08726

L = 2.0000 SIGMA = .2923

XU	CPU	XL	CPL
1.000	.0058	.0477	.7609
.9876	.0734	.1743	.6186
.9498	.1429	.3417	.5108
.8851	.2151	.5135	.4234
.7911	.2916	.6666	.3460
.6666	.3748	.7911	.2735
.5135	.4689	.8851	.2032
.3417	.5822	.9498	.1337
.1743	.7347	.9876	.0642
.0477	1.003	1.000	-.0098

L = 10.000 SIGMA = .0783

XU	CPU	XL	CPL
1.000	.0029	.0271	.0826
.9779	.0501	.1049	.1865
.9132	.1022	.2238	.1814
.8105	.1605	.3696	.1605
.6779	.2271	.5263	.1367
.5263	.3051	.6779	.1121
.3696	.4005	.8106	.0865
.2238	.5270	.9132	.0593
.1049	.7232	.9779	.0296
.0271	1.163	1.000	-.0029

L = 30.000 SIGMA = .0423

XU	CPU	XL	CPL
1.000	.0026	.0252	-.5990
.9763	.0598	.0984	-.1386
.9073	.1250	.2117	-.0450
.7993	.2003	.3532	-.0080
.6621	.2806	.5084	.0194
.5084	.3946	.6621	.0285
.3531	.5283	.7993	.0302
.2117	.7134	.9074	.0255
.0984	1.020	.9763	.0165
.0252	1.785	1.000	-.0025

L = 90.000 SIGMA = .0238

XU	CPU	XL	CPL
1.000	.0024	.0247	-1.922
.9757	.0048	.0964	-.8133
.9054	.1009	.2079	-.4469
.7957	.2943	.3480	-.2909
.6570	.4298	.5027	-.1929
.5027	.5958	.6570	-.1214
.3480	.8106	.7957	-.0705
.2079	1.118	.9054	-.0347
.0964	1.654	.9757	-.0126
.0247	3.081	1.000	-.0024

ALPHA = .17452

L = 2.0000 SIGMA = .6847

XU	CPU	XL	CPL
1.000	.0273	.0477	2.155
.9876	.2132	.1743	1.718
.9498	.4032	.3417	1.411
.8851	.5999	.5135	1.163
.7911	.8072	.6666	.9460
.6666	1.031	.7911	.7432
.5135	1.284	.8851	.5479
.3417	1.587	.9498	.3558
.1743	1.996	.9876	.1646
.0477	2.706	1.000	-.0273

L = 10.000 SIGMA = .1631

XU	CPU	XL	CPL
1.000	.0121	.0271	.2247
.9779	.1137	.1049	.4262
.9132	.2251	.2238	.4064
.8105	.3495	.3696	.3597
.6779	.4913	.5263	.3001
.5263	.6570	.6779	.2436
.3696	.8598	.8106	.1857
.2238	1.128	.9132	.1248
.1049	1.544	.9779	.0592
.0271	2.475	1.000	-.0121

L = 30.000 SIGMA = .0865

XU	CPU	XL	CPL
1.000	.0106	.0252	-1.197
.9763	.1290	.0984	-.3096
.9073	.2635	.2117	-.0784
.7993	.4186	.3532	.0080
.6621	.6002	.5084	.0462
.5084	.8181	.6621	.0618
.3531	1.093	.7993	.0626
.2117	1.473	.9074	.0506
.0984	2.104	.9763	.0261
.0252	3.673	1.000	-.0106

L = 90.000 SIGMA = .0483

XU	CPU	XL	CPL
1.000	.0101	.0247	-3.876
.9757	.1775	.0964	-1.636
.9054	.3726	.2079	-.9382
.7957	.6026	.3480	-.5965
.6570	.8771	.5027	-.3881
.5027	1.213	.6570	-.2453
.3480	1.648	.7957	-.1436
.2079	2.273	.9054	-.0731
.0964	3.359	.9757	-.0296
.0247	6.252	1.000	-.0100

ALPHA = .26178

L = 2.0000 SIGMA = 1.239

XU	CPU	XL	CPL
1.000	.0741	.0477	4.009
.9876	.4809	.1743	3.798
.9498	.8951	.3417	3.105
.8851	1.322	.5135	2.551
.7911	1.770	.6666	2.065
.6666	2.253	.7911	1.615
.5135	2.794	.8851	1.184
.3417	3.441	.9498	.7623
.1743	4.308	.9876	.3641
.0477	5.807	1.000	-.0741

L = 10.000 SIGMA = .2551

XU	CPU	XL	CPL
1.000	.0284	.0271	.4409
.9779	.1929	.1049	.7310
.9132	.3723	.2238	.6845
.8105	.5721	.3696	.5931
.6779	.7991	.5263	.4961
.5263	1.064	.6779	.3991
.3696	1.388	.8106	.3006
.2238	1.817	.9132	.1981
.1049	2.481	.9779	.0891
.0271	3.961	1.000	-.0283

L = 30.000 SIGMA = .1327

XU	CPU	XL	CPL
1.000	.0244	.0252	-1.794
.9763	.2084	.0984	-.4389
.9073	.4168	.2117	-.0982
.7993	.6566	.3532	.0280
.6621	.9369	.5084	.0814
.5084	1.273	.6621	.1007
.3531	1.697	.7993	.0977
.2117	2.284	.9074	.0785
.0984	3.257	.9763	.0348
.0252	5.674	1.000	-.0244

L = 90.000 SIGMA = .0733

XU	CPU	XL	CPL
1.000	.0230	.0247	-5.864
.9757	.2784	.0964	-2.469
.9054	.5755	.2079	-1.413
.7957	.9253	.3480	-.8986
.6570	1.342	.5027	-.5855
.5027	1.854	.6570	-.3717
.3480	2.516	.7957	-.2199
.2079	3.465	.9054	-.1193
.0964	5.117	.9757	-.0511
.0247	9.515	1.000	-.0229

FROUDE NO = 4.0

ALPHA = .08726

L = 2.0000 SIGMA = .2923

XU	CPU	XL	CPL
1.000	.0014	.0477	.8568
.9876	.0700	.1743	.6621
.9498	.1394	.3417	.5375
.8851	.2106	.5135	.4405
.7911	.2848	.6666	.3568
.6666	.3640	.7911	.2803
.5135	.4519	.8851	.2077
.3417	.5554	.9498	.1372
.1743	.6911	.9876	.0677
.0477	.9154	1.000	-.0014

L = 10.000 SIGMA = .0783

XU	CPU	XL	CPL
1.000	.0007	.0271	.4880
.9779	.0424	.1049	.3877
.9132	.0861	.2238	.3110
.8105	.1328	.3696	.2505
.6779	.1840	.5263	.1998
.5263	.2419	.6779	.1552
.3696	.3105	.8106	.1143
.2238	.3974	.9132	.0754
.1049	.5219	.9779	.0373
.0271	.7502	1.000	-.0007

L = 30.000 SIGMA = .0423

XU	CPU	XL	CPL
1.000	.0006	.0252	.2949
.9763	.0428	.0984	.2834
.9073	.0876	.2117	.2393
.7993	.1365	.3532	.1975
.6621	.1910	.5084	.1601
.5084	.2539	.6621	.1260
.3531	.3298	.7993	.0940
.2117	.4289	.9074	.0628
.0984	.5781	.9763	.0315
.0252	.8910	1.000	-.0006

L = 90.000 SIGMA = .0238

XU	CPU	XL	CPL
1.000	.0006	.0247	-.0457
.9757	.0482	.0964	.1120
.9054	.1000	.2079	.1276
.7957	.1575	.3480	.1183
.6570	.2230	.5027	.1028
.5027	.3000	.6570	.0852
.3480	.3952	.7957	.0664
.2079	.5239	.9054	.0461
.0964	.7289	.9757	.0239
.0247	1.205	1.000	-.0006

ALPHA = .17452

L = 2.0000 SIGMA = .6847

XU	CPU	XL	CPL
1.000	.0068	.0477	2.362
.9876	.1950	.1743	1.821
.9498	.3854	.3417	1.477
.8851	.5804	.5135	1.209
.7911	.7832	.6666	.9781
.6666	.9995	.7911	.7672
.5135	1.239	.8851	.5674
.3417	1.521	.9498	.3736
.1743	1.890	.9876	.1828
.0477	2.499	1.000	-.0068

L = 10.000 SIGMA = .1631

XU	CPU	XL	CPL
1.000	.0030	.0271	1.068
.9779	.0933	.1049	.8486
.9132	.1875	.2238	.6771
.8105	.2881	.3696	.5447
.6779	.3984	.5263	.4339
.5263	.5232	.6779	.3365
.3696	.6707	.8106	.2472
.2238	.8577	.9132	.1624
.1049	1.125	.9779	.0796
.0271	1.631	1.000	-.0030

L = 30.000 SIGMA = .0865

XU	CPU	XL	CPL
1.000	.0026	.0252	.6289
.9763	.0904	.0984	.5980
.9073	.1837	.2117	.5035
.7993	.2851	.3532	.4148
.6621	.3983	.5084	.3357
.5084	.5287	.6621	.2637
.3531	.6861	.7993	.1961
.2117	.8915	.9074	.1304
.0984	1.200	.9763	.0647
.0252	1.846	1.000	-.0026

L = 90.000 SIGMA = .0483

XU	CPU	XL	CPL
1.000	.0025	.0247	-.0785
.9757	.0998	.0964	.2369
.9054	.2054	.2079	.2659
.7957	.3227	.3480	.2484
.6570	.4561	.5027	.2124
.5027	.6129	.6570	.1795
.3480	.8068	.7957	.1361
.2079	1.068	.9054	.0939
.0964	1.486	.9757	.0480
.0247	2.453	1.000	-.0025

ALPHA = .26178

L = 2.0000 SIGMA = 1.239

XU	CPU	XL	CPL
1.000	.0185	.0477	5.183
.9876	.4296	.1743	3.989
.9498	.8453	.3417	3.231
.8851	1.270	.5135	2.642
.7911	1.712	.6666	2.135
.6666	2.182	.7911	1.673
.5135	2.703	.8851	1.235
.3417	3.315	.9498	.8121
.1743	4.117	.9876	.3984
.0477	5.433	1.000	-.0185

L = 10.000 SIGMA = .2551

XU	CPU	XL	CPL
1.000	.0071	.0271	1.760
.9779	.1540	.1049	1.387
.9132	.3070	.2238	1.109
.8105	.4703	.3696	.8914
.6779	.6491	.5263	.7092
.5263	.8512	.6779	.5491
.3696	1.090	.8106	.4024
.2238	1.392	.9132	.2635
.1049	1.825	.9779	.1280
.0271	2.640	1.000	-.0071

L = 30.000 SIGMA = .1327

XU	CPU	XL	CPL
1.000	.0061	.0252	1.006
.9763	.1433	.0984	.9472
.9073	.2888	.2117	.7953
.7993	.4470	.3532	.6540
.6621	.6233	.5084	.5283

.5084	.8263	.6621	.4142
.3531	1.071	.7993	.3072
.2117	1.391	.9074	.2035
.0984	1.871	.9763	.0999
.0252	2.873	1.000	-.0061

L = 90.000 SIGMA = .0733

XU	CPU	XL	CPL
1.000	.0057	.0247	-.0972
.9757	.1548	.0964	.3755
.9054	.3164	.2079	.4158
.7957	.4958	.3480	.3818
.6570	.6997	.5027	.3293
.5027	.9392	.6570	.2711
.3480	1.235	.7957	.2095
.2079	1.635	.9054	.1437
.0964	2.272	.9757	.0724
.0247	3.747	1.000	-.0097

FROUDE NO = 6.0

ALPHA = .08726

L = 2.0000 SIGMA = .2923

XU	CPU	XL	CPL
1.000	.0006	.0477	.8731
.9876	.0693	.1743	.6702
.9498	.1388	.3417	.5425
.8851	.2098	.5135	.4436
.7911	.2836	.6666	.3588
.6666	.3620	.7911	.2815
.5135	.4487	.8851	.2085
.3417	.5504	.9498	.1378
.1743	.6831	.9876	.0683
.0477	.8992	1.000	-.0006

L = 10.000 SIGMA = .0783

XU	CPU	XL	CPL
1.000	.0003	.0271	.5630
.9779	.0410	.1049	.4250
.9132	.0831	.2238	.3350
.8105	.1276	.3696	.2671
.6779	.1760	.5263	.2115
.5263	.2302	.6779	.1632
.3696	.2938	.8106	.1194
.2238	.3734	.9132	.0783
.1049	.4846	.9779	.0387
.0271	.6832	1.000	-.0003

L = 30.000 SIGMA = .0423

XU	CPU	XL	CPL
1.000	.0002	.0252	.4605
.9763	.0396	.0984	.3652
.9073	.0807	.2117	.2920
.7993	.1247	.3532	.2343
.6621	.1730	.5084	.1862
.5084	.2278	.6621	.1441
.3531	.2931	.7993	.1058
.2117	.3763	.9074	.0697
.0984	.4962	.9763	.0346
.0252	.7254	1.000	-.0002

L = 90.000 SIGMA = .0238

XU	CPU	XL	CPL
1.000	.0002	.0247	.3016
.9757	.0415	.0964	.2834
.9054	.0850	.2079	.2377
.7957	.1322	.3480	.1952
.6570	.1848	.5027	.1576
.5027	.2452	.6570	.1235
.3480	.3183	.7957	.0917
.2079	.4138	.9054	.0610
.0964	.5576	.9757	.0306
.0247	.8576	1.000	-.0002

ALPHA = .17452

L = 2.0000 SIGMA = .6847

XU	CPU	XL	CPL
1.000	.0030	.0477	2.400
.9876	.1916	.1743	1.841
.9498	.3821	.3417	1.489
.8851	.5768	.5135	1.217
.7911	.7788	.6666	.9841
.6666	.9936	.7911	.7717
.5135	1.230	.8851	.5710
.3417	1.509	.9498	.3768
.1743	1.871	.9876	.1862
.0477	2.461	1.000	-.0030

L = 10.000 SIGMA = .1631

XU	CPU	XL	CPL
1.000	.0013	.0271	1.224
.9779	.0895	.1049	.9232
.9132	.1805	.2238	.7273
.8105	.2767	.3696	.5797
.6779	.3812	.5263	.4587
.5263	.4984	.6779	.3537
.3696	.6357	.8106	.2585
.2238	.8075	.9132	.1694
.1049	1.047	.9779	.0834
.0271	1.475	1.000	-.0013

L = 30.000 SIGMA = .0865

XU	CPU	XL	CPL
1.000	.0011	.0252	.9672
.9763	.0833	.0984	.7653
.9073	.1689	.2117	.6113
.7993	.2604	.3532	.4902
.6621	.3609	.5084	.3893
.5084	.4751	.6621	.3011
.3531	.6108	.7993	.2208
.2117	.7838	.9074	.1452
.0984	1.033	.9763	.0718
.0252	1.508	1.000	-.0011

L = 90.000 SIGMA = .0483

XU	CPU	XL	CPL
1.000	.0011	.0247	.6248
.9757	.0854	.0964	.5038
.9054	.1744	.2079	.4890
.7957	.2709	.3480	.4013
.6570	.3782	.5027	.3237
.5027	.5016	.6570	.2534
.3480	.6508	.7957	.1880
.2079	.8458	.9054	.1249
.0964	1.139	.9757	.0624
.0247	1.750	1.000	-.0011

ALPHA = .26178

L = 2.0000 SIGMA = 1.239

XU	CPU	XL	CPL
1.000	.0082	.0477	5.252
.9876	.4201	.1743	4.025
.9498	.8361	.3417	3.255
.8851	1.260	.5135	2.659
.7911	1.701	.6666	2.148
.6666	2.169	.7911	1.684
.5135	2.686	.8851	1.245
.3417	3.292	.9498	.8213
.1743	4.081	.9876	.4049
.0477	5.363	1.000	-.0082

L = 10.000 SIGMA = .2551

XU	CPU	XL	CPL
1.000	.0031	.0271	2.005
.9779	.1468	.1049	1.509
.9132	.2949	.2238	1.188
.8105	.4514	.3696	.9466
.6779	.6213	.5263	.7486
.5263	.8118	.6779	.5768
.3696	1.035	.8106	.4213
.2238	1.314	.9132	.2756
.1049	1.703	.9779	.1352
.0271	2.396	1.000	-.0031

L = 30.000 SIGMA = .1327

XU	CPU	XL	CPL
1.000	.0027	.0252	1.524
.9763	.1312	.0984	1.203
.9073	.2651	.2117	.9607
.7993	.4082	.3532	.7699
.6621	.5652	.5084	.6111
.5084	.7435	.6621	.4723
.3531	.9554	.7993	.3460
.2117	1.225	.9074	.2272
.0984	1.614	.9763	.1119
.0252	2.354	1.000	-.0027

L = 90.000 SIGMA = .0733

XU	CPU	XL	CPL
1.000	.0025	.0247	.9707
.9757	.1319	.0964	.9024
.9054	.2684	.2079	.7546
.7957	.4162	.3480	.6189
.6570	.5806	.5027	.4987
.5027	.7698	.6570	.3901
.3480	.9983	.7957	.2890
.2079	1.296	.9054	.1917
.0964	1.745	.9757	.0993
.0247	2.679	1.000	-.0025

CAVITY SHAPE-GRAV-WEDGE FLOW

ALPHA = .17450

SIGMA =.0865 GBAR/U =.01366

X	YU	YL
1.533	.2381	-.2413
4.041	.3911	-.4213
9.164	.5282	-.5959
15.43	.5760	-.6533
20.69	.5429	-.5983
24.21	.4758	-.4987
26.37	.4065	-.4000
27.65	.3465	-.3173
28.44	.2975	-.2520
28.93	.2584	-.2011
29.24	.2270	-.1615
29.45	.2018	-.1302
29.59	.1813	-.1054
29.69	.1645	-.0853
29.76	.1505	-.0690

SIGMA =.0483 GBAR/U =.02325

X	YU	YL
1.552	.2378	-.2474
4.345	.3866	-.4851
11.28	.5434	-.8349
23.11	.6623	-1.167
37.81	.7230	-1.349
51.94	.7304	-1.346
63.27	.7027	-1.220
71.44	.6579	-1.047
77.04	.6077	-.8735
80.82	.5586	-.7196
83.38	.5133	-.5904
85.14	.4729	-.4843
86.36	.4372	-.3976
87.23	.4060	-.3269
87.86	.3787	-.2689

SIGMA =.0865 GBAR/U =.03072

X	YU	YL
1.533	.2361	-.2431
4.041	.3715	-.4393
9.164	.4840	-.6365
15.43	.5255	-.6997
20.69	.5067	-.6316
24.21	.4609	-.5124
26.37	.4108	-.3960
27.65	.3655	-.2998
28.44	.3273	-.2247
28.93	.2957	-.1668
29.24	.2698	-.1222
29.45	.2484	-.0874
29.59	.2308	-.0599
29.69	.2161	-.0380
29.76	.2037	-.0202

SIGMA =.0483 GBAR/U =.05225

X	YU	YL
1.552	.2314	-.2529
4.345	.3204	-.5422
11.28	.3475	-1.004
23.11	.3225	-1.461
37.81	.3019	-1.713
51.94	.3162	-1.704
63.27	.3546	-1.521
71.44	.3962	-1.272
77.04	.4291	-1.027
80.82	.4504	-.8130
83.38	.4616	-.6351
85.14	.4652	-.4909
86.36	.4638	-.3747
87.23	.4591	-.2811
87.86	.4525	-.2052

SIGMA =.0865 GBAR/U =.12270

X	YU	YL
1.533	.2239	-.2522
4.041	.2530	-.5275
9.164	.2177	-.8347
15.43	.2214	-.9260
20.69	.2886	-.7939
24.21	.3709	-.5794
26.37	.4367	-.3768
27.65	.4803	-.2144
28.44	.5065	-.0913
28.93	.5207	.0006
29.24	.5275	.0695
29.45	.5297	.1219
29.59	.5292	.1621
29.69	.5271	.1935
29.76	.5242	.2183

SIGMA =.0483 GBAR/U =.20875

X	YU	YL
1.552	.1887	-.2784
4.345	-.1182	-.8041
11.28	-.9503	-1.779
23.11	-1.928	-2.805
37.81	-2.487	-3.378
51.94	-2.427	-3.342
63.27	-1.951	-2.898
71.44	-1.336	-2.307
77.04	-.7540	-1.734
80.82	-.2664	-1.241
83.38	.1185	-.8400
85.14	.4145	-.5211
86.36	.6399	-.2695
87.23	.8111	-.0709
87.86	.9415	.0867

APPENDIX G
Supercavitating Flow about a Slender Wedge in a Transverse Gravity Field

Here the results of Section 3.1 are used to calculate the flow parameters for a supercavitating flow about a slender wedge in a transverse gravity field. The corresponding flow about a supercavitating, flat-plate hydrofoil has been studied by Parkin [4], while Acosta [5] considered the flow about a slender wedge in a longitudinal gravity field. The purpose of this work is to complete the studies of gravity effects in linearized flow. As in Parkin's work, this treatment of the problem is not capable of describing cavity flows with large, bouyant effects. The theory is expected to be valid when the effects of gravity are of first order smallness consistent with the linearization approximations. The notation used here is consistent with that used previously.

The base flow is an irrotational, inviscid, and incompressible uniform flow extending to infinity. The upstream velocity far from the wedge is U_∞, and the origin of the coordinates (x,y) is taken at the nose of the unit length wedge which is aligned symmetrically in the flow. The reference elevation at infinity is, then, zero. The flow is sketched in Figure 31. The acceleration g due to gravity is directed downward in the minus y-direction, perpendicular to the freestream velocity and wedge path.

In this flow, Bernoulli's equation is given by

$$p_\infty + \tfrac{1}{2}\rho U_\infty^2 = p_o + \tfrac{1}{2}\rho q_o^2 + \rho g y_o = p_c + \tfrac{1}{2}\rho q_c^2 + \rho g y_c, \tag{G-1}$$

with the subscripts referring to infinity, the wedge surface, and the cavity surface respectively. Since the condition of constant pressure in the cavity must be satisfied in steady flow, the non-dimensional cavitation number may be defined as

$$\sigma = \frac{p_\infty - p_c}{\tfrac{1}{2}\rho U_\infty^2}. \tag{G-2}$$

Another characteristic non-dimensional parameter peculiar to gravity flows is the Froude Number F which is given by

$$F^2 = U_\infty^2/g(1),$$

when based on the unit length of the wedge.

In accordance with the assumptions of the linearized theory developed in Section 2, the flow velocities near the body are assumed to be represented by the perturbation components u and v such that

$$\vec{q} = \overrightarrow{(U_\infty + u, v)}$$

at any point in the flow. From equation (G-1), one has, to the first order, on the cavity

$$\frac{u}{U_\infty} = \frac{\sigma}{2} - \frac{gy_c}{U_\infty^2} \, . \tag{G-3}$$

In accordance with the basic assumption of slenderness in the linearized theory, one can argue that the variations in the gravity term in equation (G-3) are small over most of the cavity (see Section 2.1). Thus, the term gy_c/U_∞ may be replaced by an average term $\pm \bar{g}$. The boundary condition (G-3) becomes

$$\left.\begin{aligned} \frac{u}{U_\infty} &= \frac{\sigma}{2} - \frac{\bar{g}}{U_\infty}, \qquad y > 0, \\ \text{and} \qquad \frac{u}{U_\infty} &= \frac{\sigma}{2} + \frac{\bar{g}}{U_\infty}, \qquad y < 0, \end{aligned}\right\} \tag{G-3a}$$

on the cavity surfaces. On the wedge, the boundary condition is given by

$$\frac{dy_o(x)}{dx} = \alpha = \frac{v(x,y_o)}{U_\infty + u(x,y_o)} \, . \tag{G-4}$$

If one lets $U_c = U_\infty \left(1 + \frac{\sigma}{2}\right)$ - a result from the zero gravity case - and expands equation (G-4) in terms of U_c, he finds, to the first order, that and

$$\left.\begin{array}{l} v = \alpha U_c, \ y > 0, \\ \\ v = -\alpha U_c, \ y < 0, \end{array}\right\} \qquad \text{(G-4a)}$$

on the wedge.

From the results of Section 2.2, it follows that the boundary conditions (G-3a) and (G-4a), together with three assumptions - cavity closure, the vanishing of the perturbation velocities at infinity, and smooth separation at the trailing edges of the wedge - are sufficient to determine a solution to a boundary value problem for the complex perturbation velocity w. Recall that w was defined in Section 2.2 as

$$w = u - iv,$$

with w analytic outside the slit x-axis of the physical z-plane. The complete boundary value problem is as follows:

To find $w(z)$, analytic off the slit, such that

D. E. $$\frac{\partial^2 w}{\partial z \partial \bar{z}} = 0$$

B. C.

a) $\text{Real } (w) = \frac{U_\infty \sigma}{2} - \bar{g}, \qquad 1 < x \leq \ell, \ y = 0^+$

b) $\text{Real } (w) = \frac{U_\infty \sigma}{2} + \bar{g}, \qquad 1 < x \leq \ell, \ y = 0^-$

c) $\text{Im } (w) = -\alpha U_c, \qquad 0 \leq x \leq 1, \ y = 0^+$

d) $\text{Im } (w) = \alpha U_c, \qquad 0 \leq x \leq 1, \ y = 0^-$

e) the cavity closes, i.e., the net source strength is zero on the slit.

f) $w(z) \to 0$ as $z \to \infty$.

g) there are no singularities at the trailing edges of the wedge.

As before, $z = x + iy$, and the boundary conditions are applied on the slit x-axis in the complex z-plane.

If $\bar{g} = -\bar{\epsilon}$, the above boundary value problem for a "gravity flow" is precisely the same as that given in Table 1 for a uniform shear flow past a wedge. Again, one sees the similarity, at least in the linearized case, of rotational and gravity flows. Because of this similarity, the results of Section 3.1 may be used directly after appropriate changes of notation.

One finds first that the gravity field has no effect on the cavitation number - cavity length equation or the cavity area. Thus,

$$\frac{\sigma}{2+\sigma} = \frac{\alpha}{\pi}\left(\ln \frac{\sqrt{\ell}+1}{\sqrt{\ell}-1} + \frac{2\sqrt{\ell}}{\ell-1}\right) \tag{G-5}$$

and

$$A_c = \alpha(\ell^{3/2} - 1). \tag{G-6}$$

Second, on the cavity surfaces the horizontal component of the velocity is

$$U_\infty\left(1 + \frac{\sigma}{2}\right) \mp \bar{g}$$

on the upper and lower surfaces respectively. Thus, one has for the cavity shape

$$\frac{y_c}{\ell} = \frac{\alpha}{\ell} + \int_1^x \left(\frac{v}{U_c - \bar{g}}\right) dx$$

on the upper surface and

$$\frac{y_c}{\ell} = -\frac{\alpha}{\ell} + \int_1^x \left(\frac{v}{U_c + \bar{g}}\right) dx$$

on the lower surface. From equations (3.13) of Section 3.1, following substitution of $-\bar{g}$ for $\bar{\epsilon}$, one finds that

a. $$\frac{y_c}{\ell} = \frac{\alpha}{\ell} - \frac{8(\ell-1)}{U_c-\bar{g}} \int_1^t \left[A\left(\zeta - \frac{1}{\zeta}\right) + D\,\frac{\zeta^2-1}{\zeta^2+1} - \frac{2}{\pi}\,\bar{g}\,\ln\zeta - \frac{4\alpha U_c}{\pi}\tan^{-1}\frac{1}{\zeta}\right] \frac{\zeta(\zeta^4-1)\,d\zeta}{(\zeta^2+T)^2(\zeta^2+R)^2}, \qquad t \geq 1, \qquad \text{(G-7)}$$

on the upper surface.

b. $$\frac{y_c}{\ell} = -\frac{\alpha}{\ell} + \frac{8(\ell-1)}{U_c+\bar{g}} \int_1^{|t|} \left[A\left(\zeta - \frac{1}{\zeta}\right) - D\,\frac{\zeta^2-1}{\zeta^2+1} + \frac{2}{\pi}\,\bar{g}\,\ln\zeta - \frac{4\alpha U_c}{\pi}\tan^{-1}\frac{1}{\zeta}\right] \frac{\zeta(\zeta^4-1)\,d\zeta}{(\zeta^2+T)^2(\zeta^2+R)^2}, \qquad t \leq -1, \qquad \text{(G-8)}$$

on the lower surface.

c. $$\frac{x}{\ell} = \left[1 - \frac{4(\ell-1)t^2}{(t^2+T)(t^2+R)}\right]. \qquad \text{(G-9)}$$

Also, from Section 3.1, the constants A and D are

$$A = \frac{\alpha U_c}{\pi(\ell-1)}$$

and

$$D = \frac{-2\bar{g}}{\pi}\,\frac{(1-T)}{(1+T)}\,\ln\left(\sqrt{\ell} + \sqrt{\ell-1}\right).$$

In the above, $T = 2\ell - 1 + 2\sqrt{\ell(\ell-1)}$

and $R = 2\ell - 1 - 2\sqrt{\ell(\ell-1)}$.

The pressure force coefficients are calculated next. The major difference between the rotational and gravity cases occurs in these calculations. This difference is due to the fact that while the rotational effect enters the pressure coefficient C_p only through the perturbation velocity terms, the gravity effect enters through both the velocities and the term $\rho g y_c$ in the Bernoulli equation (G-1). The pressure coefficient C_p is defined to be

$$C_p = \frac{p_o - p_c}{\frac{1}{2}\rho U_\infty^2}. \qquad \text{(G-10)}$$

Thus,

$$C_p = \sigma + \frac{p_o - p_\infty}{\frac{1}{2}\rho U_\infty^2}$$

and, from equation (G-1), one obtains

$$C_p = \sigma + 1 - \frac{q_o^2}{U_\infty^2} - \frac{2gy_o}{U_\infty^2} .$$

In accordance with Parkin's discussion[4] regarding the linear contribution from the second order term $(u/U_\infty)^2$, one obtains after linearization the relation

$$C_p = \mp 2\left(\frac{\bar{g}}{U_\infty}\right)x - (2+\sigma)\left(\frac{u}{U_\infty} - \frac{\sigma}{2}\right), \qquad \text{(G-11)}$$

where $\pm \bar{g}x/U_\infty$ replaces gy_o/U_∞^2 on the upper and lower wedge surfaces respectively. One should refer to Section 2.3 for a detailed discussion of this substitution and should compare equation (G-11) with its rotational equivalent equation (3.14). By using the results of that section, one has

$$C_p = \mp 2\left(\frac{\bar{g}}{U_\infty}\right)x + (2+\sigma)\left\{\frac{\alpha}{\Pi}(2+\sigma)\left(\frac{\sin\theta}{\ell-1} + \ln\left|\frac{1+\sin\theta}{1-\sin\theta}\right|\right)\right.$$
$$\left. - \frac{\bar{g}}{U_\infty}\left[\frac{2\theta}{\Pi} - 1 + \frac{2(1-T)}{\Pi(1+T)}\ln\left(\sqrt{\ell} + \sqrt{\ell-1}\right)\tan\theta\right]\right\} \qquad \text{(G-11a)}$$

with $x = \ell\cos^2\theta/(\ell-\sin^2\theta)$. The minus sign and $0 \leq \theta \leq \Pi/2$ apply to the upper wedge surface; the plus sign and $\Pi/2 \leq \theta \leq \Pi$ apply to the lower surface.

The remainder of the force coefficients are determined from equation (G-11). First, the drag coefficient C_D is given in Table 4 as

$$C_D = \frac{D}{\frac{1}{2}\rho U_\infty^2(2\alpha)} = -\frac{1}{2\alpha}\oint_{\text{BODY}} C_p\,dy. \qquad \text{(G-12)}$$

Since $U_c dy = v dx$ on the wedge and $2uv = -\operatorname{Im} w^2(z)$, one may write

$$C_D = -\frac{1}{2\alpha}\left[\operatorname{Im}\oint_{\text{BODY}}\frac{w^2}{U_\infty^2}\,dz + 2\oint_{\text{BODY}}\mp\left(\frac{\bar{g}}{U_\infty}\right)x\,dy + (2+\sigma)\frac{\sigma}{2}\oint_{\text{BODY}}dy\right].$$

From Section 3.1.2,

$$\operatorname{Im}\oint_{\text{BODY}}\frac{w^2}{U_\infty^2}\,dz = -\operatorname{Im} J_T + (2+\sigma)\oint_{\text{CAV}}\mp\left(\frac{\bar{g}}{U_\infty}\right)dy + (2+\sigma)\frac{\sigma}{2}\oint_{\text{CAV}}dy.$$

The closure condition for this cavity model requires that $\displaystyle\oint_{\text{BODY + CAV}} dy = 0.$

By using these results, one obtains

$$C_D = \frac{1}{2\alpha}\operatorname{Im} J_T - \frac{2+\sigma}{\alpha}\oint_{\text{CAV}}\mp\left(\frac{\bar{g}}{U_\infty}\right)dy - \frac{1}{\alpha^2}\oint_{\text{BODY}}\mp\left(\frac{\bar{g}}{U_\infty}\right)y\,dy$$

since $x = y/\alpha$ on the wedge. Finally, it is easily shown that the last two contour integrals in the above are zero; hence, with the value of J_T given in Appendix B,

$$C_D = \frac{(2+\sigma)^2\alpha}{\pi}\cdot\frac{\ell}{\ell-1}\,. \tag{G-13}$$

Second, the lift coefficient C_L is defined in Table 4 as

$$C_L = \frac{L}{\frac{1}{2}\rho U_\infty^2(\text{CHORD})} = \oint_{\text{BODY}} C_p\,dx.$$

From Equation (G-11),

$$C_L = 2\left(\frac{\bar{g}}{U_\infty}\right)\left(\int_0^1 x\,dx - \int_1^0 x\,dx\right) - (2+\sigma)\oint_{\text{BODY}}\frac{u}{U_\infty}\,dx.$$

After one performs the indicated integrations and notes that $\operatorname{Re}(w/U_\infty)dz = (u/U_\infty)dx$ on the slit, the above equation becomes

$$C_L = 2\left(\frac{\bar{g}}{U_\infty}\right) - (2+\sigma)\operatorname{Re}\oint_{\text{BODY}}\frac{w}{U_\infty}\,dz.$$

The results of Section 3.1.2 show that

$$\mathrm{Re}\oint_{\mathrm{BODY}} \frac{w}{U_\infty}\, dz = \frac{\bar{g}}{U_\infty}\left[2\sqrt{\ell(\ell-1)}\left(1 + \frac{4T}{T^2-1}\,\ln\left(\sqrt{\ell} + \sqrt{\ell-1}\right)\right) - 2(\ell-1)\right].$$

Thus,

$$C_L = 2\,\frac{\bar{g}}{U_\infty}\left[1 - (2+\sigma)\left\{\sqrt{\ell(\ell-1)}\left[1 + \frac{4T}{T^2-1}\,\ln(\sqrt{\ell} + \sqrt{\ell-1})\right] - \ell + 1\right\}\right]. \tag{G-14}$$

Third, the moment coefficient about the nose of the wedge is defined in Table 4 as

$$C_{MO} = \frac{L\cdot(\text{dist. to } L)}{\frac{1}{2}\rho U_\infty^2(\text{CHORD})^2} = \oint_{\mathrm{BODY}} C_p\, x dx.$$

To the first order,

$$C_{MO} = 2\,\frac{\bar{g}}{U_\infty}\left(\int_0^1 x^2 dx - \int_1^0 x^2 dx\right) - (2+\sigma)\oint_{\mathrm{BODY}} u\; x dx.$$

Following simplification and introduction of complex notation, this equation becomes

$$C_{MO} = \frac{4}{3}\left(\frac{\bar{g}}{U_\infty}\right) - (2+\sigma)\;\mathrm{Re}\oint_{\mathrm{BODY}} w z dz.$$

In Section 3.1.2, it is shown that

$$\mathrm{Re}\oint_{\mathrm{BODY}} w z dz = \frac{\bar{g}}{2U_\infty}\left[\sqrt{\ell(\ell-1)}\,(2\ell+1)\left\{1 + \frac{4T\ln(\sqrt{\ell}+\sqrt{\ell-1})}{(T^2-1)(1-T)}\left[\frac{2\sqrt{\ell(\ell-1)}\,(1+T)}{2\ell+1} + 1-T\right]\right\} - 2(\ell^2-1)\right].$$

Thus,

$$C_{MO} = \frac{\bar{g}}{U_\infty}\left[\frac{4}{3} - \frac{2+\sigma}{2}\left(\sqrt{\ell(\ell-1)}\,(2\ell+1)\left[1 + \frac{4T\ln(\sqrt{\ell}+\sqrt{\ell-1})}{(T^2-1)(1-T)}\left(\frac{2\sqrt{\ell(\ell-1)}\,(1+T)}{2\ell+1} + (1-T)\right)\right] - 2(\ell^2-1)\right)\right]. \tag{G-15}$$

Finally, it remains to define the gravitation parameter $\bar{g}/U_\infty$. On the basis of the analogy between the linearized rotational and gravity problems, this definition is taken directly from equation (3.23) of Section 3.1.2; hence,

$$\frac{\bar{g}}{U_\infty} = \left(\frac{g}{U_\infty^2}\right) \frac{A_c}{2(\ell-1)} .$$

By introducing equation (G-6) and the Froude Number F into this result, one has

$$\frac{\bar{g}}{U_\infty} = \frac{\alpha(\ell^{3/2} - 1)}{2F^2(\ell-1)}. \tag{G-16}$$

The complete solution is summarized in Table 9.

Certain results of the gravity flow analysis are the same as those previously obtained in the study of uniform shear flow past a wedge. These duplicated results include the cavity length-cavitation number relationship, the cavity area, and the drag coefficient - all of which are independent of gravity effects. Figures 7 and 8 show the drag coefficient C_D and cavity area A_c as functions of σ. The ℓ-σ relationship is plotted in Figures 16 and 17; the curve for gravity flow is the same as that for irrotational gravity-free flow, i.e., the curve labelled $\epsilon/U_\infty = 0$. As in the gravity-free case, the cavity length is limited in this linearized theory so

$$1 + \frac{2\alpha}{\Pi}\left(1 + \frac{\alpha}{\Pi} \ln \frac{2\Pi}{\alpha}\right) < \ell < \infty.$$

It is possible, however, that as $\ell \to \infty$ $(\sigma \to 0)$, the effects of gravity may be exaggerated. Finally, since $\bar{\epsilon}/\epsilon$ is equal in magnitude to $(\bar{g}/U_\infty)F^2$, Figure 9 gives a plot of both parameters.

The remainder of the numerical results are listed in Appendix F and illustrated in Figures 32 through 37. Figures 32 through 35 picture the pressure force coefficients. The first two figures show the effect of cavitation number on C_L and C_{MO} in a gravity field. Note that both coefficients are linear functions of $1/F^2$. Hence, independent of σ, both coefficients are inverse functions of the square of the Froude number. As σ approaches zero, the lift and moment become negatively infinite for all finite Froude numbers. The limitations of the theory are seen clearly in Figures 34 and 35, which show the pressure coefficient. When the Froude number is small, the gravity effects are large and the pressure coefficient on the lower side of the wedge is negative over the whole body surface. Such a condition (one in which the pressure on the body is always less than the pressure in the cavity) is contradictory. However, as in the case of uniform shear flow past a wedge, it seems permissible to allow a negative pressure in the immediate vicinity of the nose of the wedge for the reasons presented in Section 3.1.3. Thus, in Figure 35 for example, the curve of C_{p_2} vs x for $F^2 = 16$ is a reasonable approximation, while when $F^2 = 4$ it is seen that the limits of the theory have been exceeded. This behavior corresponds to that found by Parkin [4] in his study of gravity effects on hydrofoils. In the present case, the behavior is due to the increased size of the gravity effects, represented by $\bar{g}/U_\infty$, for small Froude numbers. Since this theory was expected to hold only for flows with small gravity effects, its use must be restricted accordingly. The behavior of C_p acts, then, as a guide to the limits of the theory.

The final figures, Figures 36 and 37, show the effect of Froude number on cavity shape and the effect of cavitation number on the location of the center of lift at an arbitrary Froude number (since C_{MO}/C_L is not a function of F). The cavity shape is seen to be distorted downward in the middle and upward at the end. The effect of the transverse gravity field is exactly opposite to the effect of a uniform shear flow with positive vorticity (see page 38 and Figure 10). The fact that the cavity is not inclined upward by bouyancy is no longer surprising since the same result was predicted by Parkin's analysis and has been confirmed by experiments on cavitation behind two-dimensional bluff bodies at the California Institute of Technology [25].

REFERENCES

1. Tulin, M. P., "Steady two-dimensional cavity flows about slender bodies," Report No. 834, David Taylor Model Basin, Washington, D. C., May 1953.

2. Chen, C. F., "Second-order supercavitating hydrofoil theory," Technical Report 121-1, Hydronautics, Inc., Rockville, Md., Oct 1961.

3. Schot, S. H., "Surface tension and free surface effects in steady two-dimensional cavity flow about slender bodies," Report No. 1566, David Taylor Model Basin, Washington, D. C., Jan 1962.

4. Parkin, B. R., "A note on the cavity flow past a hydrofoil in a liquid with gravity," Report No. 47-9, Engineering Division, California Institute of Technology, Pasadena, Calif., Dec 1957.

5. Acosta, A. J., "The effect of a longitudinal gravitational field on the supercavitating flow over a wedge," J. Appl. Mech., 28, Series E, No. 2, Jun 1961, pp. 188-192.

6. Tulin, M. P., "Supercavitating flow past foils and struts," Proc. of Symposium on Cavitation in Hydrodynamics, N.P.L., Teddington, Middlesex, Philosophical Library, Inc., New York, 1957.

7. Tulin, M. P., "Cavitation, II. Supercavitating flows," Handbook of Fluid Dynamics, McGraw-Hill Book Co., Inc., New York, 1961.

8. Parkin, B. R., "Linearized theory of cavity flow in two-dimensions," Report P-1745, RAND Corp. Santa Monica, Calif., Jul 1959.

9. Lamb, Sir Horace, Hydrodynamics, 6th Ed., Dover Publications, New York, 1945.

10. Groen, P., "Two fundamental theorems on gravity waves in inhomogeneous incompressible fluid," Physica, 14 (Haag) 1948, pp. 294-300.

11. Yih, C-S, "Two solutions of inviscid rotational flow with corner eddies," J. Fluid Mech., 5, 1959, pp. 36-40.

12. Tsien, H-S, "Symmetrical Joukowsky airfoils in shear flow," Quarterly of Appl. Math., I, 2, Jul 1943, pp. 130-148.

13. Kronauer, R. D., "Secondary flow in fluid dynamics," Proc. First U. S. National Congress of Applied Mechanics, 1951, pp. 747-56.

14. Fabula, A. G., "Thin-airfoil theory applied to hydrofoils with a single finite cavity and arbitrary free-streamline detachment," J. Fluid Mech., 12, 2, 1962, pp. 227-240.

15. Cohen, H., Sutherland, C. D., and Tu, Y., "Wall effects in cavitating hydrofoil flow," J. Ship Research, I, 3, Nov 1957, pp. 31-39.

16. Birkhoff, G. and Zarantonello, E. H., Jets, Wakes, and Cavities, Academic Press, Inc., New York, 1957, p 139.

17. Milne-Thomson, L. M., Theoretical Hydrodynamics, 4th Ed., The Macmillan Co., New York, 1960.

18. Wu, T. Y., "A simple method for calculating the drag in the linear theory of cavity flows," Report No. 85-5, Engineering Division, California Institute of Technology, Pasadena, Calif., Aug 1957.

19. Wu, T. Y., "A note on the linear and nonlinear theories for fully cavitated hydrofoils," Report No. 21-22, Hydrodynamics Laboratory, California Institute of Technology, Pasadena, Calif., Aug 1956.

20. Geurst, J. A. and Timman, R., "Linearized theory of two-dimensional cavitational flow around a wing section," IXth International Congress of Applied Mechanics, Brussels, 1956.

21. Churchill, R. V., Complex Variables and Applications, 2nd Ed., McGraw-Hill Book Co., Inc., New York, 1960, p. 158.

22. Tricomi, F. G., Integral Equations, Interscience Publishers, Inc., New York, 1957.

23. Communications of the ACM, vol. 1, no. 12, Dec 1958, pp. 8-22; and vol. 3, no. 5, May 1960, pp. 299-313.

24. "Burroughs Algebraic Compiler, A Reference Manual," Bulletin 220-21011-P, Burroughs Corp., Detroit, Michigan, Jan 1961.

25. Acosta, A. J., "The effect of a longitudinal gravitational field on the supercavitating flow over a wedge," J. Appl. Mech., 29, Series E, No. 1, Mar 1962, p.219.

TABLE 1. BOUNDARY VALUE PROBLEMS FOR COMPLEX PERTURBATION VELOCITY

	Wedge	Hydrofoil
D.E.	$\frac{\partial^2 w(z)}{\partial z \partial \bar{z}} = 0$	$\frac{\partial w(z)}{\partial z \partial \bar{z}} = 0$
B.C.		
	a. $Re(w) = \frac{U_\infty \Sigma}{2} + \bar{\epsilon}$, $1 < x \leq \ell$, $y \to 0^+$	a. $Re(w) = \frac{U_\infty \Sigma}{2} + \bar{\epsilon}$, $0 \leq x \leq \ell$, $y \to 0^+$
	b. $Re(w) = \frac{U_\infty \Sigma}{2} - \bar{\epsilon}$, $1 < x \leq \ell$, $y \to 0^-$	b. $Re(w) = \frac{U_\infty \Sigma}{2} - \bar{\epsilon}$, $1 < x \leq \ell$, $y \to 0^-$
	c. $Im(w) = -\alpha U_c$, $0 \leq x \leq 1$, $y \to 0^+$	c. None
	d. $Im(w) = \alpha U_c$, $0 \leq x \leq 1$, $y \to 0^-$	d. $Im(w) = +\alpha U_c$, $0 \leq x \leq 1$, $y \to 0^-$

e. The cavity is closed, i.e., the net source strength on the slit is zero.

f. $w(z) \to 0$ as $z \to \infty$, i.e., $(u,v) = 0$ at infinity.

g. $w(z)$ must not contain nonintegrable singularities on the slit or have multiple values off the slit.

h. The flow is characterized by a smooth separation from the rear of the body, i.e., $w < \infty$ at $x = 1$, $y \to 0$.

TABLE 2. TRANSFORMATIONS

Wedge	Hydrofoil
$t = k^2 \frac{z}{\ell - z}$	(Mobius) $t = k^2 \frac{z}{\ell - z}$
$Q = t^{1/2} = k\left(\frac{z}{\ell - z}\right)^{1/2}$	(Square root) $Q = t^{1/2} = k\left(\frac{z}{\ell - z}\right)^{1/2}$
$2Q = \zeta + \frac{1}{\zeta}$	(Joukowsky) $2Q + 1 = \frac{1}{2}(\zeta + \frac{1}{\zeta})$
	$k = \sqrt{\ell - 1}$

TABLE 3. SINGULARITIES

	$w_i(\zeta)$	Purpose	Value of Re(w) on $\mathrm{Im}(\zeta) = 0$	Value of Im(w) on Unit Circle	Remarks
1	$\ln \frac{\zeta+i}{\zeta-i}$	To satisfy jump in Im(w) at nose of wedge	0	$\begin{cases} +\frac{\pi}{2}, & \mathrm{Re}(\zeta) > 0 \\ -\frac{\pi}{2}, & \mathrm{Re}(\zeta) < 0 \end{cases}$	Regular at trailing edges of wedge
2	$i(\zeta - \frac{1}{\zeta})$	Vortex pair to provide closure singularity - branching of streamlines at end of cavity	0	0	Simple poles; regular at trailing edges of wedge and hydrofoil
3	$i \ln \zeta$	To satisfy jump in Re(w) from upper to lower cavity surfaces	$\begin{cases} 0, & \zeta > 0 \\ -\pi, & \zeta < 0 \end{cases}$	0	Regular at trailing edges of wedge and hydrofoil
4	$i \frac{\zeta^2-1}{\zeta^2+1}$	A function symmetric about the $\mathrm{Im}(\zeta)$ axis. To satisfy condition that $w(\zeta) \to 0$ at $\zeta_1 (z = -\infty)$ in wedge flow	0	0	Equivalent to $\frac{i(\zeta^2-1)}{(\zeta+i)(\zeta-i)}$; a simple pole at wedge nose and regular at trailing edge
5	$i \frac{1}{\zeta-1}$	Vortex at nose of hydrofoil to satisfy Im(w) = constant on foil in ζ-plane	0	$-\frac{1}{2}$	Regular at trailing edge of hydrofoil

TABLE 4. PRESSURE FORCE COEFFICIENTS

Coefficient	Wedge	Hydrofoil
1. $C_p = \dfrac{P - P_c}{\frac{1}{2}\rho U_\infty^2}$	$(2+\Sigma)\left(\pm \dfrac{\bar{\epsilon}}{U_\infty} x + \dfrac{\Sigma}{2} - \dfrac{u}{U_\infty}\right)$	$-(2+\Sigma)\left(\dfrac{\bar{\epsilon}}{U_\infty} x + \dfrac{u}{U_\infty} - \dfrac{\Sigma}{2}\right)$
2. $C_N = \dfrac{N}{\frac{1}{2}\rho U_\infty^2 \text{ (CHORD)}}$	-	$\int_0^1 C_p \, dx$
3. $C_D = \dfrac{D}{\frac{1}{2}\rho U_\infty^2 \text{ (LENGTH)}}$	$-\dfrac{1}{2\alpha} \oint_W C_p \, dy$	αC_N*
4. $C_L = \dfrac{L}{\frac{1}{2}\rho U_\infty^2 \text{ (CHORD)}}$	$\oint_W C_p \, dx$	C_N*
5. $C_{MO} = \dfrac{L(\bar{x})}{\frac{1}{2}\rho U_\infty^2 \text{ (CHORD)}^2}$**	$\oint_W C_p x \, dx$	$\int_0^1 C_p x \, dx$

*Based on first-order smallness of angle of attack α.

**Taken at leading edge of body; positive in the counter-clockwise direction.

TABLE 5. FLOW CIRCULATIONS

Quantity	Wedge	Hydrofoil
Γ	$\int_1^{\ell} (U_c + \epsilon y_c)_L \, dx + \int_{\ell}^{1} (U_c + \epsilon y_c)_U \, dx$ $+ \int_1^0 (U_\infty + u)_U \, dx + \int_0^1 (U_\infty + u)_L \, dx$	$\int_1^{\ell} (U_c + \epsilon y_c)_L \, dx + \int_{\ell}^{0} (U_c + \epsilon y_c)_U \, dx$ $+ \int_0^1 (U_\infty + u)_L \, dx$
$\overline{\Gamma}$	$\int_1^{\ell} (U_c - \overline{\epsilon})_L \, dx + \int_{\ell}^{1} (U_c + \overline{\epsilon})_U \, dx$ $+ \int_0^1 (U_\infty + u)_U \, dx + \int_0^1 (U_\infty + u)_L \, dx$	$\int_1^{\ell} (U_c - \overline{\epsilon})_L \, dx + \int_{\ell}^{0} (U_c + \overline{\epsilon})_U \, dx$ $+ \int_0^1 (U_\infty + u)_L \, dx$
$\dfrac{\overline{\epsilon}}{U_\infty}$	$\dfrac{(\epsilon/U_\infty)}{2(\ell-1)}\left(\int_1^{\ell} \lvert y_c \rvert_L \, dx + \int_1^{\ell} \lvert y_c \rvert_U \, dx\right)$	$\dfrac{(\epsilon/U_\infty)}{2(\ell-1)}\left(\int_1^{\ell} \lvert y_c \rvert_L \, dx + \int_0^{\ell} \lvert y_c \rvert_U \, dx\right)$

NOTE: The subscripts U and L refer respectively to the upper and lower surfaces of the body or cavity.

TABLE 6. SUMMARY OF RESULTS FOR ASYMMETRIC WEDGE FLOW.

Quantity	Equation	No.
Cavity Length	$\frac{\Sigma}{2+\Sigma} = \frac{\alpha}{\pi}\left(\ln\frac{\sqrt{\ell}+1}{\sqrt{\ell}-1} + \frac{2\sqrt{\ell}}{\ell-1}\right)$	(3.8)
Cavity Area	$A_c = \alpha(\ell^{3/2} - 1)$	(3.11b)
Cavity Shape	(See equations 3.13 a, b, and c)	(3.13)
Pressure Coefficient Upper Surface	$C_{pu} = (2+\Sigma)\left[\frac{\alpha}{\pi}(2+\Sigma)\left(\frac{\sin\theta}{\ell-1} + \ln\left\lvert\frac{1+\sin\theta}{1-\sin\theta}\right\rvert\right) + \frac{\bar{\epsilon}}{U_\infty}\left(\frac{2\theta}{\pi} - 1 + \frac{2(1-T)}{\pi(1+T)}\tan\theta\cdot\ln(\sqrt{\ell}+\sqrt{\ell-1}) + x\right)\right]$, $0 \le \theta \le \pi/2$	(3.16)
Lower Surface	$C_{pL} = (2+\Sigma)\left[\frac{\alpha}{\pi}(2+\Sigma)\left(\frac{\sin\theta}{\ell-1} + \ln\left\lvert\frac{1+\sin\theta}{1-\sin\theta}\right\rvert\right) + \frac{\bar{\epsilon}}{U_\infty}\left\{\frac{2\theta}{\pi} - 1 + \frac{2(1-T)}{\pi(1+T)}\tan\theta\cdot\ln(\sqrt{\ell}+\sqrt{\ell-1}) - x\right\}\right]$, $\pi/2 \le \theta \le \pi$	(3.16)
	$x = \frac{\ell\cos^2\theta}{\ell - \sin^2\theta}$	(3.15)
Drag Coefficient	$C_D = (2+\Sigma)^2\,\alpha\ell/\pi(\ell-1)$	(3.18)
Lift Coefficient	$C_L = \left(\frac{\bar{\epsilon}}{U_\infty}\right)(2+\Sigma)\left\{\sqrt{\ell(\ell-1)}\left[1+\frac{4T}{T^2-1}\ln(\sqrt{\ell}+\sqrt{\ell-1})\right] + \frac{1}{2} - \ell\right\}$	(3.20)
Moment Coefficient	$C_{MO} = \left(\frac{\bar{\epsilon}}{U_\infty}\right)(2+\Sigma)\left\{\sqrt{\ell(\ell-1)}\left(\frac{2\ell+1}{2}\right)\cdot\left(1+\frac{4T\ln(\sqrt{\ell}+\sqrt{\ell-1})}{(T^2-1)(1-T)}\cdot\left[1-T+\frac{2\sqrt{\ell(\ell-1)}\,(T+1)}{2\ell+1}\right]\right)+\frac{1}{3}-\ell^2\right\}$	(3.22)
Vorticity Parameter	$\frac{\bar{\epsilon}}{U_\infty} = \left(\frac{\epsilon}{U_\infty}\right)\frac{\alpha(\ell^{3/2}-1)}{2(\ell-1)}$	(3.23)

NOTE: $T = 2\ell - 1 + 2\sqrt{\ell(\ell-1)}$.

TABLE 7. SUMMARY OF RESULTS FOR SYMMETRIC WEDGE FLOW

Quantity	Equation	No.
Cavity Length	$\frac{1}{2+\sigma}\left[\sigma + \left(\frac{\epsilon}{U_\infty}\right)\frac{\alpha(\ell^{3/2}-1)}{\ell-1}\right] = \frac{\alpha}{\pi}\left(\ln\frac{\sqrt{\ell}+1}{\sqrt{\ell}-1} + \frac{2\sqrt{\ell}}{\ell-1}\right)$	(3.26)
Cavity Area	$A_c = \alpha(\ell^{3/2}-1)$	(3.28b)
Cavity Shape	$y_c = \alpha - \frac{8\ell\alpha}{\pi}\int_1^t \left[\zeta - \frac{1}{\zeta} - 4(\ell-1)\tan^{-1}\frac{1}{\zeta}\right]\frac{\zeta(\zeta^4-1)\,d\zeta}{(\zeta^2+T)^2(\zeta^2+R)^2},\quad t \geq 1$	(3.29a)
	$x = \ell[1-4(\ell-1)t^2/(t^2+T)(t^2+R)]$	(3.13c)
Pressure Coefficient	$C_p = (2+\sigma)\left[\left(\frac{\bar{\epsilon}}{U_\infty}\right)(x-1) + \frac{\alpha}{\pi}(2+\sigma)\left(\frac{\sin\theta}{\ell-1} + \ln\left\lvert\frac{1+\sin\theta}{1-\sin\theta}\right\rvert\right)\right]$ $0 \leq \theta \leq \pi/2$	(3.32)
	$x = \ell\cos^2\theta/(\ell-\sin^2\theta)$	(3.31)
Drag Coefficient	$C_D = (2+\ )^2\,\alpha\ell/\pi(\ell-1)$	(3.33)
Vorticity Parameter	$\frac{\bar{\epsilon}}{U_\infty} = \left(\frac{\epsilon}{U_\infty}\right)\frac{\alpha(\ell^{3/2}-1)}{2(\ell-1)}$	(3.34)

NOTE: $T = 2\ell-1+2\sqrt{\ell(\ell-1)}$; $R = 2\ell-1-2\sqrt{\ell(\ell-1)}$.

TABLE 8. SUMMARY OF RESULTS FOR HYDROFOIL FLOW

Quantity	Equation	No.
Cavity Length	$\alpha = \frac{k\Sigma}{2+\Sigma} - \frac{\bar{\epsilon}}{U_\infty}\frac{2}{\pi(2+\Sigma)}\left[\ln\left\{\left(1+\sqrt{k}\,s\right)^2 + \left(2k+\sqrt{k}\,r\right)^2\right\} - \left\{k\pi\left[1-\frac{2}{\pi}\tan^{-1}\left(\frac{2k+\sqrt{k}\,r}{1+\sqrt{k}\,s}\right)\right] + \frac{2\sqrt{k\ell}\,s}{k+\sqrt{\ell}}\right\}\right]$	(3.46)
Cavity Area	$A_c = \frac{\pi\sqrt{k\ell}}{16(2+\Sigma)}\left\{4A_o[k(4k^2+5)r + (2k^2+1)s] - \frac{D_o}{2}[(2k+\frac{1}{k})r-s] - \frac{4}{\pi}\left(\frac{\bar{\epsilon}}{U_\infty}\right)(kr-s)\right\}^*$	(3.50)
Cavity Shape		
Upper	$\frac{y_c}{\ell} = \frac{-4k^2}{(2+\Sigma)}\left[4A_oI_1 + \frac{D_oI_2}{2} + \frac{2}{\pi}\left(\frac{\bar{\epsilon}}{U_\infty}\right)I_3 + \frac{\alpha(2+\Sigma)q^2}{4k^2(k^2+q^2)}\right] \quad , 0 \le x,\ 0 \le q$	(3.48a)
	$\frac{x}{\ell} = \frac{q^2}{k^2+q^2}$	(3.49)
Lower	$\frac{y_c}{\ell} = -\frac{\alpha}{\ell} + \frac{4k^2}{(2+\Sigma)}\left[4A_oI_4 - \frac{D_oI_5}{2} - \frac{2}{\pi}\left(\frac{\bar{\epsilon}}{U_\infty}\right)I_6 - \frac{\alpha(2+\Sigma)(q^2-1)}{4\ell(k^2+q^2)}\right] \quad , \quad 1 \le x,\ 1 \le q$	(3.48b)
Pressure Coefficient	$C_p = -(2+\Sigma)\left\{-4A_o\sqrt{\xi(1-\xi)} + \frac{D_o}{2}\sqrt{\frac{1-\xi}{\xi}} + \left(\frac{\bar{\epsilon}}{U_\infty}\right)\left[1 + \frac{\ell\xi^2}{k^2+\xi^2} - \frac{2}{\pi}\tan^{-1}\frac{2\sqrt{\xi(1-\xi)}}{1-2\xi}\right]\right\},\ \frac{x}{\ell} = \frac{\xi^2}{k^2+\xi^2},\ 0 \le \xi \le 1$	(3.52)
Normal Pressure Coefficient	$C_N = \frac{\pi}{4}(2+\Sigma)(\sqrt{\ell}-k)\left[\alpha k(2+\Sigma) + \Sigma + \frac{2}{\pi}\left(\frac{\bar{\epsilon}}{U_\infty}\right)\left\{k\ln\left[(1+\sqrt{k}\,s)^2 + (2k+\sqrt{k}\,r)^2\right] + \pi - 2\tan^{-1}\frac{2k+\sqrt{k}\,r}{1+\sqrt{k}\,s} + \frac{2\sqrt{\ell k}\,r - (4\ell-1)}{\sqrt{\ell}-k}\right\}\right],\ C_L = C_N, C_D = \alpha C_N$	(3.54)
Moment Coefficient	$C_{MO} = \frac{\pi\sqrt{\ell k}\,(2+\Sigma)}{32}\left\{\frac{4}{\pi}\left(\frac{\bar{\epsilon}}{U_\infty}\right)\left[\frac{8}{\sqrt{\ell k}}\left(\frac{1}{6}-\ell^2\right) + (4\ell+1)r + ks\right] + 4A_o[(6\ell-1)r-(12\ell+1)ks] + \frac{D_o}{2}[r-(2k+\frac{3}{k})s]\right\}^{**}$	(3.56)
Vorticity Parameter	$\frac{\bar{\epsilon}}{U_\infty} = \frac{1}{4(2\ell-1)}\left(\frac{\epsilon}{U_\infty}\right)\left[\left(\frac{-kX_4+(k-\alpha)X_3}{H} + \alpha X_1 + X_2\right) \underset{(-)}{+} \sqrt{\left(\frac{-kX_4+(k-\alpha)X_3}{H} + \alpha X_1 + X_2\right)^2 + \frac{4\alpha X_4}{H}(kX_1+X_2)}\right]$	(3.58)

NOTES: *See equations (3.38) for A_o and D_o.
**See Appendix E for notation.

TABLE 9. SUMMARY OF RESULTS FOR WEDGE FLOW IN TRANSVERSE GRAVITY FIELD

Quantity	Equation	No.
Cavity Length	$\frac{\sigma}{2+\sigma} = \frac{\alpha}{\pi}\left(\ln\frac{\sqrt{\ell}+1}{\sqrt{\ell}-1} + \frac{2\sqrt{\ell}}{\ell-1}\right)$	(G-5)
Cavity Area	$A_c = \alpha(\ell^{3/2}-1)$	(G-6)
Cavity Shape	(See equations G-7, 8, and 9)	(G-7,8,9)
Pressure Coefficient Upper Surface	$C_{p_u} = -2\left(\frac{\bar{g}}{U_\infty}\right)x + (2+\sigma)\left\{\frac{\alpha}{\pi}(2+\sigma)\left(\frac{\sin\theta}{\ell-1} + \ln\left\lvert\frac{1+\sin\theta}{1-\sin\theta}\right\rvert\right) - \frac{\bar{g}}{U_\infty}\left[\frac{2\theta}{\pi} - 1 + \frac{2(1-T)}{\pi(1+T)}\ln(\sqrt{\ell}+\sqrt{\ell-1})\tan\theta\right]\right\}$ $0 \le \theta \le \pi/2$	(G-11a)
Lower Surface	$C_{p_l} = +2\left(\frac{\bar{g}}{U_\infty}\right)x + (2+\sigma)\left\{\frac{\alpha}{\pi}(2+\sigma)\left(\frac{\sin\theta}{\ell-1} + \ln\left\lvert\frac{1+\sin\theta}{1-\sin\theta}\right\rvert\right) - \frac{\bar{g}}{U_\infty}\left[\frac{2\theta}{\pi} - 1 + \frac{2(1-T)}{\pi(1+T)}\ln(\sqrt{\ell}+\sqrt{\ell-1})\tan\theta\right]\right\}$ $\pi/2 \le \theta \le \pi$ $x = \frac{\ell\cos^2\theta}{\ell-\sin^2\theta}$	
Drag Coefficient	$C_D = (2+\sigma)^2\alpha\ell/\pi(\ell-1)$	(G-13)
Lift Coefficient	$C_L = 2\frac{\bar{g}}{U_\infty}\left[1-(2+\sigma)\left\{\sqrt{\ell(\ell-1)}\left[1+\frac{4T}{T^2-1}\ln(\sqrt{\ell}+\sqrt{\ell-1})\right]-\ell+1\right\}\right]$	(G-14)
Moment Coefficient	$C_{MO} = \frac{\bar{g}}{U_\infty}\left[\frac{4}{3} - \frac{(2+\sigma)}{2}\left\{\sqrt{\ell(\ell-1)}(2\ell+1)\left[1+\frac{4T\ln(\sqrt{\ell}+\sqrt{\ell-1})}{(T^2-1)(1-T)}\cdot\left(\frac{2\sqrt{\ell(\ell-1)}(1+T)}{2\ell+1}+1-T\right)\right]-2(\ell^2-1)\right\}\right]$	(G-15)
Gravity Parameter	$\frac{\bar{g}}{U_\infty} = \alpha(\ell^{3/2}-1)/2F^2(\ell-1)$	(G-16)

NOTE: $T = 2\ell-1+2\sqrt{\ell(\ell-1)}$

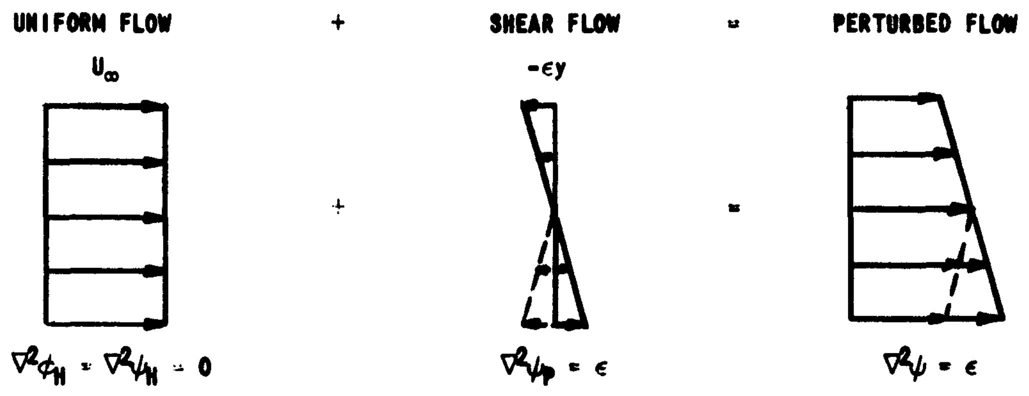

a. Flows

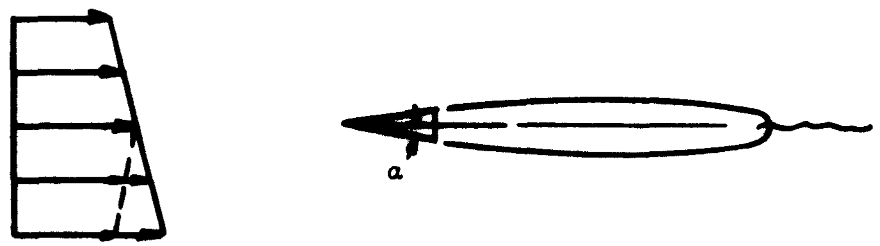

1. WEDGES

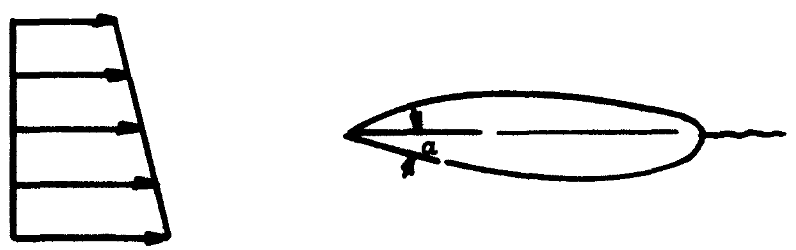

2. HYDROFOIL

b. Problems

FIGURE 1. FLOW PATTERNS AND PROBLEMS.

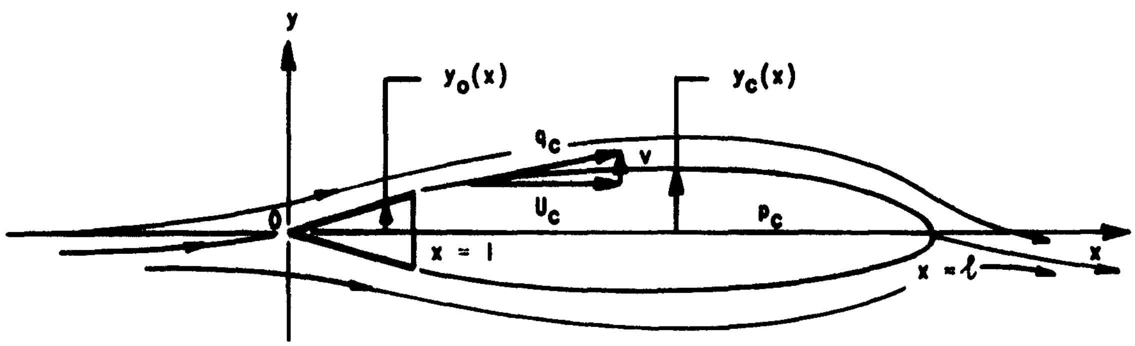

a. Wedge

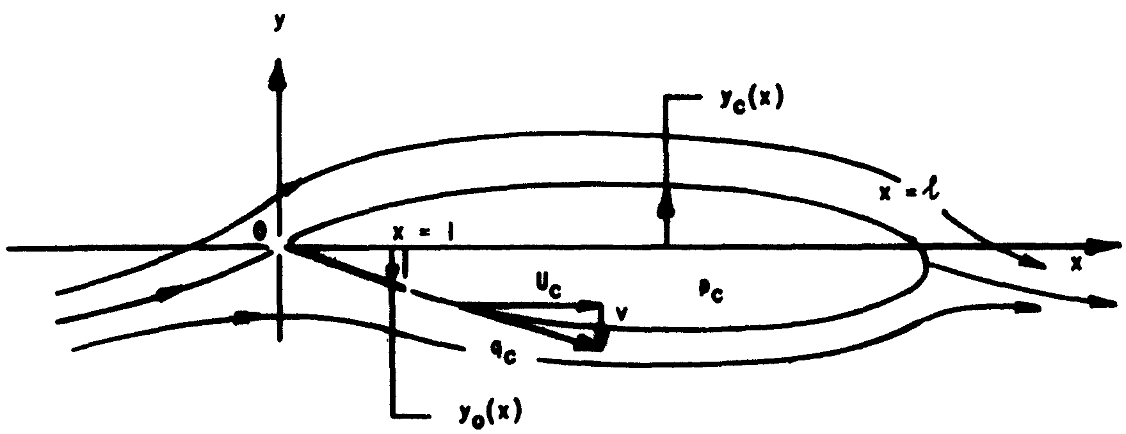

b. Hydrofoil

FIGURE 2. FULLY CAVITATED FLOWS.

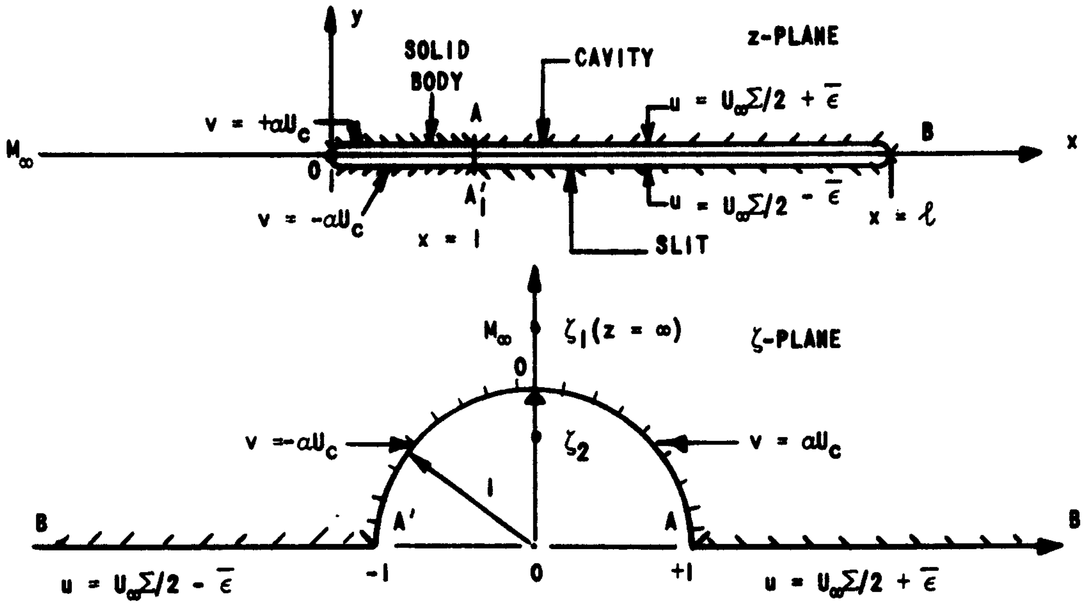

a. Wedge flow

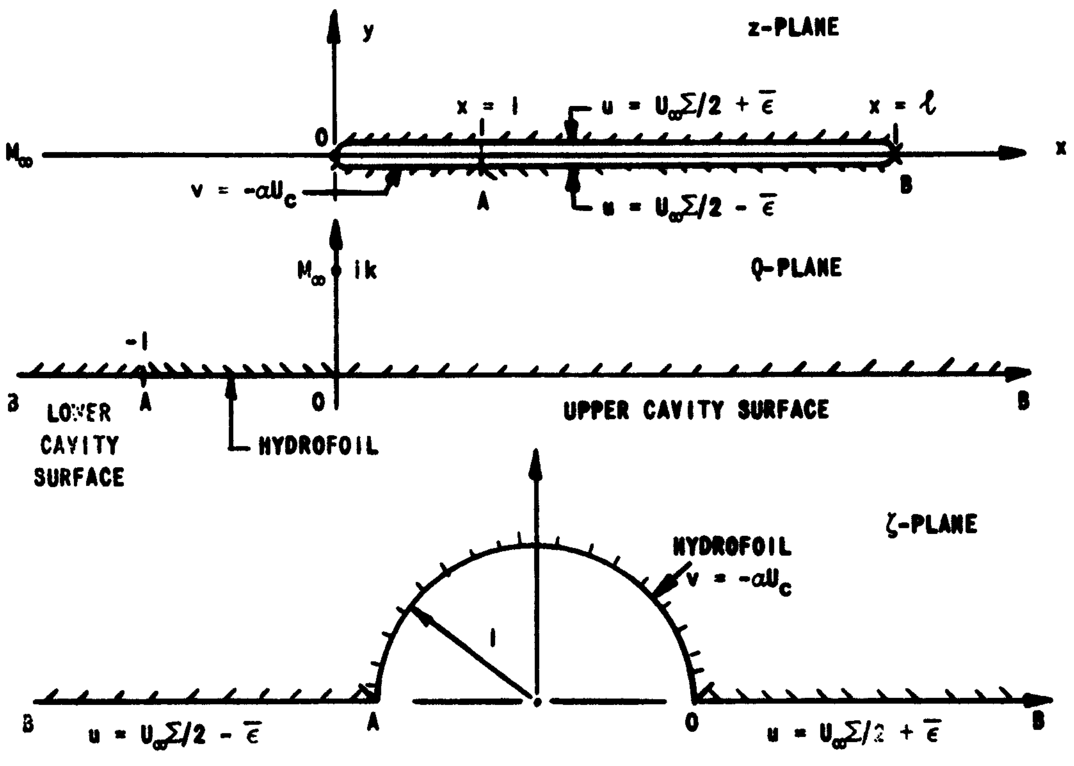

b. Hydrofoil flow

FIGURE 3. MAPPING OF z-PLANE ONTO UNIT CIRCLE.

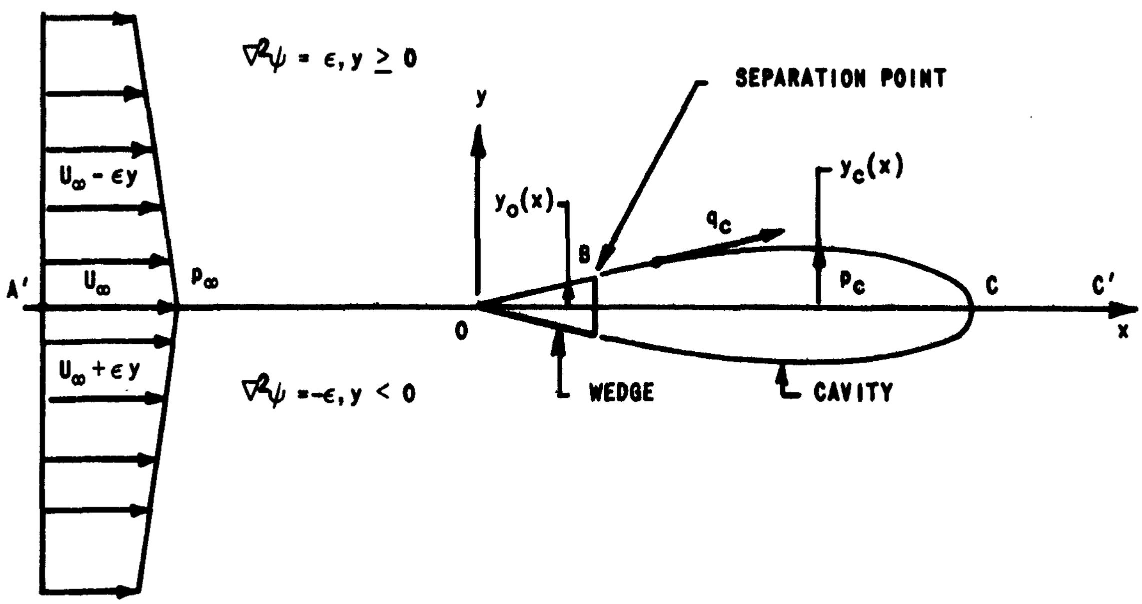

FIGURE 4. SYMMETRIC SHEAR FLOW PAST A WEDGE.

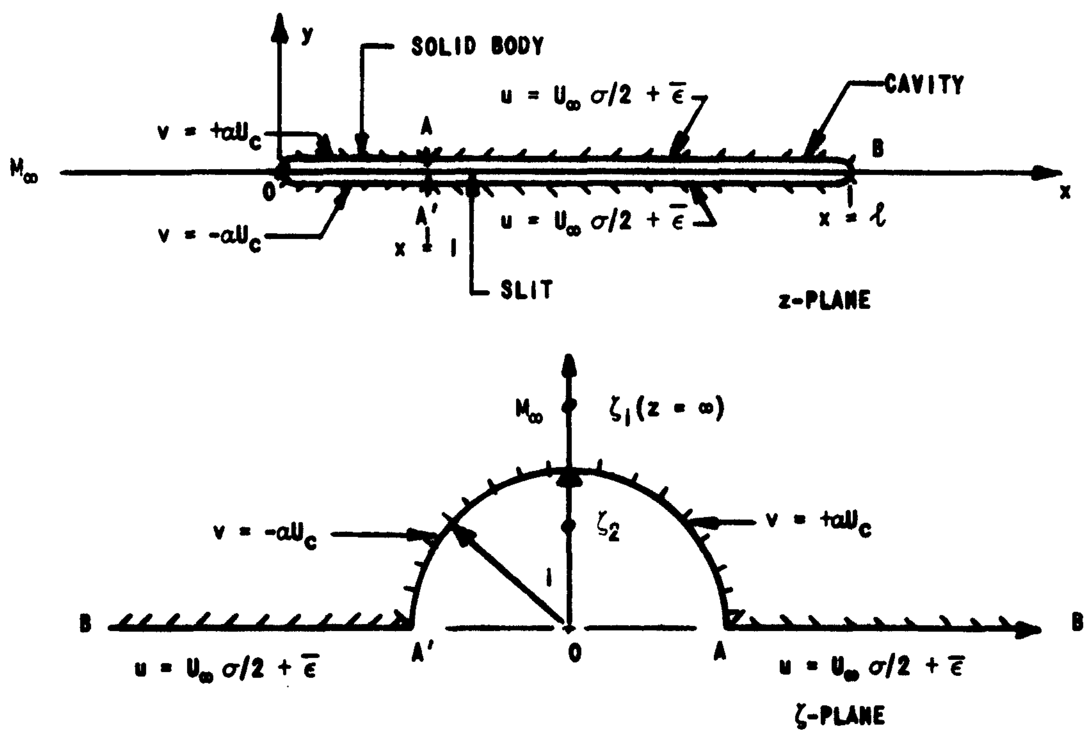

Symmetric wedge flow

FIGURE 5. MAPPING OF z-PLANE ONTO UNIT CIRCLE.

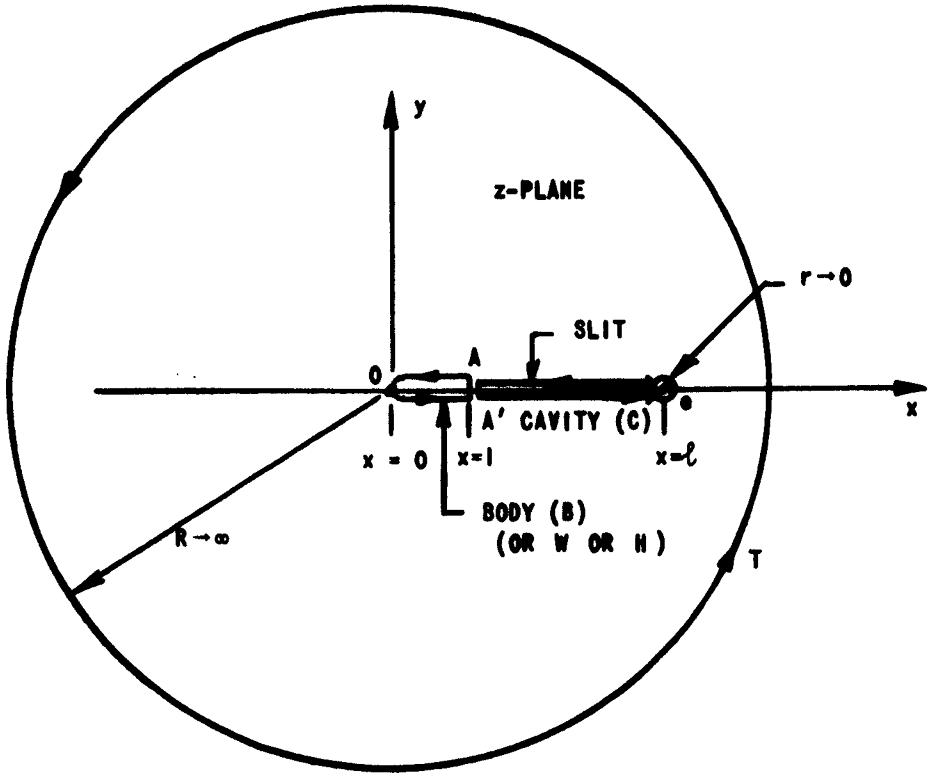

FIGURE 6. CONTOUR PATHS FOR COMPLEX INTEGRATION.

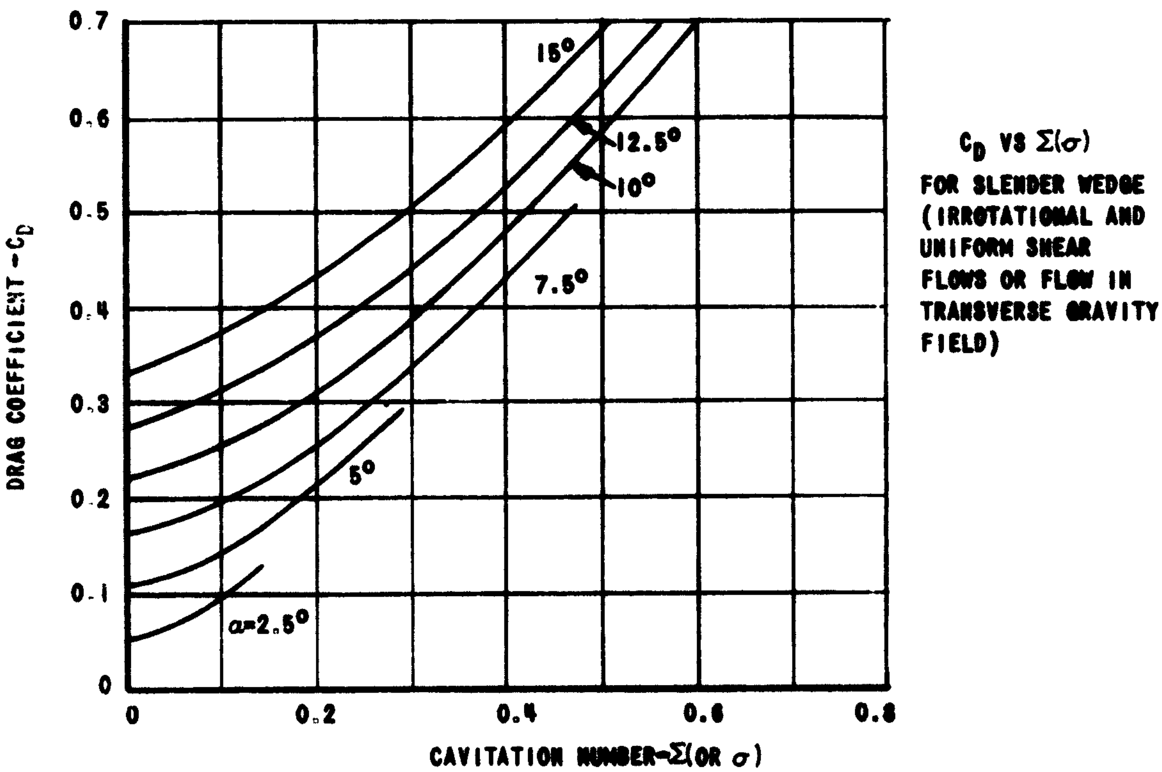

FIGURE 7. DRAG COEFFICIENT VS CAVITATION NUMBER FOR FLOW PAST A UNIT WEDGE.

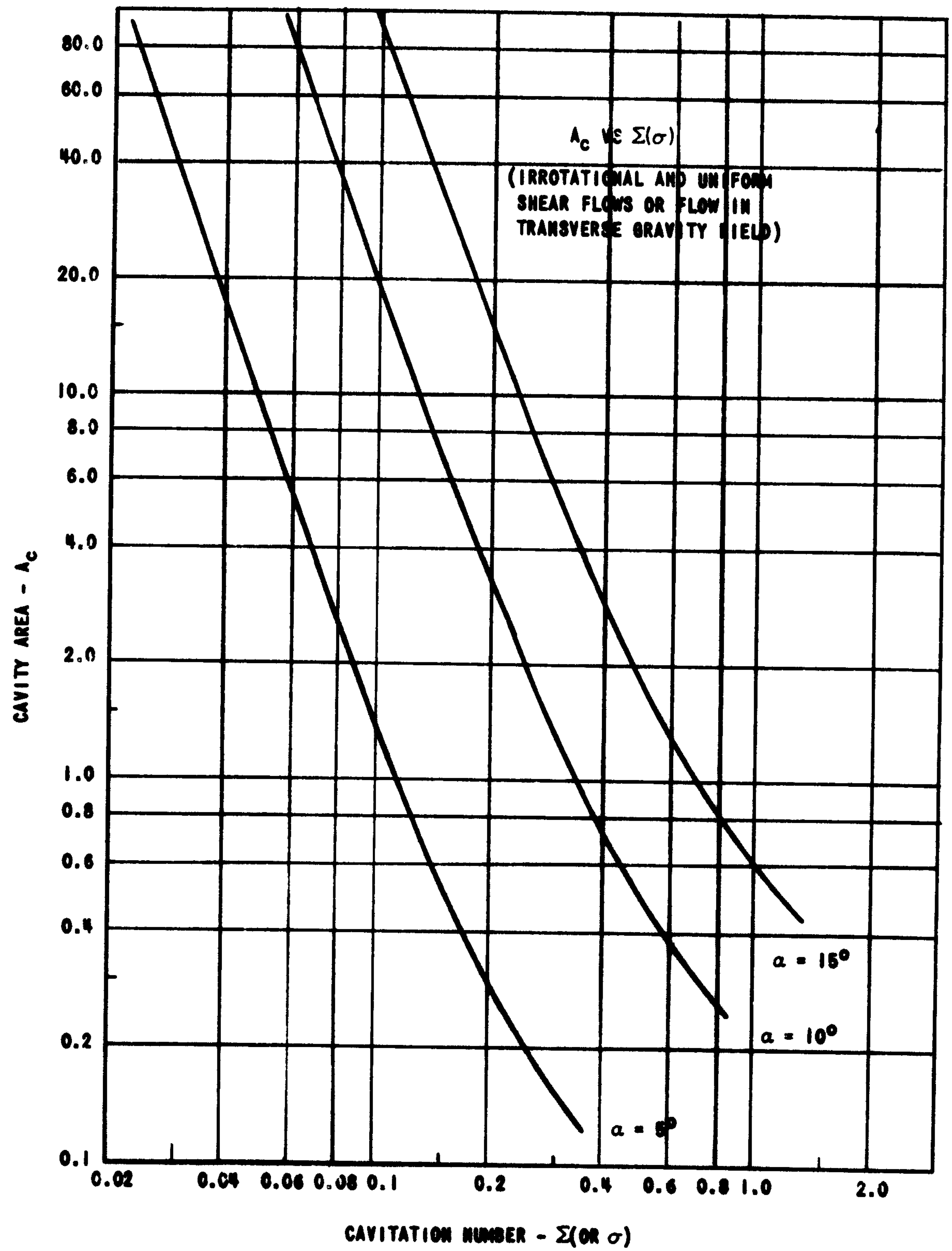

FIGURE 8. CAVITY AREA VS CAVITATION NUMBER FOR FLOW PAST A UNIT WEDGE.

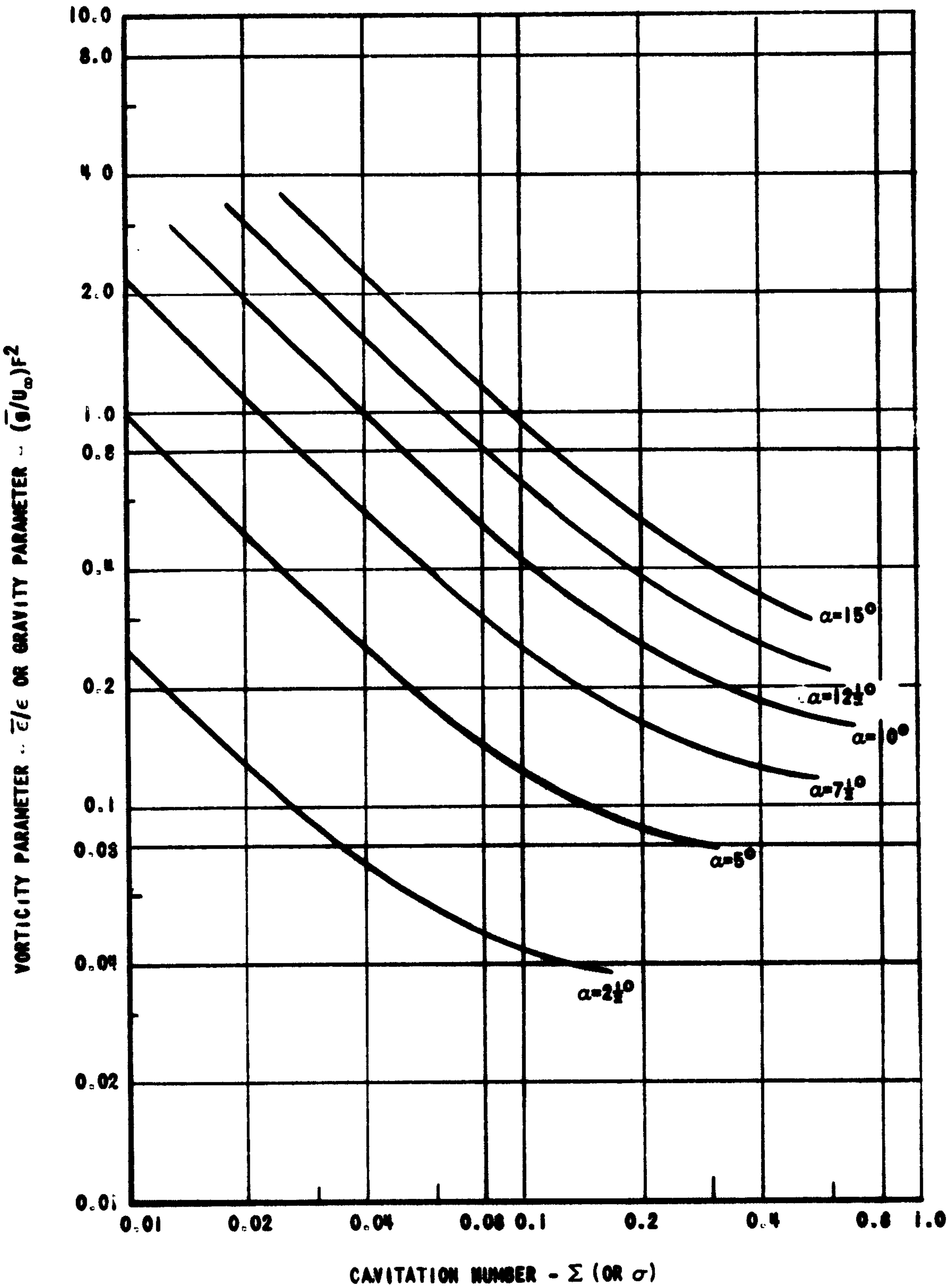

FIGURE 9. VORTICITY PARAMETER OR GRAVITY PARAMETER VS CAVITATION NUMBER FOR FLOW PAST A UNIT WEDGE.

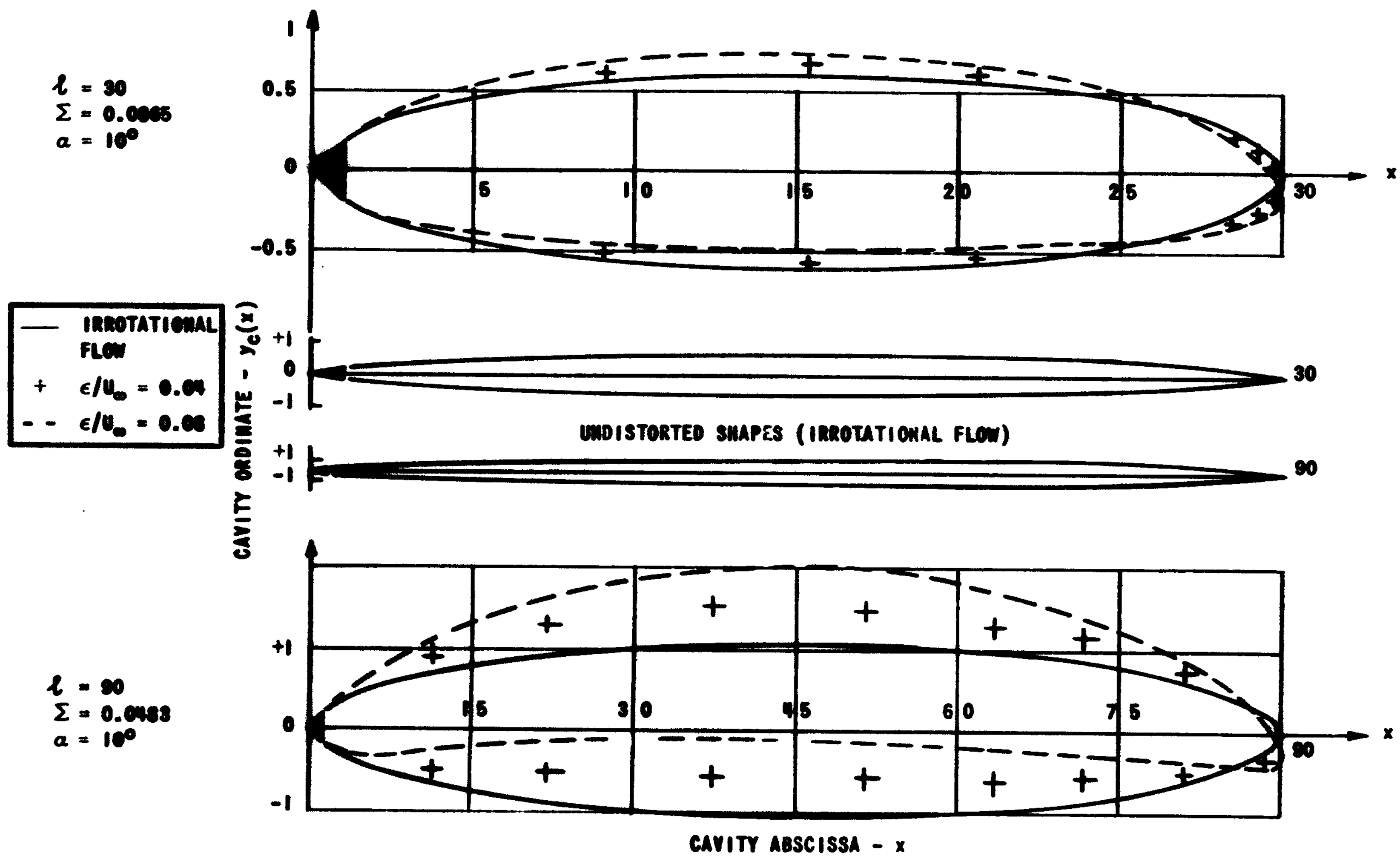

FIGURE 10. CAVITY SHAPES AT CONSTANT CAVITATION NUMBER IN UNIFORM SHEAR FLOW PAST A UNIT WEDGE.

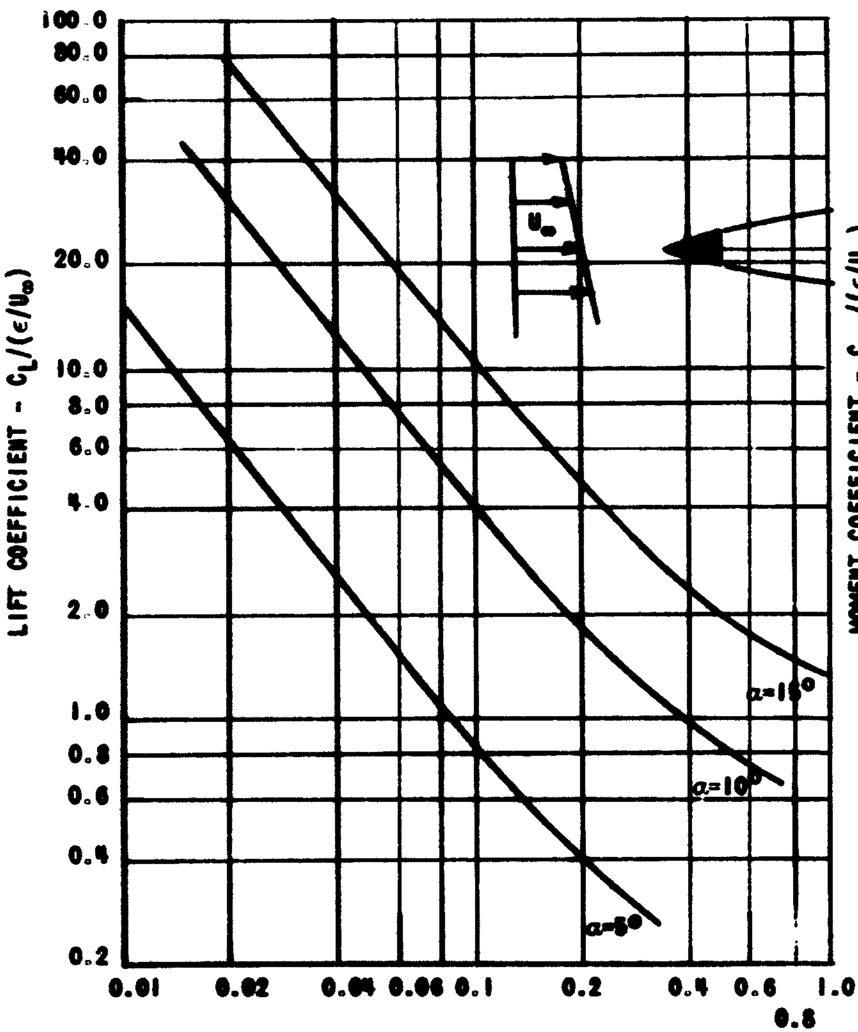

FIGURE 11. LIFT COEFFICIENT FOR SHEAR FLOW PAST A WEDGE.

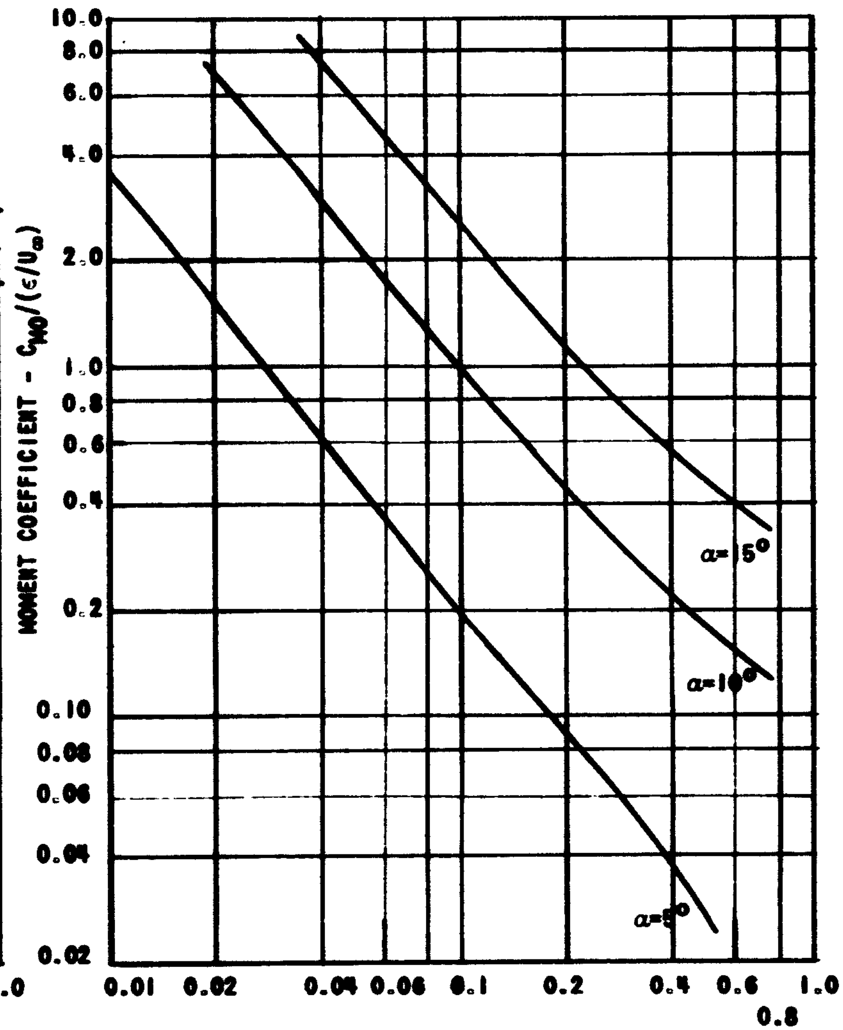

FIGURE 12. MOMENT COEFFICIENT FOR SHEAR FLOW PAST A WEDGE.

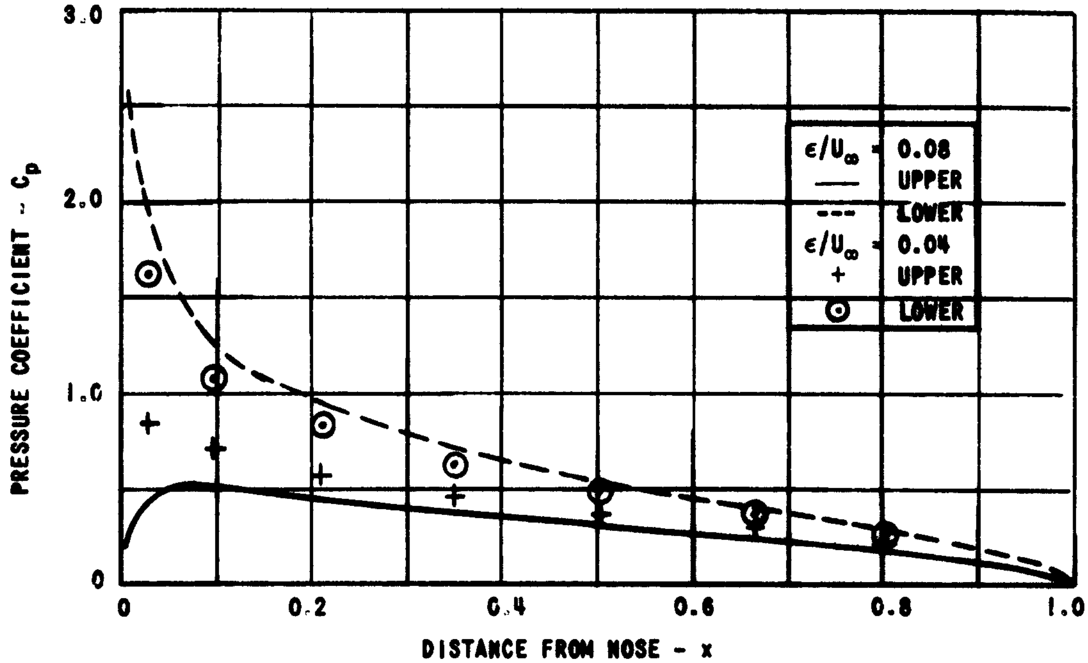

FIGURE 13. $\Sigma = 0.0865$, $\ell = 30$, $\alpha = 10°$ PRESSURE COEFFICIENT FOR SHEAR FLOW PAST A WEDGE.

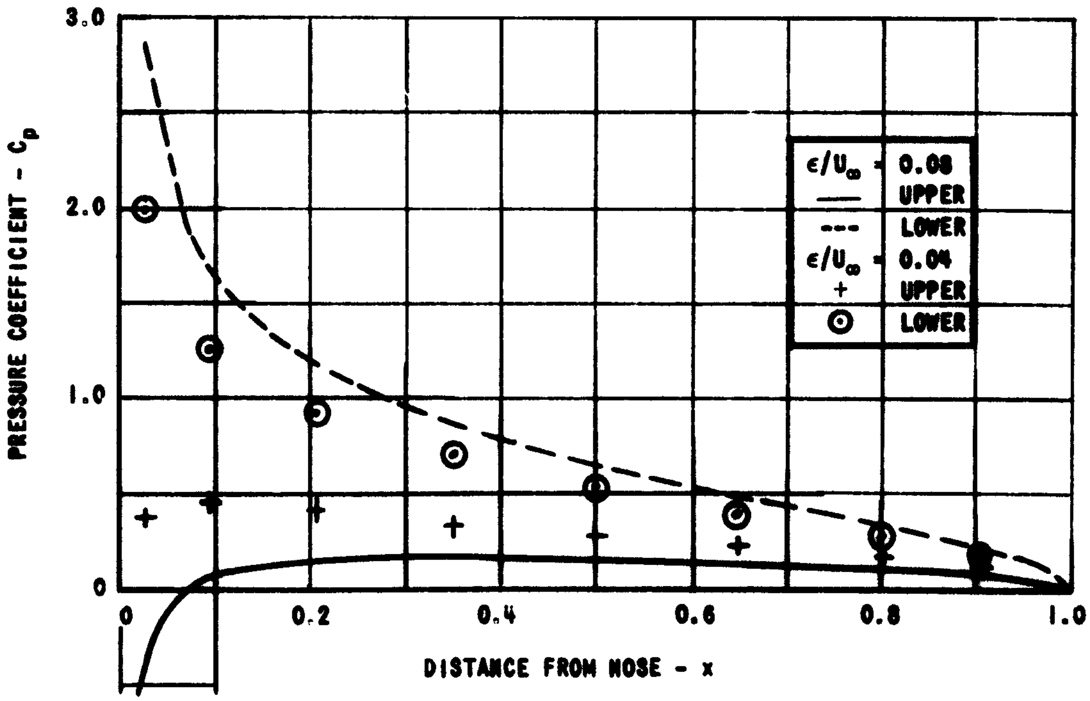

FIGURE 14. $\Sigma = 0.0483$, $\ell = 90$, $\alpha = 10°$ PRESSURE COEFFICIENT FOR SHEAR FLOW PAST A WEDGE.

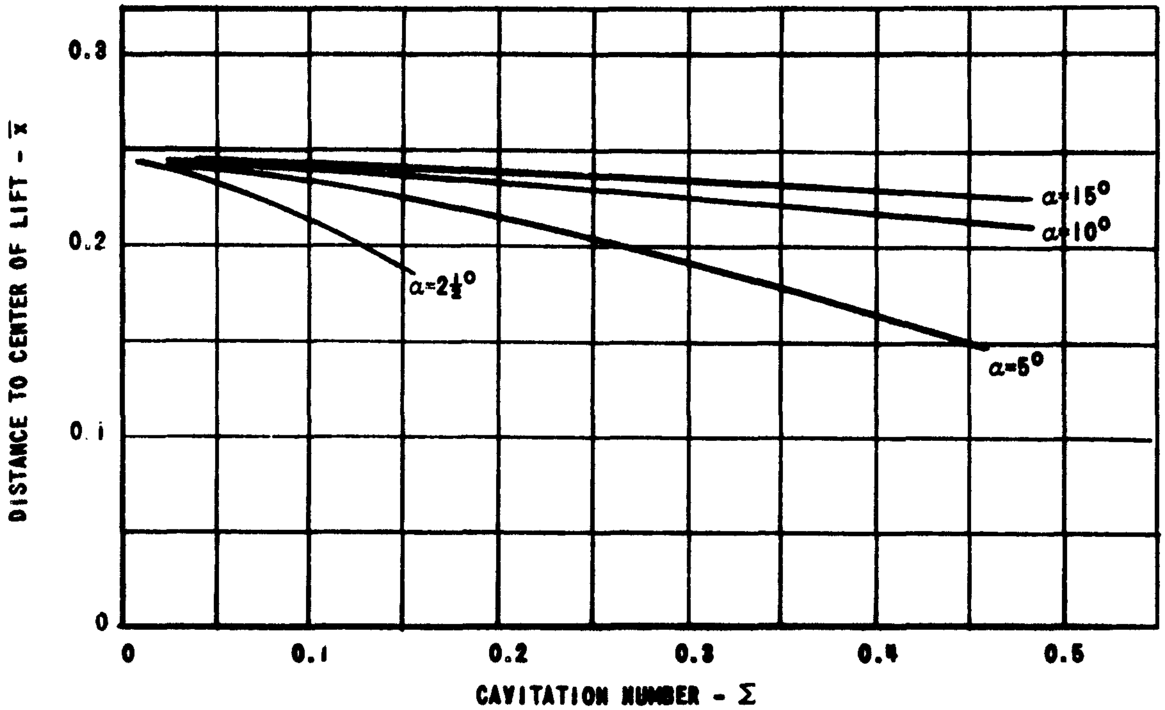

FIGURE 15. CENTER OF LIFT FOR SHEAR FLOW PAST A WEDGE.

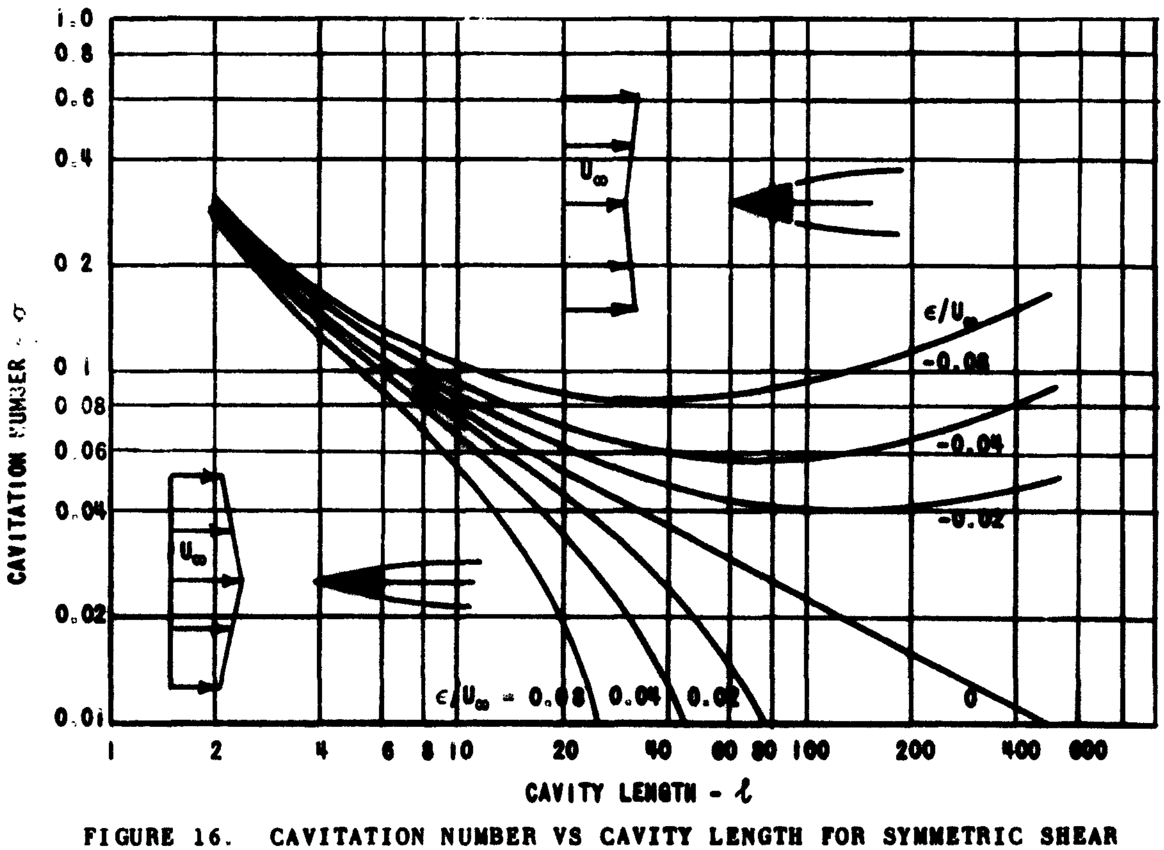

FIGURE 16. CAVITATION NUMBER VS CAVITY LENGTH FOR SYMMETRIC SHEAR FLOW PAST A WEDGE: $\alpha = 5^\circ$.

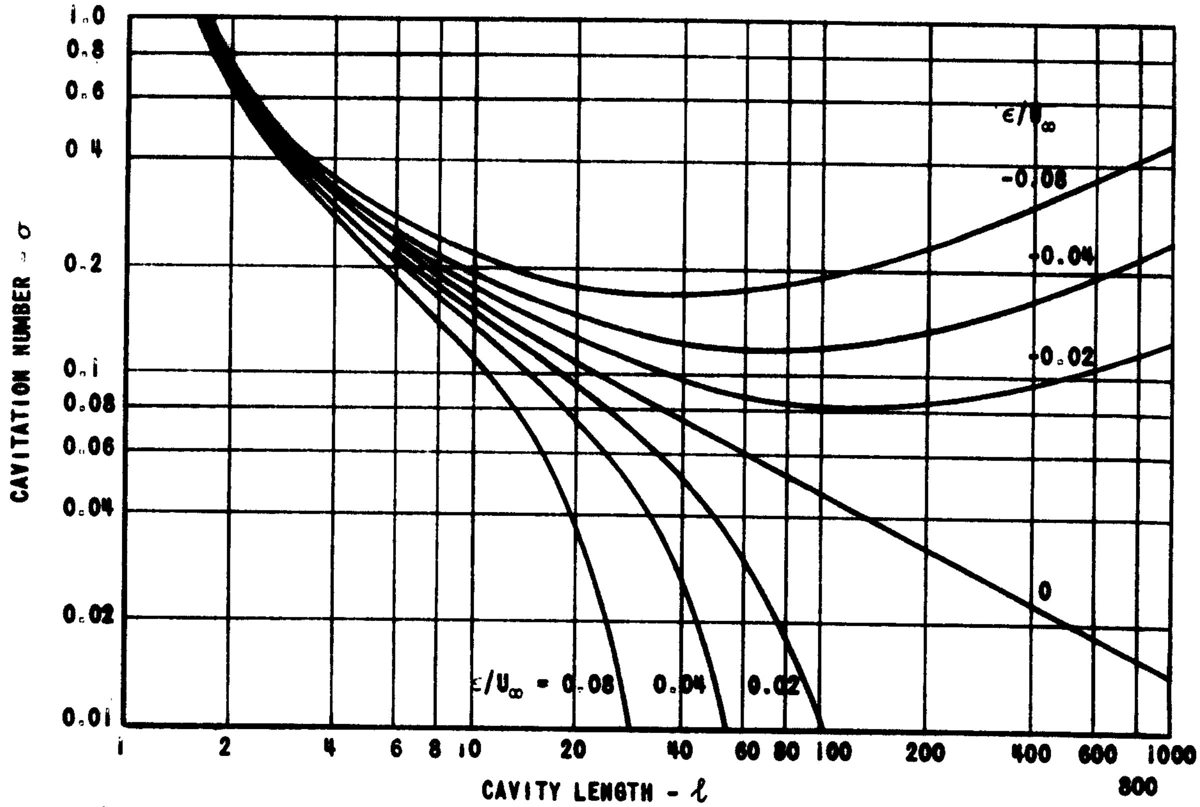

FIGURE 17. CAVITATION NUMBER VS CAVITY LENGTH FOR SYMMETRIC SHEAR FLOW PAST A WEDGE. $\alpha = 10°$.

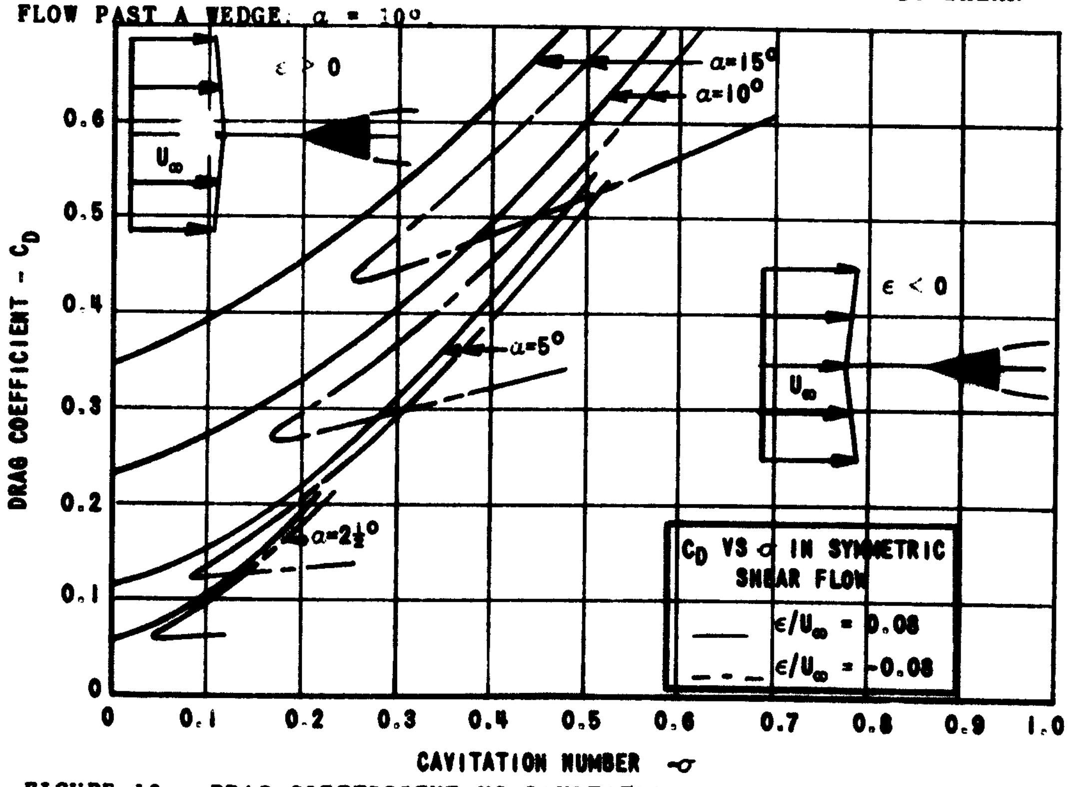

FIGURE 18. DRAG COEFFICIENT VS CAVITATION NUMBER FOR SYMMETRIC SHEAR FLOW PAST A WEDGE.

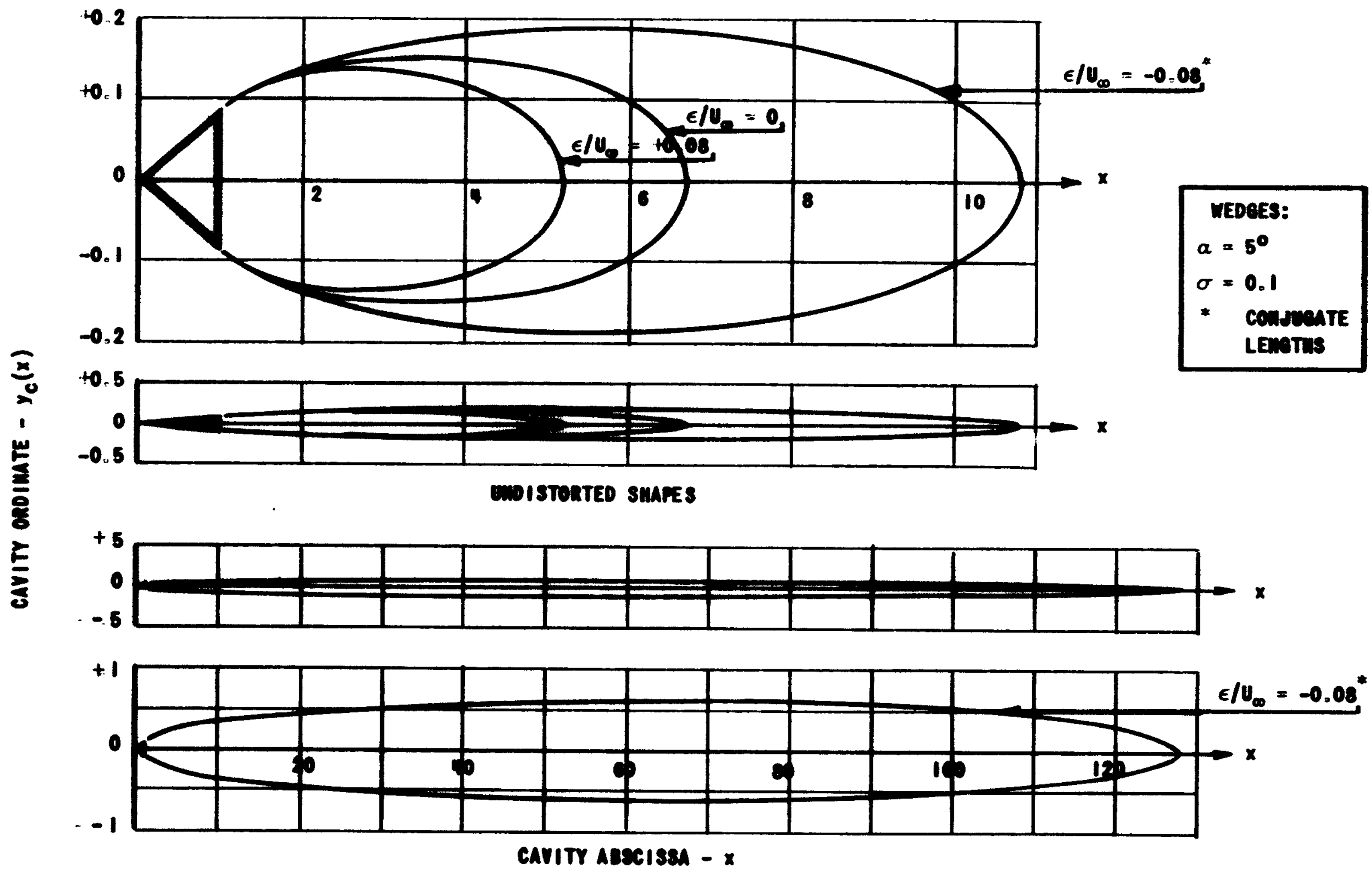

FIGURE 19. CAVITY SHAPES FOR WEDGE IN SYMMETRIC SHEAR FLOW AT CONSTANT CAVITATION NUMBER.

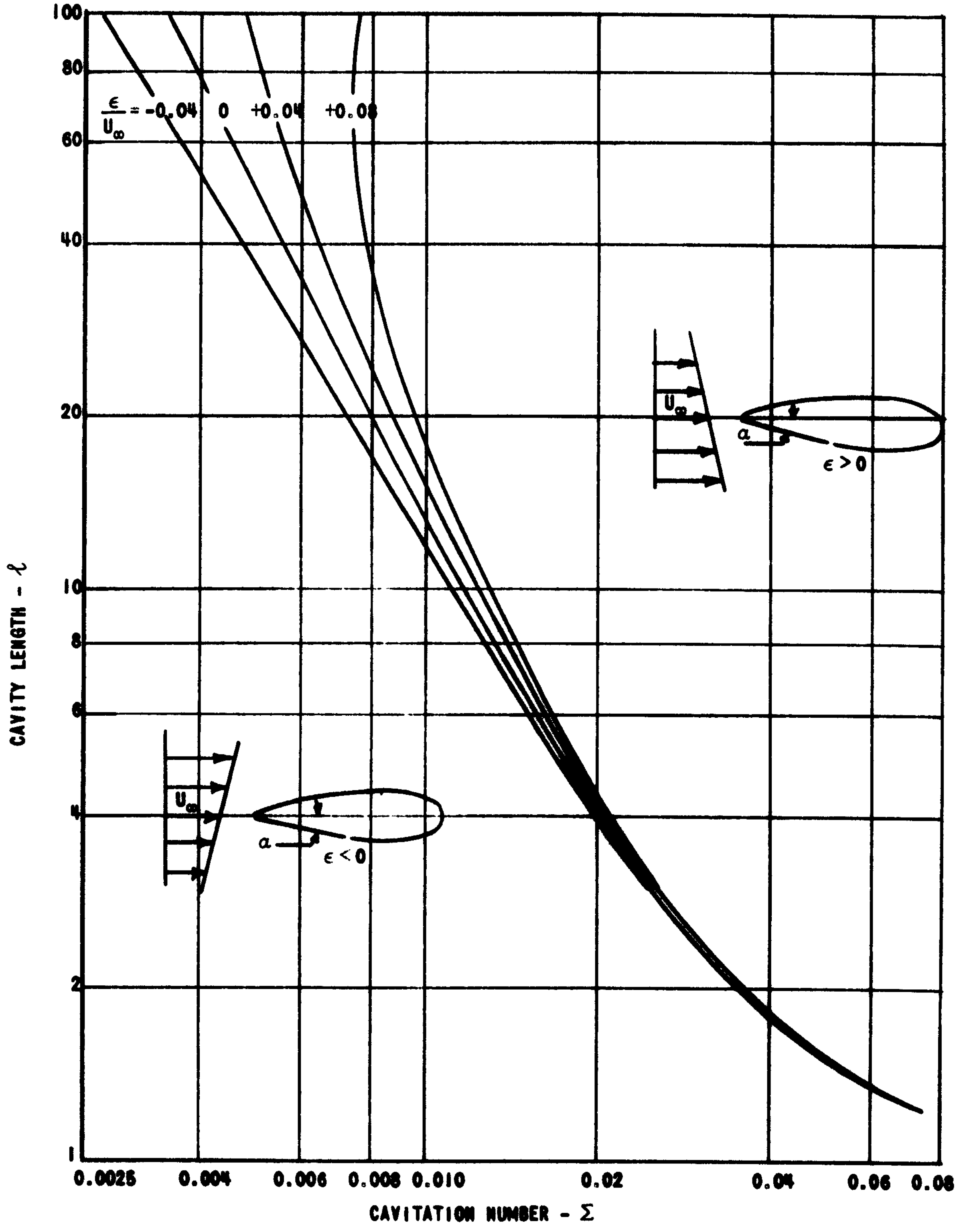

FIGURE 20. CAVITY LENGTH VS CAVITATION NUMBER FOR SHEAR FLOW PAST A HYDROFOIL: α = 1°.

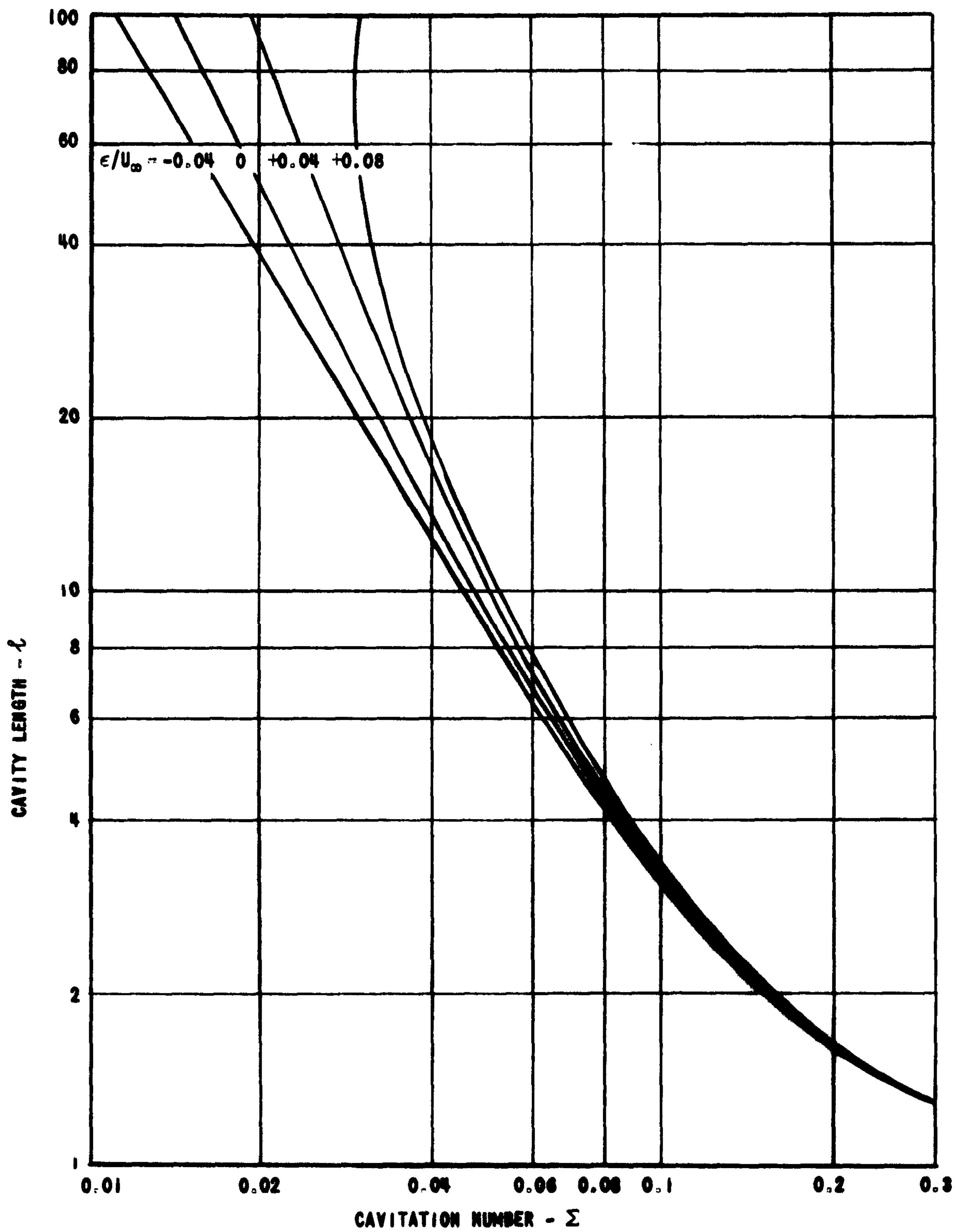

FIGURE 21. CAVITY LENGTH VS CAVITATION NUMBER FOR SHEAR FLOW PAST A HYDROFOIL: $\alpha = 4°$.

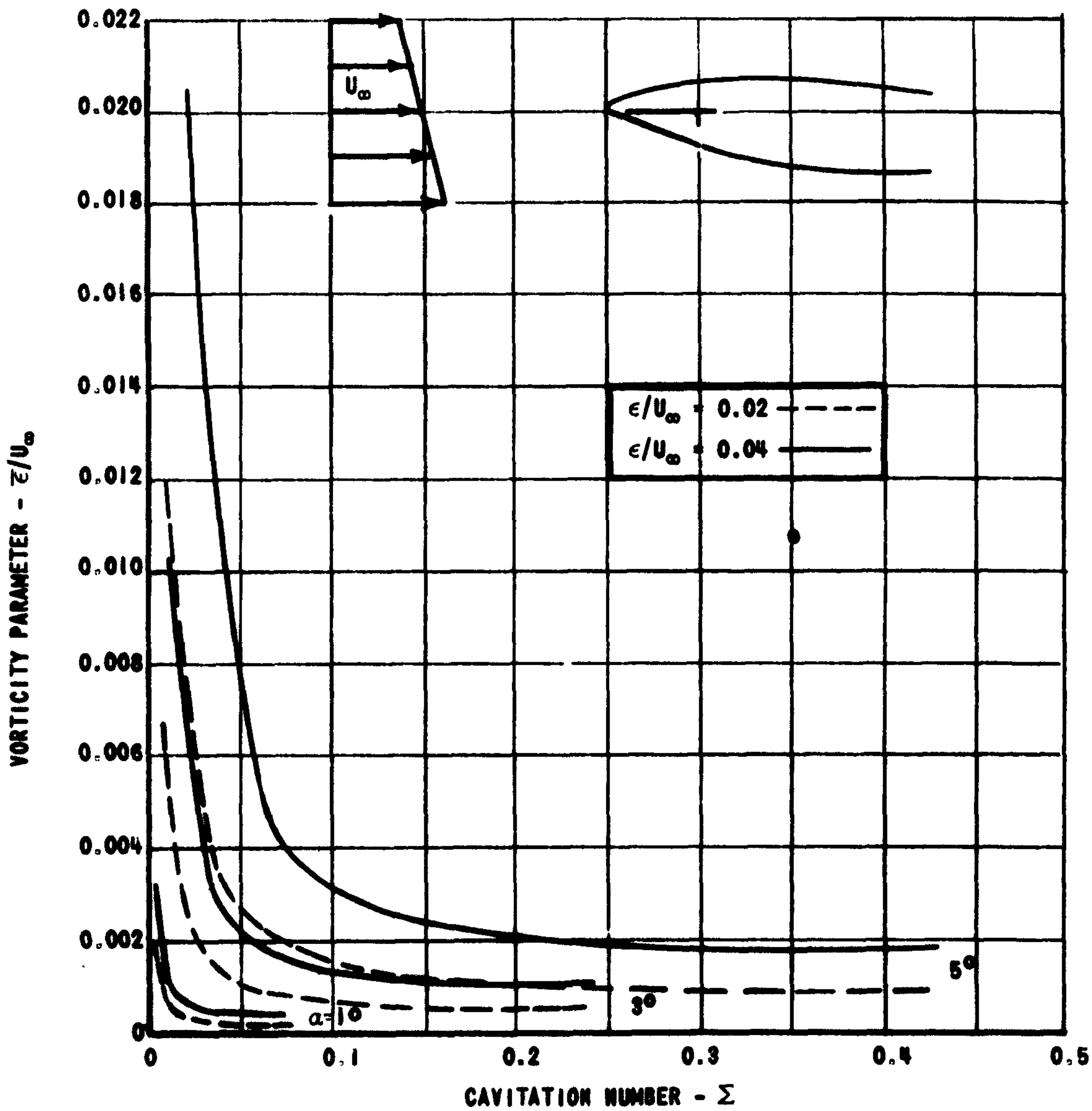

FIGURE 22. EFFECT OF VORTICITY AND CAVITATION NUMBER ON VORTICITY PARAMETER FOR SHEAR FLOW PAST A HYDROFOIL.

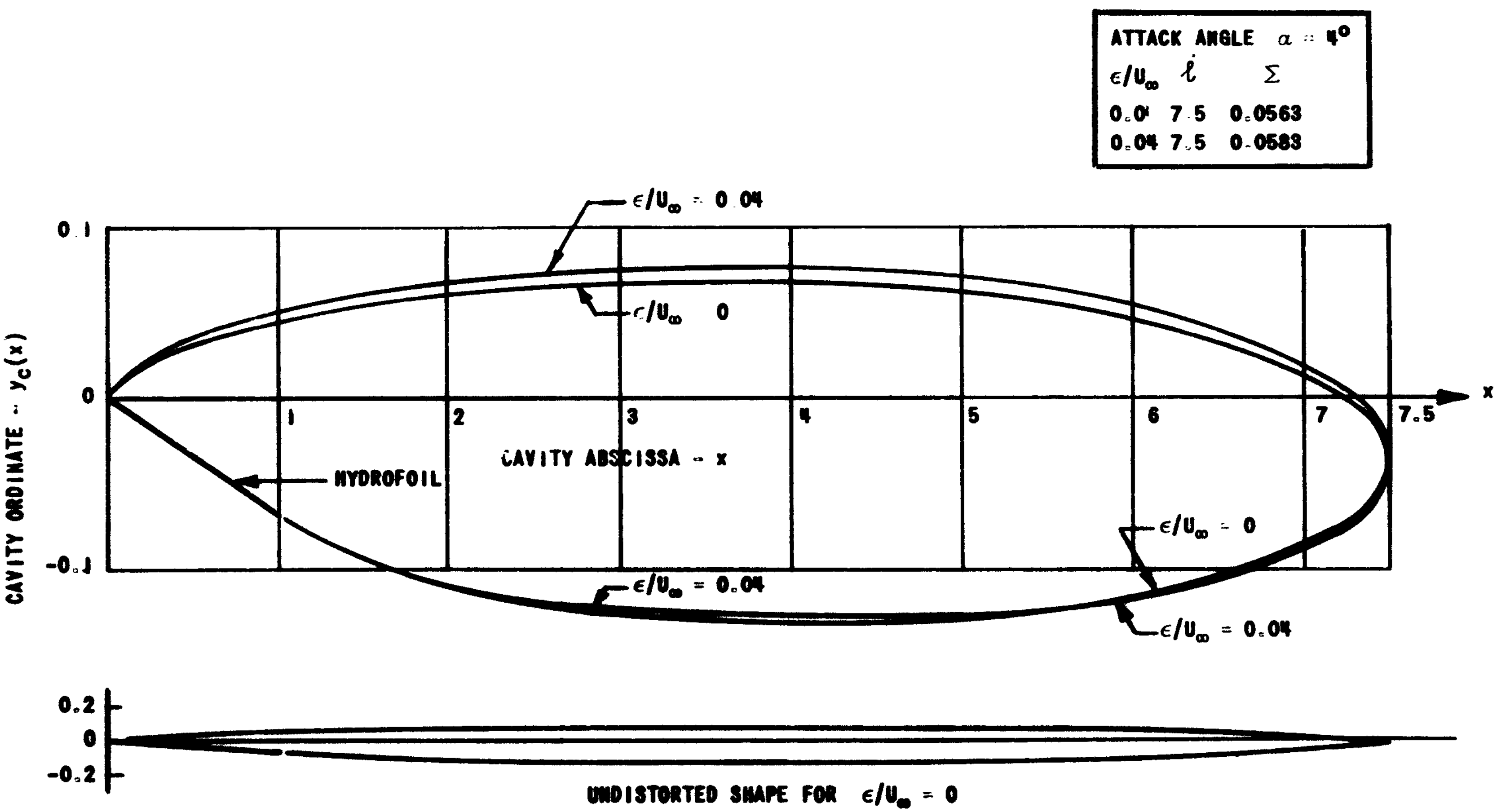

FIGURE 23. CAVITY SHAPES AT CONSTANT LENGTH IN UNIFORM SHEAR FLOW.

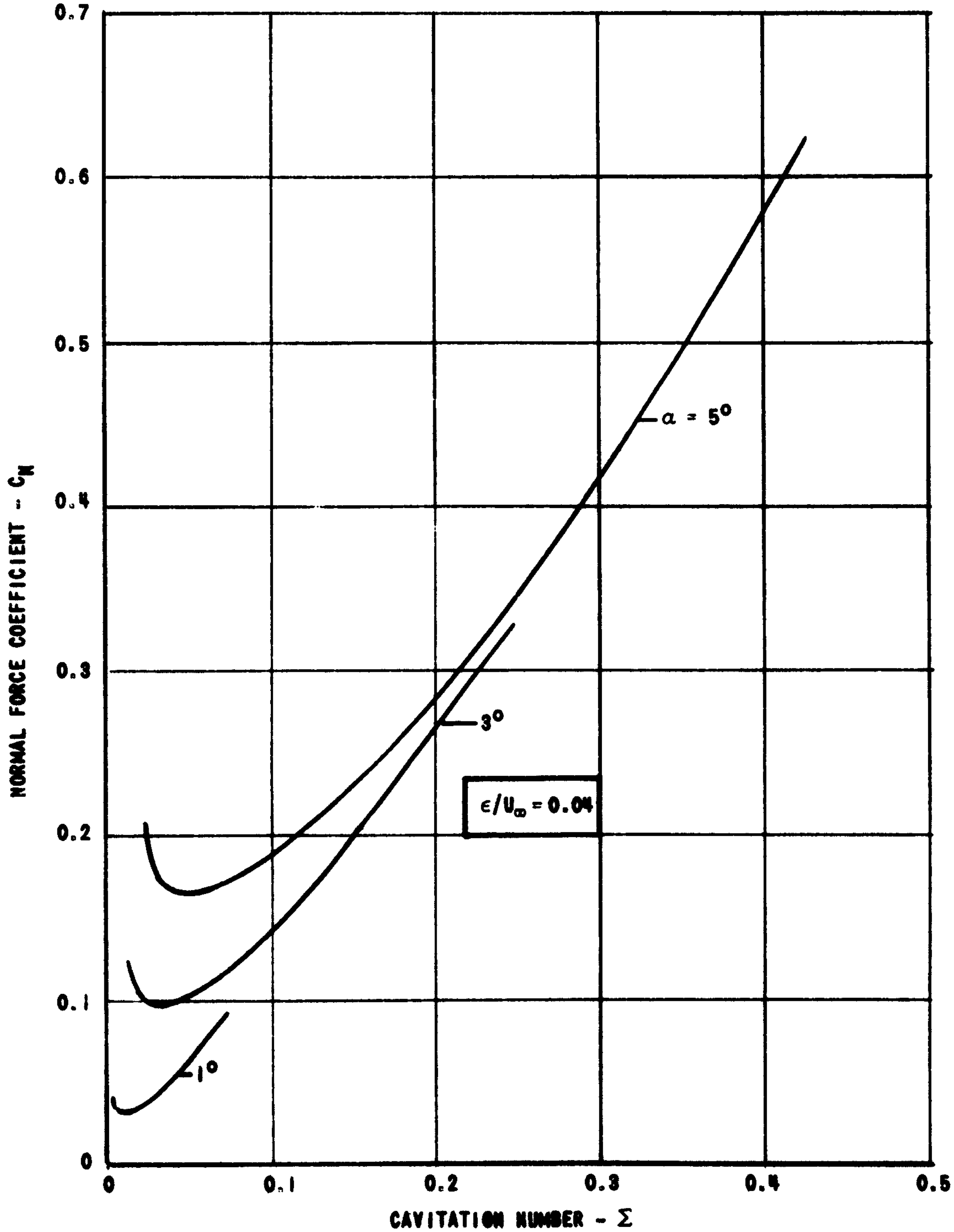

FIGURE 24. NORMAL FORCE COEFFICIENT VS CAVITATION NUMBER FOR SHEAR FLOW PAST A HYDROFOIL.

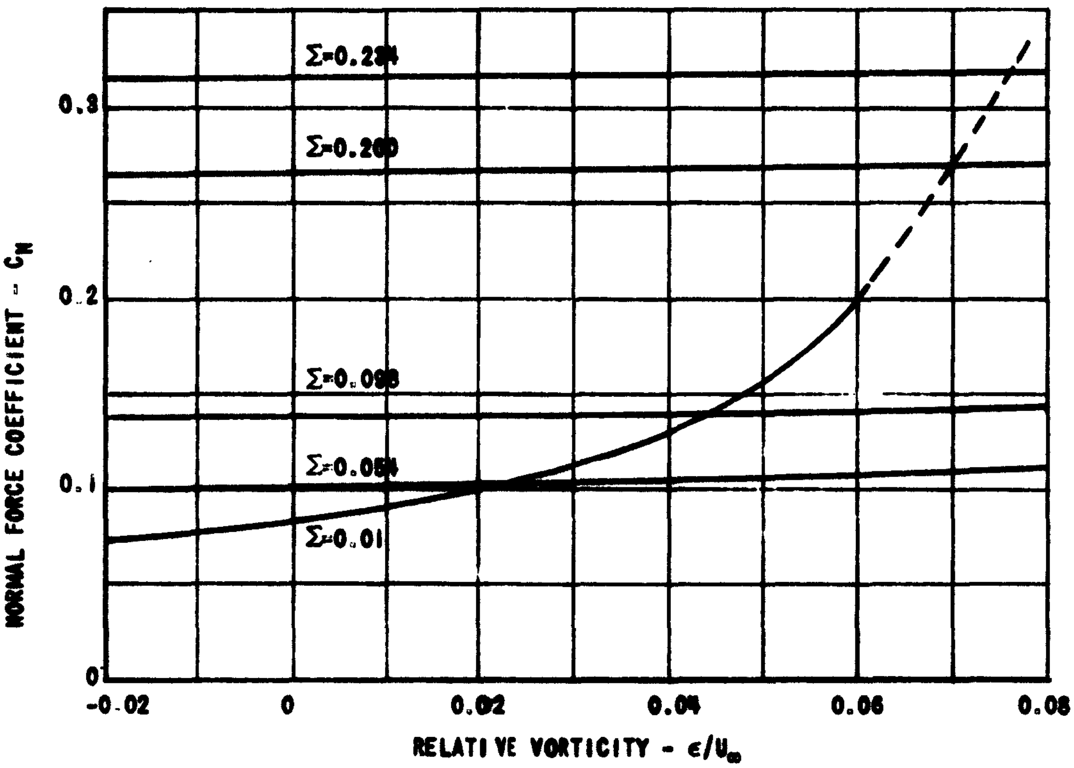

FIGURE 25. EFFECT OF VORTICITY ON C_N: $\alpha = 3°$.
FLOW PAST A HYDROFOIL.

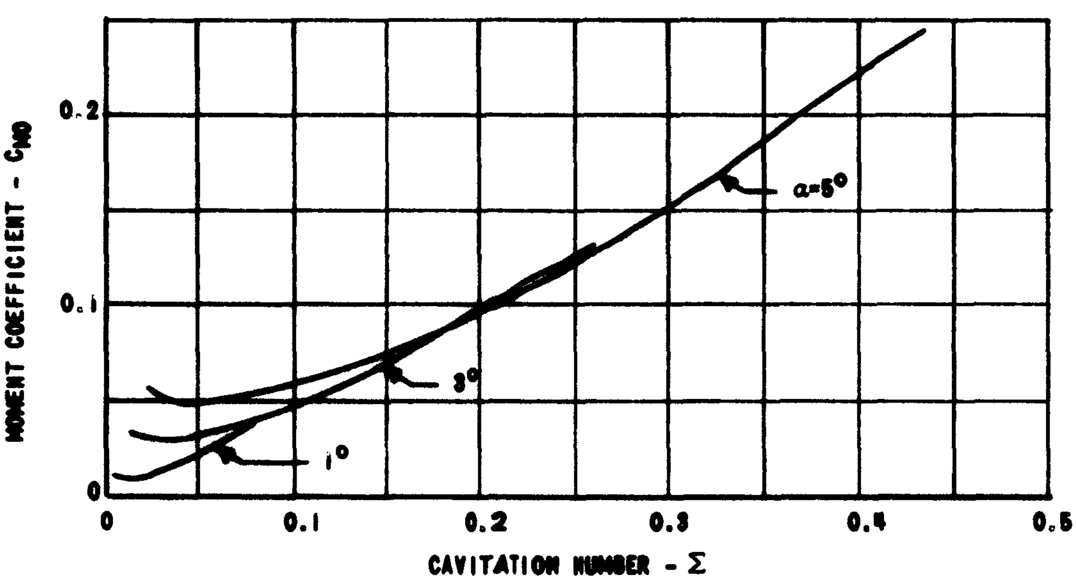

FIGURE 26. MOMENT COEFFICIENT VS CAVITATION NUMBER
FOR FLOW PAST A HYDROFOIL AT $\epsilon/U_\infty = 0.04$.

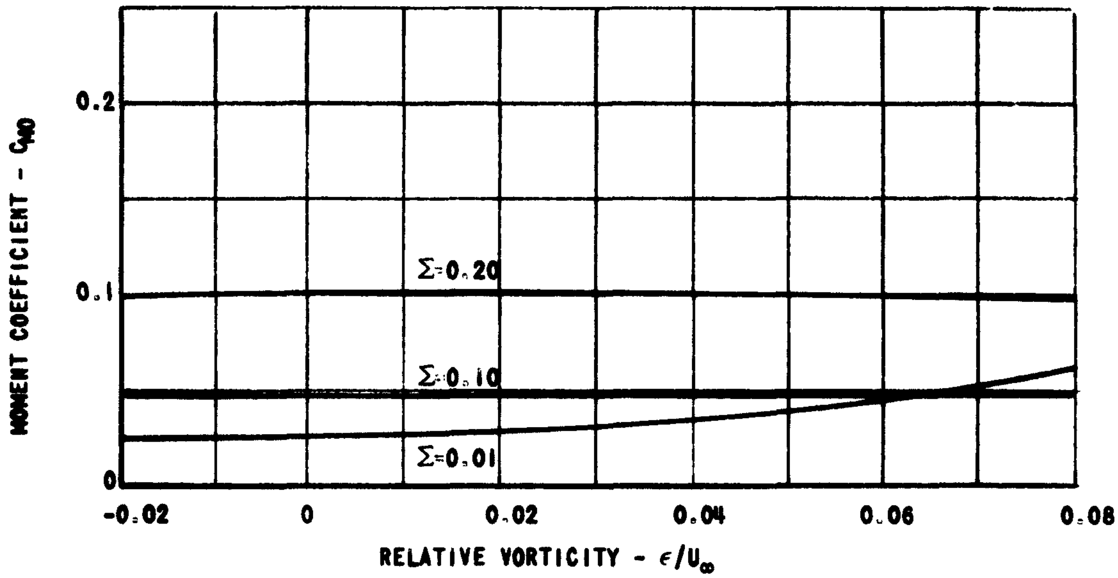

FIGURE 27 EFFECT OF VORTICITY ON C_{MO} $\alpha = 3°$ FLOW PAST A HYDROFOIL.

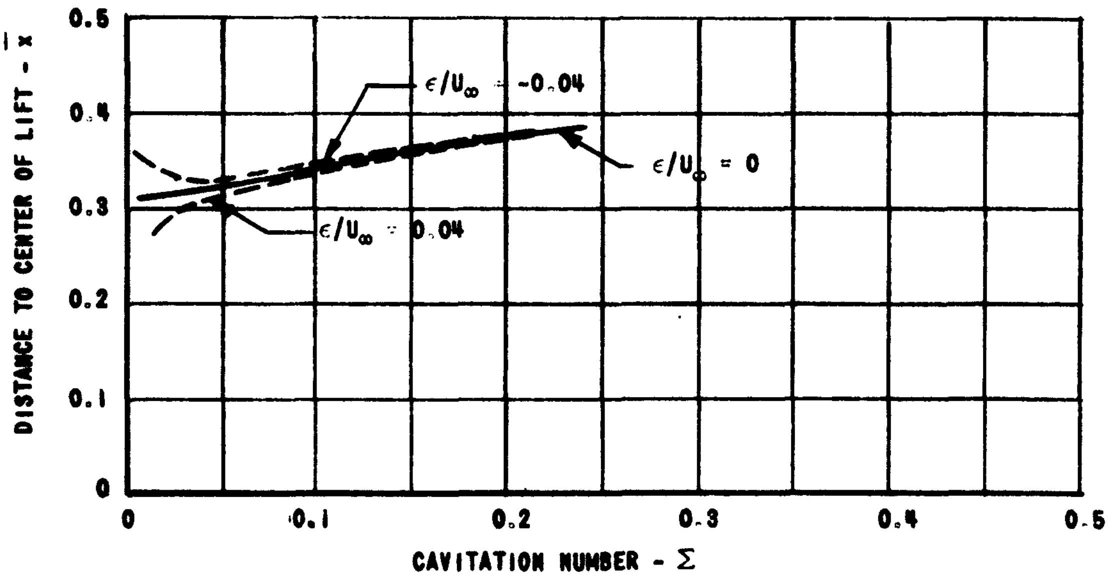

FIGURE 28. EFFECT OF VORTICITY ON $\bar{x}$ AT $\alpha = 3°$ AND VARYING Σ FOR FLOW PAST A HYDROFOIL.

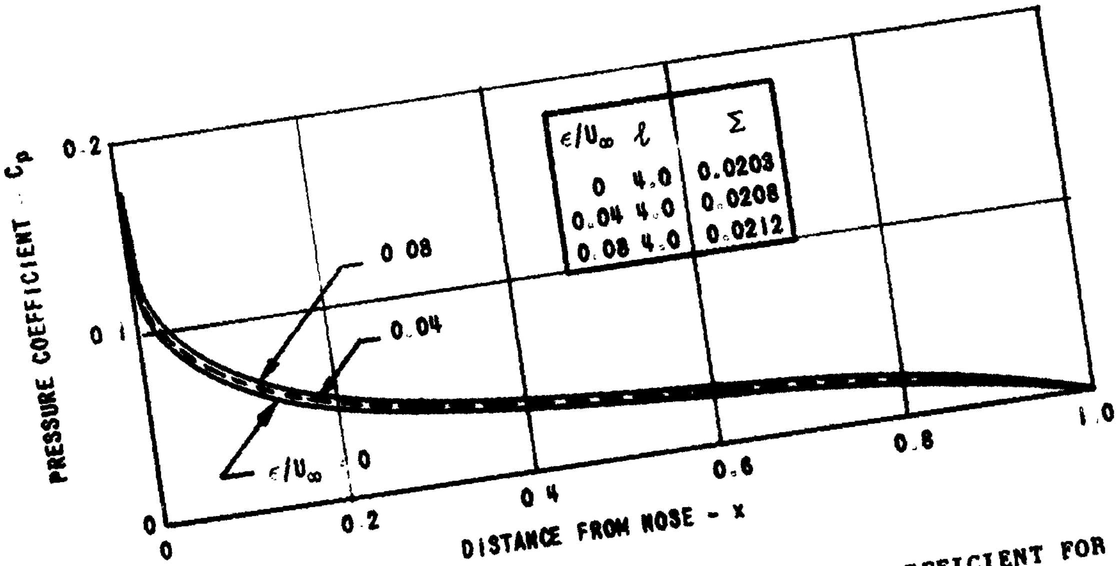

FIGURE 29 EFFECT OF VORTICITY ON PRESSURE COEFFICIENT FOR SHEAR FLOW PAST A HYDROFOIL $\alpha = 1°$.

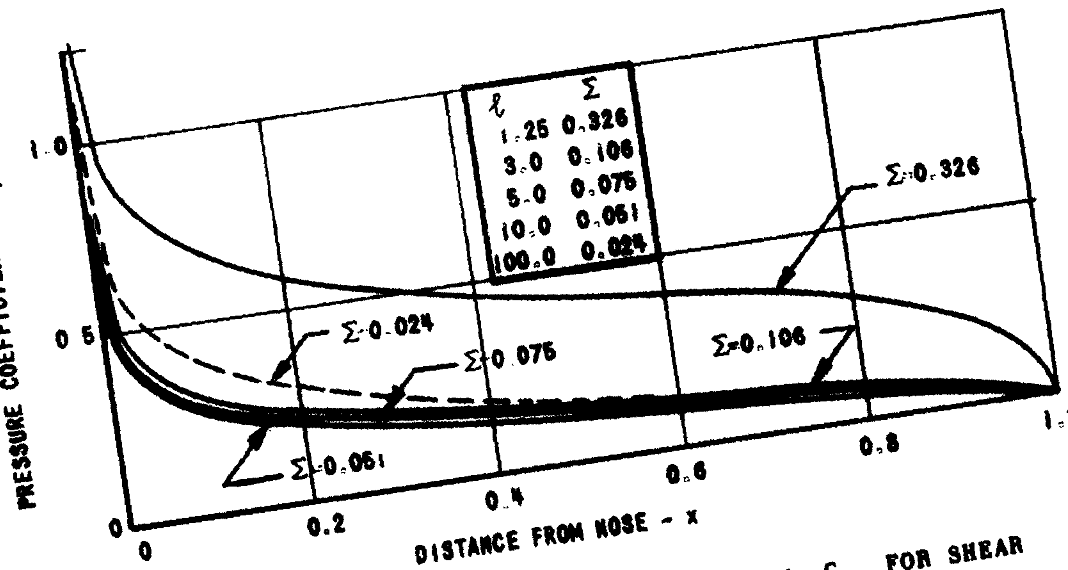

FIGURE 30 EFFECT OF CAVITATION NUMBER ON C_p FOR SHEAR FLOW PAST A HYDROFOIL. $\alpha = 4°$; $\epsilon/U_\infty = 0.06$

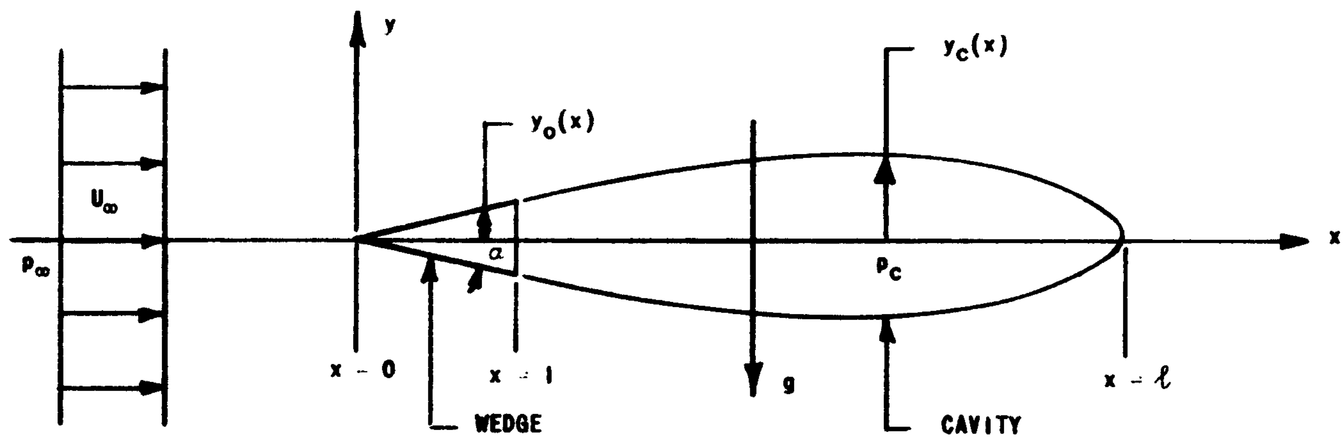

z-PLANE

FIGURE 31 SUPERCAVITATING FLOW PAST A WEDGE IN A TRANSVERSE GRAVITY FIELD

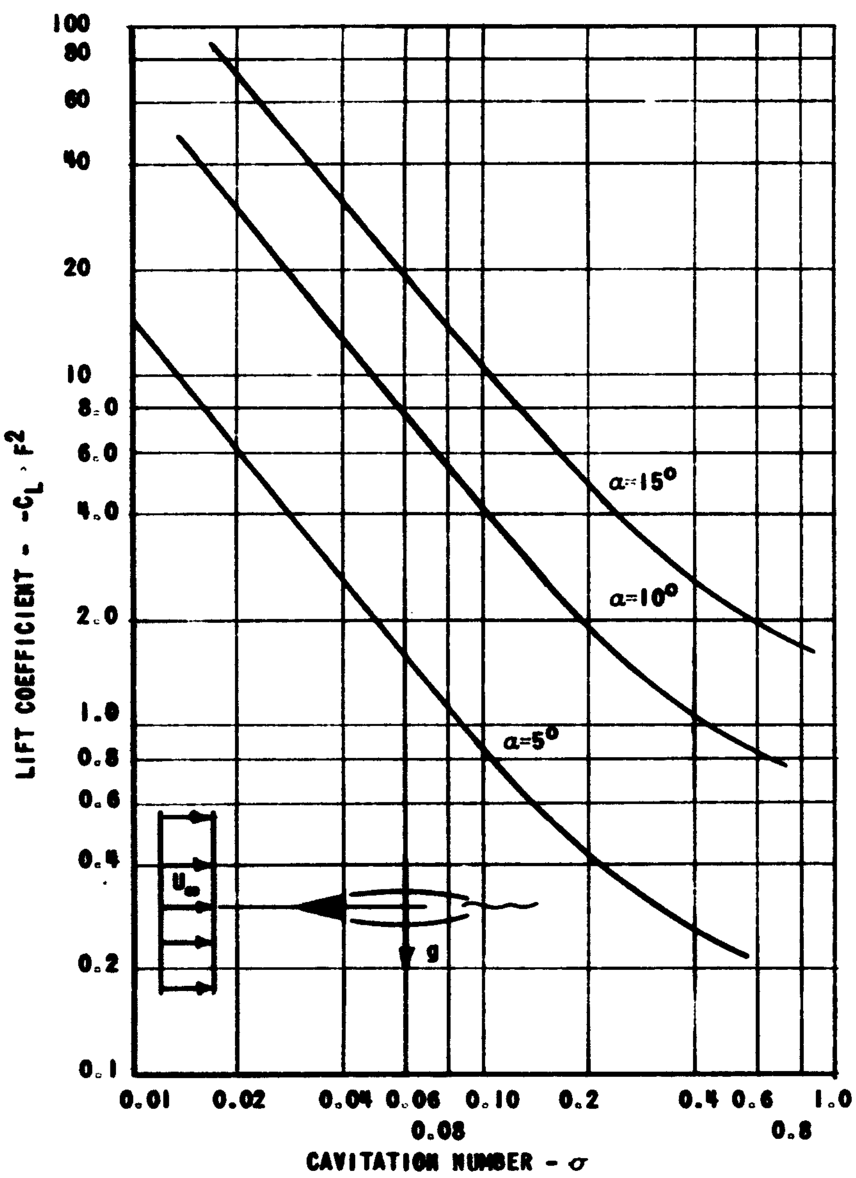

FIGURE 32. EFFECT OF CAVITATION NUMBER ON LIFT COEFFICIENT IN GRAVITY FIELD.

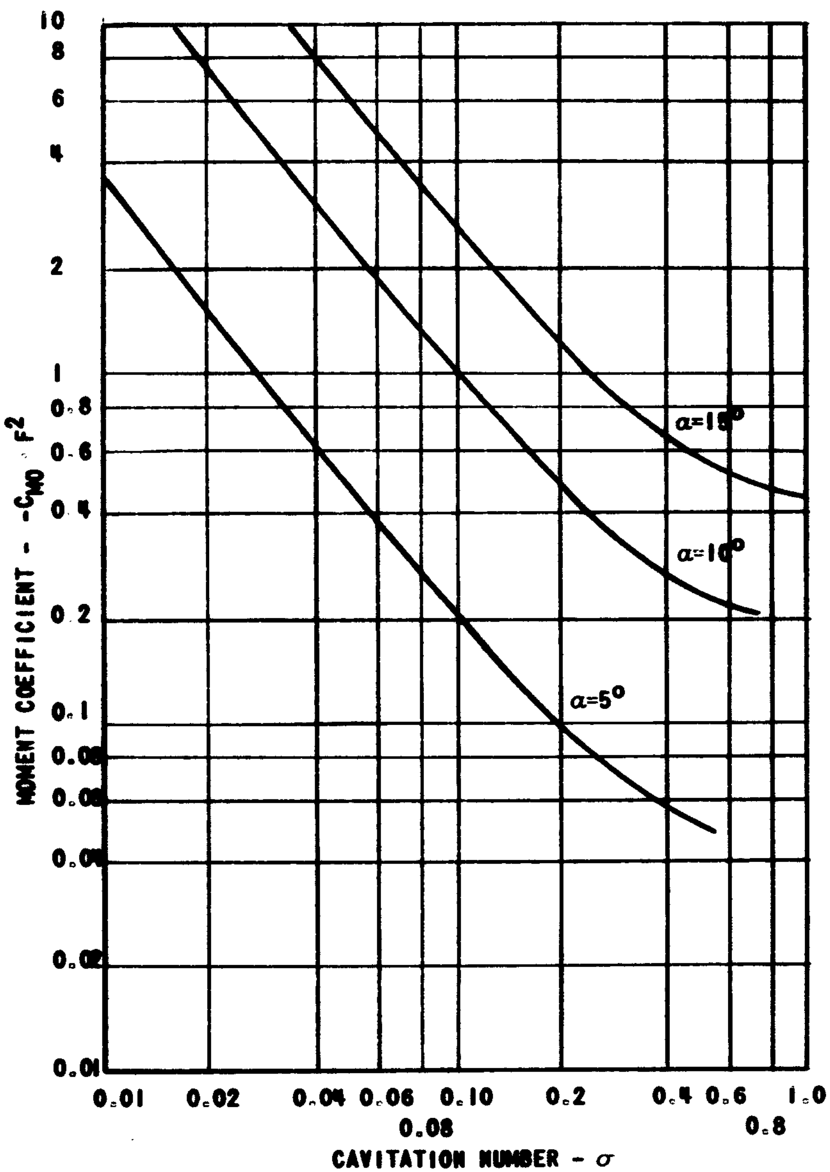

FIGURE 33. EFFECT OF CAVITATION NUMBER ON MOMENT COEFFICIENT IN GRAVITY FIELD.

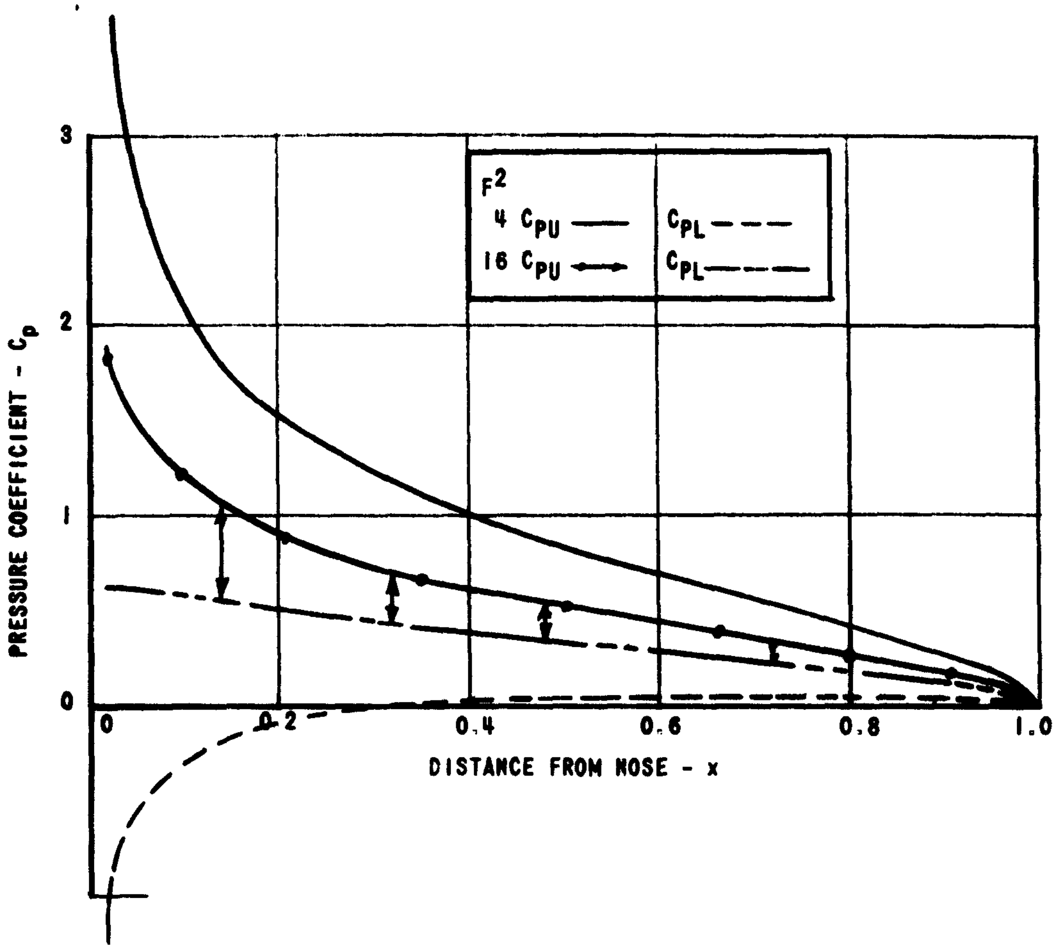

FIGURE. 34. $\sigma = 0.0865$, $\ell = 30$, $\alpha = 10°$ **EFFECT OF FROUDE NUMBER ON** C_p **FOR FLOW PAST A WEDGE.**

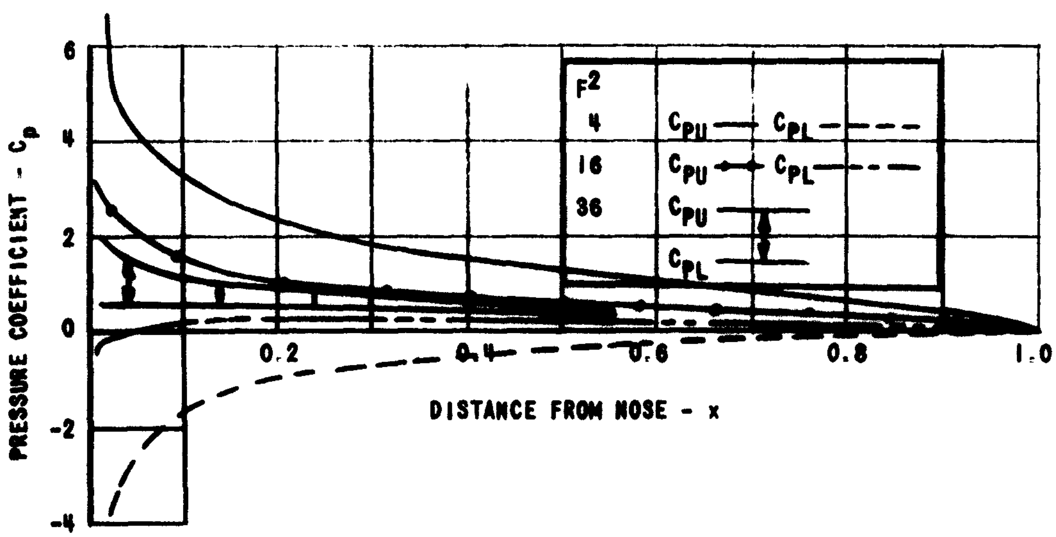

FIGURE 35. $\sigma = 0.0483$, $\ell = 90$, $\alpha = 10°$ **EFFECT OF FROUDE NUMBER ON** C_p **FOR FLOW PAST A WEDGE.**

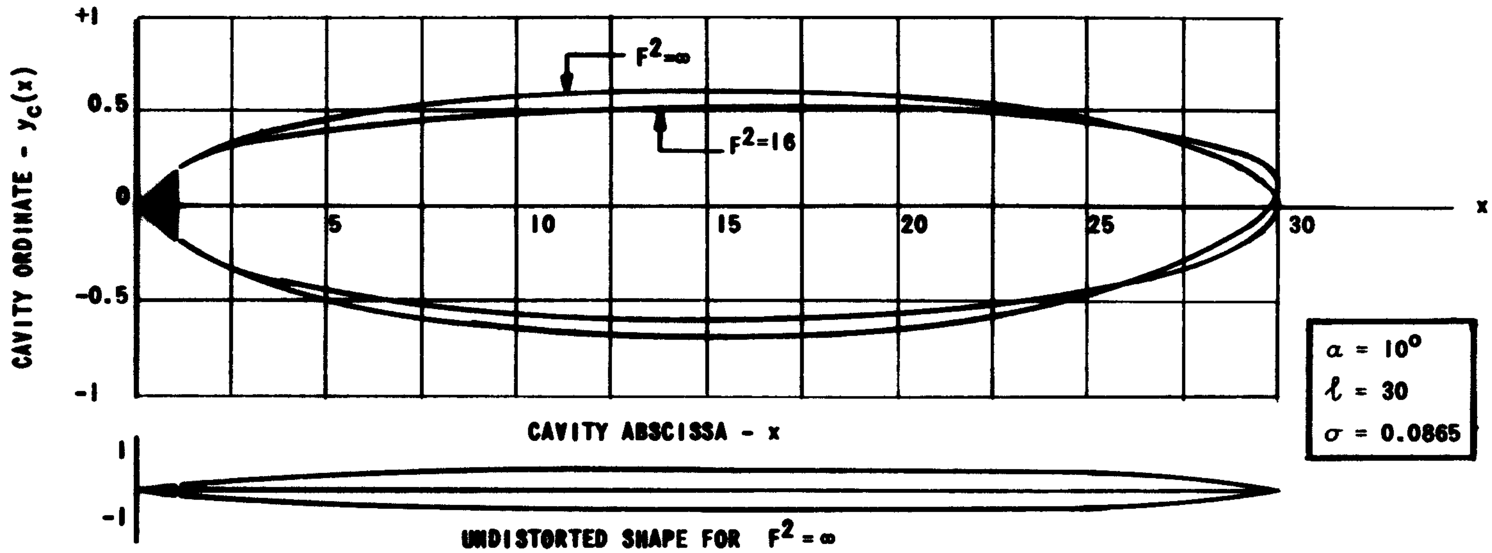

FIGURE 36. EFFECT OF FROUDE NUMBER ON CAVITY SHAPE FOR WEDGE IN TRANSVERSE GRAVITY FIELD.

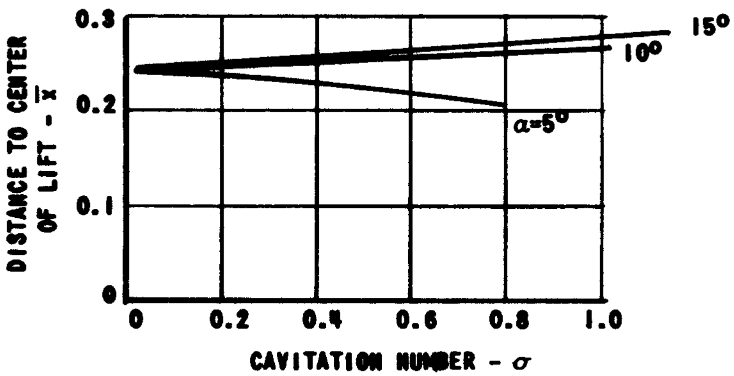

FIGURE 37. EFFECT OF CAVITATION NUMBER ON $\bar{x}$ FOR ARBITRARY FROUDE NUMBER FOR FLOW PAST A WEDGE.

DISTRIBUTION LIST

75 CO and Director
DTMB, Code 513
Washington 7, D. C.

Chief, Bu Ships
Navy Dept
Washington 25, D. C.
1 Codes 320
2 335
1 420
2 440

1 CO and Director
U. S. NEL
San Diego 52, Calif

1 CO and Director
U. S. NUSL
New London, Conn

CNO
Washington 25, D. C.
3 Codes 438
1 461
1 463
1 466

1 Chief, Bureau of Yards and Docks
Navy Dept
Washington 25, D. C.

1 CO
ONRBR
495 Summer St.
Boston 10, Mass

1 CO
ONRBR
207 West 24th St.
New York 11, N Y

1 CO
ONRBR
The John Crerar Library Bldg, 10th Floor, 86 E. Randolph St.
Chicago 1, Ill

1 CO
ONRBR
1000 Geary St.
San Francisco 9, Calif

1 CO
ONRBR
1030 E. Green St.
Pasadena 1, Calif

1 CO and Director
U. S. Naval Civil Engg Lab
Port Hueneme, Calif

1 Commander, U. S. NOL
White Oak, Silver Spring, Md

1 Commander, U. S. NOTS
China Lake, Calif
Code 753

1 Director
U. S. Naval Engg Exp Sta
Annapolis, Md

1 U. S. Navy Hydrographer
Navy Dept
Washington 25, D. C.

1 Dept of Meteorology and Oceanography
U. S. NPGS
Monterey, Calif

1 Beach Erosion Board, Corps of Engineers
U. S. Army
5201 Little Falls Rd., N. W.
Washington 16, D. C.

1 U. S. Director
Waterways Exp Sta
Corps of Engineers, U. S. Army
P. O. Box 637
Vicksburg, Miss

1 Commanding General
R and D Div
Dept of the Army
Washington 25, D. C.

1 Chief of Engineers
Dept of the Army
Washington 25, D. C.

1 NBS
Hydraulic Lab
Washington 25, D. C.
Fluid Mechanics Div

1 U. S. Coast and Geodetic Survey
Washington 25, D. C.

1 Commandant (OAO)
U. S. CG
Washington 25, D. C.

1 Library of Congress
Washington 25, D. C.

1 Chesapeake Bay Institute
John Hopkins U
Baltimore, Md

1 Dept of Oceanography
U of Washington
Seattle, Wash

1 Dept of Oceanography
Oregon State College
Corvallis, Ore

1 Oceanographic Inst
Florida State U
Tallahassee, Fla

1 Stevens Institute of Technology
Davidson Lab
Castle Point Sta
Hoboken, N. J.
Dr. J. P. Breslin

3 Calif Inst of Tech
Pasadena 4, Calif
Dr. M. S. Plesset
Dr. T. Y. Wu
Dr. A. J. Acosta

1 M. I. T.
Fluid Dynamics Research Lab
Cambridge 39, Mass

1 UCLA
Dept of Engg
Los Angeles 24, Calif
Dr. A. Powell

1 U of Minnesota
St. Anthony Falls
Hydraulic Lab
Minneapolis 14, Minn
Dr. L. G. Straub

1 Penn State U
Ordnance Research Lab
University Park, Pa
Dr. G. F. Wislicenus

1 Colorado State U
Dept of Civil Engg
Fort Collins, Colo
Prof. J. E. Cermak

1 State U of Iowa
Iowa Inst Hydraulic Research
Iowa City, Iowa
Dr. Hunter Rouse

Stanford U
Stanford, Calif
1 Applied Math and Stat Lab
3 Dept of Civil Engg
Dr. E. Y. Hsu
Dr. B. Perry
Prof. R. L. Street

1 New York U
Courent Inst of Math Sci
25 Waverly Place
New York 3, N Y
Prof. J. J. Stoker

1 New York U
University Heights
Bronx, N Y
Dept of Oceanography

1 U of Maryland
Inst for Fluid Dynamics and Appl Math
College Park, Md

1 U of Illinois
College of Engg
Dept of Theor and Appl Mech
Urbana, Ill
Dr. J. M. Robertson

1 Reneselaer Polytechnic Inst
Dept of Math
Troy, N Y
Dr. Hirsh Cohen

1 Cornell Aeronautical Lab
4455 Genesee St.
Buffalo, N Y
Mr. R. White

2 The John Hopkins U
Dept of Mech
Baltimore 18, Md
Dr. R. R. Long
Prof. S. Correin

1 U of Michigan
Dept of Aeronautical Engg
Ann Arbor, Mich
Prof. R. B. Couch

2 U of California
Dept of Engg
Berkeley 4, Calif
Dr. Wehausen

1 Texas A. and M. Research Foundation
College Sta., Tex
Mr. B. W. Wilson

1 U of Connecticut
School of Engg
Storrs, Conn

Southwest Research Inst
8500 Culebra Rd
San Antonio 6, Tex
1 Dept of Mech Sci
Dr. H. N. Abramson
1 Appl Mech Reviews

1 Midwest Research Inst
425 Volker Blvd.
Kansas City 10, Mo
Mr. Zeydel

1 General Appl Sci Labs, Inc
Merrick and Stewart Ave.
Westbury, L. I., N Y
Dr. F. Lane

1 Technical Research Group
2 Aerial Way
Syosset, L. I., N Y
Dr. L. Kotik

1 Allied Research Assoc, Inc
43 Leon St., Boston 15, Mass

2 Hydronautics, Inc
200 Monroe St.
Rockville, Md
Dr. M. P. Tulin
Mr. P. Eisenberg

1 Oceanics, Inc
114 E. 40 St.
New York 16, NY
Dr. P. Kaplan

1 Hydro-Space Assoc
3775 Sheridge Dr.
Sherman Oaks, Calif

1 General Dynamics Corp
Electric Boat Div
Groton, Conn
Mr. R. McCandliss

1 AiResearch Mfg Co
9851-9951 Sepulveda Blvd.
Los Angeles 9, Calif
Dr. B. R. Parkin

1 Gibbs and Cox, Inc
21 West St.
New York, N Y

1 Aerojet-General Corp
6352 N. Irwindale Ave.
Azusa, Calif
C. A. Gongwer

1 Lockheed Aircraft Corp
Missiles and Space Div
Palo Alto, Calif
R. W. Kermeen

1 Douglas Aircraft Co
3000 Ocean Park Blvd.
Santa Monica, Calif
A. E. Raymond

1 The Martin-Marietta Co
Middle River, Md
J. D. Pierson

1 Sperry Gyroscope Co
3 Aerial Way
Syosset, L. I., N Y

1 General Dynamics Corp
Convair Div
San Diego, Calif
Mr. H. E. Brooke

1 Grumman Aircraft Engg Corp
Dynamic Developments Div
Babylon, L. I., N Y
G. Wennagel

1 Boeing Aircraft Co
Seattle Div
Seattle, Wash
M. J. Turner

1 Edo Corp
College Point, N Y

1 North American Aviation, Inc
Columbus Div
4300 E. Fifth Ave.
Columbus, Ohio
D. A. King

1 NASA
1512 H St., N. W.
Washington 25, D. C.

1 Dept of the Navy
Bu Weaps
Airframe Design Div
Washington 25, D. C.
R. H. Handler

10 ASTIA
Arlington Hall Sta
Arlington 12, Va

Engg Societies Library
345 E. 47 St.
New York 17, N Y

1 Inst of Aerospace Sciences
Aerospace Engg
2 E. 64 St.
New York 21, N Y

1 Woods Hole Oceanographic Inst
Woods Hole, Mass

Scripps Inst of Oceanography
La Jolla, Calif